Untersuchungen zur Regulation der humanen Xylosyltransferase-I bei Fibrosen

Kumulative Dissertation

zur Erlangung des Doktorgrades

der Naturwissenschaften

(Dr. rer. nat.)

Universität Bielefeld

Fakultät für Chemie

vorgelegt von

Thanh-Diep Ly

aus Bad Soden-Salmünster

Bielefeld / Bad Oeynhausen, Januar 2021

Diese Arbeit entstand unter der Leitung von **Herrn Prof. Dr. med. Cornelius Knabbe**
am Institut für Laboratoriums- und Transfusionsmedizin,
Herz- und Diabeteszentrum Nordrhein-Westfalen,
Universitätsklinik der Ruhr-Universität Bochum
in Bad Oeynhausen
in der Zeit von November 2017 bis Januar 2021.

Erstgutachter: Prof. Dr. med. Cornelius Knabbe

Zweitgutachter: Prof. Dr. rer. nat. Torben Lübke

Danksagung

Mit dieser Seite möchte ich mich bei allen Personen bedanken, die auf ganz individuelle Weise zum Gelingen dieser Arbeit beigetragen haben. Daher formuliere ich an dieser Stelle zunächst ein unscheinbares, aber aus tiefstem Herzen kommendes „Danke“.

Beginnen möchte ich diese Danksagung mit Herrn Prof. Dr. med. Cornelius Knabbe. Ihm danke ich für die Möglichkeit, meine Doktorarbeit am Herz- und Diabeteszentrum durchführen zu können sowie für das Interesse am Fortgang dieser Arbeit.

Herrn Prof. Dr. rer. nat. Torben Lübke danke ich für die Übernahme des Zweitgutachtens und für die freundliche Beantwortung offener Fragen.

Mein besonderer Dank gilt Frau Dr. rer. nat. Isabel Faust für die Unterstützung meiner Arbeit. Ich möchte mich vor allem für ihr stetiges Engagement am Fortgang dieser Arbeit und die anregenden Gespräche während des gesamten Betreuungszeitraums bedanken.

Unserem Kooperationspartner Herrn Prof. Dr. med. Jörg H. W. Distler danke ich für die Bereitstellung der Patientenfibroblasten und die gute Zusammenarbeit.

Ein großer Dank gilt meinen ehemaligen Masterstudentinnen Ricarda Plümers und Anika Kleine für ihren Beitrag zum Gelingen dieser Arbeit.

Danken möchte ich außerdem all meinen gegenwärtigen und ehemaligen Kolleginnen und Kollegen aus Labor 11 für die gute Zusammenarbeit, die vielfältige Unterstützung und die sehr angenehme Arbeitsatmosphäre.

Allen weiteren Mitarbeitern des Instituts für Laboratoriums- und Transfusionsmedizin danke ich für die gute und zuverlässige Zusammenarbeit.

Letztlich richte ich auch ein Dankeschön an meine Mitbewohnerin für das Korrekturlesen meiner Arbeit sowie an meinen Freund, der mich auf meinem Weg durch das Studium begleitet hat.

Inhaltsverzeichnis

Zusammenfassung

Die systemische Sklerodermie (SSc) ist eine prototypische fibrotische Erkrankung, die durch eine Akkumulation von Myofibroblasten und Komponenten der extrazellulären Matrix (ECM) gekennzeichnet ist. Der Anstieg der Proteoglykan (PG)-Biosynthese bei SSc steht in einem engen Zusammenhang mit der Serumaktivitätserhöhung der humanen Xylosyltransferase (XT), die das initiale Enzym der PG-Biosynthese ist. Diese Arbeit zielte darauf ab, das Verständnis der fibrotischen XT-I-Regulation zu verbessern sowie XT-I-Inhibitoren zu identifizieren, die als Grundlage für die zukünftige Entwicklung einer antifibrotischen Therapie dienen können.

Im ersten Teilprojekt dieser Arbeit wurde Activin A, ein Zytokin der *transforming growth factor-β* (TGF-β)-Familie, als Induktor der *XYLT1* mRNA-Expression und XT-Aktivität in normalen humanen Dermalfibroblasten (NHDF) identifiziert. Unter Verwendung von Inhibitoren und gerichteter RNA-Interferenz wurde gezeigt, dass die Activin A-vermittelte XT-I-Erhöhung den Activin-Rezeptor-Typ-IB sowie Komponenten des intrazellulären MAP-Kinase- und SMAD-Signalwegs involviert. Neben profibrotischen Proteinen spielen miRNAs eine zentrale Rolle bei der Entstehung und Regulation fibrotischer Prozesse. In dieser Arbeit wurde eine Regulation der XT-I in NHDF über die TGF-β1-induzierte miRNA-145 und miRNA-21 gezeigt. Eine direkte Bindung der miRNA-145 und -21 an die 3'-untranslatierte Region der *XYLT1* mRNA wurde über einen Reporter-Luciferaseassay ausgeschlossen und somit eine miRNA-vermittelte *XYLT1* Regulation über sekundäre Mediatoren bestätigt. Die Involvierung des Transkriptionsfaktors KLF4 bei der miRNA-145-vermittelten XT-I-Regulation wurde über eine *in silico* Analyse, gerichtete RNA-Interferenz und quantitative Echtzeit-PCR nachgewiesen. Hinsichtlich der TGF-β1-induzierten *XYLT1* mRNA-Expressionsregulation durch die miRNA-21 wurde SMAD7 als Sekundärmediator bestimmt. Für die Einordnung der XT-I als validen Biomarker der Fibrosierung bei SSc fehlte bisher die Verknüpfung der erhöhten XT-Serumaktivität mit einer verstärkten zellulären *XYLT1* mRNA-Expression und XT-I-Aktivität. Im Rahmen des zweiten Teilprojekts wurden sowohl die *XYLT1* mRNA-Expression als auch die XT-I-Aktivität als Biomarker für die TGF-β1-abhängige Dysregulation der PG-Biosynthese bei SSc eruiert. So zeigten SSc-Fibroblasten im Vergleich zu NHDF eine höhere extrazelluläre XT-I-Aktivität, die auf einer Interleukin-1β-vermittelten TGF-β-Rezeptor-Typ-II-Expressionserhöhung basiert. Naturstoffe besitzen ein breites biologisches Aktivitätsspektrum und stellen eine wichtige Quelle für die Medikamentenentwicklung dar. Daher wurde im dritten Teilprojekt eine Naturstoff-Bibliothek verwendet, um nicht-substratbasierte Inhibitoren der XT-I über die massenspektrometrische Quantifizierung der XT-I-Aktivität zu ermitteln. In Kombination mit zellbasierter Methodik sowie *in silico* Analysen der Protein-Ligand-Interaktion wurden die beiden Wirkstoffe Amphotericin B und Celastrol als potenzielle XT-I-Inhibitoren identifiziert. Die Inhibition der XT-I-Enzymaktivität erfolgte bei Amphotericin B über einen unkompetitiven und bei Celastrol über einen kompetitiven Mechanismus. Das zelluläre *XYLT1* Expressionsniveau und die zelluläre XT-I-Aktivität wurden ebenfalls durch die beiden XT-I-Inhibitoren reduziert. Hierbei konnten die Inhibitor-vermittelten zellulären Effekte der Regulation von Komponenten des TGF-β/miRNA-21-Signalwegs zugeordnet werden.

Zusammengefasst verbessern die Resultate dieser Arbeit das Verständnis der zugrunde liegenden zellulären Mechanismen der dysregulierten *XYLT1* Expression bei Fibrosen. Mit der Entdeckung potenzieller XT-I-Inhibitoren liefert diese Arbeit eine wissenschaftliche Grundlage für die mögliche zukünftige Therapie fibroproliferativer Erkrankungen.

Abstract

Systemic sclerosis (SSc) is considered a prototypic fibrotic disorder that is characterized by a pathological accumulation of myofibroblasts and extracellular matrix (ECM) components including collagens and proteoglycans (PG). The increase of PG biosynthesis in SSc is closely related to an elevated serum activity of human xylosyltransferase (XT), the initial enzyme in PG biosynthesis. As a basis for future development of an antifibrotic therapy for SSc, this work aimed to enhance understanding of XT-I regulation in fibrosis and to identify XT-I inhibitory molecules.

This study revealed activin A, a cytokine of the transforming growth factor-β (TGF-β) family, as a potent regulator of *XYLT1* mRNA expression and XT activity in normal human dermal fibroblasts (NHDF). Using small molecule inhibitors and small interfering RNAs, the activin A-mediated XT-I increase was shown to involve activin receptor type 1B and the intracellular MAPK and SMAD pathways. In addition to profibrotic proteins, miRNAs play a central role in the development und regulation of fibrotic processes. In this work, the TGF-β1-inducible miRNAs miRNA-145 and -21 were shown to regulate XT-I in NHDF. The direct binding of miRNA-145 and -21 to the 3' untranslated region of the *XYLT1* mRNA was excluded by reporter luciferase assays, indicating an indirect miRNA-mediated *XYLT1* regulation through secondary mediators. The involvement of the zinc-finger transcription regulator KLF4 in the miRNA-145-mediated XT-I regulation was shown by *in silico* analysis, targeted gene silencing and quantitative real-time PCR. Regarding the TGF-β1-induced *XYLT1* expression regulation by miRNA-21, the inhibitory SMAD7 was identified as secondary mediator. To address the missing association of increased XT serum activity with increased cellular *XYLT1* mRNA expression und XT-I activity in SSc, this study characterized the differences in cellular XT-I activity of SSc fibroblasts (SScF) and NHDF. A higher extracellular XT-I activity in SScF was found to be mediated by an enhanced autocrine TGF-β signaling. A dysregulated miRNA-21/TGF-β receptor II axis in SScF was shown to contribute to the enhanced autocrine TGF-β signaling. Both the *XYLT1* mRNA expression, and XT-I activity were shown to be sensitive biomarkers of the dysregulated TGF-β signaling in SSc. Natural products have a wide range of biological activities and represent an important source for drug development. Therefore, a natural product-based molecular library was used in the third subproject in order to identify non-substrate-based XT-I inhibitors by mass spectrometric quantification of the XT-I activity. In combination with cell-based experimental approaches and structure-based *in silico* analyzes, the two active ingredients amphotericin B and celastrol were identified to possess XT-I inhibitory properties. Their XT-I inhibitory effect was not restricted to the inhibition of the catalytic activity of the XT-I protein by an uncompetitive or a competitive inhibition mode, respectively, but was shown to impact cellular *XYLT1* expression level and XT-I activity in NHDF as well. These cellular inhibitor-mediated changes were shown to involve the TGF-β and miRNA-21 signaling pathway.

This work improves the mechanistic understanding of fibrotic remodeling in SSc by identifying hitherto unknown XT-I mediators and regulatory pathways in dermal fibroblasts. With the identification of putative XT-I inhibitors this study provides a strong rational for the future therapeutical application of those in fibroproliferative diseases.

1 Einleitung

Eine Fibrose ist eine pathologische Vernarbung und Gewebeverhärtung, die durch eine abnorme Akkumulation von Komponenten der extrazellulären Matrix (ECM) verursacht wird (Wynn, 2004). Obwohl klassische fibrotische Erkrankungen wie die systemische Sklerodermie (SSc) selten sind, spielt der zugrunde liegende Fibrosierungsprozess in der Pathologie zahlreicher Volkskrankheiten, wie dem Myokardinfarkt und der Leberzirrhose, eine zentrale Rolle (Kuhn *et al.*, 2009; Prante *et al.*, 2007). Trotz der erheblichen sozioökonomischen Bedeutung der Fibrose stehen bisher keine wirksamen antifibrotischen Therapieansätze zur Verfügung.

1.1 Extrazelluläre Matrix

Die ECM ist eine dreidimensionale azelluläre Struktur, die ubiquitär vorkommt und auf makroskopischer Ebene die stabile Form der Organe ermöglicht (Cox und Erler, 2011). Die Struktur und Zusammensetzung der ECM ist demnach essentiell für zahlreiche Funktionen, wie die Aufrechterhaltung der Gewebeintegrität und -elastizität oder die Wasserretention und die Signalgebung (Do und Eming, 2016). Daraus ergibt sich eine zentrale Bedeutung der ECM für zahlreiche pathobiochemische Mechanismen wie Inflammation, Fibrose und Krebs. Fibroblasten sind die Hauptproduzenten extrazellulärer Matrixproteine, zu denen Glykoproteine, Kollagene, Proteoglykane (PG) und Glykosaminoglykane (GAG) gehören (Zhao *et al.*, 2019). Unter fibrotischen Bedingungen ist die Synthese und Freisetzung der GAG und PG aus aktivierten Fibroblasten in den Extrazellulärraum gesteigert (Götting *et al.*, 1999; Kitabatake *et al.*, 1983).

1.1.1 Glykosaminoglykane und Proteoglykane

GAG sind stark polyanionische lineare Polydisaccharide, die frei im extrazellulären Raum oder als glykosidische Seitenketten an Glykoproteine gebunden vorkommen. Die an Proteine gebundene Form der GAG wird als PG bezeichnet. Die PG-Biosynthese beginnt am rauen endoplasmatischen Retikulum mit der Synthese des PG-*Core*-Proteins und wird im Golgi-Apparat mit dessen post-translationalen Modifikation fortgesetzt (Prydz und Dalen, 2000). Die Bindungsregion zwischen PG-*Core*-Protein und GAG besteht aus der Tetrasaccharid-Sequenz Glukuronyl-β-(1→3)-Galaktosyl-β-(1→3)-Galaktosyl-β-(1→4)-Xylosyl-β-1-*O*-(Serin), die kovalent an spezifische

Serinreste des PG-*Core*-Proteins gebunden ist (**Abbildung 1**) (Mikami und Kitagawa, 2013).

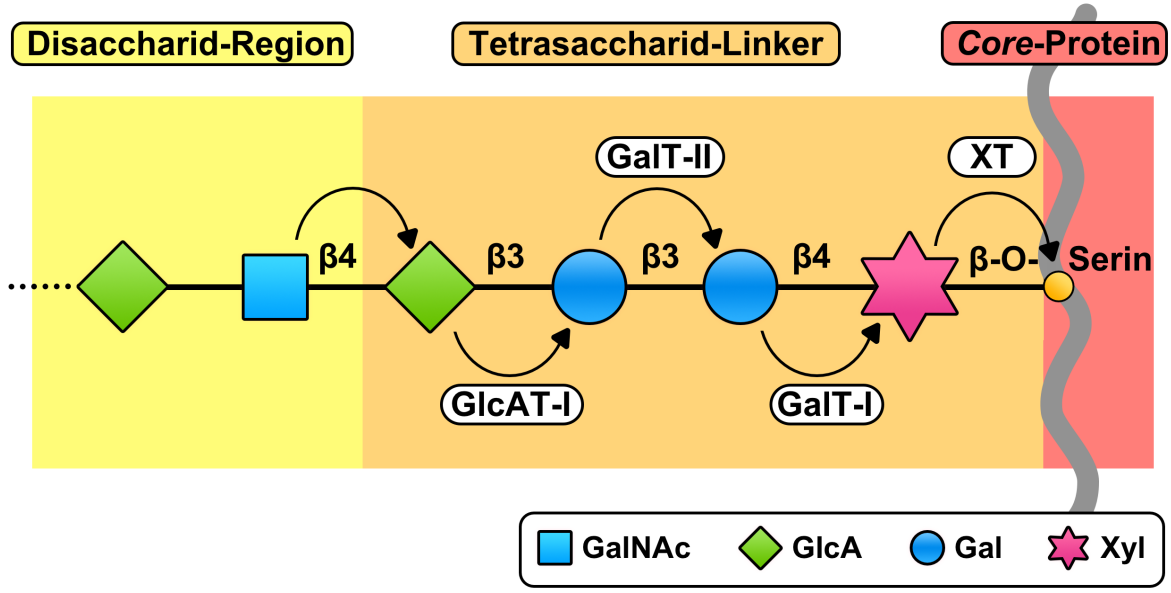

Abbildung 1: Schematische Darstellung der GAG-Tetrasaccharid-Linkerregion. Die Synthese der Linkerregion erfolgt durch die Übertragung einer Xylose (Xyl), zweier Galaktosen (Gal) und einer Glukuronsäure (GlcA), welche durch die Enzyme Xylosyltransferase (XT), Galaktosyltransferase-I (GalT-I), Galaktosyltransferase-II (GalT-II) und Glukuronyltransferase-I (GlcAT-I) katalysiert werden. Die Übertragung einer fünften Saccharid-Einheit legt fest welches GAG gebildet wird. Wird *N*-Acetylgalaktosamin (GalNAc) übertragen, bildet sich ein Chondroitinsulfat/Dermatansulfat aus (Mikami und Kitagawa, 2013).

Die Anknüpfung jeder Saccharid-Einheit des Tetrasaccharid-Linkers wird von einem spezifischen Enzym katalysiert, wodurch eine mehrschichtige Regulation der GAG-Synthese erfolgt (Kitagawa *et al.*, 1998; Robinson *et al.*, 1966; Stoolmiller *et al.*, 1972). Der Transfer der initialen Xylose-Einheit wird von der humanen Xylosyltransferase (XT, EC 2.4.2.26) katalysiert (Götting *et al.*, 2000). Darauf folgt die Übertragung zweier Galaktose-Einheiten, welche jeweils durch die β1,4-Galaktosyltransferase-I (EC 2.4.1.133) und die β1,3-Galaktosyltransferase-II (EC 2.4.1.134) katalysiert werden (Almeida *et al.*, 1999; Bai *et al.*, 2001). Die Tetrasaccharid-Synthese wird mit dem Transfer einer Glukuronsäure (GlcA)-Einheit durch die β1,3-Glukuronyltransferase-I (EC 2.4.1.135) abgeschlossen (Kitagawa *et al.*, 1998). Die Übertragung des fünften Saccharids legt fest, welche Art von GAG-Kette das PG erhält (Prydz und Dalen, 2000). Es können mitunter Heparansulfat (HS)- und Chondroitinsulfat (CS)/Dermatansulfat (DS)-PG unterschieden werden (Hardingham und Fosang, 1992). Im Fall von

CS/DS wird eine *N*-Acetylgalaktosamin (GalNAc)-Einheit an die Linkersequenz übertragen, wohingegen beim HS eine *N*-Actetylglukosamin (GlcNAc)-Einheit transferiert wird (Fritz *et al.*, 1994). Neben den proteingebundenen GAG-Formen gibt es noch freie GAG wie das Hyaluronan (HA), welches nicht über den sekretorischen Weg synthetisiert wird. Daher liegt es im Gegensatz zu den anderen GAG nicht sulfatiert vor (Mikami und Kitagawa, 2013; Wang *et al.*, 2011).

Die alternierende Verknüpfung von GlcA und GalNAc bildet die repetitive Disaccharid-Einheit des CS aus. Das DS ist das Stereoisomer des CS, das durch die Epimerisierung der GlcA zu Iduronsäure (IdoA) gebildet wird. Im HS und HA sind die repetitiven Einheiten hingegen aus GlcA und GlcNAc aufgebaut (**Abbildung 2**) (Prydz und Dalen, 2000).

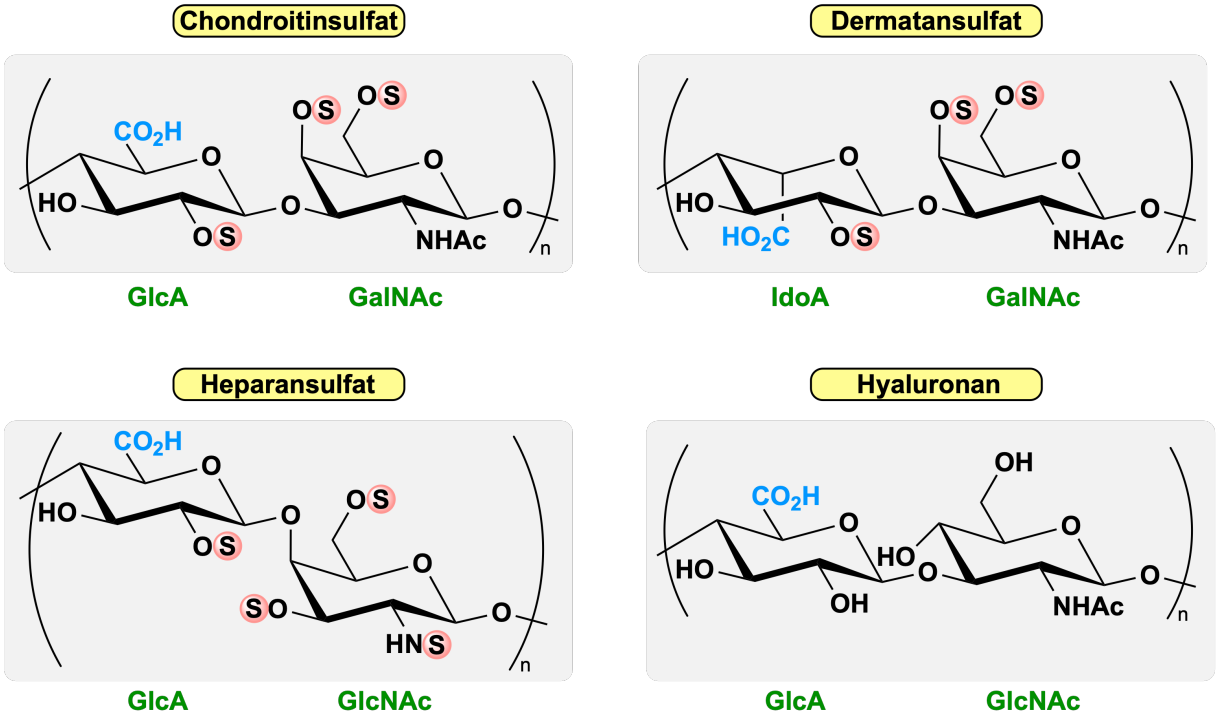

Abbildung 2: Disaccharid-Einheiten der CS-, DS-, HS- und HA-GAG-Ketten. Die repetitive Disaccharid-Einheit des CS besteht aus GlcA und GalNAc. DS ist ein Stereoisomer von CS, das IdoA anstelle von GlcA enthält. Das HS besteht aus GlcA und GlcNAc. Die Saccharide können an verschiedenen Positionen sulfatiert (rot) werden. HA ist gleichermaßen wie HS aus GlcA und GlcNAc aufgebaut und wird im Vergleich zu den proteingebundenen GAG nicht sulfatiert (Mikami und Kitagawa, 2013).

Die diversen Funktionen der PG können sowohl dem *Core*-Protein als auch den GAG-Ketten zugeschrieben werden (Yanagishita, 1993). Als eines der Hauptbestandteile der ECM besitzen PG die Eigenschaft mit HA und Kollagen multimolekulare Komplexe zu bilden, welche für die Stabilisierung der ECM sorgen. Darüber hinaus sind sie ein

Reservoir für Proteine und Signalmoleküle (Ghatak *et al.*, 2015), und besitzen teilweise Funktionen als Korezeptoren für Wachstumsfaktoren (Bishop *et al.*, 2007; Klagsbrun, 1990).

1.2 Xylosyltransferasen

Die humane XT ist das erste von vier Enzymen, das an der GAG-Linkersynthese beteiligt ist (Kearns *et al.*, 1991; Kitagawa *et al.*, 1998). Die XT katalysiert den initialen Xylose-Transfer ausgehend von UDP-D-Xylose auf definierte Serinreste im PG-*Core*-Protein. Hierbei wird eine *O*-glykosidische Bindung generiert (Götting *et al.*, 2000). Die enzymatische Aktivität der XT kann *in vitro* sowohl radiochemisch als auch massenspektrometrisch aus dem Zelllysat oder Zellkulturüberstand detektiert werden. Als Basis der XT-Analytik fungiert die Endpunktbestimmung der relativen XT-katalysierten Menge an xylosyliertem *Core*-Peptid unter standardisierten Reaktionsbedingungen (Kuhn *et al.*, 2006; Roch *et al.*, 2010).

1.2.1 Strukturelle und enzymatische Charakteristik der XT-Isoformen

Im humanen Organismus kommen die zwei XT-Isoformen XT-I und XT-II vor, die durch die Gene *XYLT1* und *XYLT2* kodiert werden (Voglmeir *et al.*, 2007; Wilson, 2004). Die XT-I-Primärstruktur besteht aus 959 Aminosäuren (AS) und besitzt ein Molekulargewicht von 108 kDa. Das XT-II-Protein hat eine Länge von 865 AS und umfasst ein Molekulargewicht von 97 kDa (Götting *et al.*, 2000). Es handelt sich um Golgi-residente Typ-II-Transmembranproteine, die eine AS-Sequenzhomologie von 52% aufweisen. Die homologen AS sind hierbei nicht gleichmäßig über die beiden Proteinsequenzen verteilt. So wurde eine 80%ige Sequenzhomologie der XT-I und XT-II dem katalytischen Bereich zugeordnet (Götting *et al.*, 2000; Müller *et al.*, 2006; Pönighaus *et al.*, 2007).

Beide XT-Isoformen bestehen aus einer kurzen *N*-terminalen Region, welche dem Zytosol zugewandt ist, einer singulären Transmembranhelix und einer Stammregion, die essentiell für die Golgi-Retention ist (Schön *et al.*, 2006). Außerdem besitzen die XT eine katalytische Glykosyltransferase-A-Domäne, die dem Lumen des Golgi-Apparats zugewandt ist (Briggs und Hohenester, 2018; Lairson *et al.*, 2008), sowie eine *C*-terminale Domäne, die laut der Pfam-Datenbank die Bezeichnung Xylo_C trägt (Briggs und Hohenester, 2018; Punta *et al.*, 2012) (**Abbildung 3**).

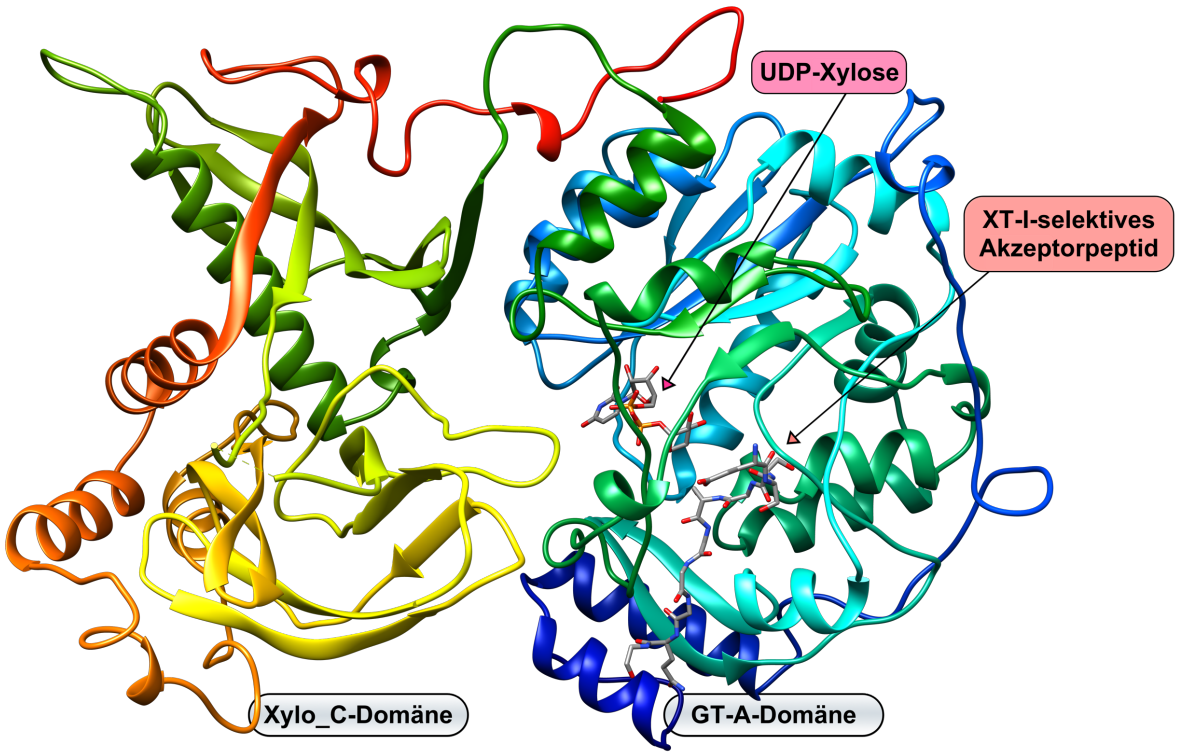

Abbildung 3: Kristallstruktur der XT-I komplexiert mit UDP-D-Xylose und Bikunin-abgeleitetem Akzeptorpeptid. Die dreidimensionale XT-I-Proteinstruktur mit UDP-D-Xylose und XT-I-selektivem Akzeptorpeptid wurde mit dem Programm MatchMaker (Meng *et al.*, 2006) in UCSF Chimera 1.14 (Pettersen *et al.*, 2004) erstellt. Hierfür wurde die Struktur des XT-I-Apoproteins (PDB ID: 6FOA) mit der XT-I-Struktur im Komplex mit UDP-D-Xylose und Bikunin-abgeleitetem Akzeptorpeptid (PDB ID:6EJ7) aus der Arbeit von Briggs *et al.* verwendet (Briggs und Hohenester, 2018). Die AS-Sequenz des Bikunin-abgeleiteten Akzeptorpeptids entspricht der AS-Sequenz des XT-I-selektiven Akzeptorpeptids aus der Arbeit von Fischer *et al.* (Fischer *et al.*, in Revision). Die dreidimensionale Struktur ist vom *N*-Terminus (blau) bis zum *C*-Terminus (rot) in Regenbogenoptik dargestellt. Die komplexierte UDP-D-Xylose und das modifizierte Akzeptorpeptid sind in der Stabdarstellung gezeigt. Die Atome sind farblich hervorgehoben: C (grau), N (blau), O (rot) und P (orange). Auf die Darstellung der vorhandenen Disulfidbrücken im XT-I-Protein wurde verzichtet.

Obwohl sich die natürliche Akzeptorspezifität von XT-I- und XT-II nur geringfügig voneinander unterscheidet (Roch *et al.*, 2010), gelang es kürzlich ein XT-I-selektives Akzeptorpeptid zu identifizieren. Mit dessen Verwendung ist eine isoformselektive XT-I-Aktivitätsbestimmung mittels *ultra-performance liquid chromatography-electrospray ionization-tandem mass spectrometry* (UPLC-ESI-MS/MS) möglich (Fischer *et al.*, in Revision).

Beide XT-Isoformen besitzen eine hohe Affinität zu Heparin, das zu einer verminderten Enzymaktivität führt (Casanova *et al.*, 2009). Eine Inhibition der XT-Aktivität durch Nukleotide und Endprodukte der PG-Biosynthese wurde ebenfalls gezeigt (Casanova *et al.*, 2008; Müller *et al.*, 2005).

1.2.2 Expression der beiden XT-Isoformen

Die beiden XT-Isoformen werden in den meisten Geweben gleichermaßen exprimiert. Jedoch existieren auch Gewebe, die eine dominantere XT-II-Expression aufweisen (Pönighaus *et al.*, 2007; Roch *et al.*, 2010). Die Expressionsunterschiede können mitunter auf eine differentielle Transkriptionsregulation zurückgeführt werden. Im *XYLT1* Promotor befinden sich Transkriptionsfaktorbindestellen für *specifity protein 1* (SP1), *early growth response factors* (EGR), und *krueppel like transcription factors* (KLF) (Faust *et al.*, 2014; Riedel *et al.*, 2018), während im *XYLT2* Promotor hauptsächlich Bindestellen für Transkriptionsfaktoren der SP1-Familie existieren (Müller *et al.*, 2013).
Über die Genotypisierung von 100 gesunden Blutspendern wurde eine Einzelnukleotidvariation (SNV, *single nucleotide variation*) identifiziert, die in der Entstehung einer potenziellen SMAD3-Bindestelle resultiert und mit einer signifikanten Reduktion der *XYLT1* Promotoraktivität assoziiert ist (Faust *et al.*, 2014).

1.2.3 Zelluläre Lokalisation und Sekretion der XT

Obwohl es sich bei der XT-I und XT-II um intrazelluläre Proteine handelt, ist ein Teil ihrer Enzymaktivität extrazellulär nachweisbar (Pönighaus *et al.*, 2007; Pönighaus *et al.*, 2010). Bei XT-defizienten pgsA-745 *Chinese hamster ovary* (CHO)-Zellen, die mit XT-I-kodierendem Plasmid transfiziert wurden, kann 90% der Gesamt-XT-Aktivität im Zellkulturüberstand nachgewiesen werden (Pönighaus *et al.*, 2010). Die membranständige XT-I wird über einen unbekannten Mechanismus, der die Aktivität einer Cysteinprotease voraussetzt, durch proteolytische Spaltung an der Transmembrandomäne in den Extrazellularraum freigesetzt (Götting *et al.*, 1999; Pönighaus *et al.*, 2010). Aufgrund des fehlenden Donorsubstrats UDP-D-Xylose im Extrazellularraum wird davon ausgegangen, dass die zelluläre Enzymfreisetzung zur Regulation der aktiven Enzymmenge dient (Pönighaus *et al.*, 2010). Die Sekretion der XT ist zelltyp- und organunabhängig und erfolgt simultan mit der Sekretion von CS-PG (Götting *et al.*, 1998; Götting *et al.*, 1999; Pönighaus *et al.*, 2007; Prante *et al.*, 2006; Schön *et al.*, 2006). Der Nachweis der XT-Aktivität ist in verschiedenen humanen Körperflüssigkeiten wie Blut, Samen und Synovialflüssigkeit möglich (Götting *et al.*, 1999; Götting *et al.*, 2002; Kleesiek *et al.*, 1987). Im physiologischen Zustand kann die Serum-XT-Aktivität vornehmlich auf die von Thrombozyten sekretierte XT-II zurückgeführt werden (Condac *et al.*, 2009).

1.2.4 XT-I als Biomarker der Fibrosierung und Gewebsremodellierung

Die zelluläre Sekretion der XT kann in der Labordiagnostik zur Quantifizierung der XT-Aktivität im Blut und in anderen Körperflüssigkeiten verwendet werden, um Rückschlüsse über die PG-Biosyntheserate zu ziehen. Die Fibrosierung der Leber oder des Herzgewebes wurde in vergangenen Studien bereits mit einer erhöhten Serum-XT-Aktivität in Verbindung gebracht (Götting *et al.*, 2005; Kuhn *et al.*, 2009; Prante *et al.*, 2007). In diesem Zusammenhang wurde auch eine Erhöhung der XT-Aktivität im Serum von SSc-Patienten gezeigt, welche mit einem hohen HA-Level korreliert. Patienten, die an der diffusen Form der SSc leiden, zeigten eine höhere Serum-XT-Aktivität als Patienten mit der limitierten Form der SSc (Götting *et al.*, 1999).
In vitro Studien an normalen humanen Dermalfibroblasten (NHDF) und kardialen Fibroblasten zeigten, dass die zelluläre *XYLT1* mRNA-Expression und extrazelluläre XT-Aktivität mit der Zahl differenzierter Fibroblasten und der Proteinexpression des Myofibroblastenmarkers α-Glattmuskelaktin (α-SMA) und der *ACTA2* mRNA-Expression korreliert. Die fibrotische Stimulation wirkte sich dabei nicht auf die relative *XYLT2* mRNA-Expression der Zellen aus (Faust *et al.*, 2013; Prante *et al.*, 2007). Kardiale Fibroblasten, die zyklisch mechanischem Stress ausgesetzt wurden, zeigten ebenfalls eine erhöhte XT-I-Expression und GAG-Synthese (Prante *et al.*, 2007). Demnach steht die *XYLT1* Expression mit einer persistierenden Fibrose im Zusammenhang und kann als Biomarker der Myofibroblastendifferenzierung von *in vitro* kultivierten NHDF herangezogen werden (Faust *et al.*, 2013).

1.3 Zelluläre und molekulare Mechanismen der Fibrose

Die Gewebereparatur stellt einen wichtigen biologischen Prozess dar, bei dem nach einer Gewebsverletzung geschädigten Zellen zunächst durch ECM ersetzt werden. Während der Gewebshomöostase befinden sich die beiden Prozesse Synthese und Abbau der ECM im Gleichgewicht. Während des Wundheilungsprozesses findet eine Verschiebung dieses Gleichgewichtes zugunsten der ECM-Synthese statt. Eine starke Regulation der ECM-Synthese ist erforderlich, um der Entstehung einer Fibrose vorzubeugen (Do und Eming, 2016; Gurtner *et al.*, 2008). Die fibrotische Zellantwort geht mit einer chronischen Inflammation einher und wird durch diverse Stimuli, darunter infektiöse Pathogene, Autoimmunreaktionen, mechanischen Stress und Toxine initiiert (Allanore *et al.*, 2015; Wynn, 2008).

1.3.1 Mediatoren der Wundheilung und Fibrogenese

Die physiologische Antwort auf eine Gewebsschädigung umfasst die temporal überlappenden Phasen Hämostase, Inflammation, Proliferation und Remodellierung. Es sind verschiedene Zelltypen, darunter Blutzellen, Epithelzellen, Bindegewebszellen und Immunzellen involviert (**Abbildung 4**). Neben den zellulären Komponenten sind lösliche Faktoren wie Koagulationsfaktoren, Wachstumsfaktoren und Zytokine an der Wundheilung beteiligt (Ghatak *et al.*, 2015).

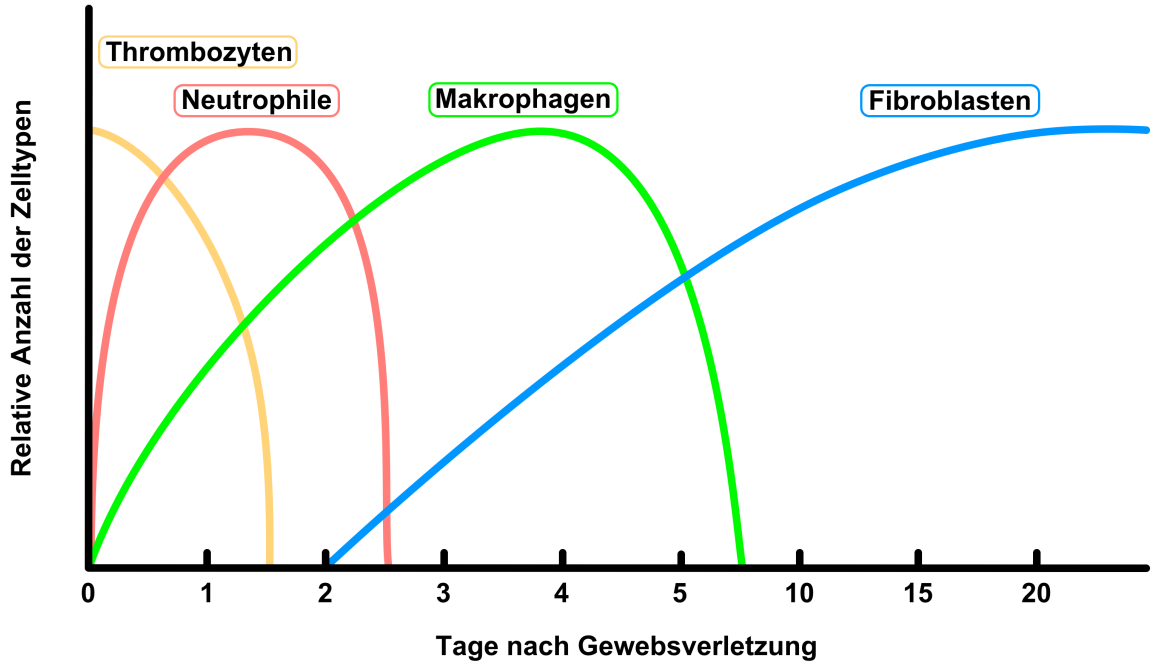

Abbildung 4: Zelluläre Phasen der Wundheilung. Relative Anzahl der verschiedenen zellulären Bestandteile pro Zeiteinheit (modifiziert nach Ramasastry, 2005).

Initial werden bei einem Endothelschaden zirkulierende Thrombozyten aktiviert und ein Fibringerinnsel ausgebildet, das als provisorische Matrix dient (Gauglitz *et al.*, 2011). Hierin können Keratinozyten, Immunzellen und Fibroblasten migrieren. Neben der Aktivierung der Koagulationskaskade setzen Thrombozyten inflammatorische Mediatoren wie Chemokine und Interleukine (IL), darunter IL-8, IL-1β und IL-6 frei, welche Immunzellen des angeborenen Immunsystems wie Neutrophile und Monozyten rekrutieren. Die aktivierten Thrombozyten setzen ebenfalls Wachstumsfaktoren wie den *transforming growth factor-β1* (TGF-β1) frei, der ein fibrogener Wachstumsfaktor ist und die ECM-Synthese von Fibroblasten stimuliert (Barrientos *et al.*, 2008). Die rekrutierten Neutrophilen beteiligen sich an der Beseitigung von Gewebetrümmern

und der Abtötung von eindringenden Bakterien. Des Weiteren sekretieren sie Mediatoren wie das *monocyte chemoattractant protein-1*, IL-1β und IL-6, wodurch weitere Immunzellen angelockt werden. Monozyten differenzieren am Ort des Gewebsschadens zu Makrophagen, welche das Fibringerinnsel und Zelltrümmer phagozytieren (Ellis *et al.*, 2018; Wynn und Ramalingam, 2012). Bei einer Gewebsverletzung wird ebenfalls zelluläres Material, wie DNA, RNA, Adenosintriphosphat (ATP) und HA freigesetzt (Mack, 2018), das die Produktion von Chemokinen und pro-inflammatorischen Zytokinen durch Monozyten und Makrophagen stimuliert (Li *et al.*, 2011). Darüber hinaus sorgen die Moleküle zusammen mit *interferon-γ* (INF-γ), das von rekrutierten natürlichen Killerzellen sezerniert wird, für die Polarisierung von Makrophagen zu einem M1-Phänotyp. Dieser pro-inflammatorische Phänotyp zeichnet sich unter anderem durch die Sekretion von IL-1β, IL-6 und *tumor necrosis factor-α* (TNF-α) aus (Ellis *et al.*, 2018). Obwohl die Rekrutierung der Monozyten und Neutrophilen für den Wundheilungsprozess essentiell ist, sezernieren diese Zellen eine Vielzahl an toxischen Mediatoren, mitunter reaktive Sauerstoff- und Stickstoffspezies, die das umliegende Gewebe schädigen. Ein wichtiger Schritt für die Termination der initialen Inflammation stellt die Phagozytose von apoptotischen Neutrophilen durch Makrophagen dar (Ellis *et al.*, 2018).

Unter physiologischen Bedingungen werden Zelltrümmer und apoptotische Zellen innerhalb von 48 h bis 72 h entfernt und der Wundheilungsprozess geht in die Proliferationsphase über (Gauglitz *et al.*, 2011). In dieser Phase der Wundheilung verändern Makrophagen ihren pro-inflammatorischen M1-Phänotyp zu einem anti-inflammatorischen M2-Phänotypen, der Fibroblasten stimuliert und die Gewebsregeneration vermittelt (Mosser und Edwards, 2008). M2-Makrophagen produzieren anti-inflammatorische Moleküle wie den IL-1-Rezeptorantagonisten, aber auch Wachstumsfaktoren der TGF-β-Superfamilie, wie TGF-β1 und Activin A, welche die ECM-Synthese vermitteln. Zellen des adaptiven Immunsystems wie T-Lymphozyten wandern verstärkt in die Wunde ein. Diese CD4-positive Helfer-T (T_H)-Zellen lassen sich in Typ 1 (T_H1)- und Typ 2 (T_H2)-Zellen einteilen. T_H1-Zellen sezernieren ein hohes Level an TNF-α und INF-γ, während T_H2-Zellen unter anderem IL-4, IL-13 und Activin A produzieren und die Fibroblastenaktivierung vermitteln (Antsiferova und Werner, 2012; Gauglitz *et al.*, 2011; Ogawa *et al.*, 2006).

Die Remodellierungsphase des Wundheilungsprozesses beginnt einige Wochen nach der Gewebsverletzung und kann bis zu einem Jahr andauern (Ellis *et al.*, 2018). Die in

den ersten Wundheilungsphasen ausgeschütteten Mediatoren aus den Thrombozyten, dem geschädigten Gewebe und den rekrutierten Immunzellen führen zur Fibroblastenaktivierung und Differenzierung zu Myofibroblasten (Borthwick *et al.*, 2013). Der Phänotyp dieser Zellen zeichnet sich durch die Expressionserhöhung des α-SMA und der XT-I aus (Faust *et al.*, 2013; Hinz, 2007). Myofibroblasten synthetisieren ECM-Proteine wie Prokollagene, Fibronektin, HA sowie PG und bilden das Granulationsgewebe aus. Dieses dient als Ersatz für die provisorische Fibrinmatrix und unterstützt weitere Zellmigrationen. Durch ihren kontraktilen Phänotyp initiieren Myofibroblasten die Wundkontraktion (Do und Eming, 2016; Hinz, 2007). Unter physiologischen Bedingungen werden die Myofibroblasten nach dem Wundverschluss apoptotisch (Darby und Hewitson, 2007) und die akkumulierenden ECM-Proteine werden durch Metalloproteasen abgebaut (Friedman *et al.*, 2013). In der Anwesenheit von chronischen inflammatorischen Stimuli und profibrotischen Faktoren persistieren die Myofibroblasten und die Prozesse der Gewebsregeneration bleiben bestehen. Es kommt zu einer exzessiven Akkumulation von Myofibroblasten und ECM-Komponenten, dem Charakteristikum fibrotischer Erkrankungen. Die Fibrose kann demnach auf eine gestörte Balance der Zytokin-vermittelten Synthese und Degradation von Komponenten der ECM zurückgeführt werden (Sticherling, 2012).

1.3.2 TGF-β-Signaltransduktionsweg

Der TGF-β-Signaltransduktionsweg ist ein wichtiger Teil der Fibrogenese, da er die Myofibroblastendifferenzierung vermittelt (Allanore *et al.*, 2015). Die TGF-β-Superfamilie besteht aus evolutionär konservierten Polypeptiden, darunter TGF-β1 und Activin A. Bei den TGF-β-Rezeptoren handelt es sich um Serin/Threonin-Kinase-Rezeptoren, welche in Typ I-, Typ II- und Typ III-Rezeptoren eingeteilt werden. Activin A bindet an den *activin A receptor type-IB* (ACVR1B), der auch als *activin receptor-like kinase 4* (ALK) bezeichnet wird, während TGF-β1 an den *transforming growth factor beta receptor 1* (TGFBR), auch ALK5 genannt, bindet. Nach Ligandenbindung an ein Typ-II-Rezeptordimer (TGFBR2/ACVR2A,B) wird ein Typ-I-Rezeptordimer rekrutiert. Nach Bildung des heterotetrameren Ligand-Rezeptor-Komplexes werden die Typ-I-Rezeptoren durch Typ-II-Rezeptor-vermittelte Phosphorylierung aktiviert (Antsiferova und Werner, 2012; Mishra *et al.*, 2014; Yamashita, 2004).

Die Ligandenbindung an die Oberflächenrezeptoren führt *downstream* zur Aktivierung zahlreicher Signaltransduktionskaskaden. Ein involvierter Signalweg ist der

kanonische *small mothers against decapentaplegic* (SMAD)-Signalweg. Der aktivierte Typ-1-Rezeptor phosphoryliert Rezeptor-aktivierte SMAD (R-SMAD)-Proteine. *Downstream* von TGF-β und Activin A werden die beiden Proteine SMAD2 und SMAD3 aktiviert. Diese bestehen aus zwei *Mad-homology* (MH)-Domänen und einer Linkerregion. Die *N*-terminale MH1-Domäne besitzt DNA-Bindungskapazitäten, während die *C*-terminale MH2-Domäne die Bindungen an Proteine vermittelt (Massagué und Chen, 2000). Die phosphorylierten R-SMAD-Proteine bilden mit dem Co-SMAD, SMAD4, einen heteromeren Komplex aus. Dieser kann in den Nukleus translozieren und als Transkriptionsfaktor (TF) wirken. Die SMAD-vermittelte Transkriptionsregulation erfolgt entweder direkt über DNA-Bindung oder indirekt über die Bindung anderer TF (Ihn, 2008). Der SMAD-Signalweg wird durch verschiedene Faktoren sowohl positiv als auch negativ reguliert. Negative Regulatoren des SMAD-Signalwegs stellen inhibitorische SMAD (I-SMAD)-Proteine dar. I-SMAD-Proteine, wie SMAD7, binden an den Typ-I-Rezeptor und verhindern dadurch die Phosphorylierung von R-SMAD-Proteinen (Yan und Chen, 2011). Eine positive Regulation des SMAD-Signalwegs kann über die Phosphorylierung der SMAD2-Linkerregion durch Proteinkinasen vermittelt werden (Rostam *et al.*, 2016). In Bezug auf die Transkriptionsregulation von ECM-Genen existieren jedoch wenige direkte SMAD-Zielgene. Für die Regulation der Fibronektin-Expression durch TGF-β wurde beispielsweise ein SMAD-unabhängiger Mechanismus gezeigt (Hocevar, 1999). Neben dem SMAD-Signalweg sind demnach alternative Signalwege im fibrotischen Geschehen von Relevanz. Activin A und TGF-β1 aktivieren unter anderem den *mitogen-activated protein kinase* (MAPK)-Signalweg (Hu *et al.*, 2016; Yan und Chen, 2011). Der MAPK-Signalweg wird über die *extracellular signal-regulated kinase* (ERK), die MAPK p38 und c-*Jun N-terminal kinase* (JNK) vermittelt (Derynck und Zhang, 2003). Die phosphorylierte JNK aktiviert das Onkogen c-Jun, das als Homo- oder Heterodimer den TF Aktivatorprotein-1 (AP-1) bildet (Papachristou *et al.*, 2003). AP-1-Bindestellen kommen auch im *XYLT1* Promotor vor (Faust *et al.*, 2014; Müller *et al.*, 2009).

1.3.3 Epigenetische Veränderungen und microRNAs

Fibroblasten, die aus einem fibrotischen Gewebe entnommen wurden, zeigen auch *in vitro* einen aktivierten Phänotyp, der durch eine erhöhte Expression von kontrakti-

len Fasern und ECM-Proteinen gekennzeichnet ist. Die stabile Expression dieses zellulären Phänotyps ist unter anderem auf epigenetische Modifikationen zurückzuführen, die in Folge einer profibrotischen Umgebung entstehen. Neben der DNA-Methylierung und Histonmodifikation zählen nicht-kodierende RNAs, zu denen microRNAs (miRNA) gehören, zu epigenetischen Veränderungen, die mit fibrotischen Veränderungen assoziiert werden (Distler *et al.*, 2019).

Als miRNAs werden nicht-kodierende RNA-Moleküle bezeichnet, die eine Länge von 20-25 Nukleotiden besitzen. Sie regulieren die Genexpression auf der post-transkriptionalen Ebene, indem sie die Ziel-mRNAs über die 3'-untranslatierte Region (3'-UTR) des mRNA-Transkripts binden. Je nach Komplementarität der miRNA-mRNA-Bindesequenz wird entweder der mRNA-Abbau vermittelt oder die Translation der mRNA gehemmt (Liu *et al.*, 2016; O'Reilly, 2016). Die miRNA-21-5p (miRNA-21) ist eine dieser Fibrose-assoziierten miRNAs. Eine erhöhte Expression der miRNA-21 wurde im murinen Fibrosemodell und in primären SSc-Fibroblasten (SScF) gezeigt. Die miRNA-21 verstärkt den kanonischen TGF-β-Signalweg, indem sie nach TGF-β1-Induktion die *SMAD7* Expression supprimiert (Zhu *et al.*, 2013a). Eine Expressionserhöhung der miRNA-145-5p (miRNA-145) wurde ebenfalls nach TGF-β-Supplementation von humanen dermalen und kornealen Fibroblasten gezeigt. Hierbei steht die fibrotische miRNA-145-Induktion mit dem Expressionsanstieg des Myofibroblastenmarkers α-SMA im Zusammenhang (Gras *et al.*, 2015; Ratuszny *et al.*, 2015). Eine andere Fibrose-assoziierte miRNA ist die miRNA-29b-3p (miRNA-29b). Im Gegensatz zur miRNA-21 und -145 ist die miRNA-29b eine antifibrotische miRNA, welche die Translation verschiedener Gene für Enzyme der ECM-Remodellierung und Kollagen inhibiert (Riedel *et al.*, 2018). Das Expressionslevel der miRNA-29b ist bei fibrotischen Erkrankungen wie der SSc, der kardialen oder der pulmonalen Fibrose erniedrigt (Cushing *et al.*, 2011; Maurer *et al.*, 2010; van Rooij *et al.*, 2008). Die supprimierte miRNA-29b-Expression steht hierbei ebenfalls im engen Zusammenhang mit einer dysregulierten TGF-β-Signaltransduktion (Maurer *et al.*, 2010). Eine indirekte miRNA-29b-vermittelte Regulation der *XYLT1* mRNA-Expression und XT-Aktivität in NHDF ist bekannt (Riedel *et al.*, 2018).

1.4 Systemische Sklerodermie

Die SSc ist eine chronisch inflammatorische Multiorganerkrankung, die durch Fibrosen der Haut und inneren Organe gekennzeichnet ist, und mit einer Prävalenz

von 7,2–33,9 auf 100 000 Individuen pro Jahr in Europa als selten eingestuft wird (Sticherling, 2012). Bei dieser Erkrankung sind Frauen etwa drei Mal häufiger betroffen als Männer (Allanore *et al.*, 2015; Bergamasco *et al.*, 2019). Neben der Haut sind Herz, Niere und Lunge die hauptsächlich betroffenen Organe (Domsic *et al.*, 2011; Rodnan, 1962). Das klinische Krankheitsbild lässt sich in die Formen der limitierten kutanen und der diffusen SSc differenzieren. Diese Unterscheidung erfolgt anhand der Hautbeteiligung des Patienten. Bei der limitierten kutanen Form beschränkt sich die dermale Fibrose auf die Finger, das Gesicht und die distalen Extremitäten, während bei der diffusen SSc ebenfalls der Rumpf und die proximalen Extremitäten betroffen sind (LeRoy *et al.*, 1988; LeRoy und Medsger, 2001). Der serologische Nachweis antinukleärer Antikörper stellt ein Mittel zur Diagnose und Klassifizierung der SSc dar. Der Nachweis von Anti-Zentromer-, Anti-Scl-70/Topoisomerase-1- und Anti-RNA-Polymerase-III-Antikörpern gilt nach den Richtlinien der *European league against rheumatism* von 2013 als anerkannter Diagnoseparameter der SSc (van den Hoogen *et al.*, 2013).

1.4.1 Pathogenese der systemischen Sklerodermie

Bei der SSc sind das Blutgefäßsystem, das Bindegewebe und das Immunsystem involviert. Die Ursachen der SSc sind vielschichtig und konnten noch nicht abschließend geklärt werden (Grossman *et al.*, 2011; Pattanaik *et al.*, 2015). Eine genetische Prädisposition trägt zur Entstehung der SSc bei (Angiolilli *et al.*, 2018; Murdaca *et al.*, 2016). Hierbei konnten SNV in den kodierenden Genen verschiedener Zytokine und Mediatoren nachgewiesen werden (Abtahi *et al.*, 2015; Xu *et al.*, 2019). Des Weiteren werden verschiedene Infektionen als Auslöser der SSc vermutet. Basierend auf dem bei der SSc vorliegenden erhöhten Antikörpertiter gegen Bakterien und Viren wird das Phänomen des molekularen Mimikri mit der Induktion von Autoimmunantworten diskutiert (Grossman *et al.*, 2011). Autoantikörper gegen endotheliale Zellen halten die chronische Gewebsverletzung aufrecht und begünstigen die Persistenz von Myofibroblasten (Abraham und Distler, 2007; Ho *et al.*, 2014). Verschiedene Umweltexpositionen gegenüber organischen Lösungsmitteln und Silica werden ebenfalls als beteiligte Auslöser der SSc angenommen (Magnant *et al.*, 2005).

Die beschriebenen Faktoren führen zu mikrovaskulären Verletzungen, Endothelzellaktivierung und -apoptose, welche als primäre Ereignisse bei der SSc angesehen werden. Hieraus folgen Gefäßschäden, die Aktivierung von Thrombozyten sowie die

Rekrutierung von Immunzellen. Erhöhte Serumkonzentrationen von Activin A, IL-1β, -4, -6 und -13 wurden bei SSc detektiert (Kurzinski und Torok, 2011; Ogawa *et al.*, 2006; Takagi *et al.*, 2011; Xu *et al.*, 2019). In diesem Zusammenhang wurde gezeigt, dass das Inflammasom eine zentrale Rolle in der Pathogenese der SSc einnimmt. Hierbei handelt es sich um zytosolische Multiproteinkomplexe, die in Immunzellen aber auch Fibroblasten vorkommen. Die Sekretion von IL-1β durch Immunzellen und Fibroblasten setzt die proteolytische Spaltung durch das Inflammasom voraus (Artlett, 2013; Henderson *et al.*, 2018; Xu *et al.*, 2019).

Durch die sezernierten Mediatoren wird eine fibrogene Wundheilungsantwort eingeleitet, die zu einer Akkumulation von Myofibroblasten und ECM führt (Darby und Hewitson, 2007; Henderson *et al.*, 2018). Die Myofibroblasten sorgen durch auto- und parakrine Prozesse sowie Interaktion mit der fibrotischen ECM-Umgebung für die Progression der Fibrose (Allanore *et al.*, 2015). Die profibrotische Umgebung induziert demnach Veränderungen im miRNA-Expressionsniveau der Zellen, wodurch der aktivierte Phänotyp der Zellen stabilisiert wird (Distler *et al.*, 2019). Unterschiede zwischen NHDF und SScF werden nicht nur beim Vergleich der miRNA-Expressionsprofile sichtbar, sondern auch beim Vergleich der Expression von Komponenten intrazellulärer Signalkaskaden (Ihn, 2008; Kubo *et al.*, 2002; Zhu *et al.*, 2012).

1.5 Therapeutisches Potenzial und Charakterisierung von Naturstoffen

Als Naturstoffe werden isolierte oder synthetisierte Moleküle bezeichnet, die natürlich vorkommen oder ein strukturelles Äquivalent physiologisch gebildeter Verbindungen nativer Organismen darstellen (Firn, 2010). Sie zeichnen sich durch eine hohe chemische Diversität und strukturelle Komplexität aus und können als Ausgangsverbindung für die Entwicklung synthetischer Verbindungen dienen. Zu den ältesten bekannten Naturstoffen, die in der medizinischen Anwendung vorkommen, zählen mikrobielle Antibiotika (Zhang, 2005). Strukturell können verschiedene Antibiotikaklassen, darunter β-Lactame, Tetrazykline und Makrolide, unterschieden werden (Harvey *et al.*, 2015). Neben der antimikrobiellen Wirksamkeit einzelner Naturstoffe existieren auch Naturstoffe mit antikanzerogenen, anti-inflammatorischen und/oder antifibrotischen Effekten (Chen *et al.*, 2018a, Chen *et al.*, 2018b). Mit Ausnahme von Peptiden und Kohlenhydraten sind Isoprenoide, Terpenoide, Polyphenole, Phenylpropanoide, Polyketide, Alkaloide und Glukosinolate die wichtigsten Naturstoffe (Firn, 2010).

Da Naturstoffe häufig eine wichtige Quelle für die Entwicklung von Medikamenten sind, existieren Naturstoffbibliotheken, die in der Wirkstoffentwicklung in Hochdurchsatzverfahren zur Wirkstofffindung eingesetzt werden können. Neben Rohextrakt-Bibliotheken und Bibliotheken mit Naturstoff-Fraktionen gibt es Molekülbibliotheken mit reinen Naturstoffen (Wilson *et al.*, 2020). In der Wirkstoffentwicklung ist die Quantifizierung der Enzymaktivität in Zellen und humanen Körperflüssigkeiten zur Charakterisierung der Krankheitspathologie und Bestimmung der Wirkung von Enzyminhibitoren relevant (Copeland *et al.*, 2007). Zur Wirkstofffindung können neben der reinen biochemischen Analytik unter Verwendung von isolierten Enzymlösungen zellbasierte Experimente durchgeführt werden (Wilson *et al.*, 2020).

Um den Wirkmechanismus experimentell identifizierter Wirkstoffe zu charakterisieren, werden neben Datenbankanalysen molekulare Docking-Analysen durchgeführt (Trott und Olson, 2009; Xie, 2010). Hierbei handelt es sich um eine *in silico* Analyse der Protein-Ligand-Wechselwirkungen, die auch zur Leitstrukturcharakterisierung und Optimierung genutzt wird. Ein solches freizugängliches Analyseprogramm ist AutoDock Vina (Trott und Olson, 2009), das im Visualisierungsprogramm UCSF Chimera implementiert ist (Pettersen *et al.*, 2004). Voraussetzung dieser *in silico* Analytik ist die Verfügbarkeit der Proteinstruktur, z. B. aus Proteinkristallisation und Röntgenstrukturanalyse. Die Strukturdaten können von Proteindatenbanken im PDB-Format bezogen und in Grafikprogrammen wie UCSF Chimera dargestellt werden (Berman, 2000). Die räumliche Struktur benötigter Liganden steht ebenfalls über Datenbanken zur Verfügung (Pence und Williams, 2010). Die meisten Dockingprogramme verwenden eine Scoring-Funktion, welche das chemische Potenzial des Systems erfasst. Um die bevorzugte Bindungsposition des Liganden innerhalb des Apoproteins zu bestimmen, wird zunächst ein „Suchraum“ im Apoprotein/Rezeptor festgelegt. Hierbei wird das Protein als starr und die Liganden als flexible Moleküle angenommen. Der Algorithmus von AutoDock Vina berechnet anschließend die möglichen Docking-Positionen des Liganden innerhalb des definierten Rezeptors. Eine exakte Bestimmung der freien Bindungsenergien ist mit AutoDock Vina nicht möglich, da lediglich ein relativer Vergleich der verschiedenen Bindungsmodi durchgeführt wird (Trott und Olson, 2009). In dieser Arbeit wurde AutoDock Vina zur Visualisierung potenzieller Ligandenbindungsseiten innerhalb des XT-I-Proteins sowie zur Bestätigung experimenteller Resultate herangezogen (Ly *et al.*, 2020a).

2 Zielsetzung dieser Arbeit

Die SSc ist eine prototypische fibrotische Erkrankung, die durch eine Akkumulation von ECM-produzierenden Myofibroblasten gekennzeichnet ist. Die pathologische Fibroblastenaktivierung bei der SSc gilt daher als wichtiger Angriffspunkt für die therapeutische Intervention (Distler *et al.*, 2019; Ihn, 2008). Einer von mehreren Markern der Myofibroblastendifferenzierung ist die XT-I, deren erhöhte Serumaktivität bei SSc-Patienten nachgewiesen wurde (Faust *et al.*, 2019; Götting *et al.*, 1999). In der vorliegenden Arbeit sollten unterschiedliche Aspekte der Regulation der XT-I bei Fibrosen untersucht werden, um das Verständnis der pathophysiologischen Relevanz der XT-I bei der SSc zu vertiefen.

2.1 Identifizierung von XT-I-Mediatoren in der Fibrogenese

Die gesteigerte Aktivität und Expression profibrotischer Mediatoren begünstigt die im Rahmen einer Fibrose persistierende Fibroblastenaktivierung und übermäßige ECM-Produktion (Borthwick *et al.*, 2013). In diesem Teilprojekt sollten Fibrose-assoziierte biochemische Mediatoren wie Zytokine und miRNAs hinsichtlich ihrer XT-I induktiven Wirkung in NHDF untersucht werden. Hierbei sollten gegebenenfalls regulative Unterschiede zwischen den beiden XT-Isoformen untersucht und die zugrundeliegenden zellulären Signalwege ermittelt werden.

2.2 Charakterisierung der XT-I als zellulärer Biomarker der SSc

Die Arbeit von Condac *et al.* zeigte, dass die XT-II die dominierende XT-Isoform im Serum ist und vornehmlich aus Plättchen sekretiert wird (Condac *et al.*, 2009). Für die Einordnung der XT-I als validen SSc-Biomarker fehlen die zellulären Grundlagen der erhöhten XT-Serumaktivität. Daher sollte untersucht werden, ob die erhöhte XT-Serumaktivität einer potenziellen Induktion der zellulären XT-I Aktivität und *XYLT1* mRNA-Expression in SScF unterliegt. Sollte sich die XT-I als valider Fibrosemarker bei SSc herausstellen, kann das Zellkulturmodell mit SScF zur Bestätigung identifizierter molekularer Mechanismen herangezogen werden.

2.3 Identifizierung von nicht-substratbasierten XT-I-Inhibitoren

Im Hinblick auf die Entwicklung neuer therapeutische Ansätze gegen Fibrosen bestand das Ziel dieses Teilprojektes in der Identifizierung von XT-I inhibierenden Molekülen. Ein Augenmerk sollte dabei auf Molekülklassen liegen, die keine strukturelle Verwandtschaft zu den Substraten und Endprodukten der XT-I-katalysierten Enzymreaktion aufweisen. Naturstoffe weisen eine hohe strukturelle Diversität und biologische Aktivität auf und gelten daher als wichtige Rohstoffe für die Entwicklung neuer Medikamente (Kim *et al.*, 2016). Demnach sollte in diesem Teilprojekt eine kommerziell erhältliche Molekülbibliothek verwendet werden, die 96 membrangängige Verbindungen aus der Molekülklasse der Naturstoffe umfasst.

3 Übersicht zu den Publikationen mit eigenem Beitrag

Die vorliegende kumulative Dissertation beinhaltet eine zusammengefasste Darstellung der Forschungsresultate, die in den nachfolgend dargestellten Fachzeitschriften veröffentlicht oder zur Veröffentlichung eingereicht wurden:

Publikation I (P1) Ly, T.-D., Plümers, R., Fischer, B., Schmidt, V., Hendig, D., Kuhn, J., Knabbe, C. und Faust, I. (2020b). Activin A-mediated regulation of XT-I in human skin fibroblasts. *Biomolecules*, 10(4), 609. doi: 10.3390/biom10040609

Publikation II (P2) Ly, T.-D.; Kleine, A.; Plümers, R.; Fischer, B.; Schmidt, V.; Hendig, D.; Distler, H. W. J.; Kuhn, J.; Knabbe, C.; Faust, I. (eingereicht). Cytokine-mediated induction of human xylosyltransferase-I in systemic sclerosis skin fibroblasts. *Biochemical and Biophysical Research Communications*

Publikation III (P3) Ly, T.-D., Riedel, L., Fischer, B., Schmidt, V., Hendig, D., Distler, J., Kuhn, J., Knabbe, C. und Faust, I. (2020c). MicroRNA-145 mediates xylosyltransferase-I induction in myofibroblasts via suppression of transcription factor KLF4. *Biochemical and Biophysical Research Communications*, 523(4), 1001–1006. doi: 10.1016/j.bbrc.2019.12.120

Publikation IV (P4) Ly, T.-D., Kleine, A., Fischer, B., Schmidt, V., Hendig, D., Kuhn, J., Knabbe, C. und Faust, I. (2020a). Identification of putative non-substrate-based XT-I inhibitors by natural product library screening. *Biomolecules*, 10(10), 1467. doi: 10.3390/biom10101467

Die verwendete Nummerierung der Publikationen entspricht nicht der zeitlichen Abfolge der Veröffentlichungen, sondern der in Kapitel 4 aufgeführten Reihenfolge der Publikationen.

3.1 Publikation I

Activin A-vermittelte Regulation der XT-I in humanen Hautfibroblasten

(Ly *et al.*, 2020b)

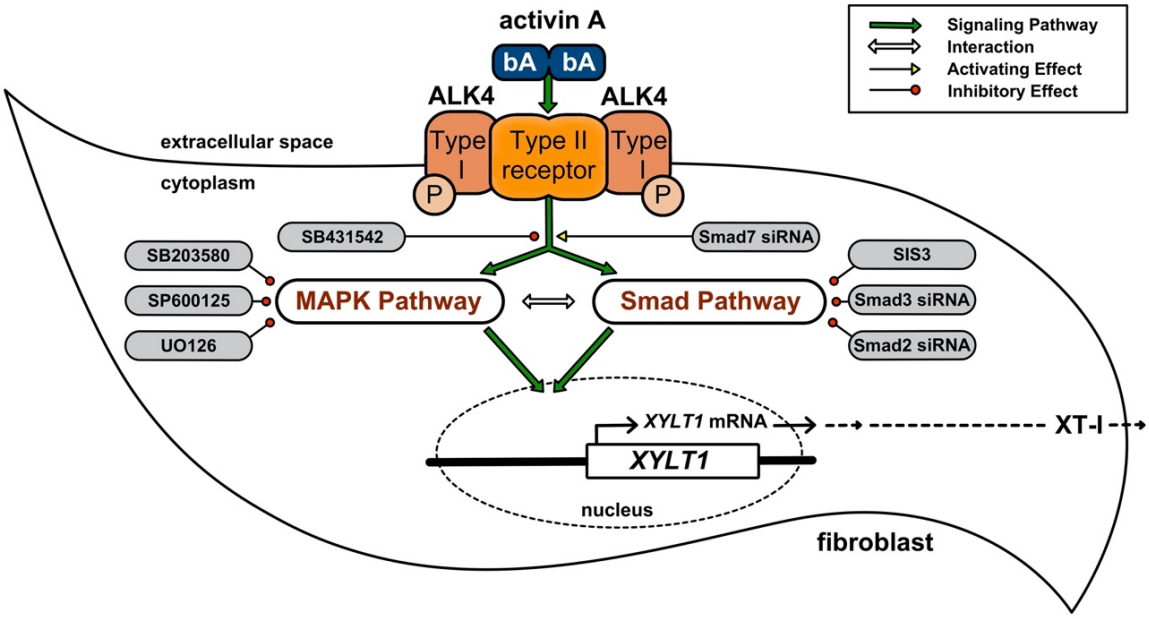

Abbildung 5: *Graphical Abstract* von Publikation I (Ly *et al.*, 2020b).

biomolecules

MDPI

Article

Activin A-Mediated Regulation of XT-I in Human Skin Fibroblasts

Thanh-Diep Ly, Ricarda Plümers, Bastian Fischer, Vanessa Schmidt, Doris Hendig, Joachim Kuhn, Cornelius Knabbe and Isabel Faust *

Institut für Laboratoriums- und Transfusionsmedizin, Herz- und Diabeteszentrum NRW, Universitätsklinik der Ruhr-Universität Bochum, Georgstraße 11, 32545 Bad Oeynhausen, Germany

* Correspondence: ifaust@hdz-nrw.de; Tel.: (+49)-5731-97-1234

Received: 9 March 2020; Accepted: 13 April 2020; Published: 14 April 2020

Abstract: Fibrosis is a fundamental feature of systemic sclerosis (SSc) and is characterized by excessive accumulation of extracellular matrix components like proteoglycans (PG) or collagens in skin and internal organs. Serum analysis from SSc patients showed an increase in the enzyme activity of xylosyltransferase (XT), the initial enzyme in PG biosynthesis. There are two distinct XT isoforms—XT-I and XT-II—in humans, but until now only XT-I is associated with fibrotic remodelling for an unknown reason. The aim of this study was to identify new XT mediators and clarify the underlying mechanisms, in view of developing putative therapeutic anti-fibrotic interventions in the future. Therefore, we used different cytokines and growth factors, small molecule inhibitors as well as small interfering RNAs, and assessed the cellular XT activity and *XYLT1* expression in primary human dermal fibroblasts by radiochemical activity assays and qRT-PCR. We identified a new function of activin A as a regulator of *XYLT1* mRNA expression and XT activity. While the activin A-induced XT-I increase was found to be mediated by activin A receptor type 1B, MAPK and Smad pathways, the activin A treatment did not alter the *XYLT2* expression. Furthermore, we observed a reciprocal regulation of *XYLT1* and *XYLT2* transcription after inhibition of the activin A pathway components. These results improve the understanding of the differential expression regulation of *XYLT* isoforms under pathological fibroproliferative conditions.

Keywords: activin A; fibrosis; MAPK; proteoglycan; Smad; systemic sclerosis; xylosyltransferase

1. Introduction

The skin is the largest organ in the human body and provides a protective barrier against microorganisms, injuries and water loss [1]. Approximately 70% of its dry weight is formed by the extracellular matrix (ECM) [2]. The synthesis, deposition and remodelling of the ECM is critical for the maintenance of tissue homoeostasis under physiological conditions. Despite being strongly regulated, disturbances of these processes can result in severe pathological diseases, such as hypertrophic scarring, scleroderma and fibrosis induced by surgery, radiotherapy or medication [3].

The hallmark of these fibroproliferative conditions is the activation and differentiation of fibroblasts into myofibroblasts due to physical or inflammatory insults. These cells secrete vast amounts of ECM proteins that accumulate in the tissue and impair proper organ function [4]. Furthermore, myofibroblasts are engaged in paracrine and autocrine interactions with their surrounding environment by secretion of growth factors and cytokines like activin A and transforming growth factor β1 (TGFβ1), which are increased in many tissues during fibrosis [5–7].

Though activin A and TGFβ1 belong to the TGFβ superfamily and provide structural similarities, activin A is secreted as an active protein, whereas TGFβ1 is secreted as an inactive precursor and requires activation [8,9]. Activin A plays a crucial role in wound healing and inflammation, therefore

providing a critical link between the process of inflammation and fibrotic response in systemic sclerosis (SSc), the prototype of fibrotic skin diseases [10–12]. Activin A production is stimulated by several pro-fibrotic mediators, including TGFβ1, interleukins (IL), endothelin-I, angiotensin-II and thrombin [6,13,14]. To promote fibroblast differentiation into myofibroblasts, exogenous activin A signals through combined type I and type II transmembrane kinase receptors, known as activin A receptor type 1B (ACVR1B) or activin receptor-like kinase 4 (ALK4) and ACVR2A or ACVR2B, which are shared by other TGFβ ligands, such as myostatin, nodal and growth and differentiation factor 11 [12,15]. In all instances, ligand complex formation leads to phosphorylation and activation of intrinsic receptor kinase domains, which facilitate phosphorylation cascades. Similar to pro-fibrotic core mediator TGFβ1, activin A mediates cellular responses via transcription factors mothers against decapentaplegic homolog 2/3 (Smad2/3)-dependent and non-canonical, Smad-independent signalling pathways, which involve the phosphorylation of the mitogen-activated protein kinases (MAPK) p38 MAPK, extracellular signal-regulated kinase (ERK) or c-Jun N-terminal kinase (JNK) in a cell type and cytokine-specific manner [16–18]. The activation of both the canonical as well as non-canonical signalling pathway has been demonstrated to be involved in fibrogenic changes [13,16,19].

Like TGFβ1, activin A has a high affinity for the ECM by binding to heparin-sulphated proteoglycans (PG), such as perlecan, which are highly up-regulated in many human fibrotic conditions, including SSc [10,16,20]. The biological roles of PGs are related to their negatively charged glycosaminoglycan (GAG) chains that were post-translationally attached to the PG core proteins [20]. The formation of these GAG chains is initiated by xylosylation of specific serine units on preformed PG core proteins by the rate-limiting enzymes xylosyltransferase-I (XT-I) and -II (XT-II) (EC 2.4.2.26) [21].

The human XT-I and XT-II are type II transmembrane proteins, which are encoded by the genes *XYLT1* and *XYLT2*. Besides their similarities regarding enzyme function, their genes are differentially expressed in tissues [22,23]. Despite the intracellular localisation of the XT-I, the enzyme is shed from the membrane of the Golgi apparatus by an unknown mechanism that involves a cysteine protease [24]. The XT activity can be measured in the human serum and provides a reliable indicator for the present rate of PG biosynthesis and is a useful serum biomarker for the assessment of fibrotic processes in patients with SSc [25]. Additional studies using human primary fibroblasts as key players of ECM remodelling and tissue repair, have shown that *XYLT1* mRNA expression und extracellular XT activity correlates with the content of differentiated myofibroblasts measured by former myofibroblast marker α-smooth muscle actin (α-SMA) or expression of *ACTA2*. Furthermore, TGFβ1 treatment of this cells leads to an increase in *XYLT1* expression and XT activity while *XYLT2* expression is unchanged after pro-fibrotic stimuli [26]. Therefore, XT-I expression is associated with persisting fibrosis and can be used as a myofibroblast differentiation marker [26,27]. However, little is known regarding the differential expressional regulation of both XT isoforms. Promoter analysis of XT-I revealed several transcription factor-binding sites for specificity protein 1 (SP1), early growth response factors (EGR) and Krueppel-like transcription factors (KLF), while the *XYLT2* promoter provides binding sites for SP1 family members. Interestingly, sequence analysis of the genomic DNA of 100 healthy blood donors revealed one single nucleotide variant (SNV), c.-1088C>A, in the *XYLT1* promoter region with an allele frequency of 38% that significantly reduced basal promoter activity by generation of a potential Smad3 binding site, but did not contribute to the measured serum XT activity of the donors [28–30].

Giving the missing link between *XYLT1* promoter analysis, identified transcription factors and the upstream cellular signalling mediating XT-I expression under fibrotic conditions, primary fibroblast cells provide a suitable model to study the relationship between exogenous pro-fibrotic stimuli and the underlying signal transduction pathways, which mediate the XT-I expression in PG biosynthesis and dermal myofibroblast differentiation.

2. Materials and Methods

2.1. Cell Culture

Adult normal human dermal fibroblasts (NHDF) from 37- to 50-year-old women and 45- to 57-year-old men were obtained from Genlantis (San Diego, CA, USA), Cambrex (Walkerville, MI, USA) and Coriell (Camden, NJ, USA). NHDF were maintained as monolayer cultures in 100 mm × 20 mm cell culture dishes with Dulbecco's modified Eagle's medium (DMEM; Thermo Fisher Scientific, San Diego, CA, USA) supplemented with 10% (v/v) foetal calf serum (Biowest, Nuaillé, France), 4 mmol/L l-glutamine and 100,000 *U*/L penicillin, 100 mg/L streptomycin, 0.25 mg/L amphotericin B (PAN Biotech, Aidenbach, Germany) at 37 °C, 5% CO_2. Cells were used in Passage 4–9, corresponding to a cumulative population doubling levels of 7 to 17. Therefore, primary NHDF were subcultured with an expansion ratio not exceeding 1:3 upon near confluence using 0.05% trypsin (PAN Biotech, Aidenbach, Germany).

2.2. Cytokine and Inhibitor Treatment

To investigate the effect of the cytokines and inhibitors, NHDF were cultured for 24 h before treatment using a formerly established cell culture model [26]. In brief, cells were cultivated with a low density of 50 cells per mm^2 on a hard tissue culture substrate (100 mm × 20 mm dish), promoting their trans-differentiation into proto-myofibroblasts. To avoid the effect of serum and to synchronize the cells, after an incubation time of 24 h fibroblasts were washed with Dulbecco's phosphate-buffered saline (Thermo Fisher, San Diego, CA, USA) and maintained in serum-free DMEM unless otherwise stated. After 24 h, serum-starved cells were treated with 1 µg/L, 10 µg/L or 50 µg/L human recombinant activin A (HumanZyme Inc., Chicago, IL, USA), or 5 µg/L or 10 µg/L human recombinant TGFβ1 for 3, 6, 24, 48 or 120 h. For inhibition studies final inhibitor concentrations of 10 µmol/L or 50 µmol/L SB431542 (Miltenyi Biotec GmbH, Bergisch Gladbach, Germany), 25 µmol/L SP600125, 10 µmol/L UO126, 20 µmol/L SB203580 (Cell Signaling Technology Inc., Danvers, MA, USA) or 10 µmol/L SIS3 (Merck KGaA, Darmstadt, Germany) diluted in serum-free DMEM were used. All inhibitors were dissolved in dimethyl sulfoxide or water and used according to the manufacturer's instructions. Negative controls treated with solvent or vehicle were included for every sampling time. All experiments were performed in biological triplicates per number (*n*) of donor-derived primary cultures.

2.3. Nucleic Acid Extraction and Synthesis of Complementary DNA

Total RNA was extracted from cells using the RNA Spin Blood kit (Machery-Nagel, Düren, Germany) according to the manufacturer's instructions. DNA extraction was performed using the DNA Spin Blood kit (Machery-Nagel, Düren, Germany). The NanoDrop 2000 spectrophotometer (Peqlab Erlangen, Germany) was used for measuring nucleic acid concentrations. An amount of 1 µg of total RNA was reverse transcribed into complementary DNA (cDNA) utilizing the SuperScript II Reverse Transcriptase kit (Thermo Fisher, Waltham, MA, USA) and diluted to 1:10 prior to storage at −20 °C or analysis.

2.4. Real-Time Polymerase Chain Reaction Analysis

Quantitative real-time polymerase chain reaction (qRT-PCR) analysis was performed in triplicate per gene and cDNA sample using 2.5 µL of diluted cDNA and 7.5 µL LightCycler 480 SYBR Green I master mix (Roche, Basel, Switzerland) and gene-specific forward and reverse primers at a final concentration of 0.625 µmol/L. The intron-spanning primer sequences are listed in Table 1. The plate-based real-time PCR amplification, detection and melting curve analysis of generated PCR products were performed using a LightCycler 480 Instrument II system (Roche, Basel, Switzerland). For PCR, 40 cycles of denaturation for 10 s at 95 °C, annealing for 15 s at 59 °C or 63 °C, followed by a thermal dissociation protocol for SYBR green detection was performed. For reaction validation and gene expression analysis the LightCycler 480 Instrument Operator's Manual Software Version

1.5.1 was used (Roche, Basel, Switzerland). The sample mRNA expression normalization was done with an internal control gene index consisting of the geometric mean of the expression level of the housekeeping genes succinate dehydrogenase complex, subunit A, flavoprotein variant (*SDHA*), ribosomal protein L13a (*RPL13A*) and β2-microglobulin (*B2M*). The relative mRNA expressions of the target genes were determined by the comparative delta–delta C_T method considering the PCR efficiency of the gene of interest and the internal control genes [31].

Table 1. Primer sequences and annealing temperatures (T_A) used for qRT-PCR analysis.

Gene	Primers	T_A (°C)	Product Size (bp)
ACTA2	5′-GACCGAATGCAGAAGGAG-3′ 5′-CGGTGGACAATGGAAGG-3′	59	169
B2M	5′-TGTGCTCGCGCTACTCTCTCTT-3′ 5′-CGGATGGATGAAACCCAGACA-3′	59	137
RPL13A	5′-CGGAAGGTGGTGGTCGTA-3′ 5′-CTCGGGAAGGGTTGGTGT-3′	63	165
SDHA	5′-AACTCGCTCTTGGACCTG-3′ 5′-GAGTCGCAGTTCCGATGT-3′	63	177
SMAD2	5′-ACAACAGGCCTTTACAGCTTCT-3′ 5′-GGAGGCAAAACTGGTGTCTCA-3′	63	239
SMAD3	5′-ACCATCCGCATGAGCTTC-3′ 5′-CACTGCAAAGGCCCATTC-3′	63	107
SMAD7	5′-AGATGCTGTGCCTTCCTC-3′ 5′-GTCTTCTCCTCCCAGTATGC-3′	63	135
TGFB1	5′-GCGATACCTCAGCAACC-3′ 5′-ACGCAGCAGTTCTTCTCC-3′	59	331
XYLT1	5′-GAAGCCGTGGTGAATCAG-3′ 5′-CGGTCAGCAAGGAAGTAG-3′	63	281
XYLT2	5′-ACACAGATGACCCGCTTGTGG-3′ 5′-TTGGTGACCCGCAGGTTGTTG-3′	63	139

2.5. Small Interfering RNA Transfection

For targeted gene silencing, small interfering RNA (siRNA) delivery into NHDF was performed by reverse transfection using the Lipofectamine 2000 transfection reagent (Thermo Fisher, San Diego, CA, USA). NHDF were maintained in antibiotic-free medium (2.9×10^5 cells, 60 mm × 50 mm dish) and reverse transfected with the transfection mixture containing one of two separate silencer pre-designed siRNAs targeting Smad2, Smad3, Smad7 or a non-targeting, fluorescently labelled negative control siRNA diluted in Opti-MEM I Reduced Serum Medium (Thermo Fisher, San Diego, CA, USA) to yield a final siRNA concentration of 40–100 nmol/L per well. A total of 24 h post-transfection the siRNA transfection efficiency was monitored by fluorescence microscopy. A transfection efficiency of nearby 100% was considered for data analysis. When compared with negative control siRNA the siRNA that provided the most efficient inhibition per target gene determined via qRT-PCR was used for future experiments. For activin A treatment, transfected cells were serum-starved for 16 h and maintained in activin A-supplemented media for 6 h until cell lysis.

2.6. Radiochemical Xylosyltransferase Activity Assay

The determination of intracellular XT activity from cell lysates and extracellular enzyme activity from cell supernatants was performed by radiochemical determination of the enzyme-catalysed incorporation of UDP-[^{14}C]-d-xylose (PerkinElmer, Foster City, CA, USA) into a silk fibroin acceptor protein as previously described [32]. The quantified disintegrations per minute (dpm) were referred to total DNA sample content and resemble the quantity of incorporated UDP-[^{14}C]-d-xylose, which is proportional to the sample XT activity. For sample preparation of the extracellular XT activity the cell culture supernatant was collected, whereas for intracellular samples the same cell culture monolayer was lysed using 0.75 mL of a Nonidet P-40 (NP-40)-based buffer (50 mM TRIS, 150 mM

NaCl, 1% NP-40, pH 7.8). After sample centrifugation (10,000 × *g*, 10 min at 4 °C), the supernatant was collected and stored at −20 °C until usage. The enzyme activities were measured 48 h and 120 h after cytokine treatment.

2.7. Statistical Analysis

The data are presented as mean values ± standard error of the mean (SEM). Statistical analysis of the variance between the experimental conditions was evaluated by non-parametric two-tailed Mann–Whitney U-tests using GraphPad Prism 7.0 (GraphPad Software, La Jolla, CA, USA) software. The lack of a Gaussian distribution was confirmed by checking normality visually (frequency distribution histogram) as well as by computing the Shapiro–Wilk normality test. The probability (P) values of less than 0.05 were considered as statistically significant. In the figures, the P values are indicated with asterisks and horizontal lines that connect the compared bars. Asterisks directly above the error bars of the treatment group indicate statistical differences between the treatment and control group, respectively.

3. Results

3.1. Identification of Pro-Fibrotic Mediators Regulating XT-I Expression in Fibroblasts

Previous work has demonstrated that TGFβ1 is a potent inducer of the XT-I gene and protein expression in primary human dermal and cardiac fibroblasts [26,27]. We wanted to examine whether other pro-fibrotic cytokines and growth factors are able to modulate *XYLT1* and *XYLT2* mRNA expression of skin fibroblasts. Using a formerly established cell culture model [26], NHDF were incubated with recombinant human TGFβ1 or different cytokines and growth factors (Figure S1). After 48 h of incubation we found significant increased activity and mRNA levels of myofibroblast marker XT-I (5.1 ± 0.9-fold and 4.2 ± 0.9-fold, both $p < 0.0001$; Figure S1A,B) and *ACTA2* mRNA level (2.4 ± 0.9, $p < 0.0001$; Figure S1C) in activin A-treated cells compared to the untreated controls, whereas no changes in *XYLT2* mRNA expression were observed ($p = 0.06$; Figure S1D). We were unable to demonstrate changes in XT activity or *XYLT1* mRNA expression after stimulation of NHDF with connective tissue growth factor (CTGF), angiotensin-II or endothelin-1 and could only show that some of them were able to exert regulatory effects on TGFβ1-induced XT-I expression (Figure S1A,B). The treatment of NHDF with cytokines IL-4, IL-6 or IL-13 alone did not increase *XYLT1* mRNA expression either (Figure S2).

In comparison to TGFβ1 treatment, activin A-mediated *XYLT1* mRNA and XT activity regulation seemed to be less pronounced (7.7 ± 1.3-fold and 5.1 ± 0.9-fold vs. 4.2 ± 0.9-fold and 5.1 ± 0.9-fold, all $p < 0.0001$; Figure S1A,B). For direct comparison of the TGFβ1 and activin A-mediated effects, serum-starved NHDF were treated with the same TGFβ1 and activin A concentration of 10 µg/L and harvested after a short incubation time of 6 h, to minimalize the side effects due to secretion of secondary metabolites and mediators (Figure 1). Activin A treatment significantly increased *XYLT1* expression 2.1 ± 0.3-fold ($p = 0.0018$), whereas treatment with TGFβ1 revealed a 6.9 ± 1.1-fold ($p < 0.0001$) increase of *XYLT1* expression (Figure 1A). In contrast, no stimulating effects ($p = 0.46$) could be observed for *XYLT2* mRNA expression after activin A or TGFβ1 treatment of NHDF (Figure 1B). In order to investigate whether the induction of *TGFB1* transcripts may play a role in activin A-mediated *XYLT1* regulation, the *TGFB1* mRNA expression changes after TGFβ1 and activin A treatment of NHDF were observed. While activin A treatment had no significant effect ($p = 0.25$) compared to the control, TGFβ1 significantly auto-induced its mRNA expression 2.3 ± 0.3-fold ($p < 0.0001$) (Figure 1C). Taken together, these results show that activin A is a TGFβ1-independent inducer of *XYLT1* mRNA expression and XT activity in NHDF.

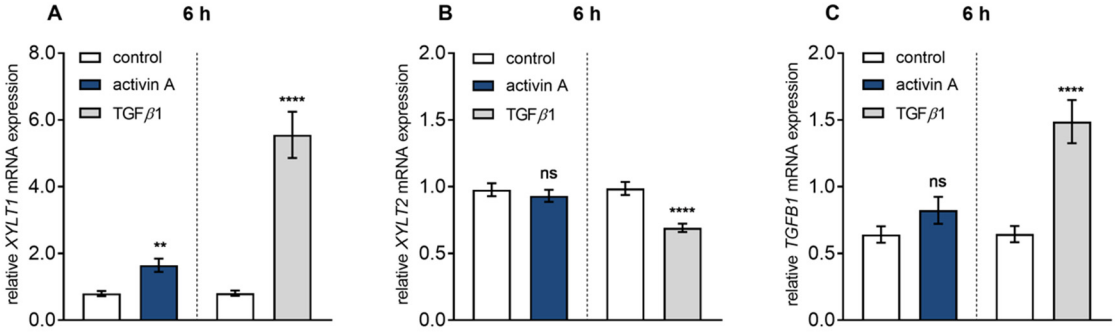

Figure 1. TGFβ superfamily cytokine regulated *XYLT* isoform and *TGFB1* mRNA expression. Human primary fibroblasts (n = 3) were cultured the day before the experiment. Cells were serum-starved for 24 h and treated with activin A (10 µg/L; left side) or TGFβ1 (10 µg/L; right side) for 6 h. The dashed line indicated that the activin A and TGFβ1 experiments were performed independently. Relative *XYLT1* (**A**), *XYLT2* (**B**) or *TGFB1* (**C**) mRNA expression levels were analysed by quantitative real-time PCR. Shown values are means ± SEM for three biological and three technical replicates per experiment. Mann–Whitney *U* test: not significant (ns), $p < 0.05$ (*), $p < 0.01$ (**), $p < 0.001$ (***), $p < 0.0001$ (****).

3.2. Activin A Induces Transient XYLT1 mRNA Expression and XT Activity Increase via ACVRIB/ALK4

Showing that activin A is a potent inducer of *XYLT1* expression under fibrotic conditions, we further examined the response of NHDF to various activin A concentrations in time-course experiments (Figure 2). The *XYLT1* mRNA expression levels were quantified 3 h, 6 h and 24 h post-treatment by qRT-PCR analysis (Figure 2A). The NHDF showed an early up-regulation of the *XYLT1* mRNA level at 3 h of activin A treatment at concentrations of 10 µg/L and 50 µg/L of 1.3 ± 0.3-fold ($p = 0.01$) and 2.3 ± 0.5-fold ($p < 0.0001$). This initial rise in *XYLT1* mRNA expression after 3 h was followed by a more pronounced expression increase in 10 µg/L and 50 µg/L activin A-treated cells of 2.7 ± 0.3-fold ($p < 0.0001$) and 3.4 ± 0.4-fold ($p < 0.0001$) after 6h in comparison to the untreated control fibroblasts. In comparison to control cells, activin A treatment at concentrations of 10 µg/L and 50 µg/L for 24 h increased the *XYLT1* expression level 1.9 ± 0.3-fold ($p = 0.0002$) and 3.2 ± 0.6-fold ($p < 0.0001$), respectively. The treatment with 1 µg/L activin A resulted in a 1.2 ± 0.1-fold ($p = 0.01$) increase in *XYLT1* mRNA expression after 6 h, though no expression changes were detectable after 3 h and 24 h treatment compared to the control (Figure 2A). These results demonstrate that activin A increases *XYLT1* mRNA expression in a time- and concentration-dependent manner in NHDF.

To confirm that the changes in *XYLT1* mRNA expression observed were caused by activin A treatment, cells were separately or simultaneously treated with the ALK4 inhibitor SB431542 [33,34] and activin A for 6 h (Figure 2B). The results showed that activin A induced a 2.1 ± 0.3-fold ($p = 0.002$) increase in *XYLT1* mRNA expression compared to the control that was completely abrogated by SB431542. Moreover, the single treatment of fibroblasts with SB431542 did not alter *XYLT1* basal expression ($p = 0.79$) compared to the vehicle-treated control cells. Treatment of NHDF with activin A or SB431542 did not alter *XYLT2* mRNA expression (Figure 2B). Together these results show an isoform-specific increase in *XYLT1* mRNA expression by activin A involving the ALK4 receptor.

Despite intracellular localization of XT-I, more than 90% of its enzyme activity is found in the culture supernatant, accumulating over time [25]. To examine if activin A-induced stimulation of *XYLT1* gene expression correlates with the changes in enzyme activity, extracellular and intracellular XT activity of NHDF were measured by radiochemical enzyme assay (Figure 2C,D). For this purpose, NHDF were treated with 10 µg/L and 50 µg/L activin A for 48 h and 120 h to promote detectable enzyme accumulation in the cell culture supernatant. In comparison to the untreated cells, the supplementation of activin A at different concentrations for 48 h increased the extracellular XT activity of NHDF 1.6 ± 0.3-fold ($p = 0.03$; 10 µg/L) and 1.5 ± 0.3-fold ($p = 0.03$; 50 µg/L), respectively. When analysing the XT activity from the corresponding cell lysates of former activin A-treated cells, a 1.7 ± 0.7-fold

(p = 0.02; 10 µg/L) and 1.8 ± 0.7-fold (p = 0.04; 50 µg/L) enhancement in intracellular XT activity was detectable in comparison to the untreated controls (Figure 2C). Compared to the untreated control cells after 120 h, no inducible effects regarding extra- and intracellular XT activity were observed after incubation of NHDF with the activin A concentration of 10 µg/L. The activin A treatment of NHDF with a concentration of 50 µg/L increased the extracellular XT activity 1.7 ± 0.3-fold (p = 0.04), while the intracellular enzyme activity was significantly raised, 1.6 ± 0.2-fold (p = 0.001) (Figure 2D). In agreement with the gene expression data (Figure 2B), the usage of the ALK4 inhibitor SB431542 suppressed the activin A-mediated increase in extra- and intracellular XT activity (Figure 2C,D). These results reveal that the activin A-induced XYLT1 mRNA expression increase correlates time- and concentration-dependently with the changes in the extracellular and intracellular XT activity of NHDF.

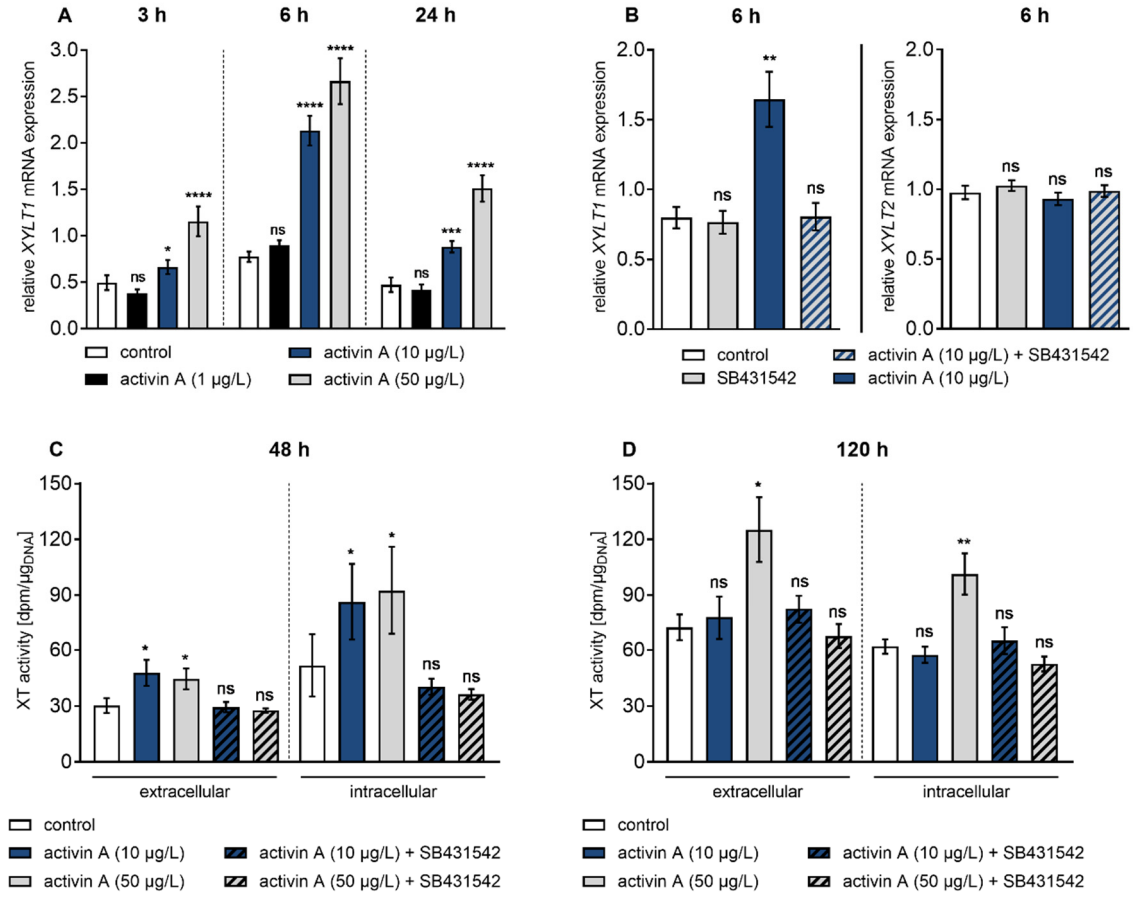

Figure 2. Time course of activin A-regulated *XYLT1* mRNA expression and XT activity. Human primary fibroblasts (n = 3) were cultured the day before the experiment. Cells were serum-starved for 24 h and treated with activin A or with activin A and the ALK4 inhibitor SB431542 (10 µmol/L) for the indicated time points. (**A**,**B**) Relative mRNA expression levels were analysed by quantitative real-time PCR. Shown values are means ± SEM for three biological and three technical replicates per donor-derived primary cell culture. Mann–Whitney *U* test: not significant (ns), $p < 0.05$ (*), $p < 0.01$ (**), $p < 0.001$ (***), $p < 0.0001$ (****). (**C**,**D**) XT activity was measured in cell supernatants and lysates by radiochemical enzyme assay and expressed as dpm per µg of DNA. Shown values are means ± SEM for three biological and one technical replicate per experiment. Mann–Whitney *U* test: not significant (ns), $p < 0.05$ (*), $p < 0.01$ (**).

3.3. ALK4–Activin A-Mediated XYLT1 mRNA Expression Requires MAPK Signalling Pathways

In order to understand the molecular mechanism of activin A–ALK4-mediated XT-I induction in NHDF, we investigated the underlying signalling pathways utilizing small-molecule inhibitors. The role of MAPK pathway on activin A-stimulated *XYLT1* expression was addressed by using

SP600125, a broad-spectrum inhibitor of JNK [35]; SB203580, inhibitor of p38 MAPK [36]; and UO126, a highly selective ERK inhibitor [37] on NHDF in presence or absence of activin A (Figure 3).

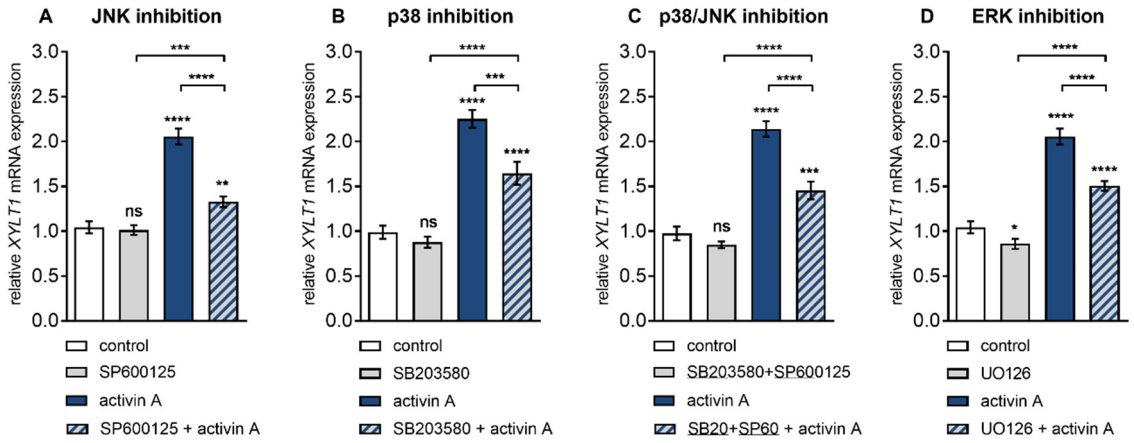

Figure 3. Inhibition of activin A-induced *XYLT1* mRNA expression by small-molecule inhibitors of MAPK pathways. Human primary fibroblasts (n = 3) were cultured the day before the experiment. Cells were serum-starved for 24 h and treated with or without activin A (10 µg/L) and (**A**) JNK inhibitor SP600125 (25 µmol/L), (**B**) p38 inhibitor SB203580 (10 µmol/L), (**C**) SP600125 (25 µmol/L) and SB203580 (10 µmol/L) or (**D**) ERK inhibitor UO126 (10 µmol/L) for 6 h. Relative mRNA expression level of *XYLT1* was analysed by qRT-PCR. Shown values are means ± SEM for three biological and three technical replicates per experiment. Mann–Whitney *U* test: not significant (ns), $p < 0.05$ (*), $p < 0.01$ (**), $p < 0.001$ (***), $p < 0.0001$ (****).

We found that the activin A-mediated increases in *XYLT1* expression at 6 h post treatment could be diminished by JNK inhibitor SP600125 and p38 MAPK inhibitor SB203580 in a concentration-dependent manner (data not shown). Both, SP600125 and SB203580 significantly reduced activin A-induced *XYLT1* expression increase (2.3 ± 0.2-fold, $p < 0.0001$) 0.6 ± 0.04-fold ($p < 0.0001$) and 0.7 ± 0.1-fold ($p = 0.0007$), respectively (Figure 3A,B). In the presence of both particular inhibitors no regulatory effects regarding the basal expression of *XYLT1* (Figure 3A,B) and *XYLT2* (Figure S3A,B) were observed compared to the vehicle-treated control cells. Combinatory treatment of NHDF with JNK inhibitor SP600125 and p38 MAPK inhibitor SB203580 resulted in a significantly decreased activin A-mediated *XYLT1* mRNA level increase of 0.7 ± 0.05-fold ($p < 0.0001$) (Figure 3C). In the presence of both inhibitors no regulatory effects regarding the basal expression of *XYLT1* (Figure 3C) and *XYLT2* (Figure S3C) mRNA were observed compared to the vehicle-treated control cells.

In comparison to the vehicle and ERK inhibitor UO126 exclusively treated cells, the presence of activin A resulted in a particular 2 ± 0.1-fold ($p < 0.0001$) and 1.8 ± 0.1-fold ($p < 0.0001$) up-regulation of *XYLT1* mRNA expression, respectively (Figure 3D). Moreover, UO126 significantly decreased the basal *XYLT1* expression 0.8 ± 0.08-fold ($p = 0.03$) and the activin A-induced *XYLT1* expression increased (2 ± 0.1-fold, $p < 0.0001$) 0.7 ± 0.04-fold ($p < 0.0001$) of that of the respective controls (Figure 3D). In addition, we found a decreased basal mRNA expression of *XYLT2* of 0.9 ± 0.03-fold ($p = 0.002$) in UO126 inhibitor single-treated cells compared with those with the vehicle treatment (Figure S3D). These data show the involvement of MAPK JNK, p38 and ERK in ALK4–activin A-mediated *XYLT1* expression. Furthermore, the results indicate a role for MAPK ERK in the maintenance of basal *XYLT1* and *XYLT2* mRNA expression in NHDF.

3.4. Smad3 is Dispensable for Activin A-Induced XYLT1 mRNA Expression in NHDF

Earlier studies by Takagi et al. on NHDF showed an activin A-induced (10 µg/L) phosphorylation of Smad2/3 after 4 h cytokine treatment [10]. On the basis of these findings, we wanted to verify the

impact of the canonical Smad pathway on basal *XYLT1* and *XYLT2* mRNA expression as well as on activin A-stimulated *XYLT1* expression increase by using siRNA knockdown experiments (Figure 4).

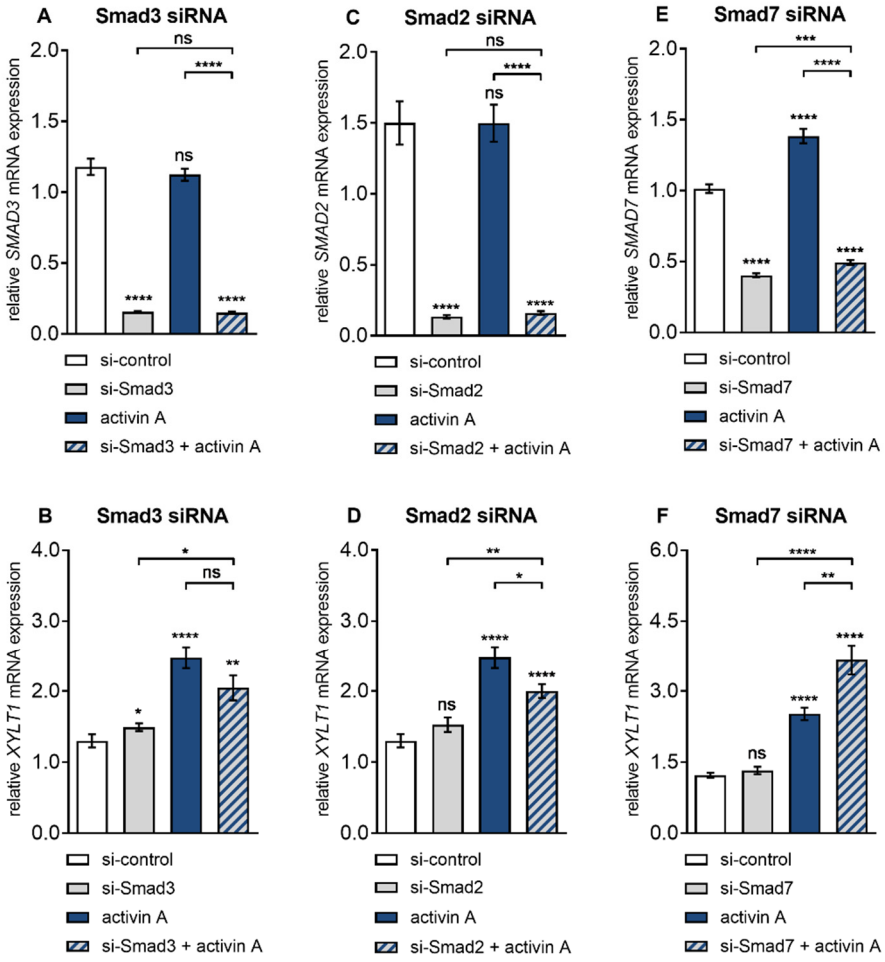

Figure 4. Basal and activin A-induced *XYLT1* mRNA expression were marginally affected by siRNA-mediated Smad knockdown. Human primary fibroblasts (n = 3) were cultured for 24 h before transfection with a negative control siRNA (si-control, 50 or 100 nmol/L) or siRNA targeting against (**A**,**B**) Smad3 (si-Smad3, 50 nmol/L), (**C**,**D**) Smad2 (si-Smad2, 50 nmol/L) or (**E**,**F**) Smad7 (si-Smad7, 100 nmol/L). A total of 24 h post-transfection, cells were serum-starved for 16 h and treated with or without activin A (10 µg/L) for 6 h. Relative *XYLT1* and *SMAD2/3/7* mRNA expression levels were analysed by qRT-PCR. Shown values are means ± SEM for three biological and three technical replicates per experiment. Mann–Whitney *U* test: not significant (ns), $p < 0.05$ (*), $p < 0.01$ (**), $p < 0.001$ (***), $p < 0.0001$ (****).

After Smad3 siRNA transfection, the basal *SMAD3* expression of the NHDF cells was knocked down 0.1 ± 0.01-fold ($p < 0.0001$), which did not change by additional activin A treatment compared to the negative control siRNA transfected cells (Figure 4A). Moreover, the Smad3 knockdown was selective, not affecting the expression levels of Smad2 or Smad7 (data not shown). Smad3 siRNA transfected NHDF showed an increased basal *XYLT1* expression of 1.1 ± 0.09-fold ($p = 0.02$) compared to the negative control siRNA transfected cells. Activin A treatment of control siRNA transfected NHDF resulted in a significant induction of *XYLT1* expression of 1.9 ± 0.2-fold ($p < 0.0001$). This induction did not significantly change ($p = 0.08$) in the presence of Smad3 knockdown. Therefore, Smad3 siRNA transfected NHDF treated with activin A exhibited an increased *XYLT1* expression of 1.6 ± 0.2-fold ($p = 0.02$) compared to the untreated control cells (Figure 4B). In contrast to basal *XYLT1* expression, the basal *XYLT2* expression level of Smad3 siRNA transfected cells fall below that of the respective

siRNA controls (0.7 ± 0.02-fold, $p < 0.0001$) (Figure S4A). These results demonstrate that the induction of *XYLT1* expression by activin A is Smad3-independent, while basal *XYLT1* and *XYLT2* expression were reversely regulated by *SMAD3* expression.

After showing the dispensability of *SMAD3* in activin A-induced *XYLT1* expression we addressed the role of Smad2 in this context with the same experimental approach. NHDF transfected with Smad2 siRNA exhibited a highly significant *SMAD2* transcription decrease of 0.1 ± 0.01-fold ($p < 0.0001$) compared to negative control siRNA-treated cells, which did not change due to activin A supplementation (Figure 4C). Specific Smad2 siRNA knockdown in NHDF did not alter basal *XYLT1* expression ($p = 0.08$) compared to the negative control siRNA transfected cells, whereas the activin A-mediated *XYLT1* mRNA expression increase (1.9 ± 0.2-fold, $p < 0.0001$) was significantly diminished 0.8 ± 0.06-fold ($p < 0.02$) (Figure 4D). In comparison to the controls, the transfection of NHDF with Smad2 siRNA significantly up-regulated the basal *XYLT2* mRNA expression 1.2 ± 0.05-fold ($p < 0.0001$) (Figure S4B). These findings show that the induction of *XYLT1* expression by activin A is dependent on Smad2, whereas basal *XYLT1* expression is Smad2-independent. Furthermore, these results demonstrate a suppressive role of Smad2 on basal *XYLT2* expression in NHDF.

To confirm the results of differential and antagonistic regulation of basal and activin A regulated *XYLT1* and *XYLT2* mRNA expression by Smad2 and Smad3 we increased the cellular availability of activated Smads 2 and 3 by selective downregulation of Smad inhibitor Smad7. Activin A treatment for 6 h resulted in an increase in *SMAD7* expression of 1.4 ± 0.06-fold ($p < 0.0001$) compared to the untreated control cells. Compared to the negative control siRNA treatment of NHDF, the basal and activin A-induced *SMAD7* expression was decreased by Smad7 siRNA knockdown to a similar extend, 0.4 ± 0.01-fold ($p < 0.0001$) and 0.5 ± 0.02-fold ($p < 0.0001$), respectively (Figure 4E). Basal *XYLT1* expression was unaffected ($p = 0.19$) by Smad7 siRNA transfection compared to the negative control siRNA treated cells. The activin A treatment for 6 h significantly induced *XYLT1* expression 2 ± 0.1-fold ($p < 0.0001$) compared to untreated controls. This activin A-induced *XYLT1* expression increase was significantly enhanced 1.5 ± 0.1-fold ($p < 0.004$) after Smad7 deletion. Smad7 siRNA transfected NHDF treated with activin A exhibited an increased *XYLT1* expression of 2.8 ± 0.3-fold ($p < 0.004$) compared to the untreated control cells (Figure 4F). In contrast to the basal expression of *XYLT1*, basal *XYLT2* mRNA expression was induced 1.3 ± 0.05-fold ($p < 0.0001$) after Smad7 knockdown compared to the controls (Figure S4C). These results demonstrate that the induction of *XYLT1* expression by activin A can be enhanced by unavailability of Smad7. Additionally, the results show an inhibitory role of Smad7 on basal *XYLT2* expression in NHDF, while basal *XYLT1* expression is independent of *SMAD7* expression.

The finding that Smad3 inhibition by siRNA-mediated gene knockdown failed to properly impair activin A-induced *XYLT1* expression in NHDF was independently confirmed by pharmacologic Smad3 inhibitor SIS3 (Figure 5), which has been shown in previous works not to inhibit the Smad2 or MAPK pathways in human fibroblasts [38]. Compared to the vehicle-treated cells, the presence of SIS3 increased the basal *XYLT1* expression 2.1 ± 0.5-fold ($p = 0.048$) at 6 h post-treatment. NHDF treated with activin A for 6 h increased the *XYLT1* expression 2.6 ± 0.5-fold ($p < 0.0001$) of that from the untreated control cells (Figure 5A). In consistency with former results obtained from siRNA experiments (Figure 4B), the activin A-mediated expression increase in NHDF was not significantly impeded ($p = 0.08$) in the presence of the Smad3 inhibitor SIS3. In direct comparison to the SIS3 treatment alone, the activin A treatment up-regulated the *XYLT1* mRNA expression 1.8 ± 0.4-fold ($p = 0.001$) (Figure 5A). On the contrary, there was a significant decrease in the basal *XYLT2* expression of 0.6 ± 0.04-fold ($p < 0.0001$) in the SIS3-treated cells in comparison to the vehicle treated control cells (Figure 5B). These results confirm the former findings about Smad3 dispensability of activin A-mediated *XYLT1* mRNA expression increase and its suppressive role in basal *XYLT1* expression. In addition, we substantiated our findings of basal *XYLT2* mRNA expression dependency on *SMAD3* expression. Figure 5C shows a schematic diagram of these findings.

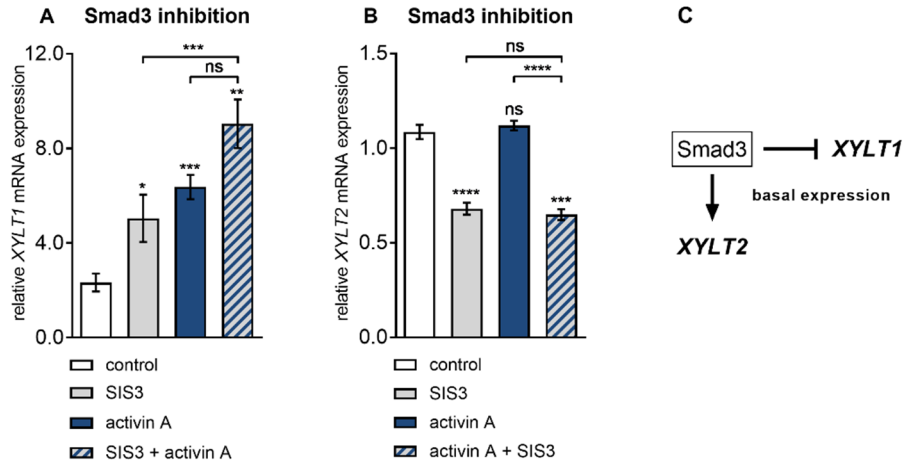

Figure 5. Differential regulation of basal *XYLT* isoform mRNA expression by Smad3. Human primary fibroblasts (n = 3) were cultured the day before the experiment. Cells were serum-starved for 24 h and treated with or without activin A (10 µg/L) in the presence or absence of the Smad3 inhibitor SIS3 (10 µmol/L) for 6 h. Relative (**A**) *XYLT1* and (**B**) *XYLT2* mRNA expression levels were analysed by qRT-PCR. Shown values are means ± SEM for three biological and three technical replicates per experiment. Mann–Whitney *U* test: not significant (ns), $p < 0.05$ (*), $p < 0.01$ (**), $p < 0.001$ (***), $p < 0.0001$ (****). (**C**) Schematic illustration of Smad3-dependent basal *XYLT2* and Smad3-independent basal *XYLT1* expression.

4. Discussion

The activity of GAG initiating key enzyme XT-I was found to be increased in the serum of patients with connective tissue diseases such as SSc or liver fibrosis [25,39]. Furthermore, long-term studies revealed that serum XT-I activity of SSc patients remains increased [25], corresponding to elevated PG metabolism and increased GAG content found in skin biopsies or cultured SSc fibroblasts [40,41]. Many TGFβ superfamily ligands are potent mediators of ECM deposition and are highly up-regulated under fibrotic conditions [42]. Until now, studies have described an induction of *XYLT1* expression in fibrotic tissue or in cultured primary cells treated with TGFβ1, IL-1β or thrombin [26,27,43–47], while the effect of other pro-fibrotic cytokines and their underlying signalling pathways remain unknown.

In the present study, we demonstrate for the first time that activin A, which was shown to be involved in wound healing processes and the pathogenesis of SSc [10,12], is a potent inducer of gene expression and activity of XT-I in dermal skin fibroblasts. Therefore, we provide evidence that one mechanism by which activin A contributes to dermal fibrosis in SSc is through the increase in *XYLT1* expression in NHDF, the major cells responsible for ECM remodelling [48].

We found that activin A-mediated *XYLT1* mRNA expression increase is time- and concentration-dependent, and considerably increased the intra- and extracellular XT enzyme activity in NHDF. The correlation of mRNA expression and enzyme activity increase regarding XT-I has been shown in this and numerous other studies using TGFβ1-treated human dermal and cardiac fibroblasts [26,27,45–47]. Furthermore, we observed, in consistency with previous results in NHDF [25], that the extracellular enzyme activity of untreated cells increased over time due to the protein accumulation in the cell supernatant, while intracellular XT activity remains constant over the test period of 120 h. These findings support the hypothesis that two regulatory mechanisms exist to control enzyme activity in NHDF: One at the transcriptional stage and another operating post-translationally, shedding the Golgi-resident, constitutive active enzyme from the membrane for release to the extracellular space controlling the rate of PG biosynthesis by reducing the cellular enzyme amount [24,29]. In contrast to TGFβ1, activin A treatment of NHDF results in a weaker *XYLT1* mRNA expression increase, which can be explained by the autocrine TGFβ*1* signalling, which is responsible for sustaining or amplifying the fibrotic responses in the pathogenesis of SSc [7].

Former sequence analysis of the human *XYLT1* promoter region revealed several downstream transcription factors of the EGR-, SP1- or KLF-family to regulate *XYLT1* mRNA expression [28,29,43]. Giving the missing link between promoter analysis, identified transcription factors and upstream cellular signalling mediating *XYLT1* expression in response to TGFβ cytokine stimulation of ALK receptors, we found a novel signalling axis involving MAPK and Smad proteins in activin A-mediated XT-I regulation in primary NHDF cells. Earlier studies by Takagi et al. on NHDF and SSc patients derived fibroblasts showed an activin A-induced phosphorylation of Smad2/3 after 4 h cytokine treatment, which could be reversed by ALK4 inhibition [10]. In agreement with the previous findings, we show here that the activin A-mediated effects on *XYLT1* mRNA and XT-I expression increases were ALK4-dependent in NHDF.

The ALK4–activin A-induced signal transduction can be promoted via canonical Smad or non-canonical, non-Smad pathways in human fibroblasts [10,16]. Regarding the role of non-canonical pathways, we found here for the first time that MAPK JNK, p38 and ERK are involved in ALK4–activin A-mediated *XYLT1* expression regulation in NHDF. The involvement of p38 MAPK in the TGFβ pathway promoted XT-I mRNA and the activity increase were observed in cultured human cardiac fibroblasts stimulated with TGFβ1 and corresponds with an elevated amount of digested GAG content in cardiac tissues from patients with myocardial fibrosis [27]. Additionally, in a recent study JNK and p38 were shown to be involved in growth factor thrombin or IL-1β-induced *XYLT1* mRNA expression increase in vascular smooth-muscle cells or primary chondrocyte cells [43,49].

While we demonstrated the contribution of the three MAPKs JNK, p38 and ERK in activin A-driven *XYLT1* expression increase in NHDF by the usage of small-molecule inhibitors, we were unable to detect a more pronounced decrease of activin A-mediated effects by simultaneous blocking of MAPK JNK and p38 compared to single p38, JNK or ERK inhibition. These data indicate reciprocal activation loops in the MAPK network itself or potential mechanisms of MAPK crosstalk and regulation by other signalling pathways [50,51]. The used SP600125 inhibitor concentration of 25 µmol/L in this study was previously shown not to block ERK1/2 and p38 phosphorylation [35], whereas blockade of p38 by SB203580 using an inhibitor concentration of 10 µmol/L resulted in a formerly identified increase on both ERK1/2 and JNK phosphorylation in primary hepatocytes and primary portal myofibroblasts [50]. Because of this cross-activation of MAPK signalling by MAPK inhibitors itself [35,50,52,53], it cannot be excluded that blocking of single MAPK JNK, p38 or ERK or simultaneous blocking of JNK and p38 MAPK pathways by the used small-molecule inhibitors in this study leads to a simultaneous activation of the other MAPKs driven by activin A. Therefore, no conclusion can be made on the basis of the observed relative extent of individual or combinatory MAPK inhibitions on the activin A-induced *XYLT1* mRNA expression increase.

Regarding the role of the canonical Smad signalling pathway, we suggest a Smad2-dependency of activin A-regulated *XYLT1* transcription, while Smad3 could be shown to be dispensable for *XYLT1* expression increase. Interestingly, we observed a slight inhibitory action of Smad3 with regard to the basal *XYLT1* expression of NHDF. In accordance with these findings, the full length *XYLT1* promoter does not provide a Smad binding element, except our group did identify the *XYLT1* promoter SNV with allele frequencies of 38%, detected in healthy blood donors, in which the base exchange c.-1088C>A results in a Smad3 transcription factor binding site that significantly reduced basal promoter activity by 48.1% ± 3% compared to promoter constructs without the mutation [54]. It might therefore be plausible that the slight increase in basal *XYLT1* expression observed in the Smad3-inhibited fibroblast cells of this study were due to this SNV. As former studies did not reveal any differences in serum enzyme activity in these blood donors harbouring the appropriate *XYLT1* promoter SNV c.-1088C>A [29], the corresponding *XYLT1* promoter SNV in this cells was therefore not considered further by sequencing for dividing into subgroups.

Additionally, the cell-type specific activation of individual MAPK JNK, p38 and ERK has been demonstrated to phosphorylate the regulatory linker region of Smad2 protein [13,49]. As Smad signalling is critical to fibroblast activation and fibrosis induced by activin A [49,55], inhibition of

Smad2 signalling by usage of MAPK inhibitors might have contributed to the suppressed *XYLT1* expression increase in activin A-stimulated cells shown in this study. Several studies using human VSMC have demonstrated the dependency of PG synthesis on the phosphorylation of the Smad2 linker region. These studies especially highlighted Smad2 linker residue Thr220 regarding the transcriptional regulation of XT-I that can undergo phosphorylation by two of the three MAPKs p38, ERK and JNK after TGFβ or thrombin stimulation of VSMC [49,56]. As our results show that activin A-mediated *XYLT1* expression increase is dependent on *SMAD2* expression and involves the activity of MAPK JNK, p38 and ERK, and thus possibly JNK, p38 and ERK initiate non-canonical phosphorylation of the Smad2 linker region, which could have an inducible effect on *XYLT1* mRNA expression in NHDF.

Deregulation of Smad7 expression has been associated with various human diseases, such as tissue fibrosis or systemic sclerosis [57]. Given the Smad3-dispensibilty of *XYLT1* expression regulation, we indirectly assumed the positive regulatory impact of increased Smad2 availability on *XYLT1* mRNA expression increase by depletion of Smad inhibitor Smad7. We could show that decreased *SMAD7* expression, mimicking SSc fibroblasts, increased activin A-driven *XYLT1* expression up-regulation but did not affect basal *XYLT1* expression. These data confirm the reliability of the used cell culture model and the role of XT-I as a marker for myofibroblast differentiation in fibrosis, as demonstrated in previous studies [26].

Former studies using activin A and a human neuroblastoma cell line demonstrated that the expression of some TGFβ superfamily target genes induced by ALK4–activin A did not require promoter bindings of SMAD2/3 [10]. By taking into consideration that of the *XYLT1* promoter does not provide the according Smad binding site [29], but Smad2 linker phosphorylation was shown to enhance the nuclear localisation of Smad2 proteins [55], we presume that a potential activin A–ALK4 signalling pathway in NHDF is transduced by the MAPK JNK, p38 and ERK pathways and potential phosphorylation of the Smad2 linker region, promoting the nuclear entrance and favoured binding of Smad2 to the former identified transcription factors AP1 and SP1/3, known to increase *XYLT1* expression [28,29,58–61].

Interestingly, we found differential dependency of *XYLT* isoform expression on Smad3 and ERK. In comparison to basal *XYLT1* expression, which is increased by ERK and supressed by Smad3, basal *XYLT2* expression is increased by Smad3 and ERK in NHDF. This observation can be explained by considering the results of this current work and the previous *XYLT1* and *XYLT2* promoter analysis performed in our group. In contrast to the promoter region of *XYLT1*, the *XYLT2* promoter does not exhibit a binding site for the AP1 transcription factor, which plays a considerable role in the regulation of *XYLT1* gene by JNK and p38 [43], explaining why basal *XYLT2* expression was not influenced by the usage of p38 and JNK inhibitors in this study. While the *XYLT1* promoter exhibits numerous transcription-binding sites for EGR1, which was previously shown to response to non-canonical, Smad3-independent TGFβ pathway MEK/ERK in SScF [60], the main transcription factors substantially involved in *XYLT2* promoter regulation are SP1/3 [29,30,62]. These findings are consistent with previously published data demonstrating dose-dependent inhibition of *SMAD3* promoter activity by ERK inhibitor UO126 that correlates with the inhibition of SP1/SP3 function by the same inhibitor [63]. Therefore, it is likely that apparent *SMAD3* expression due to ERK inhibition has led to diminish basal *XYLT2* expression. In accordance to Smad3 expression, which was shown to be down-regulated in former published data after TGFβ1 treatment [64,65], *XYLT2* expression decreases in a *SMAD3*-dependent manner.

The knockdown of Smad2 in NHDF resulted in higher basal *XYLT2* expression, suggesting that Smad2 acts as a transcriptional suppressor. Additionally, the inhibition of *SMAD7* expression mimics the effect of Smad2 silencing on basal *XYLT2* expression in NHDF. It is described that active Smad proteins interfere with transcription factor complexes mediating repression of target gene expression [66]. Therefore, Smad2 and Smad3 binding to SP1 and their relative distribution to *XYLT2* gene expression regulation in NHDF require further clarification. With the knowledge that basal *XYLT2* expression relies on Smad3, the depletion of Smad2 in this study could have raised the endogenous ratio of Smad3 in comparison to Smad2. This could have led to the observed *XYLT2* expression increase in

Smad2-depleted cells. The impact of siRNA-mediated knockdown of single Smad proteins on the endogenous Smad2/3 ratio and their respective complex formation has been shown in previous studies to change the outcome of target gene expression [67]. Future studies will be necessary to evaluate this reciprocal basal *XYLT2* expression regulation by Smads 2, 3 and 7 in NHDF.

5. Conclusions

Taken together, our data identify, for the first time, XT-I as a target of activin A-mediated pro-fibrotic effects in NHDF. *XYLT2* isoform expression was unchanged by activin A. We demonstrated the critical role for Smad2 and MAPK JNK, p38 and ERK in the underlying signalling pathways of increased *XYLT1* expression by activin A. Furthermore, we detected a differential regulation of basal *XYLT1* and *XYLT2* isoform transcription by MAPK and Smad proteins. This knowledge develops an enhanced understanding for their distinct expression pattern in tissues or under pathological conditions, and might be useful for isoform-specific activation or repression strategies of clinical relevance.

Supplementary Materials: The following are available online at http://www.mdpi.com/2218-273X/10/4/609/s1, Figure S1: Various Cytokine and growth factor treatments of NHDF. Figure S2: Interleukin treatments of NHDF. Figure S3: Inhibition of basal *XYLT2* mRNA expression by pharmacological inhibitors to MAPK JNK, p38 and ERK. Figure S4: siRNA-mediated Smads 2, 3 and 7 knockdowns.

Author Contributions: Conceptualization, T.-D.L., D.H., C.K. and I.F.; data curation, T.-D.L. and I.F; formal analysis, T.-D.L.; funding acquisition, I.F.; investigation, T.-D.L. and R.P.; methodology, R.P., V.S. and J.K.; project administration, D.H. and I.F.; resources, B.F.; supervision, C.K.; validation, B.F., V.S. and J.K.; visualization, T.-D.L.; writing—original draft, T.-D.L.; writing—review and editing, R.P., B.F., V.S., D.H., J.K., C.K. and I.F. All authors have read and agreed to the published version of the manuscript.

Funding: This research was funded by the German Research Foundation (Deutsche Forschungsgemeinschaft, DFG; FA 1381/1-1).

Acknowledgments: We thank Philip Saunders for linguistic advice and Christoph Lichtenberg for technical assistance.

Conflicts of Interest: The authors declare no conflict of interest.

References

1. Pasparakis, M.; Haase, I.; Nestle, F.O. Mechanisms regulating skin immunity and inflammation. *Nat. Rev. Immunol.* **2014**, *14*, 289–301. [CrossRef] [PubMed]
2. Zhao, X.; Psarianos, P.; Ghoraie, L.S.; Yip, K.; Goldstein, D.; Gilbert, R.; Witterick, I.; Pang, H.; Hussain, A.; Lee, J.H.; et al. Metabolic regulation of dermal fibroblasts contributes to skin extracellular matrix homeostasis and fibrosis. *Nat. Metab.* **2019**, *1*, 147–157. [CrossRef]
3. Do, N.N.; Eming, S.A. Skin fibrosis: Models and mechanisms. *Curr. Res. Transl. Med.* **2016**, *64*, 185–193. [CrossRef]
4. Yazdani, S.; Bansal, R.; Prakash, J. Drug targeting to myofibroblasts: Implications for fibrosis and cancer. *Adv. Drug Deliv. Rev.* **2017**, *121*, 101–116. [CrossRef]
5. Werner, S.; Smola, H. Paracrine regulation of keratinocyte proliferation and differentiation. *Trends in Cell Biology* **2001**, *11*, 143–146. [CrossRef]
6. Borthwick, L.A.; Wynn, T.A.; Fisher, A.J. Cytokine mediated tissue fibrosis. *Biochim. Biophys. Acta Mol. Basis Dis.* **2013**, *1832*, 1049–1060. [CrossRef]
7. Ihn, H. Autocrine TGF-β signaling in the pathogenesis of systemic sclerosis. *J. Dermatol. Sci.* **2008**, *49*, 103–113. [CrossRef]
8. Wang, X.; Fischer, G.; Hyvönen, M. Structure and activation of pro-activin A. *Nat. Commun.* **2016**, *7*. [CrossRef]
9. Annes, J.P. Making sense of latent TGFbeta activation. *J. Cell Sci.* **2003**, *116*, 217–224. [CrossRef]
10. Takagi, K.; Kawaguchi, Y.; Kawamoto, M.; Ota, Y.; Tochimoto, A.; Gono, T.; Katsumata, Y.; Takagi, M.; Hara, M.; Yamanaka, H. Activation of the Activin A-ALK-Smad pathway in systemic sclerosis. *J. Autoimmun.* **2011**, *36*, 181–188. [CrossRef]
11. Jones, K.L.; De Kretser, D.M.; Patella, S.; Phillips, D.J. Activin A and follistatin in systemic inflammation. *Mol. Cell. Endocrinol.* **2004**, *225*, 119–125. [CrossRef] [PubMed]

12. Antsiferova, M.; Werner, S. The bright and the dark sides of activin in wound healing and cancer. *J. Cell Sci.* **2012**, *125*, 3929–3937. [CrossRef] [PubMed]
13. Tsuchida, K.; Nakatani, M.; Hitachi, K.; Uezumi, A.; Sunada, Y.; Ageta, H.; Inokuchi, K. Activin signaling as an emerging target for therapeutic interventions. *Cell Commun. Signal.* **2009**, *7*, 1–11. [CrossRef] [PubMed]
14. Fibroblasts, L.; Ohga, E.; Matsuse, T.; Teramoto, S.; Katayama, H.; Nagase, T.; Fukuchi, Y.; Ouchi, Y. Effects of Activin A on Proliferation and Differentiation Activin A is a dimeric protein that was isolated from ovarian fluid as a stimulator of follicle- stimulating hormone (FSH). *Biochem. Biophys. Res. Commun.* **1996**, *228*, 391–396.
15. Yamashita, S.; Maeshima, A.; Kojima, I.; Nojima, Y. Activin A Is a Potent Activator of Renal Interstitial Fibroblasts. *J. Am. Soc. Nephrol.* **2004**, *15*, 91–101. [CrossRef]
16. Hu, J.; Wang, X.; Wei, S.M.; Tang, Y.H.; Zhou, Q.; Huang, C.X. Activin A stimulates the proliferation and differentiation of cardiac fibroblasts via the ERK1/2 and p38-MAPK pathways. *Eur. J. Pharmacol.* **2016**, *789*, 319–327. [CrossRef]
17. Bao, Y.L.; Tsuchida, K.; Liu, B.; Kurisaki, A.; Matsuzaki, T.; Sugino, H. Synergistic activity of activin A and basic fibroblast growth factor on tyrosine hydroxylase expression through Smad3 and ERK1/ERK2 MAPK signaling pathways. *J. Endocrinol.* **2005**, *184*, 493–504. [CrossRef]
18. Susarla, B.T.S.S.; Laing, E.D.; Yu, P.; Katagiri, Y.; Geller, H.M.; Symes, A.J. Smad proteins differentially regulate transforming growth factor-β-mediated induction of chondroitin sulfate proteoglycans. *J. Neurochem.* **2011**, *119*, 868–878. [CrossRef]
19. Bhattacharyya, S.; Chen, S.J.; Wu, M.; Warner-Blankenship, M.; Ning, H.; Lakos, G.; Mori, Y.; Chang, E.; Nihijima, C.; Takehara, K.; et al. Smad-independent transforming growth factor-β regulation of early growth response-1 and sustained expression in fibrosis: Implications for scleroderma. *Am. J. Pathol.* **2008**, *173*, 1085–1099. [CrossRef]
20. Li, S.; Shimono, C.; Norioka, N.; Nakano, I.; Okubo, T.; Yagi, Y.; Hayashi, M.; Sato, Y.; Fujisaki, H.; Hattori, S.; et al. Activin A binds to perlecan through its pro-region that has heparin/heparan sulfate binding activity. *J. Biol. Chem.* **2010**, *285*, 36645–36655. [CrossRef]
21. Kleesiek, K.; Reinards, R.; Okusi, J.; Wolf, B.; Greiling, H. UDP-D-Xylose: Proteoglycan Core Protein β-D-Xylosyltransferase: A New Marker of Cartilage Destruction in Chronic Joint Diseases. *Clin. Chem. Lab. Med.* **1987**, *25*. [CrossRef] [PubMed]
22. Pönighaus, C.; Speirs, H.J.L.; Morris, B.J.; Kuhn, J.; Kleesiek, K.; Götting, C. Xylosyltransferase gene variants and their role in essential hypertension. *Am. J. Hypertens.* **2009**, *22*, 432–436. [CrossRef] [PubMed]
23. Götting, C.; Kuhn, J.; Zahn, R.; Brinkmann, T.; Kleesiek, K. Molecular Cloning and Expression of Human UDP-d-Xylose:Proteoglycan Core Protein β-d-Xylosyltransferase and its First Isoform XT-II. *J. Mol. Biol.* **2000**, *304*, 517–528. [CrossRef] [PubMed]
24. Pönighaus, C.; Kuhn, J.; Kleesiek, K.; Götting, C. Involvement of a cysteine protease in the secretion process of human xylosyltransferase I. *Glycoconj. J.* **2010**, *27*, 359–366. [CrossRef] [PubMed]
25. Götting, C.; Sollberg, S.; Kuhn, J.; Weilke, C.; Huerkamp, C.; Brinkmann, T.; Krieg, T.; Kleesick, K.; Kleesiek, K.; Sollberg, S.; et al. Serum xylosyltransferase: A new biochemical marker of the sclerotic process in systemic sclerosis. *J. Investig. Dermatol.* **1999**, *112*, 919–924. [CrossRef]
26. Faust, I.; Roch, C.; Kuhn, J.; Prante, C.; Knabbe, C.; Hendig, D. Human xylosyltransferase-I – A new marker for myofibroblast differentiation in skin fibrosis. *Biochem. Biophys. Res. Commun.* **2013**, *436*, 449–454. [CrossRef]
27. Prante, C.; Milting, H.; Kassner, A.; Farr, M.; Ambrosius, M.; Schon, S.; Seidler, D.G.; Banayosy, A.E.; Korfer, R.; Kuhn, J.; et al. Transforming Growth Factor beta1-regulated Xylosyltransferase I Activity in Human Cardiac Fibroblasts and Its Impact for Myocardial Remodeling. *J. Biol. Chem.* **2007**, *282*, 26441–26449. [CrossRef]
28. Müller, B.; Prante, C.; Kleesiek, K.; Götting, C.; Muller, B.; Prante, C.; Kleesiek, K.; Gotting, C. Identification and Characterization of the Human Xylosyltransferase I Gene Promoter Region. *J. Biol. Chem.* **2009**, *284*, 30775–30782. [CrossRef]
29. Faust, I.; Böker, K.O.; Lichtenberg, C.; Kuhn, J.; Knabbe, C.; Hendig, D. First description of the complete human xylosyltransferase-I promoter region. *BMC Genet.* **2014**, *15*, 1. [CrossRef]
30. Müller, B.; Prante, C.; Knabbe, C.; Kleesiek, K.; Götting, C. First identification and functional analysis of the human xylosyltransferase II promoter. *Glycoconj. J.* **2013**, *30*, 237–245. [CrossRef]
31. Pfaffl, M.W. A new mathematical model for relative quantification in real-time RT-PCR. *Nucl. Acids Res.* **2001**, *29*, e45. [CrossRef] [PubMed]

32. Götting, C.; Kuhn, J.; Tinneberg, H.-R.; Brinkmann, T.; Kleesiek, K. High xylosyltransferase activities in human follicular fluid and cultured granulosa-lutein cells. *Mol. Hum. Reprod.* **2002**, *8*, 1079–1086. [CrossRef] [PubMed]
33. Mori, Y.; Ishida, W.; Bhattacharyya, S.; Li, Y.; Platanias, L.C.; Varga, J. Selective inhibition of activin receptor-like kinase 5 signaling blocks profibrotic transforming growth factor β responses in skin fibroblasts. *Arthr. Rheum.* **2004**, *50*, 4008–4021. [CrossRef] [PubMed]
34. Inman, G.J.; Nicolás, F.J.; Callahan, J.F.; Harling, J.D.; Gaster, L.M.; Reith, A.D.; Laping, N.J.; Hill, C.S. SB-431542 is a potent and specific inhibitor of transforming growth factor-β superfamily type I activin receptor-like kinase (ALK) receptors ALK4, ALK5, and ALK7. *Mol. Pharmacol.* **2002**, *62*, 65–74. [CrossRef]
35. Bennett, B.L.; Sasaki, D.T.; Murray, B.W.; Leary, E.C.O.; Sakata, S.T.; Xu, W.; Leisten, J.C.; Motiwala, A.; Pierce, S.; Satoh, Y.; et al. SP600125, an Anthrapyrazolone Inhibitor of Jun N-Terminal Kinase. *Proc. Natl. Acad. Sci. USA* **2001**, *98*, 13681–13686. [CrossRef]
36. Henklova, P.; Vrzal, R.; Papouskova, B.; Bednar, P.; Jancova, P.; Anzenbacherova, E.; Ulrichova, J.; Maurel, P.; Pavek, P.; Dvorak, Z. SB203580, a pharmacological inhibitor of p38 MAP kinase transduction pathway activates ERK and JNK MAP kinases in primary cultures of human hepatocytes. *Eur. J. Pharmacol.* **2008**, *593*, 16–23. [CrossRef]
37. Dumas, J. Protein kinase inhibitors: Emerging pharmacophores 1997 - 2000. *Expert Opin. Ther. Pat.* **2001**, *11*, 405–429. [CrossRef]
38. Jinnin, M.; Ihn, H.; Tamaki, K. Characterization of SIS3, a novel specific inhibitor of Smad3, and its effect on transforming growth factor-β1-induced extracellular matrix expression. *Mol. Pharmacol.* **2006**, *69*, 597–607. [CrossRef]
39. Kuhn, J.; Gressner, O.A.; Götting, C.; Gressner, A.M.; Kleesiek, K. Increased serum xylosyltransferase activity in patients with liver fibrosis. *Clin. Chim. Acta* **2009**, *409*, 123–126. [CrossRef] [PubMed]
40. Kitabatake, M.; Ishikawa, H.; Maeda, H. Immunohistochemical demonstration of proteoglycans in the skin of patients with systemic sclerosis. *Br. J. Dermatol.* **1983**, *108*, 257–262. [CrossRef] [PubMed]
41. Kuroda, K.; Shinkai, H. Decorin and glycosaminoglycan synthesis in skin fibroblasts from patients with systemic sclerosis. *Arch. Dermatol. Res.* **1997**, *289*, 481–485. [CrossRef] [PubMed]
42. Walton, K.L.; Johnson, K.E.; Harrison, C.A. Targeting TGF-β Mediated SMAD Signaling for the Prevention of Fibrosis. *Front. Pharmacol.* **2017**, *8*. [CrossRef] [PubMed]
43. Khair, M.; Bourhim, M.; Barré, L.; Li, D.; Netter, P.; Magdalou, J.; Fournel-Gigleux, S.; Ouzzine, M. Regulation of Xylosyltransferase I Gene Expression by Interleukin 1β in Human Primary Chondrocyte Cells: MECHANISM AND IMPACT ON PROTEOGLYCAN SYNTHESIS. *J. Biol. Chem.* **2013**, *288*, 1774–1784. [CrossRef] [PubMed]
44. Ye, W.; Zhou, J.; Markova, D.Z.; Tian, Y.; Li, J.; Anderson, D.G.; Shapiro, I.M.; Risbud, M.V. Xylosyltransferase-1 expression is refractory to inhibition by the inflammatory cytokines tumor necrosis factor α and IL-1β in nucleus pulposus cells: Novel regulation by AP-1, Sp1, and Sp3. *Am. J. Pathol.* **2014**, *185*, 485–495. [CrossRef]
45. Faust, I.; Donhauser, E.; Fischer, B.; Ibold, B.; Kuhn, J.; Knabbe, C.; Hendig, D. Characterization of dermal myofibroblast differentiation in pseudoxanthoma elasticum. *Exp. Cell Res.* **2017**, *360*, 153–162. [CrossRef]
46. Fischer, B.; Ly, T.; Hendig, D.; Kuhn, J.; Pécheur, E.; Reungoat, E.; Knabbe, C.; Faust, I. Biochem. Biophys. Res. Commun. First description of a compensatory xylosyltransferase I induction observed after an anti fi brotic UDP-treatment of normal human dermal fi broblasts. *Biochem. Biophys. Res. Commun.* **2019**, *512*, 7–13. [CrossRef]
47. Riedel, L.; Fischer, B.; Ly, T.-D.; Hendig, D.; Kuhn, J.; Knabbe, C.; Faust, I. microRNA-29b mediates fibrotic induction of human xylosyltransferase-I in human dermal fibroblasts via the Sp1 pathway. *Sci. Rep.* **2018**, *8*, 17779. [CrossRef]
48. Garrett, S.M.; Baker Frost, D.; Feghali-Bostwick, C. The Mighty Fibroblast and Its Utility in Scleroderma Research. *J. Scleroderma Relat. Disord.* **2017**, *2*, 100–107. [CrossRef]
49. Kamato, D.; Burch, M.; Zhou, Y.; Mohamed, R.; Stow, J.L.; Osman, N.; Zheng, W.; Little, P.J. Individual Smad2 linker region phosphorylation sites determine the expression of proteoglycan and glycosaminoglycan synthesizing genes. *Cell. Signal.* **2019**, *53*, 365–373. [CrossRef]
50. Meurer, S.K.; Weiskirchen, R. Usage of Mitogen-activated protein kinase small molecule inhibitors: More than just inhibition! *Front. Pharmacol.* **2018**, *9*, 9–11. [CrossRef]

51. Dolivo, D.M.; Larson, S.A.; Dominko, T. Crosstalk between mitogen-activated protein kinase inhibitors and transforming growth factor-β signaling results in variable activation of human dermal fibroblasts. *Int. J. Mol. Med.* **2019**, *43*, 325–335. [CrossRef] [PubMed]
52. Kempf, H.; Lecina, M.; Ting, S.; Zweigerdt, R.; Oh, S. Distinct regulation of mitogen-activated protein kinase activities is coupled with enhanced cardiac differentiation of human embryonic stem cells. *Stem Cell Res.* **2011**, *7*, 198–209. [CrossRef] [PubMed]
53. Hotokezaka, H.; Sakai, E.; Kanaoka, K.; Saito, K.; Matsuo, K.; Kitaura, H.; Yoshida, N.; Nakayama, K. U0126 and PD98059, Specific Inhibitors of MEK, Accelerate Differentiation of RAW264.7 Cells into Osteoclast-like Cells. *J. Biol. Chem.* **2002**, *277*, 47366–47372. [CrossRef]
54. Suzuki, K.; Kobayashi, T.; Funatsu, O.; Morita, A.; Ikekita, M. Biochem. Biophys. Res. Commun. Activin A induces neuronal differentiation and survival via ALK4 in a SMAD-independent manner in a subpopulation of human neuroblastomas. *Biochem. Biophys. Res. Commun.* **2010**, *394*, 639–645. [CrossRef] [PubMed]
55. Rostam, M.A.; Shajimoon, A.; Kamato, D.; Mitra, P.; Piva, T.J.; Getachew, R.; Cao, Y.; Zheng, W.; Osman, N.; Little, P.J. Flavopiridol Inhibits TGF- β -Stimulated Biglycan Synthesis by Blocking Linker Region Phosphorylation and Nuclear Translocation of Smad2. *J. Pharmacol. Exp. Ther.* **2018**, *365*, 156–164. [CrossRef] [PubMed]
56. Rostam, M.A.; Kamato, D.; Piva, T.J.; Zheng, W.; Little, P.J.; Osman, N. The role of specific Smad linker region phosphorylation in TGF-β mediated expression of glycosaminoglycan synthesizing enzymes in vascular smooth muscle. *Cell. Signal.* **2016**, *28*, 956–966. [CrossRef]
57. Mori, Y.; Chen, S.J.; Varga, J. Expression and regulation of intracellular SMAD signaling in scleroderma skin fibroblasts. *Arthr. Rheum.* **2003**, *48*, 1964–1978. [CrossRef]
58. Venkatesan, N.; Barré, L.; Bourhim, M.; Magdalou, J.; Mainard, D.; Netter, P.; Fournel-Gigleux, S.; Ouzzine, M. Xylosyltransferase-I Regulates Glycosaminoglycan Synthesis during the Pathogenic Process of Human Osteoarthritis. *PLoS ONE* **2012**, *7*, e34020. [CrossRef]
59. Ihn, H.; Yamane, K.; Asano, Y.; Jinnin, M.; Tamaki, K. Constitutively phosphorylated Smad3 interacts with Sp1 and p300 in scleroderma fibroblasts. *Rheumatology* **2006**, *45*, 157–165. [CrossRef]
60. Bhattacharyya, S.; Sargent, J.L.; Du, P.; Lin, S.; Tourtellotte, W.G.; Takehara, K.; Whitfield, M.L.; Varga, J. Egr-1 induces a profibrotic injury/repair gene program associated with systemic sclerosis. *PLoS ONE* **2011**, *6*, 1–7. [CrossRef]
61. Piera-velazquez, S.; Makul, A.; Jimenez, S.A. Increased Expression of NAPDH Oxidase 4 (NOX4) in Systemic Sclerosis Dermal Fibroblasts: Regulation by Transforming Growth Factor β. *Arthr. Rheumatol.* **2016**, *67*, 2749–2758.
62. Tan, N.Y.; Khachigian, L.M. Sp1 Phosphorylation and Its Regulation of Gene Transcription. *Mol. Cell. Biol.* **2009**, *29*, 2483–2488. [CrossRef] [PubMed]
63. Ross, K.R.; Corey, D.A.; Dunn, J.M.; Kelley, T.J. SMAD3 expression is regulated by mitogen-activated protein kinase kinase-1 in epithelial and smooth muscle cells. *Cellular Signalling* **2007**, *19*, 923–931. [CrossRef]
64. Poncelet, A.-C.; De Caestecker, M.P.; Schnaper, H.W. The transforming growth factor-βbgr/SMAD signaling pathway is present and functional in human mesangial cells. *Kidney Int.* **1999**, *56*, 1354–1365. [CrossRef] [PubMed]
65. Baugé, C.; Cauvard, O.; Leclercq, S.; Galéra, P.; Boumédiene, K. Modulation of transforming growth factor beta signalling pathway genes by transforming growth factor beta in human osteoarthritic chondrocytes: Involvement of Sp1 in both early and late response cells to transforming growth factor beta. *Arthr. Res. Ther.* **2011**, *13*, R23. [CrossRef]
66. Shi, Y.; Massagué, J. Mechanisms of TGF-β signaling from cell membrane to the nucleus. *Cell* **2003**, *113*, 685–700. [CrossRef]
67. Ungefroren, H.; Groth, S.; Sebens, S.; Lehnert, H.; Gieseler, F.; Fändrich, F. Differential roles of Smad2 and Smad3 in the regulation of TGF-β1-mediated growth inhibition and cell migration in pancreatic ductal adenocarcinoma cells: Control by Rac1. *Mol. Cancer* **2011**, *10*, 67. [CrossRef] [PubMed]

3.2 Publikation II

Zytokin-vermittelte Induktion der humanen Xylosyltransferase-I in dermalen Sklerodermiefibroblasten

(Ly *et al.*, eingereicht)

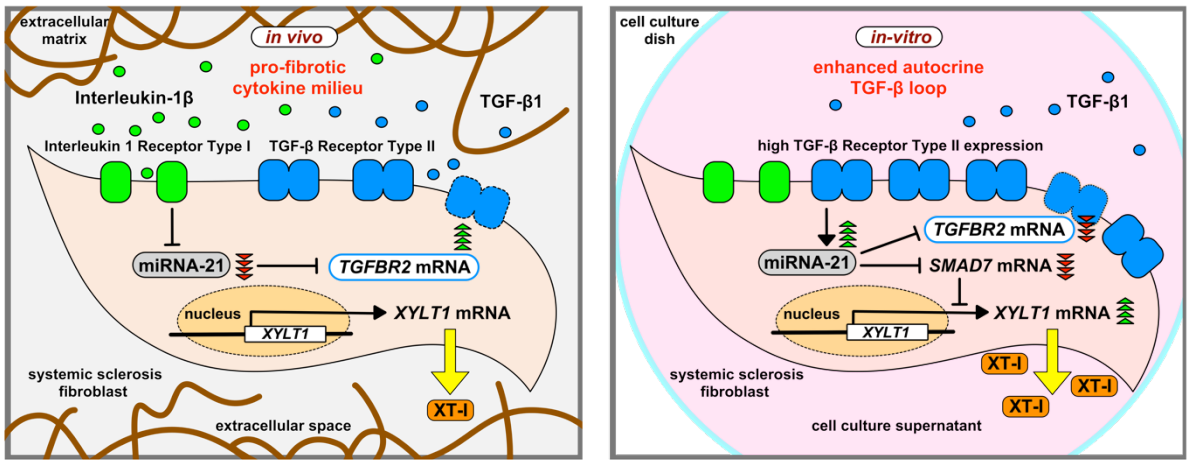

Abbildung 6: *Graphical Abstract* von Publikation II (Ly *et al.*, eingereicht).

Biochemical and Biophysical Research Communications

Cytokine-mediated Induction of Human Xylosyltransferase-I in Systemic Sclerosis Skin Fibroblasts

--Manuscript Draft--

Manuscript Number:	BBRC-20-9997
Article Type:	Short communication/Research article
Keywords:	fibrosis; systemic sclerosis; xylosyltransferase-I; interleukin-1β; TGF-β receptor II; microRNA-21
Corresponding Author:	Isabel Faust Herz- und Diabeteszentrum Nordrhein-Westfalen, Ruhr University Bochum Bad Oeynhausen, GERMANY
First Author:	Thanh-Diep Ly
Order of Authors:	Thanh-Diep Ly
	Anika Kleine
	Ricarda Plümers
	Bastian Fischer
	Vanessa Schmidt
	Doris Hendig
	Jörg H. W. Distler
	Joachim Kuhn
	Cornelius Knabbe
	Isabel Faust

Cytokine-mediated Induction of Human Xylosyltransferase-I in Systemic Sclerosis Skin Fibroblasts

Thanh-Diep Ly[1], Anika Kleine[1], Ricarda Plümers[1], Bastian Fischer[1], Vanessa Schmidt[1], Doris Hendig[1], Jörg H. W. Distler[2], Joachim Kuhn[1], Cornelius Knabbe[1] and Isabel Faust[1*]

[1]Institut für Laboratoriums- und Transfusionsmedizin, Herz- und Diabeteszentrum Nordrhein-Westfalen, Universitätsklinik der Ruhr-Universität Bochum, Georgstraße 11, 32545 Bad Oeynhausen, Germany

[2]Department of Internal Medicine 3 – Rheumatology and Immunology, Friedrich-Alexander-University Erlangen-Nürnberg, 91054 Erlangen, Germany

[*]Corresponding author:

Dr. rer. nat. Isabel Faust

Institut für Laboratoriums- und Transfusionsmedizin

Herz- und Diabeteszentrum Nordrhein-Westfalen

Universitätsklinik der Ruhr-Universität Bochum

Georgstraße 11, 32545 Bad Oeynhausen, Germany

Phone: (+49) 5731-97-1234, Fax: (+49) 5731-97-2307

E-mail: ifaust@hdz-nrw.de

Abstract

Systemic sclerosis (SSc) is an inflammatory fibrotic disease characterized by an excessive extracellular matrix deposition in the skin and internal organs. One fibrotic key event remains the fibroblast-to-myofibroblast differentiation that is controlled by a combination of mechanical and soluble factors, such as transforming growth factor-β1 (TGF-β1) and interleukin-1β (IL-1β). One important myofibroblast biomarker is human xylosyltransferase-I (XT-I), the initial enzyme in proteoglycan biosynthesis. Increased serum XT activity was quantified in SSc, but the underlying cellular mechanisms remain elusive. This study aims to determine the cellular basis of XT-I induction in SSc by using a myofibroblast cell culture model with SSc fibroblasts (SScF) and healthy control fibroblasts. We found that SScF exhibit a higher extracellular XT-I activity compared to control fibroblasts. This increased XT-I activity in SScF was demonstrated to be mediated by an enhanced autocrine TGF-β signaling. Upon IL-1β treatment, SScF showed an increased mRNA expression level of XT-I and TGF-β receptor II (*TGFBR2*), while healthy control fibroblasts did not, pointing towards an involvement of IL-1β in the cytokine-mediated XT-I induction. Performing microRNA (miRNA) inhibition experiments in the presence of TGF-β1, we showed that the pro-fibrotic effect of IL-1β may be mediated by a miRNA-21/TGF-β receptor II axis, enhancing the autocrine TGF-β signaling in SScF. Taken together, this study improves the mechanistic understanding of fibrotic XT-I induction in SSc by identifying a hitherto unknown IL-1β-mediated miRNA-21/*TGFBR2* regulation contributing to the enhanced *XYLT1* expression and XT-I activity in SScF.

Keywords: fibrosis; systemic sclerosis; xylosyltransferase-I; interleukin-1β; TGF-β receptor II; microRNA-21

Abbreviations: ECM: extracellular matrix; IL-1β: interleukin-1β; miRNA: microRNA; NHDF: normal human dermal fibroblast; PG: proteoglycan; qRT-PCR: quantitative real-time polymerase chain reaction; SSc: systemic sclerosis; SScF: SSc fibroblasts; TGF-β1: transforming growth factor β1; UTR: untranslated regions; XT-I: xylosyltransferase-I

1. Introduction

The hallmark of systemic sclerosis (SSc) is progressive tissue accumulation of extracellular matrix (ECM) components, such as collagens and proteoglycans (PGs). The synthesis of fibrotic tissue is caused by the differentiation of fibroblasts to α-smooth muscle actin-positive myofibroblasts, which express vast amounts of ECM and pro-fibrotic cytokines, such as transforming growth factor-β (TGF-β). The activin/TGF-β family consists of evolutionarily conserved polypeptides, which play a prominent role in fibrosis. The TGF-β signaling is considered an important pathogenic factor in fibrogenesis driving myofibroblast differentiation [1]. The TGF-β receptors are serine/threonine kinase receptors and are divided into type I, type II and type III receptors. Upon ligand binding to the type II receptor dimer, an active ligand-type I/type II receptor heterotetrameric complex is formed. The type I receptor is activated due to the phosphorylation by the type II receptor. The type I receptor activated subsequently phosphorylates downstream SMAD proteins which transmit the signal to the nucleus. This TGF-β signaling is regulated by inhibitory SMAD7 by negative feedback loops. The TGF-β target genes includes both proteins and microRNAs (miRNAs) [2]. The latter are noncoding endogenous RNAs which are important posttranscriptional gene regulators by binding to the 3′-untranslated regions (UTR) of their target mRNAs, preventing the translation or promoting the degradation of the mRNA. Aberrant miRNA expression and TGF-β signaling has been reported in a wide range of diseases, including fibrosis [2]. Experimentally validated interactions between TGF-β signaling and miRNAs suggest that the latter influence the TGF-β pathway at multiple levels. Downregulation of miRNA-133 and miRNA-590 via TGF-β1 and TGF-β receptor type II (*TGFBR2*), respectively, contribute to the enhancement of TGF-β signaling in cardiac fibroblasts [3], whereas decreased *SMAD7* expression was shown to involve TGF-β1-mediated miRNA-21 induction [4].

The biological role of PGs are mostly related to their glycosaminoglycan (GAG) chains [5]. The initiation of the GAG synthesis is mediated by xylosylation of the PG core protein catalyzed by the human xylosyltransferase-I and -II (XT-I, XT-II; EC 2.4.2.26). Both XT isoforms are type II transmembrane proteins localized in the Golgi apparatus. They are encoded by the genes *XYLT1* and *XYLT2* that are regulated differently on the transcriptional state [6,7]. Only *XYLT1* mRNA expression was shown to be induced by TGF-β1 in human fibroblasts and was therefore associated with fibrotic remodeling and myofibroblast differentiation [8,9]. In addition to the XT-I regulation on the transcriptional state, a mechanism of active XT-I secretion is thought to be regulating the amount of constitutively active XT-I within the cell [6,10]. The XT enzyme activity is measurable in human serum and provides an indicator for the present rate of GAG synthesis. Elevated serum activity of XT was found in patients with SSc [11], but the contribution of the respective XT isoform and cell type remains elusive. Therefore, the present study aimed to find the missing connection between the serum XT activity increase in SSc and the underlying cellular mechanisms in myofibroblasts.

2. Methods

2.1 Cell culture, cytokine treatment and miRNA transfection

The normal human dermal fibroblasts (NHDF) were acquired from Genlantis and Coriell (USA). Prof. Jörg Distler (University Hospital Erlangen, GER) kindly provided the age and biopsy side-matched diffuse cutaneous type SSc fibroblasts (SScF). SScF use was approved by the local ethical committee. The cells were maintained in culture medium containing serum, as formerly described [12]. All experiments using 50 cells/mm^2 were conducted in serum-free growth medium unless otherwise stated. TGF-β1 or IL-1β were obtained from Miltenyi Biotec (GER) for the cytokine treatment. Cells were serum-starved for 24 h and maintained in serum-free growth medium containing cytokine for the time points indicated. Regarding miRNA delivery, NHDF were maintained in antibiotic-free growth medium and reverse-transfected using Lipofectamine 2000 (ThermoFisher, USA), as described previously [12]. The transfection mixture contained a miRNA-21 inhibitor (UAGCUUAUCAGACUGAUGUUGA) or a miRNA inhibitor control diluted in Opti-MEM I Reduced Serum Medium (ThermoFisher, USA) at a final concentration of 50 nmol/L. Twenty-four hours post-transfection, the NHDF were maintained in serum-free growth medium for an additional 24 h.

2.2 mRNA and miRNA expression analyses

The RNA extraction, cDNA synthesis and mRNA or miRNA expression analysis by quantitative real-time polymerase chain reaction (qRT-PCR) was performed as described previously [13] using the primer sequences listed in **Table S1**. The geometric mean of the expression levels of the three housekeeping genes *SDHA*, *RPL13A* and *B2M* was used for normalization purposes. The relative target gene mRNA expressions were calculated with the $\Delta\Delta C_T$ method considering the efficiency of the PCR [14]. The TaqMan advanced miRNA Assay (ThermoFisher, USA) was performed according to the manufacturer's instructions using the primer assays miRNA-21-5p (477975_mir) and miRNA-191 (477952_mir) for the expression analysis of miRNAs. The miRNA-21-5p (miRNA-21) expression level determined was normalized to the control gene expression of miRNA-191 via the $\Delta\Delta C_T$ method. All normalized gene expression levels were related to the target gene expression of one NHDF derived sample for relative comparison among multiple biological samples.

2.3 UPLC-ESI-MS/MS XT-I activity assay

The determination of the extracellular and intracellular XT-I activity was performed by a UPLC-ESI-MS/MS assay, as described previously [15].

2.4 Bioinformatic analysis

The identification of probable miRNA-21 binding sites within an mRNA was predicted using the computational algorithm TargetScan 7.6 (http://www.targetscan.org; 2020-11-12) [16].

2.5 Verification of miRNA-21 binding to the 3'UTR of XYLT1

The interaction of miRNA-21 with the *XYLT1* 3'-UTR was determined by a luciferase reporter assay, as described previously [12,13]. In brief, luciferase reporter constructs comprising the *XYLT1* 3'-UTR were co-transfected into SW1353 cells with miRNA-21 (UAGCUUAUCAGACUGAUGUUGA) or negative control miRNA for luciferase activity determination.

2.6 Statistical analyses

Data were expressed as means with standard error of the mean (SEM). Statistical analyses were conducted by Mann-Whitney *U* test using the software GraphPad Prism 8.0 (GraphPad Software, USA). The probability of $p<0.05$ was considered statistically significant.

3. Results

3.1 Increased XT-I activity in SScF involves cytokine-mediated effects

We used a myofibroblast cell culture model with NHDF and SScF to address the underlying cellular mechanisms of the increased serum XT activity in SSc [11]. The SScF showed a significantly 1.3±0.09-fold (p=0.0003) higher extracellular XT-I activity than NHDF under standardized cell culture conditions in fully supplemented growth medium for 96 h (**Fig. 1A**). After the same culture period, no intracellular XT-I activity differences were observed (**Fig. 1A**). Since most of the SScF characteristics can be mimicked by TGF-β cytokine treatment of NHDF [6,17], we hypothesized that the extracellular XT-I activity increase observed in SScF involves exogenous cytokine stimulation. In order to address this hypothesis, we cultured NHDF and SScF in serum-free growth medium with or without the addition of TGF-β1. After 120 h, NHDF and SScF showed no differences in extracellular or intracellular XT-I activity when grown in serum-free growth medium (**Fig. 1B**). By contrast, the supplementation of TGF-β1 compared to the respective control resulted in a 2.3±0.4-fold (p<0.0001) increase in extracellular XT-I activity of SScF, while NHDF showed a 1.6±0.2-fold (p=0.008) activity increase (**Fig. 1B**). Compared to untreated cells, SScF showed a significant 2.1±0.3-fold (p<0.0001) increase in intracellular XT-I activity by TGF-β1, whereas no significant TGF-β1-induced intracellular activity changes were observed in NHDF (**Fig. 1B**). These results demonstrate that TGF-β1 is a potent inducer of cellular XT-I activity in NHDF and SScF. In comparison to NHDF, SScF showed an enhanced XT-I activity induction by TGF-β1.

3.2 XYLT1 expression is regulated differentially by TGF-β1 and IL-1β in SScF

Since the extracellular XT-I activity increase may result from former *XYLT1* mRNA expression changes [6,9,12], we examined the direct impact of TGF-β1 treatment on the *XYLT1* mRNA expression of NHDF and SScF after 6 and 48 h. Consistent with the XT-I activity observed, NHDF and SScF showed no significant differences in basal X*YLT1* mRNA expression after the culture period of 6 h (**Fig. 2A**). Compared to NHDF, SScF showed a 1.4±0.2-fold (p=0.03) increase in X*YLT1* mRNA expression after 48 h (**Fig. 2B**). After 6 h, the supplementation of TGF-β1 resulted in a 4.4±0.9-fold (p<0.0001) increase in *XYLT1* mRNA expression of SScF, while NHDF showed a 2.9±0.5-fold (p=0.0003) expression increase compared to the untreated control (**Fig. 2A**). Compared to untreated cells after the culture period of 48 h, TGF-β1 treatment resulted in a significant 4.5±0.6-fold (p<0.0001) increase in *XYLT1* mRNA expression in SScF and a significant 5.7±1.4-fold (p < 0.0001) expression increase in NHDF (**Fig. 2B**). In addition to TGF-β1, we used the pro-inflammatory cytokine IL-1β, which had been shown to be increased in serum and skin samples of SSc patients [18,19]. In comparison to untreated control cells after 6 h, the IL-1β treatment resulted in a pronounced 1.9±0.3-fold (p<0.0001) *XYLT1* mRNA expression increase in SScF, whereas no significant *XYLT1* mRNA changes were detectable in NHDF (**Fig. 2A**). In relation to the untreated controls, IL-1β treatment of SScF for 48 h resulted in a significant 0.6±0.08-fold (p=0.0006) reduced *XYLT1* mRNA expression

level. The same treatment did not influence relative *XYLT1* mRNA expression in NHDF (**Fig. 2B**). We concluded that differences in cytokine-mediated effects on *XYLT1* mRNA expression might have contributed to the differences observed in extracellular XT-I activity in SScF and NHDF.

3.3 IL-1β-mediated TGFBR2 mRNA expression in SScF

Increased expression of TGF-β receptor II has been demonstrated in SScF [20,21]. The NHDF and SScF were cultured in the presence and absence of both TGF-β1 and IL-1β to address the impact of both cytokines on *TGFBR2*. The TGF-β1 treatment for 6 and 48 h failed to induce the *TGFBR2* expression of NHDF and SScF compared to controls (**Fig. 3A**,**B**). By contrast, after a cultivation period of 6 h, IL-1β was shown to stimulate *TGFBR2* expression by 1.7±0.3-fold (p=0.0008) in SScF but not in NHDF (**Fig. 3A**). The SScF showed a significant 2.6±0.4-fold (p<0.0001) increase in *TGFBR2* mRNA expression compared to NHDF after 48 h (**Fig. 3B**), that could not be observed after a cultivation period of 6 h. The IL-1β treatment for 48 h was shown to decrease *TGFBR2* mRNA expression in SScF by 0.8±0.09-fold (p=0.1) and not to influence the *TGFBR2* mRNA expression in NHDF (**Fig. 3B**). These results indicated a dual role for IL-1β in *XYLT1* expression regulation by influencing the relative *TGFBR2* expression in SScF.

3.4 Inverse association of basal *miRNA-21* and *TGFBR2 expression in SScF*

Previous studies demonstrated that the expression of miRNA-21 was downregulated by the IL-1β stimulation of chondrocytes [22]. Showing that IL-1β is capable of inducing *TGFBR2* expression in SScF, we hypothesized that this effect might be mediated by the miRNA-21. To test this hypothesis, we performed an *in silico* target prediction analyses ([16], **Tab. S2**) and experimentally transfected NHDF with a miRNA-21 inhibitor in the presence of TGF-β1 to resemble the potential IL-1β-mediated miRNA-21 decrease in SScF. Using the computational algorithm TargetScan 7.6 [16], we could demonstrate two putative miRNA-21 binding sites within the target gene *TGFBR2*. In addition, we could exclude a direct miRNA-21 binding to the 3'-UTR of *XYLT1* by reporter luciferase assay (**Fig. S1**). In comparison to inhibitor control transfected cells, miRNA-21 inhibitor transfection significantly increased *TGFBR2* mRNA expression by 1.1±0.07-fold (p=0.04) (**Fig. 4A**). Since an inverse relationship between the miRNA expression level and its putative target gene is anticipated (**Tab. S2**), we hypothesized that the former exposure of SScF to IL-1β *in vivo* could have led to a basal miRNA-21 decrease favoring a *TGFBR2* expression increase. We determined the basal *miRNA-21* and *TGFBR2* expression in SScF after a cultivation period of 3 h in serum-free medium to confirm this hypothesis. Using this approach, we detected a significantly 0.6±0.03-fold (p<0.0001) reduced basal *miRNA-21* expression and a simultaneous 1.8±0.1-fold (p<0.0001) increased *TGFBR2* mRNA expression in SScF compared to NHDF (**Fig. 4B**,**C**). We conclude from these experiments that miRNA-21 is an indirect regulator of *XYLT1* expression by functioning as an amplifying circuit to enhance fibrotic TGF-β signaling events in SSc.

4. Discussion

Systemic sclerosis is a severe fibrotic disease characterized by an excessive accumulation of ECM components, such as PGs and collagens, in the skin and internal organs. Among the disease effector cells, myofibroblasts are considered to play a key role in the development of fibrosis in SSc and other fibrosing conditions [23,24]. Since the disease phenotype of SScF can be retained upon *in vitro* culture [23], these cells provide a valuable tool for therapeutic target discovery and studying disease mechanisms [24]. One of several myofibroblast biomarkers is human XT-I, which is the initial enzyme in PG biosynthesis [9]. Patients with SSc show an increased serum activity of XT [11], but the underlying cellular mechanisms leading to this increase remain elusive.

In this study, we have demonstrated an increased extracellular XT-I activity in SScF compared to NHDF when grown in the presence of fetal calf serum (FCS), while no extracellular XT-I activity differences were observed when grown in the absence of FCS. Since FCS contains cytokines and growth factors that activate intracellular transduction pathways [25], it can be concluded that the differences in extracellular XT-I activity observed may involve variations in cellular responses of NHDF and SScF towards exogenous cytokines. A cytokine-mediated increase in extracellular XT activity correlates with an intracellular XT activity or *XYLT1* mRNA increase [6,8,9]. Therefore, it could be possible that an enhanced cytokine-mediated *XYLT1* expression might have contributed to the XT-I activity differences in SScF and NHDF observed in this study. This conclusion was strengthened by treating NHDF and SScF with TGF-β1, a potent inducer of XT-I expression in NHDF [9]. Upon TGF-β1 treatment, SScF showed an enhanced relative *XYLT1* expression increase after 6 h and a higher extracellular and intracellular XT-I activity induction after 120 h compared to NHDF. Since there was no difference between SScF and NHDF in the production of total TGF-β1 and active TGF-β1 *in vitr*o [20], it could be thought that the increased fibroblast activation and XT-I induction in SSc may be a result of enhanced autocrine TGF-β signaling. A critical mechanism for regulating the cellular response towards cytokines and growth factors resides at the level of receptor expression [26]. The IL-1β was found to be increased in skin and serum in patient with SSc [18,19]. In our present study, IL-1β was capable of inducing *TGFBR2* expression in SScF after 6 h and slightly decreased it after 48 h in SScF. Consistent with the IL-1β-mediated effect on *TGFBR2* mRNA expression in SScF, IL-1β increased the *XYLT*1 mRNA expression significantly after 6 h and slightly decreased it after 48 h in SScF. On the contrary, IL-1β did not change the relative *TGFBR2* or *XYLT1* expression in NHDF. The results of the IL-1β-induced *XYLT1* expression in SScF are in line with the results from Khair et al. in primary chondrocytes using the same IL-1β concentration but a detection time of 6 and 24 h [27]. Our observation that the IL-1β treatment of NHDF did not considerably change the *XYLT1* mRNA expression is consistent with that reported by Mia et al., who found that IL-1β alone has no obvious pro-fibrotic effect on NHDF [28]. In addition, Mia et al. also showed that IL-1β is capable of inhibiting the TGF-β1-induced myofibroblast formation [28], which might explain the IL-1β-mediated *XYLT1* mRNA expression decrease observed in SScF after 48 h. Therefore, IL-1β has a dual effect

on *XYLT1* mRNA expression that may depend on the presence of cytokine TGF-β1. This hypothesis was strengthened by the finding that, despite the use of serum-free growth medium, a relative increase in the *XYLT1* or *TGFBR2* mRNA expression could be observed in SScF after 48 h. These relative increases may result from a higher activin A or IL-1β secretion by SScF [17–19]. In order to determine an almost cytokine-independent basal *TGFBR2* expression in NHDF and SScF, cells were maintained in serum-free growth medium for a minimum of 3 h after serum-starvation. In concordance with the literature [21], we have found that *TGFBR2* is expressed at higher levels in SScF than NHDF despite using cytokine-free culture conditions. After showing that IL-1β is capable of inducing *TGFBR2* expression in SScF, we determined the expression of *miRNA-21* that had been shown previously to be downregulated by IL-1β [22] and an experimentally validated transcriptional regulator of *TGFBR2* [29]. In contrast to previous studies that demonstrated a significantly upregulated *miRNA-21* expression in SScF cultured in the presence of FCS [4], our study showed a significant decreased basal *miRNA-21* expression in SScF compared to NHDF under cytokine-free culture conditions. Therefore, the higher responsiveness of SScF towards exogenous TGF-β1 observed in our myofibroblast model may involve elevated *TGFBR2* expression that was initiated by a former *in vivo* exposure of SScF to IL-1β. Since fibrosis is accompanied by a TGF-β1-induced increase in *miRNA-21* and *XYLT1* expression [15], we analyzed whether the IL-1β-induced miRNA-21 decrease [22] in the presence of TGF-β1 participates in abnormal XT regulation in fibrosis in SSc. We demonstrated that miRNA-21 inhibitor transfection, mimicking the effects of IL-1β on *miRNA-21* expression, significantly increased *TGFBR2* mRNA in NHDF in comparison to control transfected cells.

Taken together, our results indicate that increased XT-I expression in SScF involves a dysregulated autocrine TGF-β signaling that includes IL-1β-mediated effects on *miRNA-21* and *TGFBR2* expression. Therefore, the results shed light on an aberrant fibrogenic pathway in SScF, the key effector cells of fibrosis, that may contribute to the former increase in serum XT activity observed in SSc.

Acknowledgements

We thank Philip Saunders for linguistic advice and Christoph Lichtenberg for technical assistance. This work was supported by grant FA 1381/1-1 of the German Research Foundation.

References

[1] Y. Allanore, R. Simms, O. Distler, M. Trojanowska, J. Pope, C.P. Denton, J. Varga, Systemic sclerosis, Nat. Rev. Dis. Primer. 1 (2015) 15002. https://doi.org/10.1038/nrdp.2015.2.

[2] H. Butz, K. Rácz, L. Hunyady, A. Patócs, Crosstalk between TGF-β signaling and the microRNA machinery, Trends Pharmacol. Sci. 33 (2012) 382–393. https://doi.org/10.1016/j.tips.2012.04.003.

[3] H. Shan, Y. Zhang, Y. Lu, Y. Zhang, Z. Pan, B. Cai, N. Wang, X. Li, T. Feng, Y. Hong, B. Yang, Downregulation of miR-133 and miR-590 contributes to nicotine-induced atrial remodelling in canines, Cardiovasc. Res. 83 (2009) 465–472. https://doi.org/10.1093/cvr/cvp130.

[4] H. Zhu, Y. Li, S. Qu, H. Luo, Y. Zhou, Y. Wang, H. Zhao, Y. You, X. Xiao, X. Zuo, MicroRNA Expression abnormalities in limited cutaneous scleroderma and diffuse cutaneous scleroderma, J. Clin. Immunol. 32 (2012) 514–522. https://doi.org/10.1007/s10875-011-9647-y.

[5] S. Ghatak, E.V. Maytin, J.A. Mack, V.C. Hascall, I. Atanelishvili, R. Moreno Rodriguez, R.R. Markwald, S. Misra, Roles of proteoglycans and glycosaminoglycans in wound healing and fibrosis, Int. J. Cell Biol. 2015 (2015) 1–20. https://doi.org/10.1155/2015/834893.

[6] T.-D. Ly, R. Plümers, B. Fischer, V. Schmidt, D. Hendig, J. Kuhn, C. Knabbe, I. Faust, Activin A-mediated regulation of XT-I in human skin fibroblasts, Biomolecules. 10 (2020) 609. https://doi.org/10.3390/biom10040609.

[7] C. Götting, J. Kuhn, R. Zahn, T. Brinkmann, K. Kleesiek, Molecular cloning and expression of human UDP-D-xylose:Proteoglycan core ürotein β-D-xylosyltransferase and its first isoform XT-II, J. Mol. Biol. 304 (2000) 517–528. https://doi.org/10.1006/jmbi.2000.4261.

[8] C. Prante, H. Milting, A. Kassner, M. Farr, M. Ambrosius, S. Schön, D.G. Seidler, A.E. Banayosy, R. Körfer, J. Kuhn, K. Kleesiek, C. Götting, Transforming growth Factor β1-regulated xylosyltransferase I activity in human cardiac fibroblasts and its impact for myocardial remodeling, J. Biol. Chem. 282 (2007) 26441–26449. https://doi.org/10.1074/jbc.M702299200.

[9] I. Faust, C. Roch, J. Kuhn, C. Prante, C. Knabbe, D. Hendig, Human xylosyltransferase-I – A new marker for myofibroblast differentiation in skin fibrosis, Biochem. Biophys. Res. Commun. 436 (2013) 449–454. https://doi.org/10.1016/j.bbrc.2013.05.125.

[10] C. Pönighaus, J. Kuhn, K. Kleesiek, C. Götting, Involvement of a cysteine protease in the secretion process of human xylosyltransferase I, Glycoconj. J. 27 (2010) 359–366. https://doi.org/10.1007/s10719-010-9283-4.

[11] C. Götting, S. Sollberg, J. Kuhn, C. Weilke, C. Huerkamp, T. Brinkmann, T. Krieg, K. Kleesiek, Serum xylosyltransferase: a new biochemical marker of the sclerotic process in systemic sclerosis, J. Invest. Dermatol. 112 (1999) 919–924. https://doi.org/10.1046/j.1523-1747.1999.00590.x.

[12] T.-D. Ly, L. Riedel, B. Fischer, V. Schmidt, D. Hendig, J. Distler, J. Kuhn, C. Knabbe, I. Faust, microRNA-145 mediates xylosyltransferase-I induction in myofibroblasts via suppression of transcription factor KLF4, Biochem. Biophys. Res. Commun. 523 (2020) 1001–1006. https://doi.org/10.1016/j.bbrc.2019.12.120.

[13] L. Riedel, B. Fischer, T.-D. Ly, D. Hendig, J. Kuhn, C. Knabbe, I. Faust, microRNA-29b mediates fibrotic induction of human xylosyltransferase-I in human dermal fibroblasts via the Sp1 pathway, Sci. Rep. 8 (2018) 17779. https://doi.org/10.1038/s41598-018-36217-2.

[14] M.W. Pfaffl, A new mathematical model for relative quantification in real-time RT-PCR, Nucleic Acids Res. 29 (2001) 45e–445. https://doi.org/10.1093/nar/29.9.e45.

[15] T.-D. Ly, A. Kleine, B. Fischer, V. Schmidt, D. Hendig, J. Kuhn, C. Knabbe, I. Faust, Identification of putative non-substrate-based XT-I inhibitors by natural product library screening, Biomolecules. 10 (2020) 1467. https://doi.org/10.3390/biom10101467.

[16] V. Agarwal, G.W. Bell, J.-W. Nam, D.P. Bartel, Predicting effective microRNA target sites in mammalian mRNAs, ELife. 4 (2015). https://doi.org/10.7554/eLife.05005.

[17] K. Takagi, Y. Kawaguchi, M. Kawamoto, Y. Ota, A. Tochimoto, T. Gono, Y. Katsumata, M. Takagi, M. Hara, H. Yamanaka, Activation of the Activin A-ALK-Smad pathway in systemic sclerosis, J. Autoimmun. 36 (2011) 181–188. https://doi.org/10.1016/j.jaut.2010.09.004.

[18] M.R. Hussein, Alterations of mononuclear inflammatory cells, CD4/CD8+ T cells, interleukin 1 , and tumour necrosis factor in the bronchoalveolar lavage fluid, peripheral blood, and skin of patients with systemic sclerosis, J. Clin. Pathol. 58 (2005) 178–184. https://doi.org/10.1136/jcp.2004.019224.

[19] M.A. Martínez-Godínez, M.P. Cruz-Domínguez, L.J. Jara, A. Domínguez-López, R.A. Jarillo-Luna, O. Vera-Lastra, D.H. Montes-Cortes, R. Campos-Rodríguez, D.M. López-Sánchez, C.M. Mejía-Barradas, E.E. Castelán-Chávez, A. Miliar-García, Expression of NLRP3 inflammasome, cytokines and vascular mediators in the skin of systemic sclerosis patients, Isr. Med. Assoc. J. IMAJ. 17 (2015) 5–10.

[20] H. Ihn, K. Yamane, M. Kubo, K. Tamaki, Blockade of endogenous transforming growth factor beta signaling prevents up-regulated collagen synthesis in scleroderma fibroblasts: association with increased expression of transforming

growth factor beta receptors, Arthritis Rheum. 44 (2001) 474–480. https://doi.org/10.1002/1529-0131(200102)44:2<474::AID-ANR67>3.0.CO;2-#.

[21] M. Kubo, H. Ihn, K. Yamane, K. Tamaki, Upregulated expression of transforming growth factor-beta receptors in dermal fibroblasts of skin sections from patients with systemic sclerosis, J. Rheumatol. 29 (2002) 2558–2564.

[22] H. Zhu, X. Yan, M. Zhang, F. Ji, S. Wang, miR-21-5p protects IL-1β-induced human chondrocytes from degradation, J. Orthop. Surg. 14 (2019) 118. https://doi.org/10.1186/s13018-019-1160-7.

[23] L. Chadli, B. Sotthewes, K. Li, S.N. Andersen, E. Cahir-McFarland, M. Cheung, P. Cullen, A. Dorjée, J.K. de Vries-Bouwstra, T.W.J. Huizinga, D.F. Fischer, J. DeGroot, J.L. Viney, T.S. Zheng, J. Aarbiou, A. Gardet, Identification of regulators of the myofibroblast phenotype of primary dermal fibroblasts from early diffuse systemic sclerosis patients, Sci. Rep. 9 (2019) 4521. https://doi.org/10.1038/s41598-019-41153-w.

[24] S.M. Garrett, D. Baker Frost, C. Feghali-Bostwick, The mighty fibroblast and its utility in scleroderma research, J. Scleroderma Relat. Disord. 2 (2017) 100–107. https://doi.org/10.5301/jsrd.5000240.

[25] F. Boraldi, G. Annovi, C. Paolinelli-Devincenzi, R. Tiozzo, D. Quaglino, The effect of serum withdrawal on the protein profile of quiescent human dermal fibroblasts in primary cell culture, PROTEOMICS. 8 (2008) 66–82. https://doi.org/10.1002/pmic.200700833.

[26] L. Lillien, Changes in retinal cell fate induced by overexpression of EGF receptor, Nature. 377 (1995) 158–161. https://doi.org/10.1038/377158a0.

[27] M. Khair, M. Bourhim, L. Barré, D. Li, P. Netter, J. Magdalou, S. Fournel-Gigleux, M. Ouzzine, Regulation of xylosyltransferase I gene expression by interleukin 1β in human primary chondrocyte cells: Mechanism and impact on proteoglycan synthesis, J. Biol. Chem. 288 (2013) 1774–1784. https://doi.org/10.1074/jbc.M112.419887.

[28] M.M. Mia, M. Boersema, R.A. Bank, Interleukin-1β attenuates myofibroblast formation and extracellular matrix production in dermal and lung fibroblasts exposed to transforming growth factor-β1, PLoS ONE. 9 (2014) e91559. https://doi.org/10.1371/journal.pone.0091559.

[29] S. Mishra, J.J. Deng, P.S. Gowda, M.K. Rao, C.-L. Lin, C.L. Chen, T. Huang, L.-Z. Sun, Androgen receptor and microRNA-21 axis downregulates transforming growth factor beta receptor II (TGFBR2) expression in prostate cancer, Oncogene. 33 (2014) 4097–4106. https://doi.org/10.1038/onc.2013.374.

Figures/Table Legends

Fig. 1: Cytokine-mediated increase of extracellular XT-I activity in SScF. NHDF (n=3) and SScF (n=3) were cultured for 24 h before the experiment. (**A**) Cells were maintained in growth medium for an additional 96 h. (**B**) Cells were serum-starved for 24 h and treated with serum-free medium containing TGF-β1 (5 µg/L) or vehicle for 120 h. Intra- and extracellular XT-I activity was measured in cell lysates (intra) and cell culture supernatants (extra) by UPLC-ESI-MS/MS assay and expressed as arbitrary unit (AU)/µg protein or DNA. Values shown are means±SEM for three biological and (**A**) three or (**B**) two technical replicates per experiment. Mann-Whitney *U* test: not significant (ns), ***p*<0.01, ****p*<0.001, *****p*<0.0001.

Fig. 2: Differences in TGF-β1- und IL-1 β-induced *XYLT1* mRNA expression in NHDF and SScF. NHDF (n=3) and SScF (n=3) were cultured for 24 h before the experiment. Cells were serum-starved for 24 h and treated with TGF-β1 (5 µg/L), IL-1β (10 µg/L) or vehicle for (**A**) 6 h and (**B**) 48 h. Relative mRNA expression levels of *XYLT1* were analyzed by qRT-PCR. Values shown are means±SEM for three biological and three technical replicates per experiment. Mann-Whitney *U* test: not significant (ns), ***p*<0.01, ****p*<0.001, *****p*<0.0001.

Fig. 3: IL-1β-induced *TGFBR2 mRNA* expression in SScF. NHDF (n=3) and SScF (n=3) were cultured for 24 h before the experiment. Cells were serum-starved for 24 h and treated with TGF-β1 (5 µg/L), IL-1β (10 µg/L) or vehicle for (**A**) 6 h and (**B**) 48 h. Relative *TGFBR2* mRNA expression levels were analyzed by qRT-PCR. Values shown are means±SEM for three biological and three technical replicates per experiment. Mann-Whitney *U* test: not significant (ns), ***p*<0.01, ****p*<0.001, *****p*<0.0001.

Fig. 4: Reciprocal basal *miR-21* and *TGFBR2* mRNA expression in SScF. (**A**) NHDF (n=3) were transfected with miRNA-21 inhibitor (miR-21 inhibitor) or miRNA inhibitor control (miR IC). After 24 h, the transfection medium was replaced with serum-free medium for 24 h. (**B**,**C**) NHDF (n=3) and SScF (n=3) were cultured for 24 h before the experiment. Cells were serum-starved for 24 h and maintained in serum-free medium for an additional 3 h. Relative (**B**) *miRNA-21* and (**A**,**C**) *TGFBR2* expression levels were analyzed by qRT-PCR. Values shown are means±SEM for three biological and three technical replicates per experiment. Mann-Whitney *U* test: ***p*<0.01, ****p*<0.001, *****p*<0.0001.

Figures/Tables

Figure 1

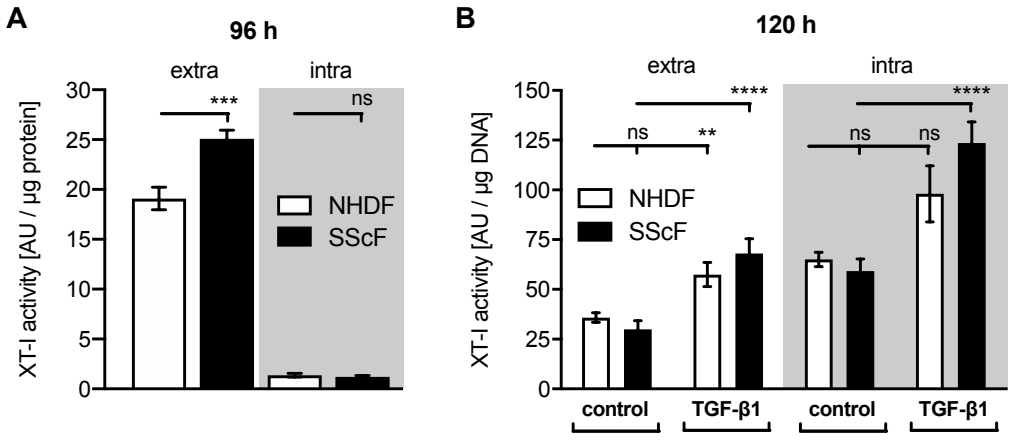

Figure 2

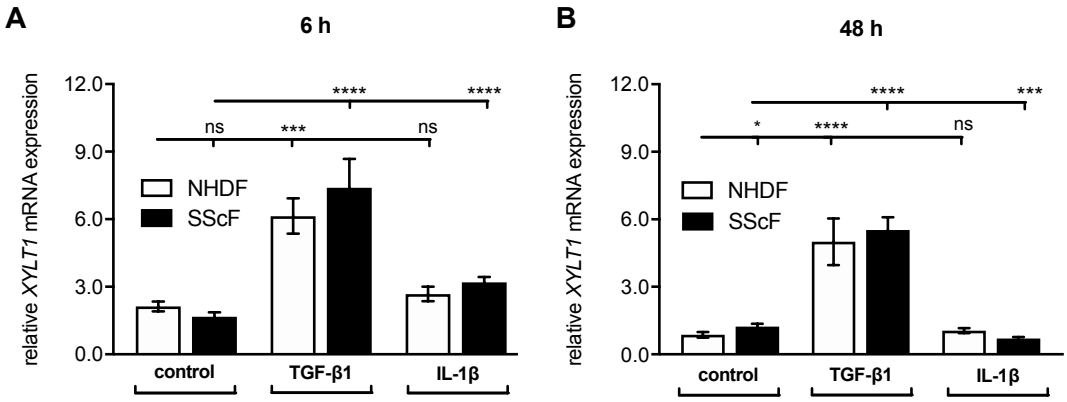

Figure 3

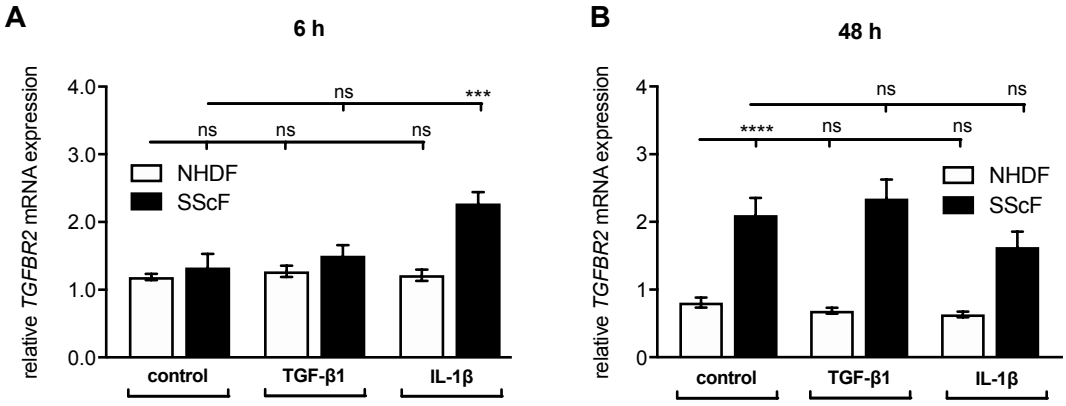

Figure 4

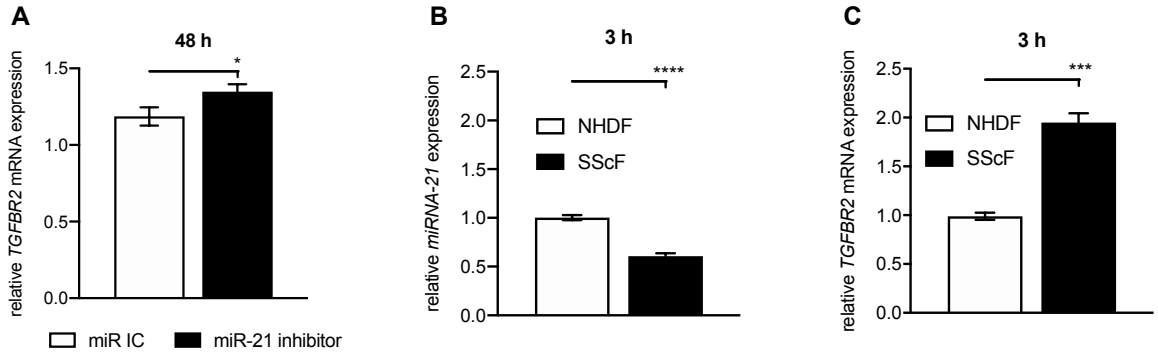
A
48 h
*
relative TGFBR2 mRNA expression
1.5
1.0
0.5
0.0
miR IC
miR-21 inhibitor
B
3 h
****
relative miRNA-21 expression
2.5
2.0
1.5
1.0
0.5
0.0
NHDF
SScF
C
3 h
***
relative TGFBR2 mRNA expression
2.5
2.0
1.5
1.0
0.5
0.0
NHDF
SScF

3.3 Publikation III

MicroRNA-145 vermittelt die Xylosyltransferase-I-Induktion in Myofibroblasten über die Suppression des Transkriptionsfaktors KLF4

(Ly *et al.*, 2020c)

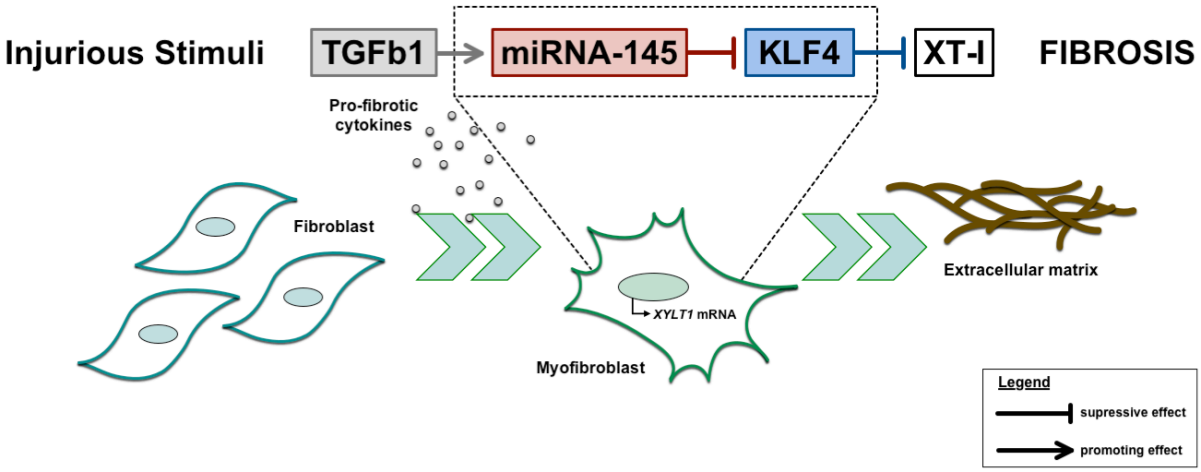

Abbildung 7: *Graphical Abstract* von Publikation III (Ly *et al.*, 2020c).

Biochemical and Biophysical Research Communications 523 (2020) 1001–1006

Contents lists available at ScienceDirect

Biochemical and Biophysical Research Communications

journal homepage: www.elsevier.com/locate/ybbrc

microRNA-145 mediates xylosyltransferase-I induction in myofibroblasts via suppression of transcription factor KLF4

Thanh-Diep Ly [a], Lara Riedel [a], Bastian Fischer [a], Vanessa Schmidt [a], Doris Hendig [a], Jörg Distler [b], Joachim Kuhn [a], Cornelius Knabbe [a], Isabel Faust [a, *]

[a] Institut für Laboratoriums- und Transfusionsmedizin, Herz- und Diabeteszentrum Nordrhein-Westfalen, Universitätsklinik der Ruhr-Universität Bochum, Georgstraße 11, 32545, Bad Oeynhausen, Germany
[b] Department of Internal Medicine 3 – Rheumatology and Immunology, Friedrich-Alexander-University Erlangen-Nürnberg, 91054, Erlangen, Germany

ARTICLE INFO

Article history:
Received 3 December 2019
Accepted 28 December 2019
Available online 20 January 2020

Keywords:
Fibrosis
Krueppel-like factor 4
microRNA-145
Systemic sclerosis
TGFβ
Xylosyltransferase

ABSTRACT

Remodelling of the extracellular matrix by myofibroblasts is crucial for wound repair, but if deregulated, it might contribute to the development of fibrosis. Fibroblast-to-myofibroblast differentiation is promoted by aberrant microRNA-145-5p (miR-145) expression in response to transforming growth factor β1 (TGFβ1). One of several myofibroblast markers is human xylosyltransferase-I (XT-I), which is the initial and rate-limiting enzyme of proteoglycan biosynthesis. Increased serum XT activity was quantified in patients with systemic sclerosis (SSc), but the underlying cellular mechanism of this disease remains unknown. This study aims to determine the underlying molecular basis of XT-I induction by considering the miR-mediated regulation of XT-I. We found that miR-145 is upregulated in TGFβ1-treated dermal fibroblasts and correlates with an increased cellular *XYLT1* expression and XT activity. Overexpression of miR-145 in dermal fibroblasts induced *XYLT1* expression and XT activity and enhanced TGFβ1-promoted XT activity increase. Since direct *XYLT1* 3′-UTR targeting by miR-145 could be experimentally excluded, an indirect effect of miR-145 on XT-I regulation was indicated. We identified six transcription factor-binding sites for Krueppel-like factor 4 (KLF4), a zinc-finger transcription regulator and putative miR-145 target, in the *XYLT1* promoter *in silico*. A suppressive role of KLF4 on *XYLT1* expression was confirmed by targeted gene silencing in dermal fibroblasts and the quantification of *KLF4* expression in SSc fibroblasts. Taken together, this study improves the mechanistic understanding of fibrotic remodelling in SSc by identifying a hitherto unknown miR-145/KLF4 pathway mediating the fibrogenic XT-I induction. This knowledge on *XYLT1* may lead to the development of novel approaches in the therapy of fibrosis.

1. Introduction

Fibrotic disorders are characterized by the excessive deposition of extracellular matrix (ECM) components like collagen and proteoglycans (PG), leading to a loss of proper organ function. Fibrosis is a hallmark of numerous human diseases, such as hypertrophic scarring or systemic sclerosis (SSc). A key event in this process remains the differentiation of fibroblasts to α-smooth muscle actin (α-SMA)-positive myofibroblasts, which synthesize vast amounts of ECM and cytokines, actively contributing to tissue remodelling. Among the cytokines found increased in fibrotic tissues, transforming growth factor β1 (TGFβ1) is considered the most relevant [1]. The TGFβ1 modulates a number of other cytokines and regulatory elements, such as microRNAs (miRNA). miRNAs are small noncoding endogenous RNAs which are important post-transcriptional gene regulators. They bind to the 3′-untranslated regions (UTR) of target mRNAs, preventing the translation or leading to the degradation of the respective mRNAs. Aberrant miRNA expression levels have been reported in a wide range of diseases including fibrosis. Therefore, crosstalk between the TGFβ1 signalling and the miRNA machinery is essential for ECM homeostasis [2]. Alterations of the TGFβ pathways in fibrosis result in constitutive fibroblast activation promoting pathological ECM remodelling. One triggering event reveals the abnormal expression of microRNA-145-5p (miR-145), which has been found to be upregulated by TGFβ stimulation in myofibroblasts derived from SSc patients [3,4]. The knowledge about direct and indirect targets of this miRNA that contributes to fibrosis will facilitate the

* Corresponding author.
E-mail address: ifaust@hdz-nrw.de (I. Faust).

https://doi.org/10.1016/j.bbrc.2019.12.120
0006-291X/

Abbreviations

α-SMA	α-smooth muscle actin
UTR	untranslated regions
dpm	disintegrations per minute
ECM	extracellular matrix
KLF4	Krüppel-like factor 4
miR-145	microRNA-145-5p
miRNA	microRNA
NHDF	normal human dermal fibroblast
PG	proteoglycan
qRT-PCR	quantitative real-time polymerase chain reaction
SEM	standard error of the mean
siRNA	small interfering RNA
SSc	systemic sclerosis
SScF	SSc fibroblasts
TGFβ1	transforming growth factor β1
XT-I	xylosyltransferase-I

development of selective therapeutic strategies. One known miR-145 target is Krüppel-like factor 4 (KLF4), a zinc-finger transcription factor expressed in a variety of tissues including the skin [3,5]. The KLF4 also plays an important role in induced pluripotent stem cells [6]. In the context of fibrosis, miR-145 expression increases α-SMA and collagen expression in myofibroblasts via suppression of KLF4 expression [3,7].

Serum analysis from SSc patients revealed an increase in the activity of xylosyltransferase (XT; EC 2.4.2.26), which is the initial key enzyme in PG biosynthesis, therefore, contributing to the increase PG synthesis and accumulation in fibrotic tissue [8–10]. Despite the intracellular localization of the XT, the enzyme is shed from the membrane of the Golgi apparatus and secreted into the extracellular space. Therefore, XT activity can be quantified in human serum and provides a reliable indicator of the present PG synthesis rate. Two distinct XT isoforms, XT-I and XT-II encoded by the *XYLT1* and *XYLT2* gene, exist in humans. Pro-fibrotic TGFβ1 stimulation has been shown to increase *XYLT1* mRNA expression and XT activity in skin and cardiac fibroblasts, while *XYLT2* is unaffected by TGFβ1. In summary, only XT-I is associated with fibrotic remodelling and provides a reliable marker for myofibroblast differentiation [11]. Given the missing link between the fibrotic XT activity increase and the underlying mechanisms in myofibroblasts, the present study aimed to investigate the role of an aberrant TGFβ/miR-145 pathway in this context.

2. Materials and methods

2.1. Materials

Recombinant human TGFβ1 was purchased from Miltenyi Biotec (GER). miRNAs, small interfering RNAs (siRNA), transfection reagents and media were obtained from ThermoFisher (USA).

2.2. Cell culture, transfection and treatment

Normal human dermal fibroblasts (NHDF) were obtained from Genlantis and Coriell (USA). Age-, sex- and biopsy side-matched diffuse cutaneous type SSc fibroblasts (SScF) were kindly provided by Prof. Jörg Distler from University Hospital Erlangen (GER). The usage of SScF was approved by the local ethical committee. The NHDF were maintained in Dulbecco's modified Eagle's medium (ThermoFisher, USA), as described previously [12]. For cytokine treatment, 50 cells/mm^2 were cultured for 24 h and serum-starved for another 24 h. Thereafter, TGFβ1 (5 μg/L) or vehicle supplemented media was added for 48, 72 or 144 h until cell lysis. For siRNA delivery, 2.9 × 10^5 cells were maintained in antibiotic-free medium and reverse-transfected using Lipofectamine 2000. The transfection mixture contained a siRNA targeting KLF4 (sense: GGGUAUAAAUUAUAUCCGUtt; antisense: ACGGAUAUAAUUUAUACCCtg) or a non-targeting negative control siRNA diluted in Opti-MEM I Reduced Serum Medium (final siRNA concentration: 50 nmol/L). Transfected cells were serum-starved for 16 h and treated with TGFβ1 (5 μg/L) for 6 h. An amount of 50 cells/mm^2 were transfected with a miR-145 mimic (GUCCAGUUUUCCCAGGAAUCCCU) or the corresponding miRNA negative control, as described above, to analyse the effect of miRNAs under TGFβ1 supplementation. Six or 24 h post-transfection cells were stimulated with TGFβ1 or vehicle supplemented media for 48 or 144 h.

2.3. Nucleic acid extraction and synthesis of complementary DNA

Cell lysis, RNA extraction from cell lysates and the corresponding cDNA synthesis for mRNA and miRNA expression analysis was performed as described previously [12].

2.4. mRNA and miRNA expression analyses

Quantitative real-time polymerase chain reaction (qRT-PCR) analysis was performed, as described previously [12]. Additional primer sequences are listed in Table S1. The geometric mean of the expression levels of three of the following housekeeping genes: *SDHA*, *RPL13A*, *B2M*, *HPRT* or *GAPDH* was calculated for expression normalization. The relative target gene mRNA expressions were determined by the $\Delta\Delta C_T$ method considering the PCR efficiency [13]. The TaqMan advanced miRNA Assay (ThermoFisher, USA) was performed, according to the manufacturer's instructions, for the miRNA expression analyses. The following primer assays were used: miR-145 (477916_mir) and miR-191 (477952_mir). The expression level of miR-145 was normalized to internal control gene expression of miRNA-191 via the $\Delta\Delta C_T$ method. All normalized gene expression levels were referred to the respective target gene expression of one sample for relative comparison of multiple biological samples per experiment.

2.5. XT activity assay

The determination of XT activity from cell supernatants was performed by radiochemical determination of enzyme catalysed incorporation of UDP-[^{14}C]-D-xylose (PerkinElmer, USA) into silk fibroin acceptor protein, as described previously [14]. The quantified disintegrations per minute (dpm) were referred to total DNA sample content and resemble the quantity of incorporated UDP-[^{14}C]-D-xylose which is proportional to the sample XT activity.

2.6. Bioinformatic analysis

The computational algorithms TargetScan (http://www.targetscan.org; 2019-10-28) [15], miRDB (http://mirdb.org/; 2019-10-28) [16] and miRwalk (http://zmf.umm.uni-heidelberg.de/; 2019-10-28) [17] were utilised to predict the probability of a functional miR-145 binding site within a given mRNA target. The *in silico* analysis of transcription factor binding sites in the full length *XYLT1* promoter [18] described previously was performed with the Genomatix software suite MatInspector v3.9 [19].

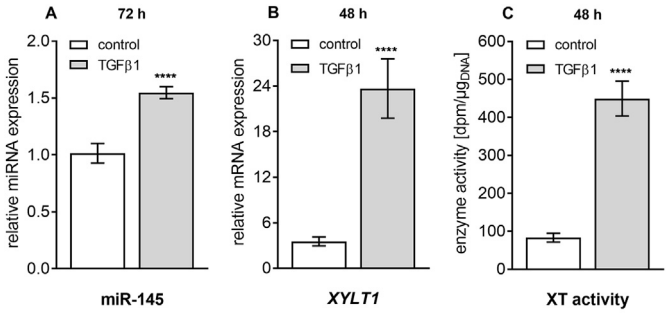

Fig. 1. TGFβ1 upregulates miR-145 and myofibroblast marker XT-I. The NHDF were cultured for 24 h before the experiment. Cells were serum-starved for 24 h and treated with TGFβ1 or vehicle for the time points indicated. (**A**) miR-145 expression levels (n = 2) were analysed by qRT-PCR using Taqman probes. (**B**) Relative mRNA expression levels of *XYLT1* (n = 4) were analysed by qRT-PCR. (**C**) XT activity was measured in cell supernatants (n = 2) by radiochemical enzyme assay and expressed as dpm/μg of DNA. Values shown are means ± SEM for three biological and technical replicates per experiment. Mann-Whitney *U* test: ****P < 0.0001.

2.7. Verification of miR-145 binding to the 3′-UTR of XYLT1

The experimental validation of miR-145 interaction with *XYLT1* transcripts was assessed by the reporter system, as described previously [12]. Briefly, luciferase reporter constructs harbouring the *XYLT1* 3′-UTR were transfected into host SW1353 cells with miRNA mimics and luciferase activity was determined.

2.8. Statistical analyses

Data are expressed as mean values ± standard error of the mean (SEM). Statistical analysis was performed by the Mann-Whitney *U* test using GraphPad Prism 7.0 (GraphPad Software, USA) software. The probability P values of less than 0.05 were considered as statistically significant and indicated with asterisks and horizontal lines that connect the bars. Asterisks above the error bars of the treatment group indicate statistical differences between treatment and control groups, respectively.

3. Results

3.1. TGFβ1 upregulates miR-145 and XT-I in NHDF

miR-145 expression has previously been shown to be increased in tissue samples of patients with idiopathic pulmonary fibrosis compared to healthy controls [7]. Taqman-based gene expression analysis was performed to verify this in our myofibroblast cell culture model. We found that miR-145 expression was increased by 1.5 ± 0.1-fold (P < 0.0001) in NHDF after TGFβ1 supplementation (Fig. 1A). Furthermore, TGFβ1 treatment significantly increased the *XYLT1* expression by 6.7 ± 1.6-fold (P < 0.0001) compared to untreated cells (Fig. 1B). The relative *XYLT2* expression was unchanged by TGFβ1 treatment (Fig. S1A). The determination of corresponding extracellular XT activity depicted a 5.4 ± 0.9-fold (P < 0.0001) increase compared to cells cultivated without TGFβ1 (Fig. 1C). The TGFβ1 treatment also increased the myofibroblast marker *ACTA2* expression by 5.0 ± 1.4-fold (P = 0.001) (Fig. S1B). Taken together, our cell culture system represents a suitable model to study the relationship between the fibrotic TGFβ1-induced miR-145 expression increase and TGFβ1-mediated XT-I upregulation.

3.2. XT-I regulation by miR-145

Showing that TGFβ1 is a potent inducer of miR-145 and XT-I, we further examined the direct impact of miR-145 on *XYLT1* expression and XT activity. Therefore, NHDF were transfected with a miR-145 mimic to resemble the fibrotic miRNA increase. In comparison to negative control miRNA-transfected cells, miR-145 transfection strongly increased *XYLT1* mRNA expression by 4.3 ± 0.6-fold (P < 0.0001) (Fig. 2A). In accordance with these changes, XT activity was increased by 1.5 ± 0.3-fold (P = 0.03) in cell culture supernatants of miR-145-treated cells compared to the control (Fig. 2B). Next, we analysed the impact of miR-145 overexpression on the induced XT activity increase by TGFβ1. We observed an XT activity increase by 4.2 ± 0.3-fold (P < 0.0001) in TGFβ1-treated cells compared to the control. This TGFβ1-mediated XT activity increase was enhanced by 1.3 ± 0.09-fold (P = 0.01) in miR-145-transfected cells (Fig. 2C). The *XYLT2* mRNA expression was unaffected by TGFβ1 supplementation or by additional miR-145 overexpression of TGFβ1-treated cells (Fig. S2A). Furthermore, we observed that the TGFβ1-induced *ACTA2* expression increase by 2.9 ± 0.6-fold (P = 0.03) was enhanced by 1.8 ± 0.5-fold (P = 0.03) in miR-145-transfected cells (Fig. S2B). We conclude from these experiments that miR-145 itself is not only a potent inducer of *XYLT1* mRNA expression and XT activity, but can also increase TGFβ1-mediated XT activity in NHDF.

3.3. XYLT1 expression is indirectly regulated by miR-145

Since an inverse relationship between the miRNA expression level and its putative target gene is anticipated, we hypothesized that *XYLT1* is an indirect target of miR-145. We performed two approaches to confirm this hypothesis: an *in silico* analysis to identify *XYLT1* as prospective miR-145 target and an experimental validation of miR-145 binding to the 3′-UTR of *XYLT1*. None of the target prediction algorithms used, except TargetScan 7.2 (Table 1), depicted *XYLT1* as a putative miR-145 target. A reporter luciferase assay excluded the direct binding of miR-145 to the 3′-UTR of *XYLT1*, which was in agreement with most of the computational results obtained (Fig. S3).

3.4. KLF4 is a negative regulator of XYLT1 expression

As microRNAs act by inhibiting translation and/or promoting degradation of their target mRNAs, we suggested that this indirect *XYLT1* regulation by miR-145 might be mediated via down-regulation of an inhibitory transcription factor. This hypothesis was evaluated by computational miR-145 target identification, literature search and *in silico* analysis of transcription factor binding sites in the *XYLT1* promoter region. The resulting comparison of the *in silico* miRNA target prediction analysis by TargetScan 7.2 (Table 1) and the search for transcription factor binding sites by MatInspector (Table 2), identified KLF4 as the overlapping target. Our literature-based analysis, focusing on experimental cell culture data of miR-145 overexpression or inhibition experiments and luciferase assays, revealed numerous previous studies (Table S2), which have experimentally approved *KLF4* as a direct miR-145 target gene [5-7,27-31].

Since *XYLT1* promoter region harbours six predicted KLF4 binding sites (Table 2), we further elucidated the function of KLF4 in fibrogenic *XYLT1* induction by targeted gene silencing. After KLF4 siRNA transfection, the basal *KLF4* expression of NHDF was knocked down by 0.1 ± 0.01-fold (P < 0.0001). The TGFβ1 treatment of control siRNA-transfected cells resulted in the *KLF4* suppression by 0.8 ± 0.06-fold (P = 0.02) (Fig. 3A). Additional TGFβ1 treatment of KLF4 siRNA-treated cells decreased the *KLF4* expression level by 0.7 ± 0.07-fold (P = 0.0004) (Fig. 3A).

The KLF4-silenced NHDF showed a 1.3 ± 0.1-fold (P = 0.003) increase in the basal *XYLT1* expression compared to negative

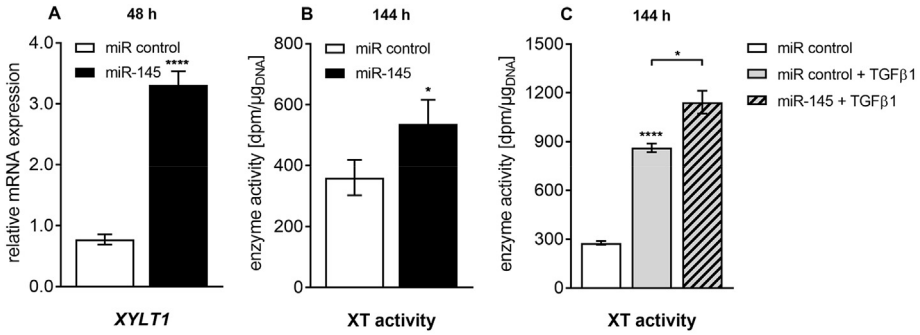

Fig. 2. miR-145 upregulates XT-I and enhances TGFβ1-induced XT activity. The NHDF (n = 2) were transfected with a miR-145 mimic (miR-145) or negative control miRNA mimic (miR control). (**A**) Cells were stimulated 24 h post-transfection with TGFβ1 or vehicle for 48 h. The relative mRNA expression level of *XYLT1* was analysed by qRT-PCR. Values shown are means ± SEM for three biological and three technical replicates per experiment. (**B**, **C**) Cells were stimulated 6 h post-transfection with TGFβ1 or vehicle for 144 h. XT activity was measured in cell supernatants by radiochemical enzyme assay and expressed as dpm/µg of DNA. Values shown are means ± SEM for three biological and two technical replicates per experiment. Mann-Whitney *U* test: *P < 0.05, ****P < 0.0001.

Table 1
Bioinformatic analyses of the miR-145−5p binding sites that are predicted to target gene *XYLT1* and *KLF4* (TargetScan 7.2). Value ranges: Site types (8_{mer}>7_{mer}>$7_{mer\text{-}A1}$>6_{mer}; matching sites in the seed region), context ++ score (1 to −1; the more negative the score, the greater the repression).

Conserved sites	Predicted consequential pairing of target region (top) and miRNA (bottom)	Site type	Context ++ score
Position 5689-5695 of *XYLT1* 3′-UTR	5′ ...UUUCAUAGGAAAUUCACUGGAAU...	7mer-A1	−0.03
hsa-miR-145-5p	3′ UCCCUAAGGACCCUUUUGACCUG		
Position 278-284 of *KLF4* 3′-UTR	5′ ...AAUGCCAAGGGGGUGACUGGAAG...	7mer-A1	−0.12
hsa-miR-145-5p	3′ UCCCUAAGGACCCUUUUGACCUG		

Table 2
In silico analysis of transcription factor binding sites in the full-length *XYLT1* promoter sequence (GenBank Accession Number KM079589 and NG_015843.1) using MatInspector (Genomax GmbH). The DNA-5′-3′-strand harbouring the KLF4 binding site is marked with (+), and the DNA-3′-5′-strand with (−). The binding site core sequence is shown in capital letters, while essential nucleotides within the binding site are shown in bold letters.

From (bp)	To (bp)	Strand	Sequence
c.−1376	c.−1358	(+)	a**a**ga**g**gacaA**GGG**agggaa
c.−1152	c.−1134	(+)	c**a**ga**c**aggaA**GGG**ggactt
c.−627	c.−654	(−)	c**a**gg**a**agagA**GGG**ggtccc
c.−502	c.−484	(−)	g**g**g**a**a**g**gaA**GGG**ggtggg
c.−497	c.−479	(−)	g**a**gg**a**ggga**AAGG**aagggg
c.−492	c.−474	(−)	a**a**aa**g**gagg**AGGG**aaagga

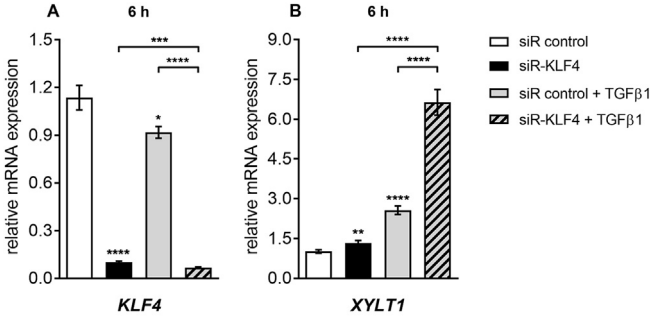

Fig. 3. Basal and TGFβ1-induced *XYLT1* mRNA expressions are increased by siRNA mediated *KLF4* knockdown. The NHDF (n = 2) were transfected with a negative control siRNA (si control) or siRNA targeting against the KLF4 (si-KLF4). Cells were treated 48 h post-transfection with or without TGFβ1 for 6 h. Relative (**A**) *KLF4* and (**B**) *XYLT1* expression levels were analysed by qRT-PCR. Values shown are means ± SEM for three biological and technical replicates per experiment. Mann-Whitney *U* test: not significant (ns), *P < 0.05, **P < 0.01, ***P < 0.001, ****P < 0.0001.

control siRNA-transfected cells (Fig. 3B). The TGFβ1 treatment of the control siRNA-transfected NHDF resulted in a significant induction of the *XYLT1* expression by 2.5 ± 0.2-fold (P < 0.0001). This TGFβ1-induced *XYLT1* expression increase was significantly enhanced by 2.6 ± 0.3-fold (P < 0.0001) after the KLF4 deletion. The KLF4 siRNA-transfected NHDF treated with TGFβ1 exhibited an increased *XYLT1* expression by 5.0 ± 0.5-fold (P < 0.0001) compared to TGFβ1-treated control siRNA-transfected cells. These results demonstrate that KLF4 is a transcriptional suppressor of basal and TGFβ1-induced *XYLT1* mRNA expression.

3.5. Reciprocal XYLT1 and KLF4 expression in SSc fibroblasts

After showing that KLF4 is a negative regulator of *XYLT1* expression, we independently confirmed this reciprocal *XYLT1* and *KLF4* expression using SScF. The SScF secrete a high amount of profibrotic mediators, such as activin A or TGFβ1 [20,21], leading potentially to the increase in serum XT activity of SSc patients observed previously [8]. Compared to NHDF, we observed an increased basal *XYLT1* expression by 2.2 ± 0.3-fold (P = 0.003) in SScF (Fig. 4A). This *XYLT1* induction in SScF correlates with a decreased *KLF4* expression level by 0.5 ± 0.07-fold (P = 0.0003) (Fig. 4B). These results confirm the suppressive role of KLF4 in the transcriptional regulation of *XYLT1* and highlight a potential deregulated TGFβ1-mediated miRNA pathway that might participate in abnormal XT regulation in fibrosis.

4. Discussion

Extensive ECM accumulation in fibrosis is caused by the uncontrolled production of profibrotic cytokines, driving

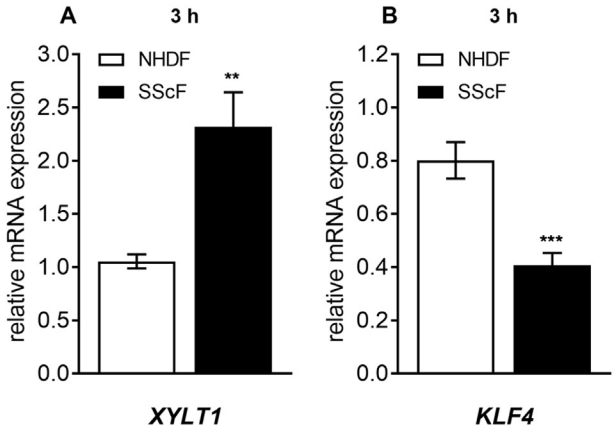

Fig. 4. Increased *XYLT1* mRNA expression in SSc fibroblasts. The NHDF (n = 2) and SScF (n = 2) were cultured for 24 h before the experiment. Cells were maintained in serum-free culture media for 24 h and an additional 3 h. Relative mRNA expression levels of (**A**) *XYLT1* and (**B**) *KLF4* were analysed by qRT-PCR. Values shown are means ± SEM for three biological and technical replicates per experiment. Mann-Whitney *U* test: $^{**}P < 0.01$, $^{***}P < 0.001$.

myofibroblast transdifferentiation and matrix synthesis. It has been reported recently that the pathogenesis of fibrosis involves aberrant miR-145 expression [2,22]. Patients suffering from the fibrotic disorder SSc show an increased serum enzyme activity of XT [8,10]. Until now, the underlying cellular mechanism leading to this XT activity increase in SSc has remained elusive. Despite the increasing numbers of studies describing the involvement of cytokines and miRNAs in the pathogenesis of fibrosis, miRNA-mediated XT-I regulation has been sparsely discussed. A recent study by Riedel et al. revealed a miRNA-29b/SP1-mediated XT regulatory pathway in human fibroblasts [12], while Theis et al. demonstrated *XYLT1* to be a direct miRNA-133b target in the context of murine spinal cord injury [23]. Since fibrosis is accompanied by TGFβ1-induced changes in miRNA and *XYLT1* expression, we analysed whether miR-145 participates in abnormal XT regulation in fibrosis in SSc.

In our present study, the expression of miR-145 was induced by the TGFβ1 stimulation of human fibroblasts *in vitro*. This is consistent with studies on lung or conjunctiva fibrosis, which demonstrated the transcriptional regulation of miR-145 and α-SMA expression by TGFβ1 in fibroblasts or hepatic stellate cells [5,7,22]. In accordance with the changes in miR-145 expression detected, we observed an increase in extracellular XT activity and a TGFβ1-induced expression of the myofibroblast markers *XYLT1* and *ACTA2*. The increase in myofibroblast marker expression observed after TGFβ1 treatment is in line with data shown previously [11]. The link between X*YLT1* mRNA expression and extracellular XT activity has been shown in previous studies using human dermal and cardiac fibroblasts [11,24]. In agreement with former studies [11,12], we found no regulation of *XYLT2* isoform expression by TGFβ1.

Performing miR-145 overexpression experiments in NHDF, we identified a novel regulatory mechanism of *XYLT1* expression and XT activity by miR-145. We also detected an enhancement of the TGFβ1-induced XT activity increase in these miR-145 overexpressing cells. Furthermore, we observed, in agreement with previous results in dermal fibroblasts [3], that miR-145 increases *ACTA2* expression in our model. Since an inverse relationship between the miRNA expression level and its putative target gene is anticipated, we excluded *XYLT1* as a direct 3′-UTR binding partner of miR-145 by bioinformatics and experimental validation and hypothesize *XYLT1* to be a secondary miR-145 target.

We and others demonstrated that miR-145 directly targets KLF4, a known negative regulator of α-SMA expression in skin fibroblast that is downregulated by TGFβ1 [3]. In agreement with these findings, we also found a reciprocal expression regulation of miR-145 or *ACTA2* and *KLF4* in our model. Previous sequence analyses of the human *XYLT1* promoter region revealed several transcription factor binding sites for KLF to regulate *XYLT1* mRNA expression [18,25]. In agreement with the previous findings, we here identified six putative KLF4 binding sites in the *XYLT1* promoter, which are located in the near neighbourhood of the SP1 binding sites identified previously [12]. A competitive regulatory action of KLF4 and SP1 transcription factors in promoting promoter activities has been shown previously [26]. Despite the similar regulation of both myofibroblast markers *ACTA2* and *XYLT1* observed here and in previous studies [11], the role of KLF4 in basal and TGFβ1-induced expression regulation of *XYLT1* was unknown until now. By performing siRNA-mediated KLF4 knockdown, we identified KLF4 as a negative regulator of both basal and TGFβ1-mediated *XYLT1* expression in NHDF. This negative regulation of KLF4 expression could be one of the mechanisms of miR-145-mediated myofibroblast transdifferentiation, increasing the *ACTA2* and *XYLT1* expression in these cells. Additionally, we demonstrated, for the first time, that basal *KLF4* expression was significant decreased in SScF compared to matched control fibroblasts, whereas the corresponding basal *XYLT1* expression was enhanced in these cells. Altogether, these results shed light on an aberrant TGFβ1-and miR-145-mediated cellular pathway in myofibroblasts that promotes increased *XYLT1* expression and fibrogenic ECM remodelling in these cells.

Acknowledgements

We thank Philip Saunders for linguistic advice and Christoph Lichtenberg for technical assistance. This work was supported by grant FA 1381/1-1 of the German Research Foundation.

Appendix A. Supplementary data

Supplementary data to this article can be found online at https://doi.org/10.1016/j.bbrc.2019.12.120.

References

[1] X. Zhao, P. Psarianos, L.S. Ghoraie, K. Yip, D. Goldstein, R. Gilbert, I. Witterick, H. Pang, A. Hussain, J.H. Lee, J. Williams, S.V. Bratman, L. Ailles, B. Haibe-Kains, F.-F. Liu, Metabolic regulation of dermal fibroblasts contributes to skin extracellular matrix homeostasis and fibrosis, Nat. Metab. 1 (2019) 147–157, https://doi.org/10.1038/s42255-018-0008-5.

[2] H. Butz, K. Rácz, L. Hunyady, A. Patócs, Crosstalk between TGF-β signaling and the microRNA machinery, Trends Pharmacol. Sci. 33 (2012) 382–393, https://doi.org/10.1016/j.tips.2012.04.003.

[3] C. Gras, D. Ratuszny, C. Hadamitzky, H. Zhang, R. Blasczyk, C. Figueiredo, miR-145 contributes to hypertrophic scarring of the skin by inducing myofibroblast activity, Mol. Med. 21 (2015) 296–304, https://doi.org/10.2119/molmed.2014.00172.

[4] S. O'Reilly, S. O'Reilly, MicroRNAs in fibrosis: opportunities and challenges, Arthritis Res. Ther. 18 (2016) 1–10, https://doi.org/10.1186/s13075-016-0929-x.

[5] R. Men, M. Wen, M. Zhao, X. Dan, Z. Yang, W. Wu, M.H. Wang, X. Liu, L. Yang, MircoRNA-145 promotes activation of hepatic stellate cells via targeting Krüppel-like factor 4, Sci. Rep. 7 (2017) 1–10, https://doi.org/10.1038/srep40468.

[6] T. Barta, L. Peskova, J. Collin, D. Montaner, I. Neganova, L. Armstrong, M. Lako, Brief report: inhibition of miR-145 enhances reprogramming of human dermal fibroblasts to induced pluripotent stem cells, Stem Cells 34 (2016) 246–251, https://doi.org/10.1002/stem.2220.

[7] S. Yang, H. Cui, N. Xie, M. Icyuz, S. Banerjee, V.B. Antony, E. Abraham, V.J. Thannickal, G. Liu, miR-145 regulates myofibroblast differentiation and lung fibrosis, FASEB J. 27 (2013) 2382–2391, https://doi.org/10.1096/fj.12-219493.

[8] C. Götting, S. Sollberg, J. Kuhn, C. Weilke, C. Huerkamp, T. Brinkmann, T. Krieg, K. Kleesiek, Serum xylosyltransferase: a new biochemical marker of the sclerotic process in systemic sclerosis, J. Investig. Dermatol. 112 (1999)

919–924, https://doi.org/10.1046/j.1523-1747.1999.00590.x.
[9] C. Prante, H. Milting, A. Kassner, M. Farr, M. Ambrosius, S. Schön, D.G. Seidler, A.E. Banayosy, R. Körfer, J. Kuhn, K. Kleesiek, C. Götting, Transforming growth factor beta1-regulated xylosyltransferase I activity in human cardiac fibroblasts and its impact for myocardial remodeling, J. Biol. Chem. 282 (2007) 26441–26449, https://doi.org/10.1074/jbc.M702299200.
[10] I. Faust, J. Weile, B. Fujita, R. Kandolf, D. Hendig, T. Vollmer, A. Stan, U. Kellner, J. Kuhn, J.F. Gummert, C. Knabbe, Heart transplantation in systemic sclerosis: new impulses for conventional scleroderma transplantation regimen and scleroderma diagnostic monitoring: 2 case reports, Transplant. Proc. 51 (2019) 865–870, https://doi.org/10.1016/j.transproceed.2019.01.025.
[11] I. Faust, C. Roch, J. Kuhn, C. Prante, C. Knabbe, D. Hendig, Human xylosyltransferase-I – a new marker for myofibroblast differentiation in skin fibrosis, Biochem. Biophys. Res. Commun. 436 (2013) 449–454, https://doi.org/10.1016/j.bbrc.2013.05.125.
[12] L. Riedel, B. Fischer, T.-D. Ly, D. Hendig, J. Kuhn, C. Knabbe, I. Faust, microRNA-29b mediates fibrotic induction of human xylosyltransferase-I in human dermal fibroblasts via the Sp1 pathway, Sci. Rep. 8 (2018) 17779, https://doi.org/10.1038/s41598-018-36217-2.
[13] M.W. Pfaffl, A new mathematical model for relative quantification in real-time RT-PCR, Nucleic Acids Res. 29 (2001) e45. http://www.ncbi.nlm.nih.gov/pubmed/11328886.
[14] C. Götting, J. Kuhn, H.-R. Tinneberg, T. Brinkmann, K. Kleesiek, High xylosyltransferase activities in human follicular fluid and cultured granulosa-lutein cells, Mol. Hum. Reprod. 8 (2002) 1079–1086. http://www.ncbi.nlm.nih.gov/pubmed/12468640.
[15] V. Agarwal, G.W. Bell, J.-W. Nam, D.P. Bartel, Predicting effective microRNA target sites in mammalian mRNAs, Elife 4 (2015), https://doi.org/10.7554/eLife.05005.
[16] W. Liu, X. Wang, Prediction of functional microRNA targets by integrative modeling of microRNA binding and target expression data, Genome Biol. 20 (2019) 18, https://doi.org/10.1186/s13059-019-1629-z.
[17] C. Sticht, C. De La Torre, A. Parveen, N. Gretz, miRWalk: an online resource for prediction of microRNA binding sites, PLoS One 13 (2018), e0206239, https://doi.org/10.1371/journal.pone.0206239.
[18] I. Faust, K.O. Böker, C. Lichtenberg, J. Kuhn, C. Knabbe, D. Hendig, First description of the complete human xylosyltransferase-I promoter region, BMC Genet. 15 (2014) 1. http://bmcgenet.biomedcentral.com/articles/10.1186/s12863-014-0129-0.
[19] K. Cartharius, K. Frech, K. Grote, B. Klocke, M. Haltmeier, A. Klingenhoff, M. Frisch, M. Bayerlein, T. Werner, MatInspector and beyond: promoter analysis based on transcription factor binding sites, Bioinformatics 21 (2005) 2933–2942, https://doi.org/10.1093/bioinformatics/bti473.
[20] K. Takagi, Y. Kawaguchi, M. Kawamoto, Y. Ota, A. Tochimoto, T. Gono, Y. Katsumata, M. Takagi, M. Hara, H. Yamanaka, Activation of the Activin A-ALK-Smad pathway in systemic sclerosis, J. Autoimmun. 36 (2011) 181–188, https://doi.org/10.1016/j.jaut.2010.09.004.
[21] H. Ihn, Autocrine TGF-β signaling in the pathogenesis of systemic sclerosis, J. Dermatol. Sci. 49 (2008) 103–113, https://doi.org/10.1016/j.jdermsci.2007.05.014.
[22] Y.H. Hwang, S.-A. Jung, J. Lyu, Y.Y. Kim, J.H. Lee, Transforming growth factor-β1–induced human subconjunctival fibrosis is mediated by microRNA 143/145 expression, Investig. Ophthalmol. Vis. Sci. 60 (2019) 2064, https://doi.org/10.1167/iovs.19-26797.
[23] T. Theis, M. Yoo, C.S. Park, J. Chen, S. Kügler, K.M. Gibbs, M. Schachner, Lentiviral delivery of miR-133b improves functional recovery after spinal cord injury in mice, Mol. Neurobiol. 54 (2017) 4659–4671, https://doi.org/10.1007/s12035-016-0007-z.
[24] C. Pönighaus, M. Ambrosius, J.C. Casanova, C. Prante, J. Kuhn, J.D. Esko, K. Kleesiek, C. Götting, Human xylosyltransferase II is involved in the biosynthesis of the uniform tetrasaccharide linkage region in chondroitin sulfate and heparan sulfate proteoglycans, J. Biol. Chem. 282 (2007) 5201–5206, https://doi.org/10.1074/jbc.M611665200.
[25] B. Müller, C. Prante, K. Kleesiek, C. Götting, B. Muller, C. Prante, K. Kleesiek, C. Gotting, Identification and characterization of the human xylosyltransferase I gene promoter region, J. Biol. Chem. 284 (2009) 30775–30782, https://doi.org/10.1074/jbc.M109.016592.
[26] W. Ai, Y. Liu, M. Langlois, T.C. Wang, Kruppel-like factor 4 (KLF4) represses histidine decarboxylase gene expression through an upstream Sp1 site and downstream gastrin responsive elements, J. Biol. Chem. 279 (2004) 8684–8693, https://doi.org/10.1074/jbc.M308278200.
[27] K. Minami, K. Taniguchi, N. Sugito, Y. Kuranaga, T. Inamoto, K. Takahara, T. Takai, Y. Yoshikawa, S. Kiyama, Y. Akao, H. Azuma, MiR-145 negatively regulates Warburg effect by silencing KLF4 and PTBP1 in bladder cancer cells, Oncotarget 8 (2017) 33064–33077, https://doi.org/10.18632/oncotarget.16524.
[28] Y. Liu, X. Sun, Y. Wu, P. Fang, H. Shi, J. Xu, M. Li, Effects of miRNA-145 on airway smooth muscle cells function, Mol. Cell. Biochem. 409 (2015) 135–143, https://doi.org/10.1007/s11010-015-2519-7.
[29] Y.T. Yeh, J. Wei, S. Thorossian, K. Nguyen, C. Hoffman, J.C. del Álamo, R. Serrano, Y.S.J. Li, K.C. Wang, S. Chien, MiR-145 mediates cell morphology-regulated mesenchymal stem cell differentiation to smooth muscle cells, Biomaterials 204 (2019) 59–69, https://doi.org/10.1016/j.biomaterials.2019.03.003.
[30] B.N. Davis-Dusenbery, M.C. Chan, K.E. Reno, A.S. Weisman, M.D. Layne, G. Lagna, A. Hata, Down-regulation of Krüppel-like Factor-4 (KLF4) by microRNA-143/145 is critical for modulation of vascular smooth muscle cell phenotype by transforming growth factor-β and bone morphogenetic protein 4, J. Biol. Chem. 286 (2011) 28097–28110, https://doi.org/10.1074/jbc.M111.236950.
[31] N. Xu, T. Papagiannakopoulos, G. Pan, J.A. Thomson, K.S. Kosik, MicroRNA-145 regulates OCT4, SOX2, and KLF4 and represses pluripotency in human embryonic stem cells, Cell 137 (2009) 647–658, https://doi.org/10.1016/j.cell.2009.02.038.

3.4 Publikation IV

Identifizierung von potenziellen nicht-substratbasierten XT-I-Inhibitoren durch Screening einer Naturstoff-Bibliothek

(Ly *et al.*, 2020a)

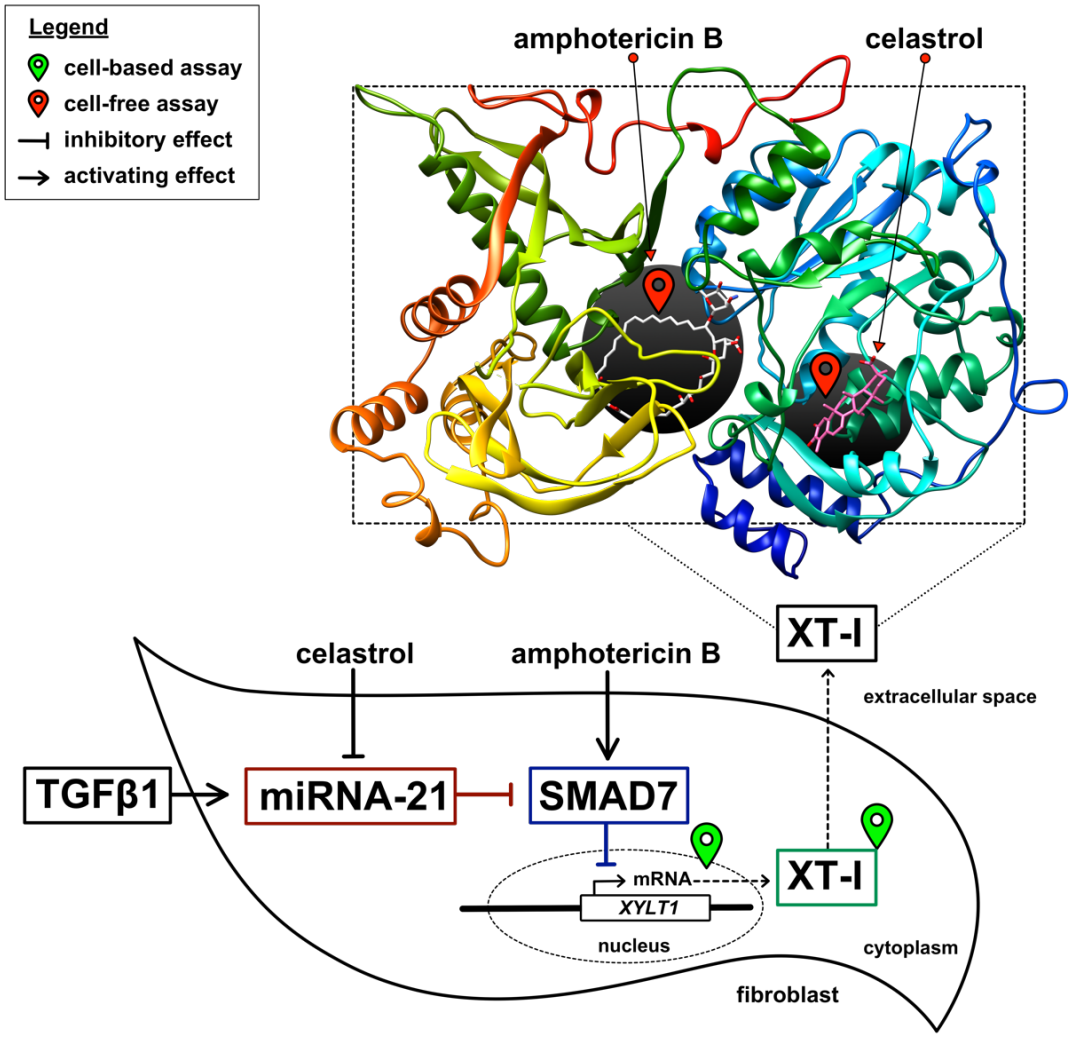

Abbildung 8: *Graphical Abstract* von Publikation IV (Ly *et al.*, 2020a).

biomolecules

MDPI

Article

Identification of Putative Non-Substrate-Based XT-I Inhibitors by Natural Product Library Screening

Thanh-Diep Ly, Anika Kleine, Bastian Fischer, Vanessa Schmidt, Doris Hendig, Joachim Kuhn, Cornelius Knabbe and Isabel Faust *

Institut für Laboratoriums- und Transfusionsmedizin, Herz- und Diabeteszentrum NRW, Universitätsklinik der Ruhr-Universität Bochum, Georgstraße 11, 32545 Bad Oeynhausen, Germany; tly@hdz-nrw.de (T.-D.L.); ankleine@hdz-nrw.de (A.K.); bfischer@hdz-nrw.de (B.F.); vschmidt@hdz-nrw.de (V.S.); dhendig@hdz-nrw.de (D.H.); jkuhn@hdz-nrw.de (J.K.); cknabbe@hdz-nrw.de (C.K.)

* Correspondence: ifaust@hdz-nrw.de; Tel.: +49-5731-97-1234

Received: 28 September 2020; Accepted: 18 October 2020; Published: 21 October 2020

Abstract: Fibroproliferative diseases are characterized by excessive accumulation of extracellular matrix (ECM) components leading to organ dysfunction. This process is characterized by an increase in myofibroblast content and enzyme activity of xylosyltransferase-I (XT-I), the initial enzyme in proteoglycan (PG) biosynthesis. Therefore, the inhibition of XT-I could be a promising treatment for fibrosis. We used a natural product-inspired compound library to identify non-substrate-based inhibitors of human XT-I by UPLC-MS/MS. We combined this cell-free approach with virtual and molecular biological analyses to confirm and prioritize the inhibitory potential of the compounds identified. The characterization for compound potency in TGF-β1-driven *XYLT1* transcription regulation in primary dermal human fibroblasts (key cells in ECM remodeling) was addressed by gene expression analysis. Consequently, we identified amphotericin B and celastrol as new non-substrate-based XT-I protein inhibitors. Their XT-I inhibitory effects were mediated by an uncompetitive or a competitive inhibition mode, respectively. Both compounds reduced the cellular *XYLT1* expression level and XT-I activity. We showed that these cellular inhibitor-mediated changes involve the TGF-β and microRNA-21 signaling pathway. The results of our study provide a strong rationale for the further optimization and future usage of the XT-I inhibitors identified as promising therapeutic agents of fibroproliferative diseases.

Keywords: library screening; amphotericin B; celastrol; fibrosis; molecular docking; miRNA-21; natural products; TGF-β1; xylosyltransferase

1. Introduction

The human xylosyltransferase (XT) isoforms XT-I and XT-II (EC 2.4.2.26), encoded by the *XYLT1* and *XYLT2* genes, are type II transmembrane proteins localized in the Golgi [1]. Both XTs catalyze the transfer of D-xylose from uridine diphosphate (UDP)-D-xylose onto defined serine residues on similar proteoglycan (PG) core proteins and, thus initiating a series of posttranslational modifications necessary for the transport and secretion of PGs [2], which are essential components of the extracellular matrix (ECM) [3]. Both XTs consist of a short amino-terminal region facing the cytosolic side, a single transmembrane helix, a stem region necessary for Golgi retention [1], a catalytic glycosyltransferase (GT)-A domain facing the Golgi lumen [4,5] and a C-terminal domain named Xylo_C according to the Pfam database [5,6]. XT-I and XT-II are differentially expressed in tissues and cell types due to variations in the promotor region and cellular transcriptional regulations [7–10], but the reason for the existence of these two isoforms in all higher organisms remains unknown. In spite of the intracellular localization of XT-I, the enzyme is shed from the Golgi membrane by an unknown

mechanism that involves a cysteine protease [11]. The XT-I secreted can be monitored by its activity in the human serum or cell culture supernatant and provides a reliable indicator of the present rate of PG biosynthesis [12–14]. This points to the important role of XT-I as a disease modifier in pathologies characterized by an altered PG metabolism, such as tissue fibrosis. Fibrosis is triggered by a variety of stimuli, leading to fibroblast activation and increased formation of ECM-producing myofibroblasts. Myofibroblasts, as central cellular mediators of this process, deposit excessive amounts of ECM components, such as type I collagen (*COL1A1*) or PG, that lead to stiffening and impaired tissue function [3,15,16]. Initiation of myofibroblast differentiation during fibrosis is mainly regulated by the pro-fibrotic mediator transforming growth factor-β1 (TGF-β1). Alpha smooth muscle actin (*ACTA2*), *COL1A1* and *XYLT1* expression were demonstrated to be upregulated in activated fibroblasts [17,18], while *XYLT2* mRNA expression is unaffected by TGF-β1 [17,19–21]. The TGF-β1-induced increase in *XYLT1* expression results in higher cellular XT-I activity and PG accumulation [3,17,18]. Therefore, elevated *XYLT1* expression is also associated with persisting fibrosis and displays a reliable marker for myofibroblast differentiation [12,17].

In addition, TGF-β1 can modulate a number of other cytokines, cellular downstream signaling pathways and microRNA (miRNA) expressions [22,23]. The miRNAs are small noncoding endogenous RNAs which bind to the 3′-untranslated regions of target mRNAs, preventing the translation or leading to the degradation of the respective mRNAs. Aberrant miRNA expression has been reported in a wide range of diseases including fibrosis [24,25]. One pathomechanism of this process involves the inhibitory SMAD7, a direct target of miRNA-21-5p (miRNA-21). Consequently, upregulation of miRNA-21 inhibits SMAD7 and results in enhanced TGF-β1 signaling in primary pulmonary and cardiac fibroblasts [26,27].

However, the broad impact of TGF-β signaling on numerous cellular functions in tissue homeostasis and disease makes developing an effective but safe TGF-β-dependent therapy challenging. Potential strategies for targeting TGF-β and its signaling pathways include focusing on modifiers and downstream products, pathway inhibition at the ligand or receptor stage and the blocking of downstream signaling components or miRNAs [28]. Therefore, targeted blocking of XT expression and activity could provide a therapeutic strategy for PG-associated diseases. To date, only substrate analogue XT inhibitors such as nucleotides and glycosaminoglycans (GAGs) have been identified, but their inhibitory activity is restricted to cell-free approaches [29,30]. The aim of this study was, therefore, to identify new non-substrate-based XT-I inhibitors from natural compounds that could potentially be suitable for therapeutic applications.

Natural products (NPs) are the earliest forms of human medicine with strong, unique, anti-inflammatory, anticancer or neuroprotective properties [31,32]. The NPs are often more efficient than artificially made compounds if a specific biological activity, such as an enzyme inhibitor, is needed. The NPs are classified based on their origins, biological functions and structures. Plants, bacteria and fungi are a vast source of many natural drugs. With the exception of peptides and carbohydrates, the most important of these NPs are terpenoids, alkaloids, steroids, phenolic compounds, vitamins, carbocyclics and heterocyclic aromatic compounds [33].

2. Materials and Methods

2.1. Materials

The 96-well plate format compound library with NPs, pre-dissolved in dimethyl sulfoxide (DMSO, 10 mM), was obtained from Selleck Chemicals Llc (Houston, Texas, United States). Celastrol and amphotericin B were purchased from Biomol GmbH (Hamburg, Germany) and Sigma-Aldrich (St. Louis, Missouri, United States), respectively, and dissolved in DMSO to gain a 10 mM stock solution. Recombinant human TGF-β1 was purchased from Miltenyi Biotec (Bergisch Gladbach, Germany). The miRNAs, transfection reagents and media were obtained from Thermo Fisher Scientific (Waltham, Massachusetts, United States).

2.2. Expression of Recombinant Human XT-I in pgsA-745 Chinese Hamster Ovary Cells

The XT-deficient pgsA-745 Chinese hamster ovary (CHO) cells [34] in which XT-I expression was complemented with a full-length *XYLT1* containing plasmid (pgsA-6HisXT1-K4) [1] were cultured as described previously [11,35]. In brief, pgsA-6HisXT1-K4 cells were grown as monolayer culture in 175 cm^2 T-flasks with 25 mL Ham's F12 medium supplemented with 10% (*v*/*v*) fetal calf serum (FCS, Biowest, Nuaillé, France) and 400 g/L Geneticin G418 (Invivogen, Toulouse, France) under standard conditions. Upon confluence, adherent cells of two T-flasks were transferred to a 100 × 20 mm cell culture dish with 10 mL of serum-free Ham's F12 medium. The cell culture supernatant was collected after four days and centrifuged at 250× *g* for 5 min to obtain the secreted recombinant XT-I protein.

2.3. Bicinchonic Acid Assay

The bicinchonic acid (BCA) assay was used to quantify the amount of protein in a sample [36]. Bovine serum albumin (Sigma Aldrich, St. Louis, Missouri, United States) was used to generate a standard curve ranging from 0 to 1000 g/L. The assay was conducted according to Smith et al. in a 96-microplate format [36]. A volume of 25 µL standard or protein sample was combined with 200 µL BCA working reagent, which was prepared by mixing 50 parts of BCA solution with 1 part of Cu^{2+} solution. The absorbance at 562 nm was measured after an incubation period of 30 min at 37 °C. The protein concentrations obtained were used for XT-I activity normalization.

2.4. Determination of XT-I Activity by Mass Spectrometry

The measurement of relative XT-I activity among different samples is based on the XT-catalyzed incorporation of xylose from UDP-D-xylose on a modified bikunin-derived peptide after a fixed reaction time. The assay was originally developed for the determination of XT activity in human- or cell-culture-derived samples [13] by ultra-performance liquid chromatography/electrospray ionization tandem mass spectrometry (UPLC/ESI-MS/MS). The UPLC/ESI-MS/MS XT assay was recently modified toward a XT-I selective activity determination in human serum and cell culture samples (unpublished data). The relative intensities of the xylosylated peptide species abundance obtained with the respective m/z ratio were directly proportional to the relative XT-I activity of the sample. The XT-I activity determined is expressed in arbitrary units and normalized to the total protein content per 1 mL sample volume in cell culture approaches. A calibrator probe with a fixed amount of recombinant XT-I enzyme was included in every UPLC-MS/MS XT-I assay for assay comparability across multiple runs. The assay reaction mixture (50 µL) contained 50% (*v*/*v*) of the respective XT-I enzyme solution and 50% (*v*/*v*) reaction buffer. The final XT-I assay contained 25 mM MES buffer (pH 6.5), 25 mM KF buffer, 5 mM $MnCl_2$, 5 mM $MgCl_2$, 7.0 µM modified acceptor peptide and 30 µM UDP-D-xylose. The sample preparation for UPLC/ESI-MS/MS was performed according to [13]. In brief, after sample incubation at 37 °C for 24 h, the reaction was stopped by heating at 99 °C for 10 min. After centrifugation (10,000× g, 10 min) the supernatant was diluted fivefold with UPLC water for analysis. All cell-based XT-I assays were carried out in three biological and three technical replicates per donor-derived primary cell culture, while the XT-I activity determination for screening or kinetic purposes was carried out at least in technical duplicates.

2.5. Inhibitor Screening Assay and Determination of IC_{50} Values

Inhibitor candidates from the NP compound library were screened using the UPLC/ESI-MS/MS XT-I assay with recombinant XT-I protein solution from pgsA-6HisXT1-K4 cells. In order to identify putative XT-I inhibitor compounds, equally concentrated XT-I protein solutions were preincubated with 1% (*v*/*v*) DMSO or 100 µM of each inhibitor for 1 h at room temperature (RT). Thereafter, 50% (*v*/*v*) of the XT-I enzyme mixture was supplemented with 50% (*v*/*v*) reaction buffer. The final screening assay contained 50 µM inhibitor or 0.75% (*v*/*v*) DMSO, 25 mM MES buffer (pH 6.5), 25 mM KF

buffer, 5 mM $MnCl_2$, 5 mM $MgCl_2$, 10.5 µM modified acceptor peptide and 15 µM UDP-D-xylose. The sample preparation for UPLC/ESI-MS/MS was performed according to [13] and diluted fivefold with UPLC water for analysis. In order to determine the IC_{50} values of the inhibitor compounds identified, equally concentrated XT-I protein solutions were preincubated with DMSO or inhibitors in the concentration range of 0.02 to 150 µM for 1 h at RT. The XT-I activity of the protein-inhibitor mixtures were determined by UPLC/ESI-MS/MS as described above. The DMSO content in this enzyme-catalyzed reaction was kept constant at a final concentration of 0.75% (*v*/*v*), which corresponds to a DMSO content of 0.15% (*v*/*v*) after the fivefold dilution step with UPLC water.

2.6. Enzyme and Inhibition Kinetics

The mode of inhibition (MOI) study was performed by evaluating the inhibitors' impact on the enzyme parameters' Michaelis constant K_m and the maximum activity V_{max}. In order to determine the enzyme and inhibition kinetics, XT-I activity determination of the recombinant XT-I protein solution with and without inhibitor supplementation was carried out in the presence of different acceptor peptide concentrations ranging from 1 to 30 µM. In addition to the modified acceptor peptide, the final reaction mixture (50 µL) contained 50% (*v*/*v*) XT-I enzyme solution with or without inhibitor at IC_{50} concentration, 25 mM MES buffer (pH 6.5), 25 mM KF buffer, 5 mM $MnCl_2$, 5 mM $MgCl_2$ and 15 µM UDP-D-xylose. The K_m and V_{max} were determined with the Michaelis–Menten equation and nonlinear regression analysis, while the slope and Y-intersection values were determined by a Lineweaver–Burk plot and simple linear regression using GraphPad Prism 8.0 (GraphPad Software, La Jolla, United States) software. The V_{max} values after a fixed reaction time are displayed in arbitrary units equaling the product generation per time d*P*/d*t*, while the K_m values are expressed in the unit of concentration.

2.7. Displaying Putative Inhibitor Binding Sites by Molecular Docking

The estimation and visualization of putative compound binding sites in the XT-I protein were conducted by molecular docking software AutoDock Vina [37] within UCSF Chimera 1.14 [38], a molecular visualization software. The PDB file for the three-dimensional structure of human XT-I apoprotein (PDB ID: 6FOA) as a target macromolecule template with a resolution of 1.867 Å was downloaded from the RCSB protein data bank [39] and processed with the Chimera tool Dockprep. The in silico receptor preparation, applied to extract only the protein chain of interest, was completed by removing all heteroatoms and water molecules, fixing nonstandard residues and adding hydrogen. The protonation state of the protein was adjusted to a neutral pH and the maximum energy difference was set to 3 kcal/mol. The structures of the active compounds were obtained from the PubChem database [40] using canonical SMILES then converted to a usable ligand molecule for subsequent in silico docking runs. After receptor and ligand preparation, the complete protein surface was defined as a binding site for docking analysis. All molecular docking simulations run with AutoDock Vina were executed with the identical setup described above and visualized with the ViewDock implementation. The binding positions of the UDP-D-xylose and acceptor peptide were adopted from the 2.0 Å resolved human XT-I structure (PDB ID: 6EJ7) for direct comparison of the binding position of inhibitors and substrate molecules. The amino acid sequence of the bikunin-derived acceptor peptide was transmuted to the amino acid sequence of the acceptor peptide applied for better illustration using the UCSF Chimera 1.14 application Rotamers. The chimera models (PDB ID: 6FOA) with the docked ligand positions identified by AutoDock Vina were then aligned with the acceptor peptide-modified human XT-I structure complexed with UDP-D-xylose (PDB ID: 6EJ7) utilizing the integrated application MatchMaker [41].

2.8. Primary Cell Culture, Treatment and Sample Preparation

Normal human dermal fibroblasts (NHDFs) from a 37- and a 50-year-old woman and a 57-year-old man were obtained commercially from Cambrex (Walkerville, United States) and Coriell (New Jersey, United States). The NHDFs were cultured in phenol red-free Dulbecco's modified Eagle's

medium (DMEM; Thermo Fisher Scientific, Waltham, Massachusetts, United States) supplemented with 10% (*v*/*v*) FCS, 4 mM L-glutamine and 100,000 *U*/L penicillin, 100 mg/L Streptomycin, 0.25 mg/L amphotericin B (PAN Biotech, Aidenbach, Germany) at 37 °C, 5% CO_2. The medium was changed twice a week until the cells reached 80% confluency. The NHDFs were subcultured with an expansion ratio of 1:3 using 0.05% trypsin (PAN Biotech, Aidenbach, Germany) and used until the ninth passage.

A former established cell culture model was utilized to investigate the effect of putative XT-I inhibitors on NHDFs [17]. The inhibition studies were carried out with final inhibitor concentrations of 0.5, 1.0, 2.0 or 4.0 µM diluted in fully supplemented DMEM. In brief, unless otherwise stated, NHDFs were cultivated with a low density of 50 cells per mm^2 on a hard tissue culture substrate (100 × 20 mm dish) in fully supplemented DMEM with or without additional TGF-β1 (5 µg/L) for 24 h, promoting their transdifferentiation into proto-myofibroblasts. Thereafter, cells were treated with celastrol or amphotericin B in the presence or absence of TGF-β1 (5 µg/L) for an additional 48 h. Negative controls treated with solvent only were included for every sampling time. The final DMSO content of 0.04% (*v*/*v*) was kept constant in all inhibition experiments.

The NHDFs (2.9×10^5 per 60 mm dish) were maintained in antibiotic-free medium and reverse transfected with miRNA-21 mimic or negative control miRNA using Lipofectamine 2000 transfection reagent to analyze miRNA-mediated effects. After 24 h, the transfection mixture containing a final miRNA concentration of 100 nM was replaced with serum-free DMEM supplemented with TGF-β1 (10 µg/L) for 48 h until cell lysis.

The cell culture supernatant was collected to analyze the extracellular XT-I activity, whereas the same cell culture monolayer was lysed using a fixed amount of 0.75 mL Nonidet P-40 (NP-40)-buffer (50 mM TRIS, 150 mM NaCl, 1% NP-40, pH 7.8) for the analysis of intracellular XT-I activities. After sample centrifugation (10,000× g, 10 min, 4 °C), the supernatant contained the intracellular XT-I protein. The lysates were also used for the BCA assay. The cellular XT-I activities were measured 48 h after inhibitor treatment (48 h) or an additional 48 h after inhibitor removal (96 h).

All cell culture experiments were conducted in biological duplicate or triplicates per number n of donor-derived primary cultures as indicated.

2.9. Cell Proliferation Assay

The tetrazolium salt WST-1 (Roche, Basel, Swiss) was used for the spectrophotometric quantification of cell proliferation in response to various inhibitor concentrations. The cell proliferation assay was carried out according to the manufacturer's instructions in a 96-well tissue culture plate with 1700 cells per cavity. Based on the inhibition studies, the cells were cultured in fully supplemented DMEM for 24 h then treated with celastrol or amphotericin B for an additional 48 h. The WST-1 reagent was added to the cell culture supernatant 4 h before the end of the treatment. The absorptions at 440 and 590 nm were measured at timepoints 0, 1, 2, 3 and 4 h after the addition of WST-1.

2.10. Nucleic Acid Extraction and Synthesis of Complementary DNA

The RNA extraction from cell lysates and cDNA synthesis for mRNA and miRNA expression analysis were performed as described previously [7,42].

2.11. mRNA and miRNA Expression Analyses

Quantitative real-time polymerase chain reaction (qRT-PCR) analysis using a LightCycler 480 Instrument II system (Roche, Basel, Swiss) was performed as previously described [7]. The qRT-PCR experiments were conducted with three biological and three technical replicates per donor-derived primary cell culture, unless otherwise stated. The intron-spanning primer sequences used are listed in [7] and Table 1. The geometric mean of the expression levels of the housekeeping genes *SDHA*, *RPL13A* and *B2M* were calculated for expression normalization. The relative target gene mRNA expressions were determined by the $\Delta\Delta C_T$ method considering the PCR efficiency [43]. All normalized

gene expression levels shown were referred to the respective target gene expression of one primary cell culture sample for the relative comparison of multiple biological samples per experiment and figures.

Table 1. Additional primer sequences and annealing temperatures (T_A) used for the qRT-PCR analysis.

Gene	Primers	T_A [°C]	Product Size [bp]
COL1A1	5′-GATGTGCCACTCTGACT-3′ 5′-GGGTTCTTGCTGATG-3′	63	151

The TaqMan advanced miRNA Assay (Thermo Fisher Scientific; Waltham, Massachusetts, United States) was performed, according to the manufacturer's instructions, for the miRNA expression analyses. The primer assays miRNA-21 (477975_mir) and miRNA-191 (477952_mir) were used. The expression level of miRNA-21 determined was normalized to internal housekeeping gene expression of miRNA-191 via the $\Delta\Delta C_T$ method.

2.12. Statistical Analysis

All data are presented as mean values ± standard error of the mean (SEM). The assumption of normality was checked visually via frequency distribution histogram and by computing a Shapiro–Wilk normality test. Due to the lack of Gaussian distribution, the statistical analysis between experimental conditions was evaluated by a nonparametric two-tailed Mann–Whitney U test using GraphPad Prism 8.0 (GraphPad Software, La Jolla, CA, USA) software. Probability P values of less than 0.05 were considered statistically significant. P values are indicated with asterisks and horizontal lines connecting the bars being compared. Asterisks shown directly above the error bars of the treatment group indicate statistical differences between treated and untreated groups.

3. Results

3.1. Identification of Putative Non-Substrate-Derived XT-I Inhibitors Celastrol and Amphotericin B

An NP library of 96 compounds was screened to identify a novel non-substrate-based XT-I inhibitor. The inhibitor screening and enzymatic activity determination were performed using pgsA-6HisXT1-K4 cell-derived XT-I protein as an enzyme source and an adapted in vitro UPLC/ESI-MS/MS XT assay for selective XT-I activity determination. The compounds (Supplementary Table S1) were applied at 50 µM, whereby the impact of 0.05 to 0.15% (*v*/*v*) DMSO on the ionization process in ESI/MS [44] was initially excluded experimentally (unpublished data). Four compounds in this preliminary screening were found to exhibit an XT-I activity reduction to less than 50% of the negative control, which was set to 100% (Table 2).

Table 2. Hit compounds of the NP library screening assay that exhibited a relative XT-I activity reduction of more than 50%. The XT-I activities shown are means from one experiment performed in technical duplicates and calculated relative to the XT-I activity of the control.

Compound	Name	XT-I Activity [%]
17	Amphotericin B	25
68	Celastrol	38
74	Oxytetracycline (Terramycin)	17
86	Curcumin	43
0	Dimethyl sulfoxide	100

The compounds identified were amphotericin B (17), celastrol (68), oxytetracycline (74) and curcumin (86). The chemical structures of these hit compounds are shown in Figure 1.

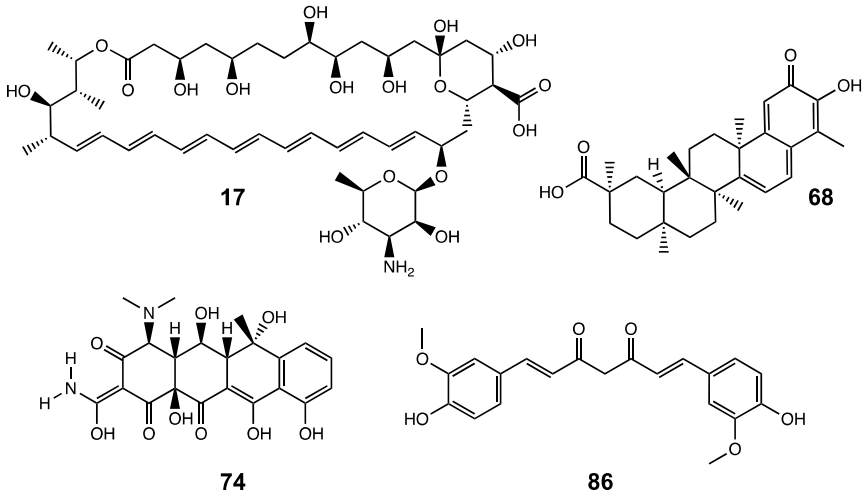

Figure 1. Structures of the compounds identified from the initial library screening assay. Amphotericin B (17), celastrol (68), oxytetracycline (74) and curcumin (86) are shown. Structures were drawn using the software ChemDraw 19.1 and retrieved from the chemical structure database ChemSpider [45].

We considered the literature-based screening results and structural features of the compounds identified to decide whether they were suitable for further cell-based analysis. Detailed information is described in the discussion part. Additionally, we performed an in silico blind docking analysis to correlate the experimental inhibition results for compounds 17, 68, 74 and 86 with the predicted ones by USCF Chimera 1.14 [38] AutoDock Vina [37]. We used the respective inhibitor structures as the ligand and apoprotein structure of XT-I previously determined by Briggs et al. [5] as the receptor input to perform a docking screen. The docking program used generates a number of potential ligand conformations and orientations relative to the XT-I protein. Those ligand-protein models (chimera model) predicted are ranked by a scoring function according to the likelihood of their binding interaction. A low negative score indicates a stable system and, thus, a likely binding interaction [37]. A summary of the docking results of the virtual screen is shown in Table 3.

Table 3. Summary of the docking scores and binding interactions of the XT-I protein with compounds 17, 68, 74, and 86, and compound 22 as a control characterized with USCF Chimera 1.14 [38] AutoDock Vina [37]. The two most favored docking modes (Chimera models) for each docked inhibitor compound with the most negative (Score) values are listed and indicated as #1 and #2. The localization of the inhibitor binding site within the XT-I protein domains (inhibitor binding) and the involvement of hydrogen bonding (^{H}Bond involvement) for inhibitor-XT-I binding are shown per chimera model predicted.

Compound	Score	Chimera Models	^{H} Bond Involvement	Inhibitor Binding
17	−11.1	Amphotericin B #1	yes	Xylo_C/GT-A domain
17	−10.1	Amphotericin B #2	yes	Xylo_C/GT-A domain
68	−9.7	Celastrol #1	no	Xylo_C domain
68	−9.1	Celastrol #2	no	GT-A domain
74	−8.6	Oxytetracycline #1	yes	Xylo_C domain
74	−8.5	Oxytetracycline #2	yes	Xylo_C/GT-A domain
86	−8.1	Curcumin #1	yes	GT-A domain
86	−7.4	Curcumin #2	yes	Xylo_C domain
22	−6.6	Sulfamethoxazole #1	yes	Xylo_C domain
22	−6.5	Sulfamethoxazole #2	no	Xylo_C domain

The virtual analysis of the two most favored inhibitor docking modes by USCF Chimera 1.14 [38] AutoDock Vina [37], ranked by the values of their scoring function, showed the most negative values for the two compounds amphotericin B (17) and celastrol (68). Compound 22, which did not possess any inhibitory effect on XT-I activity in the primary assay (Supplementary Table S1), showed the lowest AutoDock Vina docking score (Table 3). Since the value expressed by the docking score is a sum of contributions from different energy terms, such as electrostatic, H-bond, Van-der-Waals or conformation energy, we noticed the strongest discrepancy with compound 74 by comparing the ranked docking scores (Table 3) with the ranked experimental results of the initial compound screening (Table 2). Taking the results of the experimental screen, the virtual screen and the possibility of false-positive results [46], the compounds 74 and 86 were not considered for further analysis.

The two remaining compounds 17 and 68 were subjected to an IC_{50} value determination assay under the same assay conditions as the primary screening assay, except for the use of different inhibitor concentrations in the pre-incubation step with XT-I enzyme, to verify the experimental results of the preliminary screening. Consistent with the XT activity reduction observed previously (Table 2), the two compounds 17 and 68 showed comparable IC_{50} values of 12.2 ± 1 µM (amphotericin B) and 11.0 ± 1 µM (celastrol) (Figure 2A).

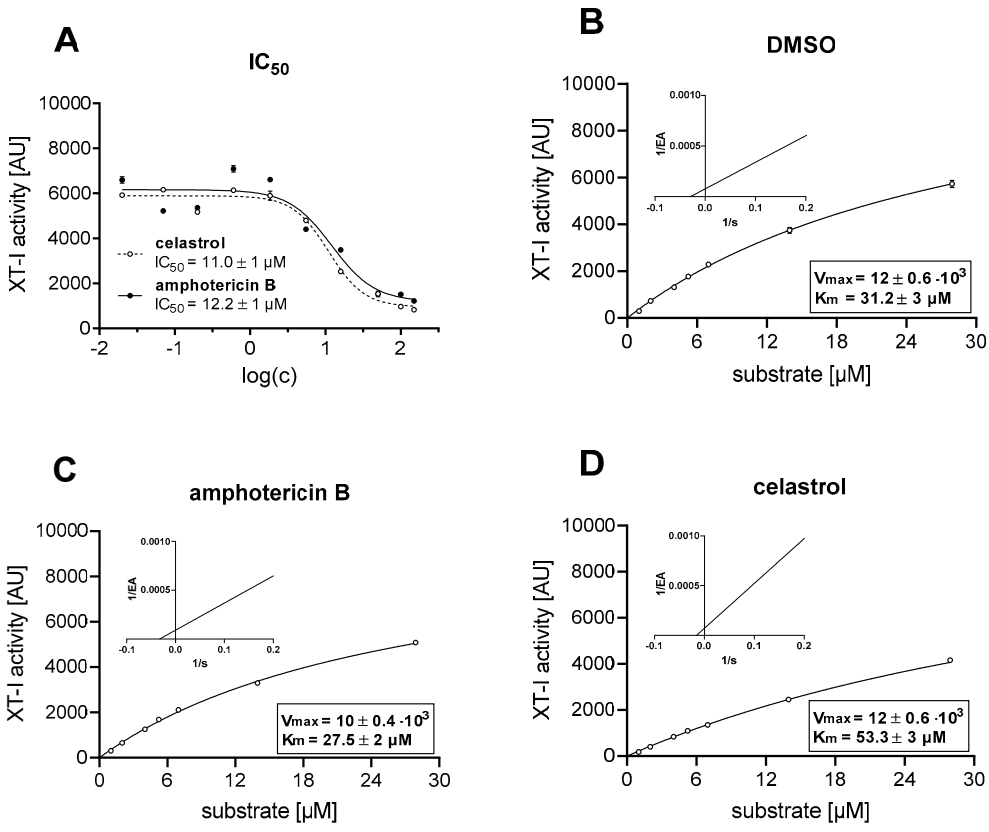

Figure 2. Enzyme and inhibition kinetics. The enzyme activity (EA) illustrated corresponds to the generated xylosylated-acceptor peptide measured by the UPLC-ESI-MS/MS XT-I assay after a fixed time point and, therefore, is expressed in arbitrary units (AU) detected at a certain retention time. (**A**) Determination of IC_{50} values of compounds 17 (amphotericin B) and 68 (celastrol) at 15 µM UDP-D-xylose, 10.5 µM acceptor peptide and various inhibitor concentrations (c). The values shown are mean ± SEM of duplicate data points per experiment. (**B**–**D**) Michaelis–Menten and Lineweaver–Burk plots for the modified acceptor peptide (substrate, s) at 15 µM UDP-D-xylose. Values are means ± SEM of triplicate data points per experiment.

We next performed kinetic studies to investigate the MOI of these potent compounds and correlated the data with the chimera models obtained with Autodock Vina. The enzyme activity of

CHO cell-derived XT-I protein samples were measured after incubation with the inhibitor compounds or DMSO for 1 h. The reaction was started by incubation of 50% (*v*/*v*) of the CHO-inhibitor mixture with 50% (*v*/*v*) reaction buffer containing UDP-D-xylose and various acceptor peptide concentrations, each at 37 °C. The Michaelis–Menten and Lineweaver–Burk plots for the modified acceptor peptide are shown in Figure 2. The Michaelis–Menten constant K_m, maximum enzyme activity V_{max} or Y-intersect and slope values derived from this analysis are summarized in Supplementary Table S2.

The compound amphotericin B (17) used at IC_{50} concentration resulted in a decreased K_m value and a concomitant decrease in the V_{max} value compared to the assay containing DMSO, indicative of an uncompetitive MOI regarding the acceptor peptide. This mechanism of inhibition is characterized by changing the Y-intercept but not the slope value in the Lineweaver–Burk plot (Figure 2B,C; Supplementary Table S2).

The usage of compound celastrol (68) at the IC_{50} concentration resulted in an increased K_m value compared to the approach containing DMSO. The V_{max} value determined did not differ between the celastrol and assay containing DMSO. Regarding the parameters extracted from the Lineweaver–Burk plot, the value of the Y-intercept was higher in the assay containing celastrol, while the slope value did not vary considerably from the assay containing DMSO (Figure 2B,D; Supplementary Table S2). The results of the Michaelis–Menten and Lineweaver–Burk plots are indicative of a competitive mechanism of inhibition.

In comparison with the most favored docking modes offered by USCF Chimera 1.14 [38] AutoDock Vina [37] (Table 3), the chimera models amphotericin B #2 and celastrol #2 were able to confirm the experimentally approved situation exactly (Figure 3).

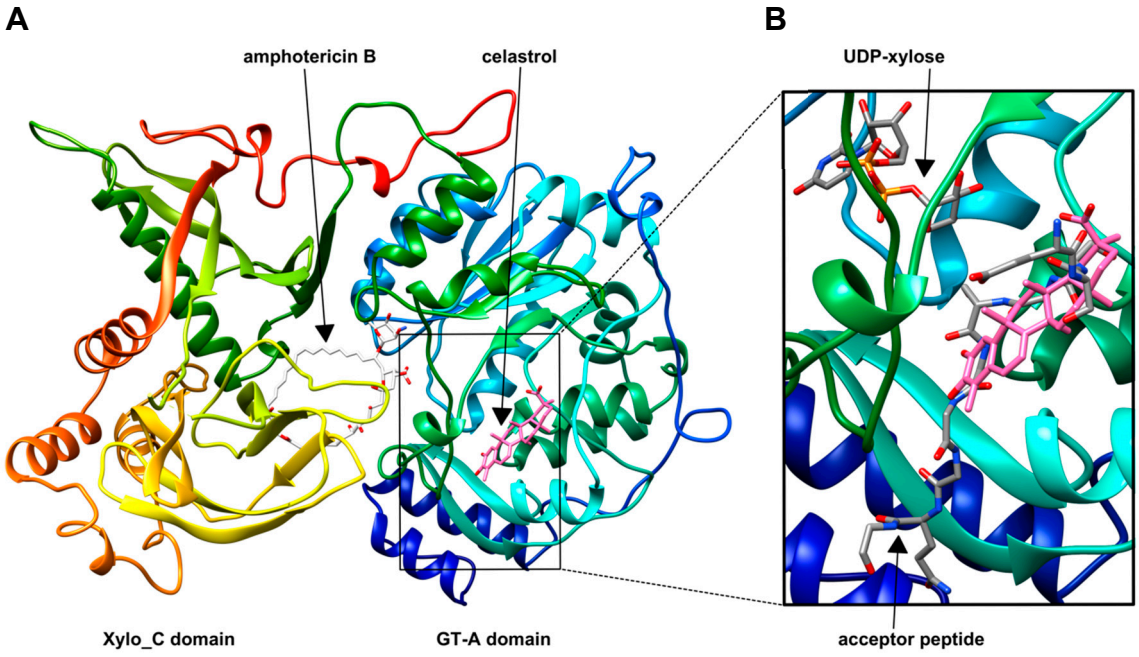

Figure 3. Three-dimensional structure of human XT-I complexed with the compounds amphotericin B (**17**) and celastrol (68). (**A**) Crystal structure of human XT-I [5], rainbow colored from the N terminus (blue) to C terminus (red), complexed with the chimera models #2 of compounds 17 (amphotericin B, white colored) and 68 (celastrol, pink colored). (**B**) UDP-D-xylose, modified acceptor peptide (atoms: C (grey), N (blue), O (red), P (orange)) and docked orientation of compound 68 (celastrol, pink) are shown in the stick representation.

It could be observed by analyzing the binding zone (< 5.0 Å) of amphotericin B #2 in the XT-I protein complexed with UDP-D-xylose and modified acceptor peptide that the binding of the acceptor peptide was unaffected by amphotericin B binding. Furthermore, an overlap of the amphotericin B binding site and UDP-D-xylose could be detected (Supplementary Figure S1). As illustrated in

Figure 3, celastrol might bind to the active site of the XT-I, preventing the acceptor peptide from binding. Binding zone (< 5.0 Å) analysis of celastrol #2 reflected a spatial proximity to the UDP-D-xylose molecule, as was shown for the modified acceptor peptide (unpublished data). The consistency of both experimental and in silico results indicate that amphotericin B is an uncompetitive inhibitor toward the acceptor peptide substrate, while celastrol seems to exhibit a competitive binding mode in this context.

3.2. Celastrol and Amphotericin B Inhibit Cellular Proliferation Dose-Dependently

The cytotoxic effects of amphotericin B and celastrol on the proliferation of NHDFs was tested with the WST-1 assay. Both compounds in these experiments were used at concentrations ranging from 0.0 to 4.0 µM (Figure 4).

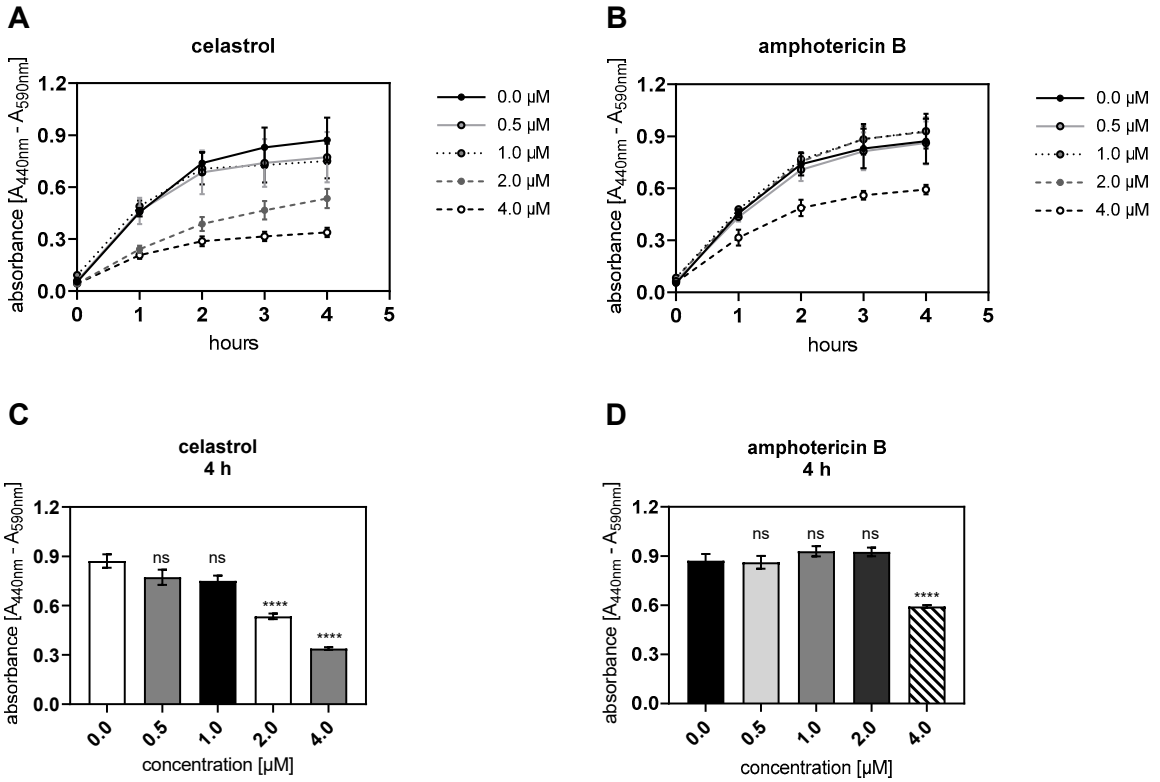

Figure 4. Celastrol and amphotericin B treatment inhibited the NHDF proliferation in a dose-dependent manner. Human primary dermal fibroblasts (n = 2) were cultured the day before the experiment for measuring the cell proliferation in response to different inhibitor treatments. Cells were treated with vehicle (0.0 µM) or 0.5, 1.0, 2.0 and 4.0 µM (**A**) celastrol or (**B**) amphotericin B for 48 h. Cellular proliferation was detected by the addition of tetrazolium salt WST-1 to the cell culture supernatants at the 44 h timepoint and measured 0, 1, 2, 3 and 4 h post-supplementation. The absorbance measured correlates directly to the number of cells viable after the inhibitor treatment. (**C**,**D**) Bar chart display of the WST-1 assay results measured 4 h post supplementation of NHDFs with WST-1. Data are means ± SEM of five biological and one technical replicate per experiment. Mann-Whitney U test: not significant (ns), $p < 0.0001$ (****).

We found significantly decreased cell proliferation in cells treated with 2.0 and 4.0 µM celastrol (both $p < 0.0001$) compared to the control after 48 h of inhibitor incubation (Figure 4A,C). The usage of 4.0 µM amphotericin B also reduced the proliferation of NHDFs significantly ($p < 0.0001$) compared to the control (Figure 4D).

Taking these results together, the treatment of NHDFs with 0.5 and 1.0 µM celastrol or the usage of amphotericin B at a concentration range of 0.5 to 2.0 µM for 48 h did not influence cellular

proliferation. Thus, these inhibitor concentrations and incubation durations could be used for the next cell-based experiments.

3.3. Dual Effect of Putative XT-I Inhibitors on XYLT1 mRNA Expression and XT Activity of NHDF

Previous studies have shown that the cellular XT-I activity is regulated on the transcriptional level [7]. After demonstrating that the DMSO content of 0.04% (*v*/*v*), the celastrol concentrations of 0.5 and 1.0 µM and the amphotericin B usage of 0.5 to 2.0 µM are well tolerated by NHDFs, we wanted to evaluate the effects of the putative XT-I inhibitors on the *XYLT1* mRNA expression and cellular XT-I activity. Consequently, NHDF cells were cultured as a monolayer in a previously established fibrosis cell culture model [17] and treated subsequently with celastrol or amphotericin B in the presence of fibrotic mediator TGF-β1, which had been previously shown to increase the *XYLT1* mRNA expression in fibroblasts [17,18]. The *XYLT1* mRNA expression levels were quantified 48 h posttreatment by qRT-PCR analysis (Figure 5).

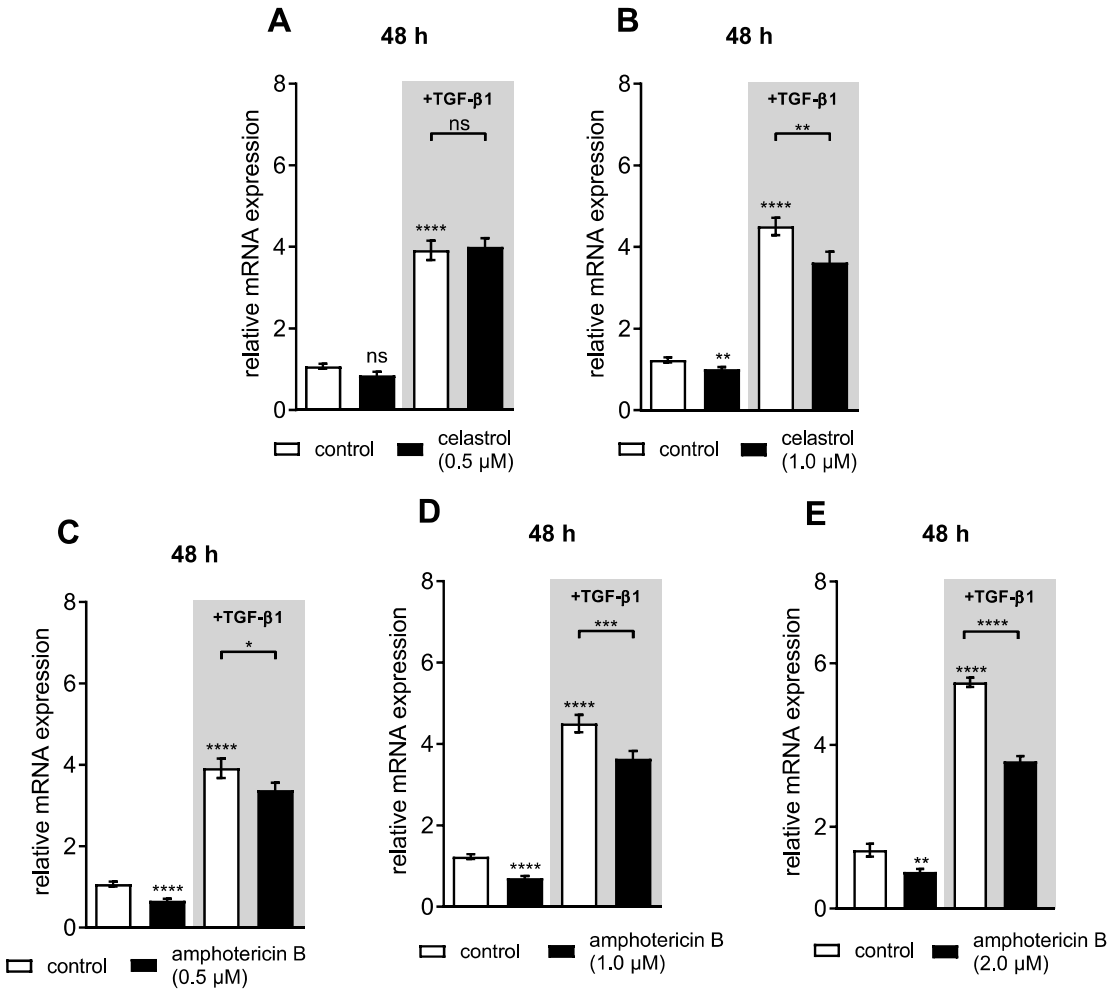

Figure 5. Celastrol and amphotericin B treatment reduced the basal and TGF-β1-mediated *XYLT1* mRNA expression in NHDFs. Human primary dermal fibroblasts ($n = 3$) were cultured the day before the experiment. Cells were treated with vehicle (control), (**A**,**B**) celastrol (0.5 or 1.0 µM) or (**C**–**E**) amphotericin B (0.5, 1.0 or 2.0 µM) for 48 h with or without additional TGF-β1 (5 µg/L) supplementation. Relative *XYLT1* mRNA expression levels were analyzed by qRT-PCR. Data are means ± SEM of three biological and three technical replicates per experiment. Mann–Whitney U test: not significant (ns), $p < 0.05$ (*), $p < 0.01$ (**), $p < 0.001$ (***), $p < 0.0001$ (****).

The NHDFs showed an increase in *XYLT1* mRNA expression after 48 h of TGF-β1 treatment (3.7 ± 0.3-fold, $p < 0.0001$; Figure 5A–D). The usage of 0.5 μM celastrol neither changed the basal *XYLT1* mRNA expression nor effected the TGF-β1-mediated *XYLT1* mRNA expression increase in NHDFs (Figure 5A). However, a significant reduction in both basal and TGF-β1-mediated *XYLT1* mRNA expression was observed with 1.0 μM celastrol (0.8 ± 0.06-fold, $p = 0.005$ and 0.8 ± 0.07-fold, $p = 0.01$) (Figure 5B). Regarding the mRNA expression of isoform *XYLT2* in NHDFs, which was unaffected by TGF-β1 supplementation, the addition of 1.0 μM celastrol in the presence of TGF-β1 did not alter the *XYLT2* mRNA expression level in these cells (Supplementary Figure S2A).

The amphotericin B treatment of NHDFs at concentrations of 0.5 and 1.0 μM significantly decreased the basal *XYLT1* mRNA expression (0.6 ± 0.06-fold and 0.6 ± 0.05-fold, respectively, both $p < 0.0001$). Furthermore, we observed a significant reduction of the TGF-β1-induced *XYLT1* mRNA expression in NHDFs due to the supplementation of amphotericin B at concentrations of 0.5 and 1.0 μM (0.9 ± 0.07-fold, $p = 0.04$ and 0.8 ± 0.06-fold, $p = 0.0003$, respectively) (Figure 5C,D). The *XYLT1* mRNA expression in cells 48 h after supplementation with amphotericin B at a concentration of 2.0 μM was considerably reduced in comparison to the mRNA expression of controls treated with DMSO (0.6 ± 0.09-fold, $p = 0.005$). The TGF-β1 treatment of NHDFs increased the basal *XYLT1* mRNA expression level significantly (4.6 ± 0.2-fold, $p < 0.0001$; Figure 5E). This TGF-β1-mediated effect on the *XYLT1* mRNA expression level was remarkedly reduced by 2.0 μM amphotericin B (0.7 ± 0.03-fold, $p < 0.0001$) (Figure 5E). In concordance with previous results [7], the isoform *XYLT2* mRNA expression level was unaffected by the TGF-β1 treatment. Furthermore, the basal *XYLT2* mRNA expression of cells treated with TGF-β1 did not differ from that of those additionally treated with amphotericin B (Supplementary Figure S2B).

Together, these results indicate that amphotericin B and celastrol were not only capable of interfering with the XT-I protein itself but could also regulate cellular *XYLT1* mRNA expression due to a yet unknown mechanism.

3.4. Inhibitor-Induced mRNA Expression Changes Lead to Decreased XT-I Protein Expression in NHDF

In order to examine whether the inhibitor-mediated reduction of *XYLT1* gene expression correlates with changes in the extracellular and intracellular XT-I activity of NHDFs, we usually determine the cellular XT-I activity by UPLC-MS/MS under the same experimental conditions as the gene expression analysis. This time, however, we had to consider that the exogenously supplemented inhibitor compounds could change the extracellular XT-I activity measured (Supplementary Figure S3). In comparison to the extracellular XT activity of untreated cells, the supplementation of celastrol for 48 h at a concentration of 0.5 μM led to a significant reduction of the XT-I activity (0.8 ± 0.07-fold, $p = 0.03$) (Supplementary Figure S3). Under the same experimental conditions, no *XYLT1* mRNA expression changes were present in cells treated with celastrol (Figure 5A). These results revealed that the XT-I activity measured in the presence of the exogenous supplemented inhibitor was artificial and did not reflect the transcriptional state of the cell.

In order to address this limitation, we decided to change the experimental setup, allowing us to determine the cellular XT-I activity changes that were caused by former inhibitor-mediated changes on the *XYLT1* mRNA expression in NHDFs by UPLC/ESI-MS/MS. The results of this XT-I activity determination after simultaneous treatment of cells for 48 h with TGF-β1 and the highest tolerated inhibitor concentrations, followed by an incubation of the NHDFs in inhibitor-free media for an additional 48 h, are shown in Figure 6.

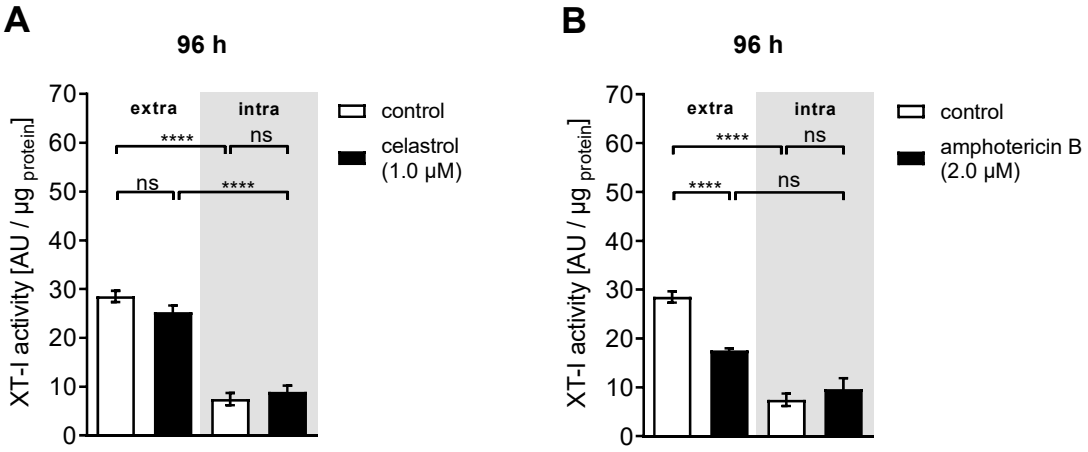

Figure 6. Amphotericin B was capable of reducing the extracellular XT-I activity in a fibrosis cell culture model. Human primary dermal fibroblasts (n = 3) were cultured in media supplemented with TGFβ1 (5 µg/L) for 24 h in order to enhance their myofibroblast differentiation. Thereafter, cells were treated with DMSO (control, white), (**A**) 1.0 µM celastrol or (**B**) 2.0 µM amphotericin B containing media supplemented with TGF-β1 (5 µg/L) for 48 h. Cells were washed twice with 1x PBS and cultured in TGF-β1- and inhibitor-free media for an additional 48 h (96 h). The intracellular XT-I activity (intra, grey) was determined from the cell lysates and the corresponding supernatants were utilized for extracellular XT-I activity (extra) determination by UPLC-ESI-MS/MS XT-I assay. The XT-I activity is expressed in arbitrary units (AU) per µg of protein in a 1 mL sample. Data are means ± SEM of three biological and three technical replicates per experiment. Mann–Whitney U test: not significant (ns), $p < 0.0001$ (****).

A slight but not significant decrease in extracellular XT activity was observed in the NHDFs upon treatment with celastrol (0.9 ± 0.06-fold, $p = 0.06$) (Figure 6A). By contrast, the usage of amphotericin B resulted in a statistically significant reduction of extracellular XT-I activity (0.6 ± 0.03-fold, $p < 0.0001$) (Figure 6B). The celastrol and amphotericin B treatments did not result in any detectable changes in the intracellular XT activities of NHDFs compared to control cells treated with DMSO. It can therefore be concluded that the celastrol- and amphotericin B-mediated changes to the *XYLT1* mRNA expression observed previously correlate with the extracellular XT-I activity changes, especially for 2 µM amphotericin B, while the intracellular XT activity seemed to return to a homeostatic state during the cell incubation in inhibitor-free media for 48 h.

3.5. Celastrol-Induced XYLT1 Suppression Might Be Mediated by the miRNA-21 Pathway

After showing that celastrol exerts a suppressive effect on *XYLT1* mRNA expression, we wanted to evaluate a putative cellular pathway underlying this regulation. miRNA-21 plays a crucial role in TGF-β1/Smad pathway-mediated tissue fibrosis [24,47]. Earlier studies by Cheng et al. showed the involvement of the miRNA-21/ERK pathway in celastrol-mediated anti-fibrotic effects in murine cardiac fibroblasts [48]. In concordance with the study by Ni et al. [49], Cheng et al. demonstrated a celastrol-induced suppression of miRNA-21 expression [48]. Based on these findings, we wanted to verify the impact of the miRNA-21 pathway on basal and TGF-β1-mediated *XYLT1* expression (Figure 7).

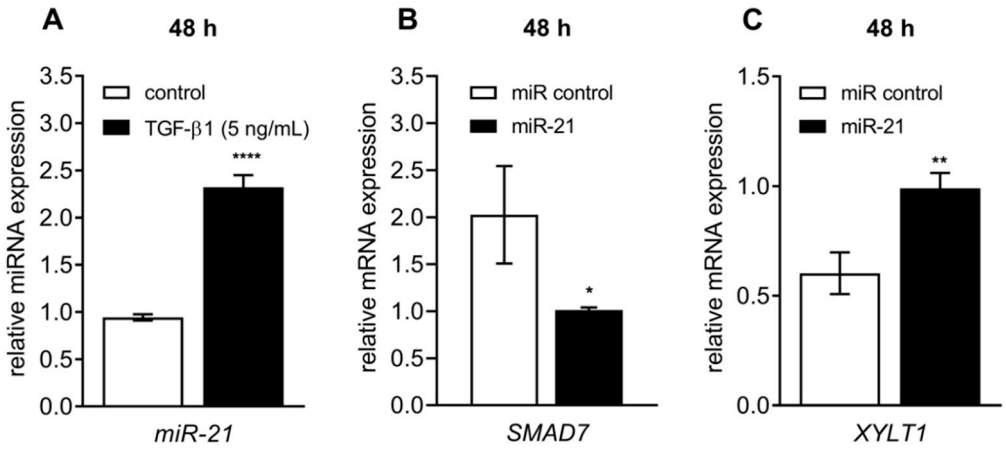

Figure 7. Reciprocal regulation of the *XYLT1* and *SMAD7* mRNA expression by miRNA-21. (**A**) Human primary dermal fibroblasts ($n = 3$) were cultured the day before the experiment. Cells were serum-starved for 24 h and treated with or without TGF-β1 (5 µg/L) for 48 h. Relative miRNA-21 (miR-21) expression levels were analyzed by qRT-PCR using Taqman probes. (**B**,**C**) The NHDFs ($n = 3$) were transfected with an miRNA-21 mimic (miR-21) or negative control miRNA mimic (miR control). After 24 h, cells were incubated in media supplemented with TGF-β1 for 48 h. Relative *XYLT1* and *SMAD7* mRNA expressions were analyzed by qRT-PCR. Data shown are means ± SEM for two biological and three technical replicates per experiment. Mann–Whitney U test: $p < 0.05$ (*), $p < 0.01$ (**), $p < 0.0001$ (****).

A Taqman-based gene expression analysis was performed to examine the role of the TGF-β1-regulated miRNA-21 expression in our myofibroblast cell culture model. We found that the miRNA-21 expression was significantly increased in NHDFs after TGF-β1 supplementation (2.5 ± 0.2-fold, $p < 0.0001$) (Figure 7A). TGF-β1 was shown to be a potent inducer of miRNA-21; therefore, we further examined the direct impact of miRNA-21 on *XYLT1* expression. Since an inverse relationship between the miRNA expression level and its putative target gene was anticipated, we determined the expression level of *SMAD7*, an miRNA-21 target gene confirmed previously [26] and negative regulator of *XYLT1* [7]. Therefore, NHDFs were transfected with an miRNA-21 mimic to resemble the fibrotic miRNA increase. In comparison to the negative control miRNA-transfected cells, miRNA-21 transfection strongly increased the *XYLT1* mRNA expression (1.6 ± 0.3-fold, $p = 0.003$) through a simultaneous decrease of inhibitory *SMAD7* expression (0.5 ± 0.1-fold, $p = 0.02$) (Figure 7B,C). These findings provide a strong argument for the role of the miRNA-21/Smad7 pathway underlying celastrol-mediated effects on *XYLT1* expression.

3.6. Amphotericin B Mediates XYLT1 Suppression by Interfering with TGF-β Pathway Components

After showing that amphotericin B is a potent XT-I inhibitor on both a transcriptional and posttranscriptional level, we hypothesized that the anti-fibrotic effect of amphotericin B was mediated by the targeting of downstream TGF-β pathway components, leading to the *XYLT1* mRNA expression decrease observed (Figure 5C–E). We determined the relative *SMAD7*, *TGFB1* and *COL1A1* mRNA expression levels in the NHDFs that were treated with 2.0 µM amphotericin B in the presence or absence of TGF-β1 for 48 h to test this hypothesis (Figure 8).

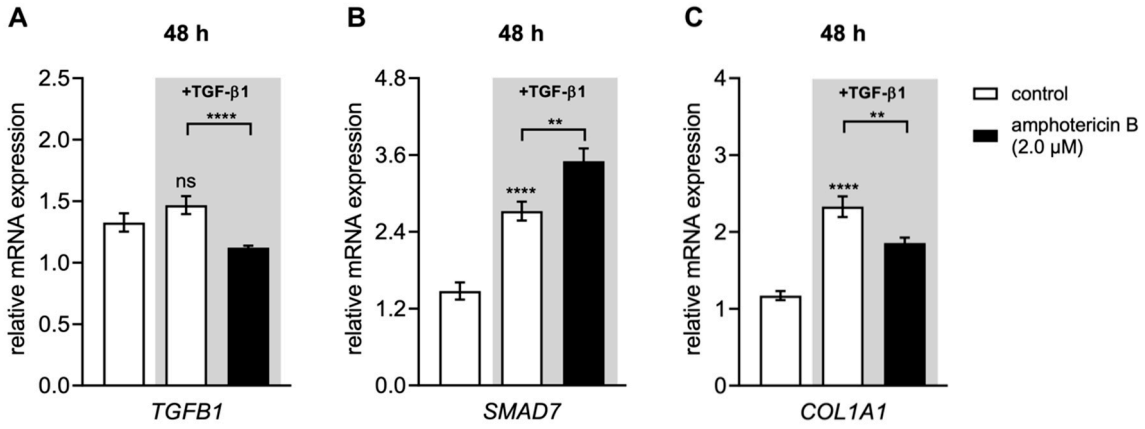

Figure 8. Amphotericin B reduces the TGF-β1-mediated *COL1A1* mRNA expression increase in NHDFs. Human primary dermal fibroblasts (n = 3) were cultured the day before the experiment. Cells were treated for 48 h with vehicle only (control), vehicle or 2.0 µM amphotericin B with additional TGF-β1 (5 µg/L) supplementation (highlighted in grey). Relative (**A**) *TGFB1*, (**B**) *SMAD7* and (**C**) *COL1A1* mRNA expression levels were analyzed by qRT-PCR. Data are means ± SEM of three biological and three technical replicates per experiment. Mann–Whitney U test: not significant (ns), $p < 0.01$ (**), $p < 0.0001$ (****).

We could show that the autoinduction of *TGFB1* mRNA expression by TGF-β1 (1.1 ± 0.08-fold, $p = 0.08$) was significantly decreased in the presence of 2 µM amphotericin B (0.8 ± 0.04-fold, $p < 0.0001$). In concordance with these changes, the TGF-β1-induced expression increase of *SMAD7* (1.8 ± 0.2-fold, $p = 0.002$), a known negative regulator of *TGFB1* expression [50], was significantly enhanced in the presence of 2 µM amphotericin B (1.3 ± 0.1-fold, $p < 0.0001$). Regarding the *COL1A1* mRNA expression, we observed a reduction in cells treated with amphotericin B that was not statistically significant compared to controls treated with DMSO (0.7 ± 0.1-fold, $p = 0.2$). In comparison to the cells treated exclusively with DMSO, the presence of TGF-β1 upregulated the *COL1A1* mRNA expression level significantly (0.8 ± 0.06-fold, $p = 0.0003$). This TGF-β1-mediated expression increase could be significantly diminished by the presence of 2.0 µM amphotericin B (0.8 ± 0.06-fold, $p = 0.008$) (Figure 8C).

We assume from these experiments that the amphotericin B-mediated *XYLT1, COL1A1* and *TGFB1* mRNA expression changes under fibrotic conditions were mediated by the simultaneous induction of *SMAD7* expression.

4. Discussion

Myofibroblasts are the key effector cells in excessive ECM synthesis under the pathophysiological conditions that characterize fibrosis [19,51]. TGF-β-driven fibroblast-to-myofibroblast transition was determined by the increased expression and activity of GAG-initiating enzyme XT-I [17,18], corresponding to elevated PG metabolism and increased GAG content in human cells and tissues [52,53]. Thus, modulating downstream TGF-β signaling by the inhibition of XT-I activity could be a promising approach to treat fibrosis. The previous studies performed focused on substrate or end-product analogues such as heparin, GAGs, nucleosides or uridine-derived nucleotides as XT inhibitors. To the best of our knowledge, no studies have been conducted to identify non-substrate-like XT-I inhibitors so far. In the present study, we adapted a previously established enzymatic XT-I activity assay for cell-free screening of an NP-inspired pure compound library with 96 substances regarding their XT-I inhibitory action. We identified four initial compounds with XT-I inhibitory properties: polyene antibiotic amphotericin B, pentacyclic triterpenoid celastrol, tetracycline antibiotic oxytetracycline and natural phenol curcumin. We performed structural- and literature-based analyses and in silico binding analyses to confirm and prioritize the active inhibitory molecules from this primary screening.

Based on the literature, curcumin is an intensively studied compound with strong assay-interfering properties and, furthermore, is an invalid metabolic panaceas candidate [46,54]. In relation to the enzymatic assay performed here, it can be concluded that curcumin could have interfered by Mg^{2+} or Mn^{2+} ion chelation via the double-activated Michael system or by the binding of the acceptor peptide that has a similar amino acid sequence to silk fibroin [55], leading to false negative screening results. The compound oxytetracycline possesses similar structural features to curcumin, such as several oxygen atoms, which make the chelation of divalent metal ions possible. The C-12 and C-11 oxygen atoms are accepted to be the major binding site for magnesium [56]. The strong ion dependency of the XT-catalyzed reaction was shown previously by Casanova et al. and Müller et al. [30,57]. Taking the molecular docking results and positions into consideration, curcumin and oxytetracycline exhibited the lowest predicted binding affinity to the XT-I protein compared to the compound amphotericin B and celastrol. The binding position for oxytetracycline was predicted to be on the Xylo_C domain (Chimera model #1) or between the Xylo_C and GT_A domain (Chimera model #2). Given that mutations in the loop region that mediate the only direct contact between the Xylo_C and GT-A domains did not impair xylose transfer of XT-I [5], we conclude that the discrepancy between the virtual and initial screening data was caused by the reactive structural features. Consequently, the compounds oxytetracycline and curcumin were not further analyzed in the current study.

The structural- and literature-based analysis of amphotericin B and celastrol showed that amphotericin B is an antibiotic used commonly in tissue culture systems and, therefore, should be suitable for cell-based analysis [58]. Amphotericin B consists of a 38-membered macrolactone ring structure, which is β-glycosylated at the C-19 hydroxyl position with a mycosamine. It could be thought that amphotericin B-protein interactions are based on the formation of hydrogen bonds or by hydrophobic interactions due to the extended conjugated system of the hydrophobic polyene subunits and the high number of hydroxyl groups in the hydrophilic polyol part of the molecule attached [59,60]. Clinical trials report the therapeutic benefit of antioxidant celastrol in inflammatory diseases, whereas cell culture experiments provided the first evidence of the anticancer and neuroprotective properties of celastrol [32,48,49]. Celastrol is structurally a quinone-contained triterpenoid made up of five cyclic rings that can form covalent Michael adducts through the binding of the electrophilic site on quinone methide rings with nucleophilic thiol groups of cysteine residues [61]. Considering the data obtained, the compounds amphotericin B (17) and celastrol (68) were subjected to further analysis.

We confirmed the results of the initial cell-free screening by the determination of the IC_{50} values, using those to evaluate their inhibitory mode experimentally. Amphotericin B was shown to be an uncompetitive inhibitor regarding the acceptor peptide. This result was consistent with the USCF Chimera [38] AutoDock Vina [37] docking modes predicted. The two docking modes of amphotericin B predicted with the highest binding affinities showed amphotericin B positioned between the Xylo_C and GT-A domains, with the β-glycosylated C-19 mycosamine structure directed towards the GT-A domain. Accordingly, amphotericin B might bind to the enzyme-peptide complex and inhibit consecutive reactions but not the binding of the acceptor peptide to the active site. This hypothesis was underlined by the binding zone analysis, showing that there is a slight overlap between the amphotericin B ring structure around the C-19 position with areas of the UDP-xylose binding site. This uncompetitive inhibitor binding mode towards a substrate is common in enzymes catalyzing bisubstrate reactions [62]. Regarding celastrol, the kinetic studies indicated a competitive inhibitory action of celastrol towards the acceptor peptide. The results were strengthened by the AutoDock Vina [37] predicted docking modes of celastrol. Docking mode #1 showed a celastrol binding at the Xylo_C domain, while docking mode #2 showed a competitive binding mode on the peptide acceptor side. Given that mutations in the Xylo_C domain did not result in XT-I activity reduction [5], the XT-I activity reduction observed experimentally is likely to have been caused by the competitive binding mode, as illustrated by docking mode #2. As has been mentioned above, celastrol is capable of forming covalent adducts with cysteine residues in the protein [61]. Based on the finding that agents (such as *N*-phenyl maleimide) that react with free cysteine residues had no effect on the activity

of XT-I [57], we conclude that the celastrol-mediated XT-I activity inhibition observed was possibly not due to covalent Micheal adduct formation. However, a complete analysis of the mechanism of action is required, including an evaluation of other potential inhibition events such as allosteric, partial, tight-binding and time-dependent inhibition, to confirm amphotericin B and celastrol as an uncompetitive and a competitive inhibitor of human XT-I, respectively [62,63].

After this initial screen and inhibitor characterization, we performed a cell-based assay to complement the biochemical screening results. The cytotoxic effects of amphotericin B and celastrol on the proliferation of NHDF cells was tested in a proliferation assay. We demonstrated that both compounds were suitable for cell-based analyses at concentrations of 0.5 and 1.0 µM, whereas amphotericin B could be used up to a concentration of 2.0 µM without resulting in proliferation changes. It should be noted that the maximum amphotericin B concentration of 4 µM (3.7 mg/L) tested here already reduced the cellular proliferation significantly and was not used for further analysis. These dose-dependent effects on cellular proliferation are comparable with those reported in the literature [49,58]. Harmsen et al. demonstrated in their in vitro study using osteoblasts and fibroblasts that amphotericin B is lethal to fibroblasts at concentrations of 100 µg/mL, and that this antifungal drug causes sublethal cytotoxicity at 5 and 10 mg/L [58]. The celastrol-mediated inhibition of cellular proliferation in different cell types was tested previously in the concentration range of 0.2 to 10 µM. In agreement with our finding, a time- and concentration-dependent reduction in cellular viability or proliferation was reported [48,49,64].

After identifying the optimal amphotericin B and celastrol concentrations for cell-based assays, we characterized their influence on TGF-β1-driven transcription in human cells. We utilized a fibrosis cell culture model established previously and assessed both the direct inhibitor binding to the cellular XT-I protein and the regulation of the *XYLT1* transcription and, thus, influencing the corresponding cellular XT activity. Consistent with the inhibition observed using recombinant CHO cell line-expressed XT-I protein, celastrol was capable of reducing the extracellular XT activity of NHDFs regardless of their *XYLT1* expression. No intracellular XT activity changes were observed, indicating a lack of the membrane permeability of the compound or an unsuited detection time point for intracellular XT activity changes. In agreement with previous results in NHDFs, the intracellular XT activity remained constant over time, while the extracellular XT activity of untreated cells increased over time due to the XT-I protein secretion and accumulation in the cell culture supernatant [7,12]. Consequently, the extracellular XT-I protein secreted can be bound by the inhibitors added exogenously, leading to the XT activity reduction that was observed when compared to samples supplemented with DMSO. The inhibitor compound containing cell culture supernatant was replaced with inhibitor-free media for XT activity detection to overcome this limiting factor of direct inhibitor-protein interaction and observe XT-I activity changes that were originally mediated by transcriptional changes. Using this experimental setup, we found a significant reduction of extracellular XT-I activity quantified 48 h post-amphotericin B treatment and only a slight but not significant reduction of extracellular XT-I activity post treatment with celastrol. The *XYLT1* mRNA expression in 2.0 µM amphotericin B- and 1.0 µM celastrol-treated cells analyzed exhibited a concentration-dependent decrease of TGF-β1-induced *XYLT1* mRNA expression compared to the control. Furthermore, this *XYLT1* transcription regulation seemed to be isoform-specific because the *XYLT2* mRNA expression in the TGF-β1-treated cells was not affected. This correlation of *XYLT1* mRNA expression level and enzyme activity has been shown in numerous studies using TGF-β1-treated human dermal and cardiac fibroblasts [7,18,29,42]. These results clearly show that amphotericin B and, to a smaller extent, celastrol are capable of dual XT-I inhibition via direct protein-ligand binding and *XYLT1* transcription regulation.

There are currently no reports from clinical trials targeting TGF-β signaling in cystic fibrosis (CF) [28], but several studies have already observed a beneficial role of amphotericin B in the treatment of CF or its secondary pulmonary complications. The exact cellular mechanisms underlying those effects have not been fully understood but have been shown as independent of loss-of-function mutation in the cystic fibrosis transmembrane conductance regulator, going beyond the antifungal activity

of amphotericin B [65,66]. Since studies of CF patients identified the activation of TGF-β signaling associated with lung fibrosis and myofibroblast differentiation [67], we presumed that amphotericin B could also regulate TGF-β-induced myofibroblast differentiation after sufficient administration [58]. In this context, we have observed a significant reduction of *COL1A1* and *TGFB1* gene expressions through the addition of 2 μM amphotericin B in our fibrosis model with primary NHDFs supplemented with TGF-β1. Furthermore, the TGF-β1-induced expression of inhibitory *SMAD7* further increased in the presence of amphotericin B. Since Smad7 is an important inhibitor of TGF-β superfamily signaling due to its upregulation by TGF-β functioning in a negative feedback loop [50,68], the *XYLT1*, *COL1A1* and *TGFB1* expression decreases observed here might be mediated by this enhanced negative feedback loop.

It has recently been reported that miRNA-21 is overexpressed during fibrosis and regulates the fibrotic process by modulation of TGF-β1 signaling pathways [24]. To date, nothing is known about the miRNA-21-mediated regulation of XT-I. Therefore, based on the study by Cheng et al. that showed the involvement of the miRNA-21/ERK pathway in celastrol-mediated anti-fibrotic effects in cardiac fibroblasts [48], we analyzed whether miRNA-21 participates in abnormal *XYLT1* regulation under fibrotic conditions. Consistent with the study by Cheng et al. described, we observed an induction of miRNA-21 expression after TGF-β1 stimulation of primary NHDFs in vitro. Performing miRNA-21 overexpression experiments in NHDFs, we identified a novel regulatory mechanism of TGF-β1-driven *XYLT1* expression by the miRNA-21/SMAD7 pathway. These results are in concordance with those of our previous study, demonstrating a suppressive role of miRNA-21 target *SMAD7* [26] in the transcriptional regulation of cytokine-driven *XYLT1* expression [7]. Only a few studies have evaluated the role of miRNAs in TGF-β1-driven *XYLT1* expression regulation so far. Recent studies by our group have revealed an miRNA-145/KLF4- and miRNA-29b/SP1-mediated XT regulatory pathway in human skin fibroblasts [42,69], while Theis et al. demonstrated *XYLT1* to be a direct target of miRNA-133b in the context of murine spinal cord injury [70]. In summary, we were not only able to identify putative XT-I inhibitors in this study but also found first evidence of a regulatory mechanism of TGF-β1-induced *XYLT1* expression by miRNA-21.

5. Conclusions

Potent and effective inhibitors of human XT-I could be useful treatment options for cytokine-driven fibrosis. Overall, this investigation identified the two compounds amphotericin B and celastrol as putative non-substrate-based XT-I inhibitors, which were hitherto unknown in this context. Their XT-I activity inhibitory actions seem to be mediated by an uncompetitive or competitive MOI, respectively, regarding the acceptor peptide substrate. In addition, both compounds were capable of decreasing *XYLT1* expression levels and, regarding amphotericin B, subsequent XT activity in myofibroblasts. Due to literature research and cell culture experiments, we suggest a critical role for TGF-β and miRNA-21 pathways in the underlying cellular mechanisms of XT-I inhibition. The results of our study provide a strong rationale for consideration of the putative XT-I inhibitors amphotericin B and celastrol as therapeutic agents in fibroproliferative diseases.

Supplementary Materials: The following are available online at http://www.mdpi.com/2218-273X/10/10/1467/s1: Table S1: Results of the NPs library screening assay. Table S2: Experimental analysis of human XT-I inhibition by celastrol and amphotericin B. Figure S1: Structure of human XT-I complexed with amphotericin B, UDP-D-xylose and the acceptor peptide. Figure S2: *XYLT2* mRNA expression is not affected by inhibitor or cytokine treatment of NHDF. Figure S3: Extracellular XT-I activity reduction by celastrol was not caused by the downregulation of *XYLT1* mRNA expression.

Author Contributions: Conceptualization, T.-D.L., D.H., C.K. and I.F.; data curation, T.-D.L. and I.F.; formal analysis, T.-D.L.; funding acquisition, I.F.; investigation, T.-D.L. and A.K.; methodology, A.K., B.F. and J.K.; project administration, D.H. and I.F.; resources, B.F.; supervision, C.K.; validation, B.F., V.S. and J.K.; visualization, T.-D.L.; Writing—Original draft, T.-D.L.; Writing—Review and editing, A.K., B.F., V.S., D.H., J.K., C.K. and I.F. All authors have read and agreed to the published version of the manuscript.

Funding: This research was funded by the German Research Foundation (Deutsche Forschungsgemeinschaft, DFG; FA 1381/1-1).

Acknowledgments: We thank Philip Saunders for linguistic advice and Christoph Lichtenberg for technical assistance.

Conflicts of Interest: The authors declare no conflict of interest.

References

1. Schön, S.; Prante, C.; Bahr, C.; Kuhn, J.; Kleesiek, K.; Götting, C. Cloning and Recombinant Expression of Active Full-length Xylosyltransferase I (XT-I) and Characterization of Subcellular Localization of XT-I and XT-II. *J. Biol. Chem.* **2006**, *281*, 14224–14231. [CrossRef] [PubMed]
2. Seo, N.-S.; McQuillan, D.J.; Höök, M. The Role of Glycosylation in the Secretion of Proteoglycans. *Sci. World J.* **2006**, *6*, 491–493. [CrossRef] [PubMed]
3. Koslowski, R.; Pfeil, U.; Fehrenbach, H.; Kasper, M.; Skutelsky, E.; Wenzel, K.-W. Changes in xylosyltransferase activity and in proteoglycan deposition in bleomycin-induced lung injury in rat. *Eur. Respir. J.* **2001**, *18*, 347–356. [CrossRef] [PubMed]
4. Lairson, L.L.; Henrissat, B.; Davies, G.J.; Withers, S.G. Glycosyltransferases: Structures, Functions, and Mechanisms. *Annu. Rev. Biochem.* **2008**, *77*, 521–555. [CrossRef] [PubMed]
5. Briggs, D.C.; Hohenester, E. Structural Basis for the Initiation of Glycosaminoglycan Biosynthesis by Human Xylosyltransferase 1. *Structure* **2018**, *26*, 801–809.e3. [CrossRef] [PubMed]
6. Punta, M.; Coggill, P.C.; Eberhardt, R.Y.; Mistry, J.; Tate, J.; Boursnell, C.; Pang, N.; Forslund, K.; Ceric, G.; Clements, J.; et al. The Pfam protein families database. *Nucleic Acids Res.* **2012**, *40*, D290–D301. [CrossRef]
7. Ly, T.-D.; Plümers, R.; Fischer, B.; Schmidt, V.; Hendig, D.; Kuhn, J.; Knabbe, C.; Faust, I. Activin A-Mediated Regulation of XT-I in Human Skin Fibroblasts. *Biomolecules* **2020**, *10*, 609. [CrossRef]
8. Müller, B.; Prante, C.; Kleesiek, K.; Götting, C. Identification and Characterization of the Human Xylosyltransferase I Gene Promoter Region. *J. Biol. Chem.* **2009**, *284*, 30775–30782. [CrossRef]
9. Müller, B.; Prante, C.; Knabbe, C.; Kleesiek, K.; Götting, C. First identification and functional analysis of the human xylosyltransferase II promoter. *Glycoconj. J.* **2013**, *30*, 237–245. [CrossRef]
10. Faust, I.; Böker, K.O.; Lichtenberg, C.; Kuhn, J.; Knabbe, C.; Hendig, D. First description of the complete human xylosyltransferase-I promoter region. *BMC Genet.* **2014**, *15*, 129. [CrossRef]
11. Pönighaus, C.; Kuhn, J.; Kleesiek, K.; Götting, C. Involvement of a cysteine protease in the secretion process of human xylosyltransferase I. *Glycoconj. J.* **2010**, *27*, 359–366. [CrossRef] [PubMed]
12. Götting, C.; Kuhn, J.; Weilke, C.; Brinkmann, T.; Kleesiek, K.; Sollberg, S.; Huerkamp, C.; Krieg, T. Serum Xylosyltransferase: A New Biochemical Marker of the Sclerotic Process in Systemic Sclerosis. *J. Invest. Dermatol.* **1999**, *112*, 919–924. [CrossRef] [PubMed]
13. Kuhn, J.; Prante, C.; Schön, S.; Götting, C.; Kleesiek, K. Measurement of Fibrosis Marker Xylosyltransferase I Activity by HPLC Electrospray Ionization Tandem Mass Spectrometry. *Clin. Chem.* **2006**, *52*, 2243–2249. [CrossRef] [PubMed]
14. Götting, C.; Kuhn, J.; Step, C. Elevated Serum Xylosyltransferase Activity Correlates with a High Level of Hyaluronate in Patients with Systemic Sclerosis. *Acta Derm. Venereol.* **2000**, *80*, 60–61. [CrossRef] [PubMed]
15. Yazdani, S.; Bansal, R.; Prakash, J. Drug targeting to myofibroblasts: Implications for fibrosis and cancer. *Adv. Drug Deliv. Rev.* **2017**, *121*, 101–116. [CrossRef]
16. Zent, J.; Guo, L.-W. Signaling Mechanisms of Myofibroblastic Activation: Outside-in and Inside-Out. *Cell. Physiol. Biochem.* **2018**, *49*, 848–868. [CrossRef]
17. Faust, I.; Roch, C.; Kuhn, J.; Prante, C.; Knabbe, C.; Hendig, D. Human xylosyltransferase-I–A new marker for myofibroblast differentiation in skin fibrosis. *Biochem. Biophys. Res. Commun.* **2013**, *436*, 449–454. [CrossRef]
18. Prante, C.; Milting, H.; Kassner, A.; Farr, M.; Ambrosius, M.; Schön, S.; Seidler, D.G.; Banayosy, A.E.; Körfer, R.; Kuhn, J.; et al. Transforming Growth Factor β_1 -regulated Xylosyltransferase I Activity in Human Cardiac Fibroblasts and Its Impact for Myocardial Remodeling. *J. Biol. Chem.* **2007**, *282*, 26441–26449. [CrossRef]
19. Hinz, B. Formation and Function of the Myofibroblast during Tissue Repair. *J. Invest. Dermatol.* **2007**, *127*, 526–537. [CrossRef]
20. Kis, K.; Liu, X.; Hagood, J.S. Myofibroblast differentiation and survival in fibrotic disease. *Expert Rev. Mol. Med.* **2011**, *13*, e27. [CrossRef]

21. Lindahl, G.E.; Chambers, R.C.; Papakrivopoulou, J.; Dawson, S.J.; Jacobsen, M.C.; Bishop, J.E.; Laurent, G.J. Activation of Fibroblast Procollagen α1(I) Transcription by Mechanical Strain Is Transforming Growth Factor-β-dependent and Involves Increased Binding of CCAAT-binding Factor (CBF/NF-Y) at the Proximal Promoter. *J. Biol. Chem.* **2002**, *277*, 6153–6161. [CrossRef] [PubMed]
22. Lafyatis, R. Transforming growth factor β—at the centre of systemic sclerosis. *Nat. Rev. Rheumatol.* **2014**, *10*, 706–719. [CrossRef] [PubMed]
23. Butz, H.; Rácz, K.; Hunyady, L.; Patócs, A. Crosstalk between TGF-β signaling and the microRNA machinery. *Trends Pharmacol. Sci.* **2012**, *33*, 382–393. [CrossRef] [PubMed]
24. Liu, R.-H.; Ning, B.; Ma, X.-E.; Gong, W.-M.; Jia, T.-H. Regulatory roles of microRNA-21 in fibrosis through interaction with diverse pathways (Review). *Mol. Med. Rep.* **2016**, *13*, 2359–2366. [CrossRef]
25. O'Reilly, S. MicroRNAs in fibrosis: Opportunities and challenges. *Arthritis Res. Ther.* **2016**, *18*, 11. [CrossRef]
26. Yuan, J.; Chen, H.; Ge, D.; Xu, Y.; Xu, H.; Yang, Y.; Gu, M.; Zhou, Y.; Zhu, J.; Ge, T.; et al. Mir-21 Promotes Cardiac Fibrosis After Myocardial Infarction Via Targeting Smad7. *Cell. Physiol. Biochem.* **2017**, *42*, 2207–2219. [CrossRef]
27. Liu, G.; Friggeri, A.; Yang, Y.; Milosevic, J.; Ding, Q.; Thannickal, V.J.; Kaminski, N.; Abraham, E. miR-21 mediates fibrogenic activation of pulmonary fibroblasts and lung fibrosis. *J. Exp. Med.* **2010**, *207*, 1589–1597. [CrossRef]
28. Kramer, E.L.; Clancy, J.P. TGFβ as a therapeutic target in cystic fibrosis. *Expert Opin. Ther. Targets* **2018**, *22*, 177–189. [CrossRef]
29. Fischer, B.; Ly, T.-D.; Hendig, D.; Kuhn, J.; Pécheur, E.-I.; Reungoat, E.; Knabbe, C.; Faust, I. First description of a compensatory xylosyltransferase I induction observed after an antifibrotic UDP-treatment of normal human dermal fibroblasts. *Biochem. Biophys. Res. Commun.* **2019**, *512*, 7–13. [CrossRef]
30. Casanova, J.C.; Kuhn, J.; Kleesiek, K.; Götting, C. Heterologous expression and biochemical characterization of soluble human xylosyltransferase II. *Biochem. Biophys. Res. Commun.* **2008**, *365*, 678–684. [CrossRef]
31. Wilson, B.A.P.; Thornburg, C.C.; Henrich, C.J.; Grkovic, T.; O'Keefe, B.R. Creating and screening natural product libraries. *Nat. Prod. Rep.* **2020**, *37*, 893–918. [CrossRef] [PubMed]
32. Cascão, R.; Fonseca, J.E.; Moita, L.F. Celastrol: A Spectrum of Treatment Opportunities in Chronic Diseases. *Front. Med.* **2017**, *4*, 69. [CrossRef] [PubMed]
33. Brahmachari, G. (Ed.) *Bioactive Natural Products: Chemistry and Biology*; Wiley-VCH: Weinheim, Germany, 2015; ISBN 978-3-527-68441-0.
34. Esko, J.D.; Stewart, T.E.; Taylor, W.H. Animal cell mutants defective in glycosaminoglycan biosynthesis. *Proc. Natl. Acad. Sci. USA* **1985**, *82*, 3197–3201. [CrossRef] [PubMed]
35. Pönighaus, C.; Ambrosius, M.; Casanova, J.C.; Prante, C.; Kuhn, J.; Esko, J.D.; Kleesiek, K.; Götting, C. Human Xylosyltransferase II Is Involved in the Biosynthesis of the Uniform Tetrasaccharide Linkage Region in Chondroitin Sulfate and Heparan Sulfate Proteoglycans. *J. Biol. Chem.* **2007**, *282*, 5201–5206. [CrossRef]
36. Smith, P.K.; Krohn, R.I.; Hermanson, G.T.; Mallia, A.K.; Gartner, F.H.; Provenzano, M.D.; Fujimoto, E.K.; Goeke, N.M.; Olson, B.J.; Klenk, D.C. Measurement of protein using bicinchoninic acid. *Anal. Biochem.* **1985**, *150*, 76–85. [CrossRef]
37. Trott, O.; Olson, A.J. AutoDock Vina: Improving the speed and accuracy of docking with a new scoring function, efficient optimization, and multithreading. *J. Comput. Chem.* **2009**. [CrossRef]
38. Pettersen, E.F.; Goddard, T.D.; Huang, C.C.; Couch, G.S.; Greenblatt, D.M.; Meng, E.C.; Ferrin, T.E. UCSF Chimera-A visualization system for exploratory research and analysis. *J. Comput. Chem.* **2004**, *25*, 1605–1612. [CrossRef]
39. Berman, H.M. The Protein Data Bank. *Nucleic Acids Res.* **2000**, *28*, 235–242. [CrossRef]
40. Xie, X.-Q.S. Exploiting PubChem for virtual screening. *Expert Opin. Drug Discov.* **2010**, *5*, 1205–1220. [CrossRef]
41. Meng, E.C.; Pettersen, E.F.; Couch, G.S.; Huang, C.C.; Ferrin, T.E. Tools for integrated sequence-structure analysis with UCSF Chimera. *BMC Bioinform.* **2006**, *7*, 339. [CrossRef]
42. Riedel, L.; Fischer, B.; Ly, T.-D.; Hendig, D.; Kuhn, J.; Knabbe, C.; Faust, I. microRNA-29b mediates fibrotic induction of human xylosyltransferase-I in human dermal fibroblasts via the Sp1 pathway. *Sci. Rep.* **2018**, *8*, 17779. [CrossRef] [PubMed]
43. Pfaffl, M.W. A new mathematical model for relative quantification in real-time RT-PCR. *Nucleic Acids Res.* **2001**, *29*, e45. [CrossRef] [PubMed]

44. Tjernberg, A.; Markova, N.; Griffiths, W.J.; Hallén, D. DMSO-Related Effects in Protein Characterization. *J. Biomol. Screen.* **2006**, *11*, 131–137. [CrossRef] [PubMed]
45. Pence, H.E.; Williams, A. ChemSpider: An Online Chemical Information Resource. *J. Chem. Educ.* **2010**, *87*, 1123–1124. [CrossRef]
46. Glaser, J.; Holzgrabe, U. Focus on PAINS: False friends in the quest for selective anti-protozoal lead structures from Nature? *MedChemComm* **2016**, *7*, 214–223. [CrossRef]
47. Bauersachs, J. miR-21: A central regulator of fibrosis not only in the broken heart: EXPERT'S PERSPECTIVE. *Cardiovasc. Res.* **2012**, *96*, 227–229. [CrossRef]
48. Cheng, M.; Wu, G.; Song, Y.; Wang, L.; Tu, L.; Zhang, L.; Zhang, C. Celastrol-Induced Suppression of the MiR-21/ERK Signalling Pathway Attenuates Cardiac Fibrosis and Dysfunction. *Cell. Physiol. Biochem.* **2016**, *38*, 1928–1938. [CrossRef]
49. Ni, H.; Han, Y.; Jin, X. Celastrol inhibits colon cancer cell proliferation by downregulating miR-21 and PI3K/AKT/GSK-3β pathway. *Int. J. Clin. Exp. Pathol.* **2019**, *12*, 808–816.
50. Gao, Y.; Wen, H.; Wang, C.; Li, Q. SMAD7 antagonizes key TGFβ superfamily signaling in mouse granulosa cells in vitro. *Reproduction* **2013**, *146*, 1–11. [CrossRef]
51. Humphrey, J.D.; Dufresne, E.R.; Schwartz, M.A. Mechanotransduction and extracellular matrix homeostasis. *Nat. Rev. Mol. Cell Biol.* **2014**, *15*, 802–812. [CrossRef]
52. Kuroda, K.; Shinkai, H. Decorin and glycosaminoglycan synthesis in skin fibroblasts from patients with systemic sclerosis. *Arch. Dermatol. Res.* **1997**, *289*, 481–485. [CrossRef] [PubMed]
53. Kitabatake, M.; Ishikawa, H.; Maeda, H. Immunohistochemical demonstration of proteoglycans in the skin of patients with systemic sclerosis. *Br. J. Dermatol.* **1983**, *108*, 257–262. [CrossRef] [PubMed]
54. Nelson, K.M.; Dahlin, J.L.; Bisson, J.; Graham, J.; Pauli, G.F.; Walters, M.A. The Essential Medicinal Chemistry of Curcumin: Miniperspective. *J. Med. Chem.* **2017**, *60*, 1620–1637. [CrossRef] [PubMed]
55. Yao, T.; Jiang, T.; Pan, D.; Xu, Z.-X.; Zhou, P. Effect of Al(III) and curcumin on silk fibroin conformation and aggregation morphology. *RSC Adv* **2014**, *4*, 40273–40280. [CrossRef]
56. Guerra, W.; Silva-Caldeira, P.P.; Terenzi, H.; Pereira-Maia, E.C. Impact of metal coordination on the antibiotic and non-antibiotic activities of tetracycline-based drugs. *Coord. Chem. Rev.* **2016**, *327–328*, 188–199. [CrossRef]
57. Müller, S.; Schöttler, M.; Schön, S.; Prante, C.; Brinkmann, T.; Kuhn, J.; Götting, C.; Kleesiek, K. Human xylosyltransferase I: Functional and biochemical characterization of cysteine residues required for enzymic activity. *Biochem. J.* **2005**, *386*, 227–236. [CrossRef]
58. Harmsen, S.; McLaren, A.C.; Pauken, C.; McLemore, R. Amphotericin B Is Cytotoxic at Locally Delivered Concentrations. *Clin. Orthop. Relat. Res.* **2011**, *469*, 3016–3021. [CrossRef]
59. Warnock, D.W. Amphotericin B: An introduction. *J. Antimicrob. Chemother.* **1991**, *28*, 27–38. [CrossRef]
60. Cuddihy, G.; Wasan, E.; Di, Y.; Wasan, K. The Development of Oral Amphotericin B to Treat Systemic Fungal and Parasitic Infections: Has the Myth Been Finally Realized? *Pharmaceutics* **2019**, *11*, 99. [CrossRef]
61. Ng, S.W.; Chan, Y.; Chellappan, D.K.; Madheswaran, T.; Zeeshan, F.; Chan, Y.L.; Collet, T.; Gupta, G.; Oliver, B.G.; Wark, P.; et al. Molecular modulators of celastrol as the keystones for its diverse pharmacological activities. *Biomed. Pharmacother.* **2019**, *109*, 1785–1792. [CrossRef]
62. Copeland, R.A. *Evaluation of Enzyme Inhibitors in Drug Discovery: A Guide for Medicinal Chemists and Pharmacologists*; Wiley: Hoboken, NJ, USA, 2013; ISBN 978-1-118-54028-2.
63. Strelow, J.; Dewe, W.; Iversen, P.W.; Brooks, H.B.; McGee, J.; Weidner, J. Mechanism of Action Assays for Enzymes. In *Assay Guidance Manual*; Eli Lilly & Company and the National Center for Advancing Translational Sciences: Bethesda, DC, USA, 2004.
64. Wang, L.-P. Celastrol inhibits migration, proliferation and transforming growth factor-β2-induced epithelial-mesenchymal transition in lens epithelial cells. *Int. J. Ophthalmol.* **2019**, *12*, 1517–1523. [CrossRef] [PubMed]
65. Proesmans, M.; Vermeulen, F.; Vreys, M.; De Boeck, K. Use of Nebulized Amphotericin B in the Treatment of Allergic Bronchopulmonary Aspergillosis in Cystic Fibrosis. *Int. J. Pediatr.* **2010**, *2010*, 1–9. [CrossRef] [PubMed]
66. Muraglia, K.A.; Chorghade, R.S.; Kim, B.R.; Tang, X.X.; Shah, V.S.; Grillo, A.S.; Daniels, P.N.; Cioffi, A.G.; Karp, P.H.; Zhu, L.; et al. Small-molecule ion channels increase host defences in cystic fibrosis airway epithelia. *Nature* **2019**, *567*, 405–408. [CrossRef] [PubMed]

67. Harris, W.T.; Kelly, D.R.; Zhou, Y.; Wang, D.; Macewen, M.; Hagood, J.S.; Clancy, J.P.; Ambalavanan, N.; Sorscher, E.J. Myofibroblast Differentiation and Enhanced Tgf-B Signaling in Cystic Fibrosis Lung Disease. *PLoS ONE* **2013**, *8*, e70196. [CrossRef]
68. Yan, X.; Chen, Y.-G. Smad7: Not only a regulator, but also a cross-talk mediator of TGF-β signalling. *Biochem. J.* **2011**, *434*, 1–10. [CrossRef]
69. Ly, T.-D.; Riedel, L.; Fischer, B.; Schmidt, V.; Hendig, D.; Distler, J.; Kuhn, J.; Knabbe, C.; Faust, I. microRNA-145 mediates xylosyltransferase-I induction in myofibroblasts via suppression of transcription factor KLF4. *Biochem. Biophys. Res. Commun.* **2020**, S0006291X20300784. [CrossRef] [PubMed]
70. Theis, T.; Yoo, M.; Park, C.S.; Chen, J.; Kügler, S.; Gibbs, K.M.; Schachner, M. Lentiviral Delivery of miR-133b Improves Functional Recovery After Spinal Cord Injury in Mice. *Mol. Neurobiol.* **2017**, *54*, 4659–4671. [CrossRef] [PubMed]

4 Ergebnisse und zusammenfassende Diskussion

Eine Fibrose ist das Endresultat chronischer Inflammationsreaktionen, die durch verschiedene Stimuli induziert werden können. Die Entwicklung einer therapeutischen Strategie, welche die Progression der Fibrosierung reduziert, ist von hoher klinischer Relevanz. Publizierte Vorarbeiten beschreiben eine im Vergleich zu einer Kontrollkohorte erhöhte XT-Aktivität im Serum von SSc-Patienten (Götting *et al.*, 1999), die mit einer Erhöhung des PG-Metabolismus und des GAG-Gehalts in Geweben und kultivierten Fibroblasten korreliert (Kitabatake *et al.*, 1983; Kuroda und Shinkai, 1997). Demnach könnte eine mögliche antifibrotische Therapiestrategie auf einer gerichteten XT-I-Inhibition aufbauen. In der vorliegenden Arbeit wurde eine detaillierte Untersuchung der Regulation der humanen XT-I bei Fibrosen durchgeführt, um das Verständnis über die pathobiochemische Relevanz der XT-I zu vertiefen. Hierfür wurden in dieser Arbeit mitunter die zellulären Regulationspfade der XT-I in Myofibroblasten analysiert und die Rolle der XT-I als zellulärer Mediator der prototypischen fibrotischen Erkrankung SSc untersucht. Weiterführend wurde eine Naturstoff-Bibliothek verwendet, um XT-I-Inhibitoren zu identifizieren und die Art der XT-I-Inhibition zu charakterisieren.

4.1 Fibrotische XT-I-Regulation in primären Dermalfibroblasten

Basierend auf den Vorarbeiten der Arbeitsgruppe wurde im Rahmen dieser Arbeit ein *in vitro* Zellkulturmodell für Fibrosen eingesetzt (**P1**–**P4**). Dieses Modell sieht die Kultivierung von primären Dermalfibroblasten als Monolayerkultur bei geringer Zelldichte von 50 Zellen/mm² auf einem harten Zellkultursubstrat vor (Faust *et al.*, 2013). Auf diese Weise werden mechanisch-aktivierte Fibroblasten generiert. Diese können zusätzlich über exogene Zugabe von profibrotischen Modulatoren wie TGF-β1 stimuliert werden, um den Einfluss fibrotischer Effekte auf die Gen- und Proteinexpression von Markern der Myofibroblastendifferenzierung und ECM-Synthese zu evaluieren (Faust *et al.*, 2013). Im Rahmen dieser Arbeit wurden neben NHDF auch SScF als Effektorzellen verwendet. SScF sind durch eine erhöhte ECM-Synthese, eine konstitutive Sekretion von Zytokinen und Chemokinen sowie eine erhöhte Expression von Oberflächenrezeptoren charakterisiert (Chadli *et al.*, 2019; Garrett *et al.*, 2017). SScF können ihren Phänotypen einige *in vitro* Populationsverdoppelungen (< 10) beibehalten (Chadli *et al.*, 2019; Garrett *et al.*, 2017).

Um die Interferenz der von den SScF konstitutiv sekretierten Faktoren in den Versuchsansätzen auszuschließen, wurden die meisten Studien unter Verwendung des Myofibroblastenmodells mit NHDF durchgeführt (**P1**–**P4**). Demnach wurde das SScF-Modell zur Validierung der aus dem NHDF-Modell gewonnenen Erkenntnisse herangezogen (**P2**, **P3**).

4.1.1 Zeit- und konzentrationsabhängige Activin A-vermittelte XT-I-Induktion

Aufgrund der zentralen Rolle der TGF-β1-vermittelten Signaltransduktionswege in der zellulären Morphogenese, dem Wachstum und der Zelldifferenzierung stellt deren therapeutische Inhibition keine realistische Option zur Fibrosebehandlung dar (Baugé *et al.*, 2011). Die Identifizierung von weiteren dysregulierten Mediatoren und Signalwegen in SScF ist demnach von hoher klinischer Relevanz. Neben der Induktion durch TGF-β1 ist eine Regulation der *XYLT1* Expression durch IL-1β in Chondrozyten und durch Thrombin in vaskulären Glattmuskelzellen nachgewiesen worden (Khair *et al.*, 2013; Ye *et al.*, 2014). Der Einfluss von IL-1β oder anderen fibrotisch- oder inflammatorisch-wirkenden Faktoren auf die XT-Aktivität und *XYLT1* Expression sowie die zugrundeliegenden Signalwege sind bisher kaum in Fibroblasten untersucht worden.

In der vorliegenden Arbeit wurde unter Verwendung des Myofibroblastenmodells über quantitative Echtzeit-PCR-Analytik und die Durchführung eines radiochemischen XT-Aktivitätsassays das Zytokin Activin A als potenter *XYLT1* mRNA und XT-Aktivität induzierender Faktor in NHDF identifiziert (**P1**). Activin A ist als zentraler Mediator in Wundheilungsprozessen bekannt (Antsiferova und Werner, 2012). Eine erhöhte Serumkonzentration dieses Zytokins wurde ebenfalls bei SSc-Patienten nachgewiesen (Takagi *et al.*, 2011). In Übereinstimmung mit vorangegangenen Arbeiten, die eine Korrelation der TGF-β1-induzierten *XYLT1* mRNA-Expression mit der extrazellulären XT-Aktivität zeigten (Faust *et al.*, 2013; Prante *et al.*, 2007; Riedel *et al.*, 2018), korreliert die hier nachgewiesene zeit- und konzentrationsabhängige Activin A-induzierte *XYLT1* mRNA-Expression ebenfalls mit einer Erhöhung der extrazellulären XT-Aktivität der Zellen (**P1**). Darüber hinaus wurde im Rahmen dieser Arbeit erstmalig eine zeitabhängige, Activin A-vermittelte Erhöhung der intrazellulären XT-Aktivität in NHDF beobachtet (**P1**), die ebenfalls mit der Activin A-induzierten *XYLT1* mRNA-Expression zusammenhängt. Ähnlich zu vorangegangenen Arbeiten mit TGF-β1 (Faust *et al.*, 2013), wurde im Rahmen dieser Arbeit keine Induktion der *XYLT2*

Expression nach Activin A-Behandlung von NHDF detektiert (**P1**). Demnach kann ein Beitrag der XT-II-Isoform zur Activin A-vermittelten XT-Aktivitätserhöhung ausgeschlossen werden. Den Resultaten zufolge könnte ein Zytokin-vermittelter fibrogener Mechanismus, der zur dermalen Fibrose in SSc beiträgt, eine Activin A-induzierte Erhöhung der *XYLT1* Expression und XT-Aktivität in Fibroblasten, den Schlüsselzellen der ECM-Remodellierung (Garrett *et al.*, 2017), verursachen.

Im Gegensatz zu Activin A zeigten die im Rahmen dieser Arbeit untersuchten inflammationsassoziierten Zytokine IL-4, -6 und -13 (**P1**) und das IL-1β (**P2**) keine *XYLT1* induzierenden Effekte in NHDF in Abwesenheit von TGF-β1. Demnach kann der alleinige Beitrag dieser Faktoren an der XT-I-Regulation bei Fibrosen ausgeschlossen werden. Die Beobachtung, dass IL-1β zu keinen *XYLT1* mRNA-Expressionsänderungen in NHDF führte, stimmt mit den Resultaten von Mia *et al.* überein, die keine profibrotischen Effekte in NHDF durch alleinige IL-1β-Supplementation detektiert haben (Mia *et al.*, 2014). Da Khair *et al.* eine *XYLT1* Expressionsregulation in primären Chondrozyten durch IL-1β gleicher Konzentration nachweisen konnten (Khair *et al.*, 2013), scheinen sich die IL-1β-vermittelten Effekte in NHDF und primären Chondrozyten zu unterscheiden. Allerdings sind weiterführende Analysen notwendig, um den möglicherweise zelltypabhängigen Beitrag dieser Zytokine im Einzelnen und in der TGF-β-vermittelten XT-I-Regulation aufzuklären. Ob die XT-I durch synergistische Effekte der Zytokine reguliert wird, bleibt ebenfalls offen.

Die zugrundeliegenden Signalwege der XT-I-Regulation in NHDF wurden im Rahmen dieser Arbeit unter Verwendung von Activin A untersucht. Die Studie von Takagi *et al.* zeigte eine Activin A-induzierte SMAD2/3-Phosphorylierung in NHDF und SScF, die in ALK4-Inhibitor-behandelten Zellen ausblieb (Takagi *et al.*, 2011). In Übereinstimmung mit der Arbeit von Takagi *et al.* wurde in dieser Arbeit eine ALK4-Abhängigkeit der Activin A-regulierten *XYLT1* mRNA-Expression und XT-Aktivität nachgewiesen (**P1**). Die ALK4-Activin A-Signaltransduktionskaskade wird zum einen über den klassischen Signalweg, an dem die SMAD-Proteine beteiligt sind, und zum anderen über den nicht-kanonischen Signalweg, der in der Aktivierung von MAPK resultiert, vermittelt (Hu *et al.*, 2016; Takagi *et al.*, 2011).

Bezüglich des nicht-kanonischen Signalwegs wurde in dieser Arbeit unter Verwendung von chemischen Molekülinhibitoren gezeigt, dass die Activin A/ALK4-vermittelte Regulation der *XYLT1* mRNA-Expression über die nachgeschalteten

MAPK p38, ERK und JNK erfolgt (**P1**). Die XT-I-Regulation durch MAPK spiegelt sich auch in anderen Zelltypen und Zytokinbehandlungen wider. So wurde in TGF-β1-behandelten humanen kardialen Fibroblasten ebenfalls die Beteiligung der MAPK p38 an der Regulation der *XYLT1* mRNA und XT-Aktivität gezeigt, während Studien mit vaskulären Glattmuskelzellen und primären Chondrozyten eine Funktion der MAPK JNK in der Thrombin- oder IL-1β-vermittelten *XYLT1* mRNA-Expressionserhöhung aufzeigen (Kamato *et al.*, 2019; Khair *et al.*, 2013).

Die Involvierung des kanonischen, SMAD-vermittelten Signalwegs wurde im Rahmen dieser Arbeit unter Verwendung des chemischen SMAD3-Inhibitors SIS3, sowie über einen siRNA-vermittelten *Knockdown* von *SMAD3* und *SMAD2* untersucht. Hierbei wurde die Involvierung des SMAD2 in der Activin A-vermittelten *XYLT1* Regulation gezeigt, während eine Beteiligung des regulatorischen SMAD3 ausgeschlossen wurde (**P1**). Da im *XYLT1* Promotor keine SMAD-Bindestellen vorkommen (Faust *et al.*, 2014), könnten die Activin A-induzierten Effekte mutmaßlich einer SMAD2-Linker-Phosphorylierung durch die MAPK p38, ERK oder JNK zugrunde liegen (Kamato *et al.*, 2019; Rostam *et al.*, 2016). Die Linker-Phosphorylierung würde den nuklearen Eintritt und somit die Interaktion von SMAD2 mit bekannten *XYLT1* regulierenden TF wie AP-1 und SP1/3 begünstigen (Faust *et al.*, 2014; Mori *et al.*, 2003; Müller *et al.*, 2009; Rostam *et al.*, 2016).

Obwohl die Signalkaskaden, die bei der durch Activin A-vermittelten XT-I-Regulation involviert sind, unter Verwendung von chemischen Molekülinhibitoren und siRNA-vermitteltem *Knockdown* identifiziert wurden, konnten die relativen Beiträge der einzelnen Signalwege auf die *XYLT1* Regulation im Rahmen dieser Arbeit nicht bestimmt werden. Eine Limitierung stellte die durch die Inhibition einer MAPK resultierende Aktivitätsverstärkung der anderen MAPK dar (Meurer und Weiskirchen, 2018). Nicht nur die gegenseitige Beeinflussung der einzelnen MAPK untereinander, sondern auch ihre Wechselwirkungen mit dem SMAD-Signalweg über die Linker-Phosphorylierung erschweren die Aufschlüsselung der relativen Beiträge. Neben weiteren experimentellen *in vitro* Ansätzen unter simultaner Inhibition mehrerer Signalwege könnten auch mathematische Modelle eingesetzt werden, um die relative *in vitro* Beteiligung der einzelnen Signalwegskomponenten zu beschreiben (Liu *et al.*, 2014).

Zusammengefasst wurden in diesem Teil der Arbeit wichtige Hinweise auf bisher unbekannte Signalpfade und deren wechselseitige Beziehung in der Activin A-vermittelten *XYLT1* Expressionsregulation in NHDF erhalten.

4.1.2 Differentielle Expressionsregulation der beiden XT-Isoformen in NHDF

Bei den durchgeführten Signaltransduktionsanalysen stellten sich Regulationsunterschiede zwischen der basalen *XYLT1* und *XYLT2* Expression in NHDF heraus (**P1**). Es konnte eine reziproke regulatorische Wirkung von SMAD3 detektiert werden. Über einen siRNA-vermittelten *Knockdown* wurde SMAD3 als ein negativer Regulator der basalen *XYLT1* Expression und als ein positiver Regulator der basalen *XYLT2* Expression nachgewiesen. Die erzielten Ergebnisse stehen im Einklang mit den Resultaten vorangegangener Promotoranalysen (Faust *et al.*, 2014; Müller *et al.*, 2009; Müller *et al.*, 2013). Im *XYLT1* Promotor gesunder Kontrollprobanden wurde unter anderem die SNV c.-1088C>A mit einer Allelfrequenz von 38% identifiziert, die in der Entstehung einer SMAD3-Bindestelle resultiert und mit einer reduzierten Promotoraktivität assoziiert werden konnte (Faust *et al.*, 2014). Demnach könnte die im Rahmen dieser Arbeit detektierte inhibitorische Wirkung von SMAD3 auf dem Vorliegen dieser SNV in den verwendeten Zellen beruhen. Eine weiterführende SNV-Analyse über Sequenzierung könnte diese Annahme verifizieren. Auch andere *in vitro* Effekte wie die Phosphorylierungsunterschiede der anderen SMAD-Proteine und ihre Interaktion mit weiteren TF nach siRNA-vermitteltem *SMAD3 Knockdown* könnten sich auf die *XYLT1* Expression auswirken und sollten demnach weiterführend untersucht werden (Lucarelli *et al.*, 2018). Promotoranalysen zufolge wird die konstitutive *XYLT2* Transkription vornehmlich durch die TF SP1/3 reguliert (Müller *et al.*, 2013). Da Zusammenhänge zwischen der Interaktion von SMAD-Proteinen mit SP1-TF und einer Transkriptionsverstärkung in Fibroblasten bestehen (Ihn *et al.*, 2006; Jinnin *et al.*, 2004; Lu *et al.*, 2010), wäre es denkbar, dass die Induktion der basalen *XYLT2* Transkription in NHDF durch SMAD3 auf einer Interaktion mit SP1/SP3-TF beruht. Weiterführende Analysen sind jedoch notwendig, um die basale *XYLT2* Expressionsregulation durch SMAD-Proteine zu charakterisieren. Über einen *electrophoretic mobility shift assay* könnte eine potenzielle SMAD3-SP1-*XYLT2*-Interaktion nachgewiesen werden (Fried und Garner, 1998). Co-Transfektionsexperimente mit Reporterkonstrukten könnten ebenfalls synergistische Effekte zwischen SP1 und SMAD3 auf die *XYLT2* Promotoraktivität aufzeigen (Botella *et al.*, 2001).

Neben der differentiellen Transkriptionsregulation der XT-Isoformen durch SMAD3 wurde im Rahmen dieser Arbeit eine Induktion der basalen *XYLT1* und *XYLT2* Expression durch ERK detektiert. Die ERK-vermittelte Regulation der basalen *XYLT1* Expression könnte auf die Vielzahl der im *XYLT1* Promotor vorhandenen Bindestellen für das EGR1 zurückgeführt werden (Faust *et al.*, 2014). Die Abhängigkeit der basalen *XYLT2* Expression von ERK kann mit der im Rahmen dieser Arbeit gezeigten Regulation der *XYLT2* Transkription durch SMAD3, und mit der von Müller *et al.* gezeigten Regulation durch SP1/3 in Zusammenhang gebracht werden (Müller *et al.*, 2013). Veröffentlichte Daten zeigten die konzentrationsabhängige Inhibition der *SMAD3* Promotoraktivität durch den verwendeten ERK-Inhibitor UO126, der simultan die Funktion von SP1/3 inhibiert (Ross *et al.*, 2007). Folglich könnte die im Rahmen dieser Arbeit detektierte relative *XYLT2* Expressionsreduktion nach ERK-Inhibition das Resultat einer verminderten SP1/3-Aktivität und *SMAD3* Expression sein.

Zusammenfassend vertiefen die dargestellten Ergebnisse das Verständnis der differentiellen XT-Isoformexpression unter physiologischen Bedingungen.

4.1.3 Regulation der XT-I durch miRNA-145 und miRNA-21 in NHDF

Neben fehlregulierten Signaltransduktionswegen nehmen aberrante miRNA-Expressionsniveaus eine zentrale Rolle bei der Pathogenese der SSc ein (Li *et al.*, 2015; Zhu *et al.*, 2013b). Die Identifizierung von miRNAs, welche die Expression zentraler Komponenten fibrogener Signalwege regulieren, könnte neue Einblicke hinsichtlich therapeutischer Angriffspunkte liefern. Im Rahmen dieses Teilprojekts wurde die Rolle der XT-I als zellulärer *Downstream*-Mediator bei Fibrosen untersucht, indem eruiert wurde, inwiefern profibrotische miRNAs die *XYLT1* Transkription regulieren. Derzeit sind wenige Studien bekannt, welche einen miRNA-vermittelten Effekt auf die *XYLT1* Expression demonstrieren. Nach der Studie von Theis *et al.* im murinen System handelt es sich bei der *XYLT1* um ein direktes Zielgen der miRNA-133b (Theis *et al.*, 2017). Ein erniedrigtes miRNA-133b-Expressionsniveau wurde in einer unabhängigen Studie bei der fibrotischen Hauterkrankung zirkumskripte Sklerodermie, Morphea, nachgewiesen (Etoh *et al.*, 2013). Die Studie von Riedel *et al.* adressiert hingegen eine miRNA-vermittelte *XYLT1* Regulation im Kontext der humanen Fibrose. Hierbei wurde ein miRNA-29b/SP1-vermittelter XT-I-Regulationsweg in NHDF aufgezeigt (Riedel *et al.*, 2018). Eine fibrotische Regulation der *XYLT1* mRNA-Expression und XT-Aktivität durch andere miRNAs wurde bisher nicht untersucht.

In dieser Dissertation wurden die Fibrose-assoziierten miRNAs miRNA-145 (**P3**) und miRNA-21 (**P2**, **P4**) hinsichtlich ihrer XT-I-regulierenden Wirkung analysiert. Über *in silico* Zielvorhersagealgorithmen wurde zunächst überprüft, ob die *XYLT1* mRNA ein direktes Zielgen der beiden miRNAs darstellt. Bis auf den verwendeten Algorithmus TargetScan 7.2 (Agarwal *et al.*, 2015), der eine Bindung zwischen miRNA-145 und *XYLT1* mRNA vorhersagte (**P3**), wurden keine Bindungen zwischen den beiden miRNAs und der 3'-UTR der *XYLT1* mRNA detektiert. Demnach ist eine direkte miRNA-145- oder miRNA-21-Bindung an die *XYLT1* mRNA unwahrscheinlich. Die Resultate der *in silico* Analysen wurden experimentell über einen Reporter-Luciferase-assay überprüft, der sowohl für die miRNA-145 als auch für die miRNA-21 eine putative Interaktion mit der 3'-UTR der *XYLT1* mRNA ausschloss (**P3**, **P2**). Demnach stellt die *XYLT1* kein direktes Zielgen der beiden miRNAs dar.

Obwohl keine Bindung der beiden miRNAs an die *XYLT1* mRNA erfolgt, ist eine Regulation der XT-I über sekundäre Mediatoren in NHDF möglich. Daher wurden die beiden miRNAs im Myofibroblastenmodell hinsichtlich ihrer XT-I regulierenden Wirkung untersucht. Die Eignung des etablierten Myofibroblastenmodells zur Adressierung der miRNA-vermittelten Effekte bei Fibrosen wurde im Rahmen dieser Arbeit durch ein Taqman-basiertes *real-time* PCR-Verfahren bestätigt. Hierbei wurde gezeigt, dass in Übereinstimmung mit publizierten Daten (Gras *et al.*, 2015; Yuan *et al.*, 2017) die Expression der miRNA-145 (**P3**) und miRNA-21 (**P4**) in NHDF durch TGF-β1 induziert wird. Die potenzielle miRNA-vermittelte XT-I-Regulation bei Fibrosen wurde anschließend im verifizierten Testsystem über miRNA-Transfektionsexperimente untersucht (**P3**, **P4**). Hierbei wurden erstmalig eine relative Erhöhung der *XYLT1* Expression und extrazellulären XT-Aktivität nach miRNA-145-Transfektion von NHDF nachgewiesen (**P3**). Zudem wurde eine Erhöhung der TGF-β1-induzierten extrazellulären XT-Aktivität durch miRNA-145-Supplementation detektiert (**P3**). Eine Überprüfung der Funktionalität der miRNA-145 als Myofibroblasten-induzierender Faktor wurde neben der relativen Quantifizierung der *XYLT1* Expression und XT-Aktivität durch die Quantifizierung des Myofibroblastenmarkers *ACTA2* sichergestellt (**P3**). Hierbei wurde gezeigt, dass in Übereinstimmung mit publizierten Daten (Gras *et al.*, 2015) die miRNA-145-Transfektion dermaler Fibroblasten die relative *ACTA2* Expression erhöht (**P3**). Demnach handelt es sich bei der miRNA-145 um einen potenten Induktor der XT-I in Myofibroblasten, der sowohl die basale als auch die TGF-β1-induzierte XT-Aktivität in NHDF reguliert. Bezüglich der miRNA-21-

vermittelten Effekte wurde eine Induktion der *XYLT1* Expression in TGF-β1-behandelten NHDF nachgewiesen (**P4**). Auch die miRNA-21 nimmt demnach einen regulierenden Effekt in der TGF-β1-induzierten *XYLT1* Expression ein.

Nachdem eine miRNA-145- und miRNA-21-vermittelte *XYLT1* Regulation über eine direkte miRNA-mRNA-Interaktion ausgeschlossen wurde, wurde das Vorliegen einer indirekten Regulation über Sekundärmediatoren weiterführend untersucht. Hinsichtlich der miRNA-145-regulierten Effekte wurde über *in silico* Zielvorhersagealgorithmen und Literaturrecherche eine mögliche Involvierung des TF KLF4 aufgezeigt (**P3**). In Übereinstimmung mit Vorarbeiten (Gras *et al.*, 2015; Yang *et al.*, 2013) wurde im Rahmen dieser Arbeit eine TGF-β1-vermittelte Reduktion der relativen *KLF4* Expression sowie eine Induktion der relativen *ACTA2* Expression in NHDF nachgewiesen (**P3**). Da die beiden Myofibroblastenmarker *ACTA2* und *XYLT1* den Resultaten zufolge einem ähnlichen Regulationsmechanismus unterliegen, ist eine Involvierung von KLF4 an der Regulation der *XYLT1* Expression denkbar. Erste Hinweise einer Beteiligung von KLF-TF bei der *XYLT1* Regulation ergaben sich aus vorangegangenen Sequenzanalysen, die SP1/KLF-Bindestellen im humanen *XYLT1* Promotor identifizierten (Faust *et al.*, 2014). Weiterführend wurden über eine *in silico* Analyse sechs potenzielle KLF4-Bindestellen im *XYLT1* Promotor identifiziert (**P3**), die sich in unmittelbarer Nachbarschaft zu SP1-Bindeseiten befinden (Riedel *et al.*, 2018). Vorangegangene DNA-Bindungsstudien haben für SP1- und KLF-Proteine eine ähnliche Affinität für GC-reiche Bereiche der DNA gezeigt (Kaczynski *et al.*, 2003). Eine Kompetition bezüglich der DNA-Bindung wurde unter anderem für die TF SP1 und SP3 sowie SP1 und KLF4 nachgewiesen (Ai *et al.*, 2004; Sun *et al.*, 2019; Zhang *et al.*, 1998). Demnach ist es möglich, dass eine KLF4-vermittelte Reduktion der *XYLT1* Transkription eine Besetzung von SP1-Bindestellen durch KLF4 im gleichen Promotorbereich involviert (Müller *et al.*, 2009; Riedel *et al.*, 2018). Über einen siRNA-vermittelten *KLF4 Knockdown* wurde im Rahmen dieser Arbeit die TGF-β1-vermittelte Degradation von KLF4 bei Fibrosen (Hu und Wan, 2011) nachgestellt (**P3**). Hierbei wurde ein relativer Anstieg der basalen und TGF-β1-induzierten *XYLT1* Expression in KLF4-supprimierten NHDF detektiert und somit die Rolle von KLF4 als negativer Regulator der *XYLT1* Expression gefestigt (**P3**). Zusammenfassend stellt die *KLF4* Suppression einen Mechanismus der TGF-β1/miR-145-vermittelten Myofibroblastendifferenzierung dar, der sich auf die Expression von *ACTA2* und *XYLT1* auswirkt.

Hinsichtlich der miRNA-21-vermittelten Effekte auf die *XYLT1* mRNA-Expression wurde in dieser Arbeit eine Involvierung des bereits experimentell bestätigten miRNA-21-Zielgens *SMAD7* (Wang *et al.*, 2018; Yuan *et al.*, 2017) untersucht. In vorangegangenen Studien wurde in SScF ein erniedrigtes *SMAD7* mRNA-Expressionsniveau im Vergleich zu NHDF detektiert. Die *SMAD7* Expressionsreduktion wurde hierbei mit einer relativen miRNA-21-Expressionserhöhung korreliert (Mori *et al.*, 2003; Varga, 2002; Zhu *et al.*, 2012). Eine ausführliche Analyse wurde von Yuan *et al.* unter Verwendung der miRNA-21 und einem miRNA-21-Inhibitor in kardialen Fibroblasten durchgeführt (Yuan *et al.*, 2017). Die verminderte *SMAD7* Expression der SScF wurde im Rahmen dieser Arbeit über eine siRNA-vermittelte Reduktion der *SMAD7* Expression in NHDF simuliert (**P1**). In Bezug auf die XT-I-Regulation in Gegenwart von Activin A ließ sich eine gesteigerte *XYLT1* mRNA-Expression in *SMAD7* supprimierten NHDF detektieren. Die *SMAD7* Suppression hatte jedoch keinen Einfluss auf die relative *XYLT1* Basalexpression in NHDF (**P1**). Die Ergebnisse der siRNA-vermittelten *SMAD7* Reduktion in NHDF stehen im Einklang mit den Resultaten der durchgeführten miRNA-21-Transfektionsexperimente, die eine Reduktion der relativen *SMAD7* mRNA-Expression in miRNA-21-transfizierten NHDF zeigten (**P4**). Angesichts der Datenlage liegt die Schlussfolgerung nahe, dass die Zytokin-induzierte *XYLT1* Expression in NHDF eine Regulation des kanonischen TGF-β-Signalwegs über miRNA-21/SMAD7 involviert.

Zusammengefasst wurden im ersten Teilprojekt neue Erkenntnisse hinsichtlich der bei der XT-I-Regulation involvierten Mediatoren und Regulationspfade gewonnen. Mitunter wurde die Beteiligung von Activin A, sowie der miRNAs miRNA-145 und -21 bei der fibrotischen XT-I Regulation aufgezeigt. Neben der Aufklärung der zugrunde liegenden Signalwege wurden basale Unterschiede in der transkriptionellen Regulation der XT-Isoformexpression durch SMAD3 und ERK identifiziert.

4.2 Zytokin-vermittelte XT-I-Regulation in SScF

Im Serum von SSc-Patienten wurde eine signifikant erhöhte XT-Aktivität nachgewiesen, die mit einem hohen HA-Level korreliert (Götting *et al.*, 1999). Um die potenzielle Rolle der XT-I als zellulärer Mediator und therapeutischer Angriffspunkt in der SSc zu evaluieren, wurden im Rahmen dieses Teilprojekts vergleichend NHDF und SScF im Myofibroblastenmodell kultiviert. Unter standardisierten Kultivierungsbedingungen mit 10%iger Supplementation von fetalem Kälberserum zeigten die SScF relativ zu den

NHDF eine signifikant erhöhte extrazelluläre XT-I-Aktivität (**P2**). Demzufolge könnte die von Götting *et al.* beschriebene Erhöhung der relativen XT-Serumaktivität bei SSc-Patienten auf einer Myofibroblasten-initiierten Erhöhung der XT-I-Expression und -Sekretion beruhen.

Da keine extrazellulären XT-I-Aktivitätsunterschiede zwischen NHDF und SScF nach einem Kultivierungszeitraum von 120 h in serumfreiem Medium auftraten (**P2**), wurde angenommen, dass Bestandteile des fetalen Kälberserums, darunter TGF-β1 (Oida und Weiner, 2010), die zellulären XT-I-Aktivitätsunterschiede verursachen. Eine Zytokin-vermittelte extrazelluläre XT-Aktivitätserhöhung korreliert *in vitro* mit einer relativen Erhöhung der *XYLT1* Expression und intrazellulären XT-Aktivität (Faust *et al.*, 2013; Ly *et al.*, 2020b; Prante *et al.*, 2007). Entsprechend könnte eine gesteigerte Zytokin-vermittelte *XYLT1* mRNA-Expression in SScF zu den detektierten XT-I-Aktivitätsunterschieden zwischen NHDF und SScF beitragen. Um den potenziell Zytokin-vermittelten XT-I-Regulationsunterschieden in NHDF und SScF nachzugehen, wurde der Einfluss von TGF-β1 und IL-1β auf die *XYLT1* mRNA-Expression und/oder XT-I-Aktivität von NHDF und SScF über definierte Zeiträume untersucht. Obwohl in *in vitro* Studien gezeigt wurde, dass NHDF und SScF keine Unterschiede bezüglich ihrer TGF-β-Gesamtproduktion oder ihres aktiven TGF-β-Anteils aufweisen (Ihn *et al.*, 2001; Kubo *et al.*, 2002), zeigten SScF in dieser Arbeit im Vergleich zu NHDF eine höhere Sensitivität für TGF-β1 (**P2**). Diese äußerte sich in Form einer verstärkten relativen *XYLT1* Expressionsinduktion und extrazellulären XT-I-Aktivitätserhöhung nach TGF-β1-Supplementation (**P2**). Unterschiede in der *XYLT1* Expressionsregulation zeigten sich auch nach IL-1β-Behandlung von NHDF und SScF. Während NHDF keine IL-1β-vermittelte Regulation der *XYLT1* Expression zeigten, wurde die *XYLT1* mRNA-Expression in SScF durch IL-1β zeitabhängig nach 6 h induziert und nach 48 h supprimiert (**P2**). Eine initiale *XYLT1* mRNA-Induktion mit nachfolgender Suppression wurde ebenfalls in Chondrozyten nachgewiesen (Khair *et al.*, 2013), die mit der gleichen IL-1β-Konzentration wie in dieser Arbeit behandelt wurden. Demnach scheint die IL-1β-vermittelte *XYLT1* Regulation in SScF der Regulation in Chondrozyten zu ähneln, während Unterschiede zur IL-1β-vermittelte *XYLT1* Expressionsregulation in NHDF bestehen. Weiterführende Analysen sind notwendig, um die zugrundeliegenden zellulären Mechanismen aufzuklären.

Ein relevanter Mechanismus, um die zelluläre Antwort auf exogene Zytokine und Wachstumsfaktoren zu regulieren, erfolgt auf Ebene der Rezeptorexpression (Ihn,

2008). Für den epidermalen Wachstumsfaktor wurde eine zehnfache Reduktion der benötigten zellulären Mediatormenge nach zweifacher Erhöhung der Rezeptorexpression nachgewiesen (Lillien, 1995). Demnach könnte die beobachtete höhere Sensitivität der SScF gegenüber TGF-β1 auf einer höheren Rezeptorexpression der Zellen beruhen. In Übereinstimmung mit der Literatur (Kawakami *et al.*, 1998; Kubo *et al.*, 2002) wurde in dieser Arbeit in SScF im Vergleich zu NHDF eine höhere *TGFBR2* Expression unter serumfreien Kultivierungsbedingungen nachgewiesen (**P2**). Dies bestätigt, dass SScF ihren aktivierten Phänotyp, auch ohne den initialen Stimulus, über mehrere *in vitro* Passagen beibehalten können (Altorok *et al.*, 2015; Chadli *et al.*, 2019).

Bei Patienten mit SSc wurde eine erhöhte IL-1β-Konzentration im Blut und eine gesteigerte Expression in der Haut nachgewiesen (Hussein, 2005; Martínez-Godínez *et al.*, 2015). Folglich sind SScF *in vivo* einer pathologischen Zytokin-Umgebung ausgesetzt, die zu epigenetischen miRNA-Expressionsänderungen führen könnte (Tsai *et al.*, 2020). Aus Vorarbeiten mit Chondrozyten ist bekannt, dass IL-1β die miRNA-21-Expression supprimiert (Zhu *et al.*, 2019). Da es sich beim *TGFBR2* um ein experimentell bestätigtes miRNA-21-Zielgen handelt (Mishra *et al.*, 2014; Yu *et al.*, 2012), ist es denkbar, dass eine ursprüngliche *in vivo* Exposition gegenüber IL-1β die relative *TGFBR2* Expressionserhöhung in SScF hervorrief. Die erhöhte Fibroblastenaktivierung und XT-I-Induktion in SSc könnte folglich einer Verstärkung des autokrinen TGF-β-Signalwegs zugrunde liegen, an der epigenetische Mechanismen beteiligt sind. Im Gegensatz zu vorangegangen Studien, die eine relative Erhöhung der basalen miRNA-21-Expression in SScF gegenüber NHDF in Gegenwart von fetalem Kälberserum zeigten (Zhu *et al.*, 2012), wurde im Rahmen dieser Arbeit eine signifikante relative Reduktion der miRNA-21-Expression in SScF unter zytokinfreien Kultivierungsbedingungen ermittelt, die reziprok mit der relativen *TGFBR2* Expression korreliert (**P2**). Demzufolge könnte die im Myofibroblastenmodell detektierte Verstärkung der TGF-β1-vermittelten Induktion der relativen *XYLT1* mRNA-Expression und XT-I-Aktivität eine durch epigenetische Variationen hervorgerufene relative *TGFBR2* mRNA-Expressionserhöhung in SScF involvieren.

Nachdem IL-1β als potenter Mediator der *TGFBR2* Expression in SScF identifiziert wurde (**P2**), ergaben sich Hinweise darauf, dass IL-1β-vermittelte Effekte am fibrotischen Geschehen der SSc beteiligt sind. Da Fibrosen mit einer TGF-β1-vermittelten miRNA-21- und *XYLT1* mRNA-Expressionserhöhung einhergehen (**P4**), wurde die IL-1β-vermittelte miRNA-21-Suppression in Gegenwart von TGF-β1 in Bezug auf die

XYLT1 Regulation analysiert (**P2**). Die miRNA-21-Inhibitorbehandlung von NHDF, welche den Effekt von IL-1β auf die miRNA-21-Expression nachstellte, führte zu einer signifikanten Erhöhung der relativen *TGFBR2* mRNA-Expression (**P2**). Neben der miRNA-21-vermittelten Verstärkung der TGF-β-Signaltransduktion über die Suppression der *SMAD7* Expression in NHDF (**P4**) scheint die miRNA-21 somit ebenfalls einen antifibrotischen Effekt in Rahmen einer *TGFBR2* Expressionsregulation zu besitzen. Diese Resultate deuten darauf hin, dass die erhöhte XT-I-Biosynthese in SScF nicht auf einer gesteigerten Basalexpression, sondern auf einer verstärkten autokrinen TGF-β-Signalgebung beruht, die durch ein pathologisches Zytokinmilieu hervorgerufen wird.

Bezogen auf die XT-I wurden sowohl die zelluläre *XYLT1* Expression als auch die extrazelluläre XT-I-Aktivität als geeignete Biomarker für die TGF-β-abhängige Myofibroblastendifferenzierung und ECM-Remodellierung bei SSc identifiziert. Demnach eignet sich das verwendete Myofibroblastenmodell sowohl für die Untersuchung intrinsischer Unterschiede zwischen NHDF und SScF, als auch zur Verifizierung der gewonnenen Erkenntnisse der XT-Regulation aus dem ursprünglichen Myofibroblastenmodell mit NHDF. So konnte unter Verwendung des Myofibroblastenmodells mit SScF bestätigt werden, dass eine durch die miRNA-145-Behandlung hervorgerufene verminderte *KLF4* mRNA-Expression zu einer relativen *XYLT1* mRNA-Expressionserhöhung beiträgt (**P3**).

Zusammenfassend wurde in diesem Teilprojekt eine Beteiligung des pro-inflammatorischen Zytokins IL-1β bei der *XYLT1* Expressionsregulation in SScF demonstriert. Darüber hinaus wurde gezeigt, dass die *XYLT1* Expression und extrazelluläre XT-I-Aktivität geeignete Biomarker für die TGF-β-abhängige Myofibroblastendifferenzierung darstellen und zur Evaluation antifibrotischer Strategien verwendet werden können.

4.3 Identifizierung von Celastrol und Amphotericin B als potenzielle XT-I-Inhibitoren

Im Hinblick auf die Entwicklung einer möglichen Therapiestrategie für Fibrosen ist neben der Charakterisierung fehlregulierter Signaltransduktionspfade und Mediatoren, die Identifizierung therapeutisch wirksamer Moleküle von hoher medizinischer Relevanz. Die vorangegangenen Arbeiten an XT-I-Inhibitoren konzentrierten sich auf eine mögliche Endprodukthemmung der XT-I. Bei den untersuchten Inhibitoren

handelte es sich um Substrat-ähnliche Moleküle wie GAG, Nukleotide und Xyloside, deren XT-I-inhibitorische Wirkung im zellfreien, nicht aber im zellbasierten System verifiziert wurde (Casanova *et al.*, 2009; Fischer *et al.*, 2019; Lee *et al.*, 1982). Eine Inhibition der XT-I-Aktivität und zellulären *XYLT1* mRNA-Expression über andere Molekülklassen wurde bisher nicht beschrieben. Da die biologische Aktivität von Naturstoffen ein breites medizinisches Wirkspektrum abdeckt (Chen *et al.*, 2015; Ng *et al.*, 2019), wurde im Rahmen dieser Arbeit eine Molekülbibliothek mit 96 zellmembrangängigen Naturstoffen für die initiale Identifikation potenzieller XT-I-Inhibitoren verwendet (**P4**). Die Identifizierung erfolgte im zellfreien System unter Verwendung von Zellkulturüberständen von XT-I-überexprimierenden CHO-Zellen. Der XT-I-Zellkulturüberstand wurde durch die Kultivierung einer stabil XT-I-exprimierenden CHO-Zelllinie erhalten, die in Vorarbeiten der Arbeitsgruppe aus der Transfektion einer XT-defizienten pgsA-745 CHO-Zelllinie mit einem XT-I-kodierenden Plasmid generiert wurde (Pönighaus *et al.*, 2010). Die Bestimmung der XT-I-Aktivität der Zellkulturüberstande, die mit oder ohne Inhibitor versetzt wurden, wurde über einen etablierten isoformselektiven UPLC-ESI-MS/MS-XT-I-Assay (Fischer *et al.*, in Revision; Kuhn *et al.*, 2006) ermittelt. Im Rahmen dieser Arbeit wurden die vier Verbindungen Curcumin, Oxytetrazyklin, Amphotericin B und Celastrol identifiziert, die zu einer signifikanten XT-I-Aktivitätsminderung im zellfreien Testsystem führten (**P4**). Über Literaturrecherche und *in silico* Bindungsanalysen der vier Liganden innerhalb des XT-I-Apoproteins ließen sich zwei geeignete Verbindungen für die Analysen im zellbasierten System identifizieren (**P4**). Die anderen beiden Verbindungen wurden aufgrund ihrer assayinterferierenden Eigenschaften ausgeschlossen (Glaser und Holzgrabe, 2016). Bei den beiden potenziellen nichtsubstratbasierten XT-I-Inhibitoren handelte es sich um das pentazyklische Triterpen Celastrol und das Polyenantibiotikum Amphotericin B. Für Celastrol wurde bereits eine anti-inflammatorische Wirkung bei Leberfibrosen sowie eine antifibrotische Wirkung bei renaler und kardialer Fibrose nachgewiesen (Cheng *et al.*, 2016; Li *et al.*, 2020; Tang *et al.*, 2018; Wang *et al.*, 2020). Für Amphotericin B, das als Antimykotikum eingesetzt wird (Warnock, 1991), sind keine antifibrotischen Effekte im Zusammenhang mit prototypischen fibroproliferativen Erkrankungen wie der SSc beschrieben.

Bezüglich des im UPLC-ESI-MS/MS-XT-I-Assay verwendeten Bikunin-abgeleiteten Akzeptorpeptids wurde für Amphotericin B im Rahmen dieser Arbeit ein unkompeti-

tiver Inhibitionsmechanismus der XT-I nachgewiesen (**P4**). Die erhobenen Kinetikdaten wurden mit Hilfe der Dockinganalysesoftware AutoDock Vina (Trott und Olson, 2009) und des Visualisierungsprogramms USCF Chimera (Pettersen *et al.*, 2004) gestützt. Es konnte eine Besetzung der UDP-Xylosebindungsseite mit der Amphotericin B-Ringstruktur gezeigt werden (**P4**). Demnach bindet Amphotericin B an den Enzym-Peptid-Komplex und inhibiert Konsekutivreaktionen, beeinflusst jedoch nicht die Bindung des Akzeptorpeptids an das freie XT-I-Protein. Der zugrundeliegende unkompetitive Bindungsmodus von Amphotericin B gegenüber einem Substrat kommt häufig bei Enzymen vor, die wie die XT-I eine Reaktion mit zwei Substraten katalysieren (Copeland, 2013).
Im Vergleich zu Amphotericin B handelt es sich beim Celastrol um einen kompetitiven XT-I-Inhibitor in Bezug auf das Akzeptorpeptid. In Übereinstimmung mit den kinetischen Daten lag eine favorisierte Dockingposition des Celastrols innerhalb der Akzeptorpeptidbindungsseite des XT-I-Proteins vor (**P4**). Durch die Substratanalogie kommt es zu einer Kompetition zwischen Celastrol und dem Bikunin-abgeleiteten Akzeptorpeptid um die Bindung an das aktive Zentrum der XT-I, wodurch die Affinität der XT-I für das Akzeptorpeptid vermeintlich herabgesetzt wird (**P4**).

Die Analyse der beiden XT-I-Inhibitoren im zellbasierten System mit primären NHDF demonstrierte eine konzentrationsabhängige relative Repression der basalen und Zytokin-induzierten *XYLT1* mRNA-Expression Inhibitor-behandelter Zellen (**P4**). Ein Einfluss der verwendeten Inhibitorkonzentrationen auf die Zellproliferation wurde mittels WST-1-Assay ausgeschlossen (**P4**). Im direkten Vergleich zur Celastrol-vermittelten *XYLT1* Repression, war der Amphotericin B-vermittelte Effekt stärker ausgeprägt. In Übereinstimmung mit den Expressionsdaten wurde eine signifikante extrazelluläre XT-I-Aktivitätsreduktion in TGF-β1-stimulierten Amphotericin B-vorbehandelten Zellen detektiert (**P4**). Zudem wurde eine nicht-signifikante Celastrol-vermittelte extrazelluläre XT-I-Aktivitätsreduktion nachgewiesen (**P4**). Bezüglich der intrazellulären XT-Aktivität ließen sich keine Unterschiede nach Inhibitorbehandlung beobachten. Dem könnte eine nicht-ausreichende Membranpermeabilität der Inhibitoren oder ein inadäquat gewählter Detektionszeitpunkt zugrunde liegen. Letzteres wird durch Resultate dieser Arbeit gestützt, die einen zeitabhängigen Anstieg der intrazellulären XT-Aktivität von NHDF nach Zytokinbehandlung zeigten (**P1**).

Zusammenfassend wurden in diesem Teilprojekt zwei potenzielle nicht-substratbasierte XT-I-Inhibitoren identifiziert, die neben der Inhibition der extrazellulären XT-I-Aktivität einen supprimierenden Effekt auf die *XYLT1* Expression haben (**P4**).

Weitere antifibrotische Effekte von Amphotericin B wurden im Rahmen dieser Arbeit in Form einer signifikanten Reduktion der *COL1A1* und *TGFB1* mRNA-Expression TGF-β1-stimulierter NHDF gezeigt (**P4**). Durch die Amphotericin B-vermittelte Induktion des inhibitorischen SMAD7 (**P4**) könnte es zur Verstärkung der TGF-β1-vermittelten Rückkopplungsschleife kommen (Yan und Chen, 2011), die sich unter anderem in Form einer verminderten *TGFB1* Autoinduktion und Reduktion der TGF-β1-induzierten *XYLT1* und *COL1A1* Expression äußert (**P4**). Diese Hypothese wird durch die Resultate des ersten Teilprojekts dieser Arbeit gefestigt, die eine inhibitorische Wirkung des SMAD7 auf die Zytokin-induzierte *XYLT1* Expression zeigten (**P1**). Eine *SMAD7* siRNA-vermittelte Reduktion der *COL1A1* mRNA- und Proteinexpression wurde bereits in der Arbeit von Zhou *et al.* unter Verwendung von NHDF nachgewiesen (Zhou *et al.*, 2017).
Cheng *et al.* zeigten, dass der antifibrotische Effekt von Celastrol über die Suppression des miRNA-21/ERK-Signalwegs in murinen kardialen Fibroblasten vermittelt wird (Cheng *et al.*, 2016). Auch im ersten Teilprojekt dieser Arbeit wurde eine Beteiligung der MAPK ERK und miRNA-21 an der Regulation der *XYLT1* Expression nachgewiesen (**P1**, **P3**). Die in diesem Teilprojekt detektierte *XYLT1* Suppression durch Celastrol in NHDF könnte somit der von Cheng *et al.* beschriebenen Inhibition des miRNA-21/ERK-Signalwegs unterliegen.

Aus den dargestellten Ergebnissen wird deutlich, dass die identifizierten XT-I-Inhibitoren sowie die zugrundeliegenden Regulationspfade sich als Therapieoption zur Zytokin-vermittelten Fibrosierung bei SSc eignen könnten und demnach näher untersucht werden sollten.

5 Ausblick

Im Rahmen dieser Arbeit wurden neue Erkenntnisse hinsichtlich der XT-I-Regulation bei Fibrosen gewonnen. Es wurden mitunter die bei der XT-I-Regulation involvierten Mediatoren und Signaltransduktionswege ermittelt sowie deren Beteiligung in der SSc näher aufgeklärt. Die erzielten Ergebnisse vertiefen nicht nur die Kenntnisse der pathobiochemischen Prozesse bei Fibrosen, sondern leisten durch die Identifizierung potenzieller XT-I-Inhibitoren auch einen wichtigen Beitrag zur Entwicklung neuer Therapieansätze für fibroproliferative Erkrankungen.

Mit dem Abschluss der Arbeit ergeben sich weiterführende Aspekte, die in einem anschließenden Forschungsvorhaben adressiert werden sollten. Erste Resultate dieser Arbeit zeigen, dass die molekularen Mechanismen der XT-I-Regulation bei Fibrosen, sich von denen der chronischen Inflammation unterscheiden. Bei der SSc scheinen die fibrotischen Aspekte zu überwiegen, welche die erhöhte Zytokin-induzierte *XYLT1* Expression und extrazelluläre XT-I-Aktivität in SScF begründen. Diese Hypothese könnte durch die Kultivierung von NHDF in konditioniertem Medium von SScF überprüft werden. Das Serum von SSc-Patienten könnte ebenfalls für diese Zwecke verwendet werden.

Ebenfalls ungeklärt sind die zugrundeliegenden Mechanismen der differentiellen IL-1β-vermittelten Zellantwort in NHDF und SScF. Durch die Variation der verwendeten IL-1β-Konzentration und Behandlungsdauer könnten die Unterschiede in der *XYLT1* Expressionsregulation zwischen NHDF und SScF weiterführend untersucht werden. Die Quantifizierung der membrangebundenen oder sekretierten IL-1-Rezeptormenge von NHDF und SScF könnte Informationen über eine differentielle zelluläre IL-1β-vermittelte Signalgebung liefern. Da erste Hinweise auf eine Involvierung des Inflammasoms bei der XT-I-Regulation unter IL-1β-Supplementation gezeigt wurden, wäre es denkbar, dass Inflammasom-vermittelte Signalwege einen regulatorischen Einfluss auf die XT-I-Expression und -Sekretion nehmen. Zur Untersuchung der Beteiligung des Inflammasoms an der XT-I-Regulation in Dermalfibroblasten könnten neben IL-1β andere bekannte Inflammasom-induzierende Faktoren, wie bakterielle Lipopolysaccharide und ATP, verwendet werden.

Neben der Verwendung von NHDF und SScF könnten weiterführend primäre Monozyten des peripheren Blutes verwendet werden, um die Aktivierung von

humanen Makrophagen im Kontext der SSc zu untersuchen. Die Untersuchung der in SSc-Geweben vorkommenden Immunzellspezies wie Makrophagen und Lymphozyten könnte ebenfalls neue Informationen über die Beteiligung einer fehlregulierten Immunantwort bei der SSc liefern. Im Zuge dessen könnte die Untersuchung der *XYLT1* Expression und XT-I-Aktivität in Monozyten und Makrophagen vorgenommen und ihr Beitrag zur erhöhten Serum-XT-Aktivität bei SSc eruiert werden. Um die Immunzellen zu charakterisieren, könnten neben der Durchflusszytometrie Einzelzellanalysen wie das *single-cell RNA-sequencing* durchgeführt werden.

Eine detaillierte Analyse der intrazellulären und extrazellulären XT-I-Aktivität von SScF mit der entsprechenden *XYLT1* Expression unter verschiedenen Kultivierungsbedingungen und Zeiträumen wäre zielführend, um potenzielle XT-I-Sekretionsunterschiede zwischen NHDF und SScF aufzuzeigen. Um jedoch die anfängliche Hypothese der erhöhten XT-I-Serumaktivität bei SSc auf die alleinige Aktivität von Myofibroblasten zurückzuführen, müssten entsprechende weitere Analysen in Myofibroblasten-depletierten Modellorganismen durchgeführt werden. Darüber hinaus könnten die im letzten Teilprojekt identifizierten XT-I-Inhibitoren strukturell modifiziert und hinsichtlich ihrer isoformspezifischen Inhibition von XT-I und XT-II analysiert werden.

Da die Kultivierung der Zellen im Monolayersystem die physiologische Umgebung der Zellen nur bedingt widerspiegelt, könnte die Testung der Hypothesen und Identifizierten XT-I-Inhibitoren in einem dreidimensionalen Kultivierungssystem mit SScF oder in *in vivo* Versuchen mit murinen SSc-Modellen erfolgen. Sollten sich die beiden XT-I-Inhibitoren als adäquate Wirkstoffe zur Therapie der SSc im Tiermodell herausstellen, könnten sich zugelassene Medikamente mit Celastrol oder Amphotericin B ebenfalls zur Therapie von SSc eignen. Da für Celastrol und Amphotericin B bereits Trägersysteme für die gezielte Applikation der Wirkstoffe in verschiedene Zielgewebe existieren (Cascão *et al.*, 2017; Cuddihy *et al.*, 2019; Li *et al.*, 2020; Proesmans *et al.*, 2010), sollten weiterführende Studien daran anknüpfen, die optimale Form des Wirkstofftransports und der Wirkstofffreisetzung zur Therapie der SSc zu ermitteln.

Literaturverzeichnis

Abraham, D. und Distler, O. (2007). How does endothelial cell injury start? The role of endothelin in systemic sclerosis. *Arthritis Research & Therapy*, *9*(Suppl 2), S2. doi: 10.1186/ar2186

Abtahi, S., Farazmand, A., Mahmoudi, M., Ashraf-Ganjouei, A., Javinani, A., Nazari, B., Kavosi, H., Amirzargar, A. A., Jamshidi, A. R. und Gharibdoost, F. (2015). *IL-1A* rs1800587, *IL-1B* rs1143634 and *IL-1R1* rs2234650 polymorphisms in Iranian patients with systemic sclerosis. *International Journal of Immunogenetics*, *42*(6), 423–427. doi: 10.1111/iji.12212

Agarwal, V., Bell, G. W., Nam, J.-W. und Bartel, D. P. (2015). Predicting effective microRNA target sites in mammalian mRNAs. *eLife*, *4*, e05005. doi: 10.7554/eLife.05005

Ai, W., Liu, Y., Langlois, M. und Wang, T. C. (2004). Kruppel-like factor 4 (KLF4) represses histidine decarboxylase gene expression through an upstream Sp1 site and downstream gastrin responsive elements. *Journal of Biological Chemistry*, *279*(10), 8684–8693. doi: 10.1074/jbc.M308278200

Allanore, Y., Simms, R., Distler, O., Trojanowska, M., Pope, J., Denton, C. P. und Varga, J. (2015). Systemic sclerosis. *Nature Reviews Disease Primers*, *1*(1), 15002. doi: 10.1038/nrdp.2015.2

Almeida, R., Levery, S. B., Mandel, U., Kresse, H., Schwientek, T., Bennett, E. P. und Clausen, H. (1999). Cloning and expression of a proteoglycan UDP-galactose:β-xylose β1,4-galactosyltransferase I: a seventh member of the human β4-galactosyltransferase gene family. *Journal of Biological Chemistry*, *274*(37), 26165–26171. doi: 10.1074/jbc.274.37.26165

Altorok, N., Tsou, P.-S., Coit, P., Khanna, D. und Sawalha, A. H. (2015). Genome-wide DNA methylation analysis in dermal fibroblasts from patients with diffuse and limited systemic sclerosis reveals common and subset-specific DNA methylation aberrancies. *Annals of the Rheumatic Diseases*, *74*(8), 1612–1620. doi: 10.1136/annrheumdis-2014-205303

Angiolilli, C., Marut, W., van der Kroef, M., Chouri, E., Reedquist, K. A. und Radstake, T. R. D. J. (2018). New insights into the genetics and epigenetics of systemic sclerosis. *Nature Reviews Rheumatology*, *14*(11), 657–673. doi: 10.1038/s41584-018-0099-0

Antsiferova, M. und Werner, S. (2012). The bright and the dark sides of activin in wound healing and cancer. *Journal of Cell Science*, *125*(17), 3929–3937. doi: 10.1242/jcs.094789

Artlett, C. M. (2013). Inflammasomes in wound healing and fibrosis: inflammasomes in wound healing and fibrosis. *The Journal of Pathology*, *229*(2), 157–167. doi: 10.1002/path.4116

Bai, X., Zhou, D., Brown, J. R., Crawford, B. E., Hennet, T. und Esko, J. D. (2001). Biosynthesis of the linkage region of glycosaminoglycans: cloning and activity of galactosyltransferase II, the sixth member of the β1,3-galactosyltransferase family (β3GalT6). *Journal of Biological Chemistry*, *276*(51), 48189–48195. doi: 10.1074/jbc.M107339200

Barrientos, S., Stojadinovic, O., Golinko, M. S., Brem, H. und Tomic-Canic, M. (2008). Perspective article: growth factors and cytokines in wound healing. *Wound Repair and Regeneration*, *16*(5), 585–601. doi: 10.1111/j.1524-475X.2008.00410.x

Baugé, C., Cauvard, O., Leclercq, S., Galéra, P. und Boumédiene, K. (2011). Modulation of transforming growth factor beta signalling pathway genes by transforming growth factor beta in human osteoarthritic chondrocytes: involvement of Sp1 in both early and late response cells

to transforming growth factor beta. Arthritis Research & Therapy, 13(1), R23. doi: 10.1186/ar3247

Bergamasco, A., Hartmann, N., Wallace, L. und Verpillat, P. (2019). Epidemiology of systemic sclerosis and systemic sclerosis-associated interstitial lung disease. *Clinical Epidemiology*, *Volume 11*, 257–273. doi: 10.2147/CLEP.S191418

Berman, H. M. (2000). The protein data bank. *Nucleic Acids Research*, *28*(1), 235–242. doi: 10.1093/nar/28.1.235

Bishop, J. R., Schuksz, M. und Esko, J. D. (2007). Heparan sulphate proteoglycans fine-tune mammalian physiology. *Nature*, *446*(7139), 1030–1037. doi: 10.1038/nature05817

Borthwick, L. A., Wynn, T. A. und Fisher, A. J. (2013). Cytokine mediated tissue fibrosis. *Biochimica et Biophysica Acta (BBA) - Molecular Basis of Disease*, *1832*(7), 1049–1060. doi: 10.1016/j.bbadis.2012.09.014

Briggs, D. C. und Hohenester, E. (2018). Structural basis for the initiation of glycosaminoglycan biosynthesis by human xylosyltransferase 1. *Structure*, *26*(6), 801-809.e3. doi: 10.1016/j.str.2018.03.014

Casanova, J. C., Ambrosius, M., Kuhn, J., Kleesiek, K. und Götting, C. (2009). Analysis of xylosyltransferase II binding to the anticoagulant heparin. *Biochemical and Biophysical Research Communications*, *383*(1), 4–10. doi: 10.1016/j.bbrc.2009.03.050

Casanova, J. C., Kuhn, J., Kleesiek, K. und Götting, C. (2008). Heterologous expression and biochemical characterization of soluble human xylosyltransferase II. *Biochemical and Biophysical Research Communications*, *365*(4), 678–684. doi: 10.1016/j.bbrc.2007.10.206

Cascão, R., Fonseca, J. E. und Moita, L. F. (2017). Celastrol: a spectrum of treatment opportunities in chronic diseases. *Frontiers in Medicine*, *4*, 69. doi: 10.3389/fmed.2017.00069

Chadli, L., Sotthewes, B., Li, K., Andersen, S. N., Cahir-McFarland, E., Cheung, M., Cullen, P., Dorjée, A., de Vries-Bouwstra, J. K., Huizinga, T. W. J., Fischer, D. F., DeGroot, J., Viney, J. L., Zheng, T. S., Aarbiou, J. und Gardet, A. (2019). Identification of regulators of the myofibroblast phenotype of primary dermal fibroblasts from early diffuse systemic sclerosis patients. *Scientific Reports*, *9*(1), 4521. doi: 10.1038/s41598-019-41153-w

Chen, D.-Q., Feng, Y.-L., Cao, G. und Zhao, Y.-Y. (2018a). Natural products as a source for antifibrosis therapy. *Trends in Pharmacological Sciences*, *39*(11), 937–952. doi: 10.1016/j.tips.2018.09.002

Chen, S.-R., Chen, X.-P., Lu, J.-J., Wang, Y. und Wang, Y.-T. (2015). Potent natural products and herbal medicines for treating liver fibrosis. *Chinese Medicine*, *10*(1), 7. doi: 10.1186/s13020-015-0036-y

Chen, S.-R., Dai, Y., Zhao, J., Lin, L., Wang, Y. und Wang, Y. (2018b). A mechanistic overview of triptolide and celastrol, natural products from tripterygium wilfordii hook F. *Frontiers in Pharmacology*, *9*, 104. doi: 10.3389/fphar.2018.00104

Cheng, M., Wu, G., Song, Y., Wang, L., Tu, L., Zhang, L. und Zhang, C. (2016). Celastrol-induced suppression of the miR-21/ERK signalling pathway attenuates cardiac fibrosis and dysfunction. *Cellular Physiology and Biochemistry*, *38*(5), 1928–1938. doi: 10.1159/000445554

Condac, E., Dale, G. L., Bender-Neal, D., Ferencz, B., Towner, R. und Hinsdale, M. E. (2009). Xylosyltransferase II is a significant contributor of circulating xylosyltransferase levels and

platelets constitute an important source of xylosyltransferase in serum. *Glycobiology*, *19*(8), 829–833. doi: 10.1093/glycob/cwp058

Copeland, R. A. (2013). *Evaluation of Enzyme Inhibitors in Drug Discovery: A Guide for Medicinal Chemists and Pharmacologists* (1. Auflage). Wiley. doi: 10.1002/9781118540398

Copeland, R. A., Harpel, M. R. und Tummino, P. J. (2007). Targeting enzyme inhibitors in drug discovery. *Expert Opinion on Therapeutic Targets*, *11*(7), 967–978. doi: 10.1517/14728222.11.7.967

Cox, T. R. und Erler, J. T. (2011). Remodeling and homeostasis of the extracellular matrix: implications for fibrotic diseases and cancer. *Disease Models & Mechanisms*, *4*(2), 165–178. doi: 10.1242/dmm.004077

Cuddihy, G., Wasan, E., Di, Y. und Wasan, K. (2019). The development of oral amphotericin B to treat systemic fungal and parasitic infections: has the myth been finally realized? *Pharmaceutics*, *11*(3), 99. doi: 10.3390/pharmaceutics11030099

Cushing, L., Kuang, P. P., Qian, J., Shao, F., Wu, J., Little, F., Thannickal, V. J., Cardoso, W. V. und Lü, J. (2011). miR-29 is a major regulator of genes associated with pulmonary fibrosis. *American Journal of Respiratory Cell and Molecular Biology*, *45*(2), 287–294. doi: 10.1165/rcmb.2010-0323OC

Darby, I. A. und Hewitson, T. D. (2007). Fibroblast differentiation in wound healing and fibrosis. *International Review of Cytology* (Band 257, S. 143–179). Elsevier. doi: 10.1016/S0074-7696(07)57004-X

Derynck, R. und Zhang, Y. E. (2003). Smad-dependent and Smad-independent pathways in TGF-β family signalling. *Nature*, *425*(6958), 577–584. doi: 10.1038/nature02006

Distler, J. H. W., Györfi, A.-H., Ramanujam, M., Whitfield, M. L., Königshoff, M. und Lafyatis, R. (2019). Shared and distinct mechanisms of fibrosis. *Nature Reviews Rheumatology*, *15*(12), 705–730. doi: 10.1038/s41584-019-0322-7

Do, N. N. und Eming, S. A. (2016). Skin fibrosis: models and mechanisms. *Current Research in Translational Medicine*, *64*(4), 185–193. doi: 10.1016/j.retram.2016.06.003

Domsic, R. T., Rodriguez-Reyna, T., Lucas, M., Fertig, N. und Medsger, T. A. (2011). Skin thickness progression rate: a predictor of mortality and early internal organ involvement in diffuse scleroderma. *Annals of the Rheumatic Diseases*, *70*(1), 104–109. doi: 10.1136/ard.2009.127621

Ellis, S., Lin, E. J. und Tartar, D. (2018). Immunology of wound healing. *Current Dermatology Reports*, *7*(4), 350–358. doi: 10.1007/s13671-018-0234-9

Etoh, M., Jinnin, M., Makino, K., Yamane, K., Nakayama, W., Aoi, J., Honda, N., Kajihara, I., Makino, T., Fukushima, S. und Ihn, H. (2013). MicroRNA-7 down-regulation mediates excessive collagen expression in localized scleroderma. *Archives of Dermatological Research*, *305*(1), 9–15. doi: 10.1007/s00403-012-1287-4

Faust, I., Böker, K. O., Lichtenberg, C., Kuhn, J., Knabbe, C. und Hendig, D. (2014). First description of the complete human xylosyltransferase-I promoter region. *BMC Genetics*, *15*(1), 129. doi: 10.1186/s12863-014-0129-0

Faust, I., Roch, C., Kuhn, J., Prante, C., Knabbe, C. und Hendig, D. (2013). Human xylosyltransferase-I – a new marker for myofibroblast differentiation in skin fibrosis. *Biochemical and Biophysical Research Communications*, *436*(3), 449–454. doi: 10.1016/j.bbrc.2013.05.125

Faust, I., Weile, J., Fujita, B., Kandolf, R., Hendig, D., Vollmer, T., Stan, A.-C., Kellner, U., Kuhn, J., Gummert, J. F. und Knabbe, C. (2019). Heart transplantation in systemic sclerosis: new impulses for conventional scleroderma transplantation regimen and scleroderma diagnostic monitoring: 2 Case Reports. *Transplantation Proceedings*, *51*(3), 865–870. doi: 10.1016/j.transproceed.2019.01.025

Firn, R. (2010). *Nature's chemicals: the natural products that shaped our world* (Oxford biology). Oxford, NY: Oxford University Press. doi: 10.1093/acprof:oso/9780199566839.001.0001

Fischer, B., Kuhn, J., Ly, T.-D., Schmidt, V., Kleine, A., Hendig, D., Knabbe, C. und Faust, I. (in Revision). Development of a xylosyltransferase-I-selective UPLC MS/MS activity assay using a specific acceptor peptide. *Biochimie*.

Fischer, B., Ly, T.-D., Hendig, D., Kuhn, J., Pécheur, E.-I., Reungoat, E., Knabbe, C. und Faust, I. (2019). First description of a compensatory xylosyltransferase I induction observed after an antifibrotic UDP-treatment of normal human dermal fibroblasts. *Biochemical and Biophysical Research Communications*, *512*(1), 7–13. doi: 10.1016/j.bbrc.2019.02.150

Fried, M. G. und Garner, M. M. (1998). The electrophoretic mobility shift assay (EMSA) for detection and analysis of protein-DNA interactions. In D. Tietz (Hrsg.), *Nucleic Acid Electrophoresis* (S. 239–271). Berlin, Heidelberg: Springer-Verlag Berlin Heidelberg. doi: 10.1007/978-3-642-58924-9_10

Friedman, S. L., Sheppard, D., Duffield, J. S. und Violette, S. (2013). Therapy for fibrotic fiseases: nearing the starting line. *Science Translational Medicine*, *5*(167), 167sr1-167sr1. doi: 10.1126/scitranslmed.3004700

Fritz, T. A., Gabb, M. M., Wei, G. und Esko, J. D. (1994). Two N-acetylglucosaminyltransferases catalyze the biosynthesis of heparan sulfate. *The Journal of Biological Chemistry*, *269*(46), 28809–28814.

Garrett, S. M., Baker Frost, D. und Feghali-Bostwick, C. (2017). The mighty fibroblast and its utility in scleroderma research. *Journal of Scleroderma and Related Disorders*, *2*(2), 100–107. doi: 10.5301/jsrd.5000240

Gauglitz, G. G., Korting, H. C., Pavicic, T., Ruzicka, T. und Jeschke, M. G. (2011). Hypertrophic scarring and keloids: pathomechanisms and current and emerging treatment strategies. *Molecular Medicine*, *17*(1–2), 113–125. doi: 10.2119/molmed.2009.00153

Ghatak, S., Maytin, E. V., Mack, J. A., Hascall, V. C., Atanelishvili, I., Moreno Rodriguez, R., Markwald, R. R. und Misra, S. (2015). Roles of proteoglycans and glycosaminoglycans in wound healing and fibrosis. *International Journal of Cell Biology*, *2015*, 1–20. doi: 10.1155/2015/834893

Glaser, J. und Holzgrabe, U. (2016). Focus on PAINS: false friends in the quest for selective anti-protozoal lead structures from nature? *MedChemComm*, *7*(2), 214–223. doi: 10.1039/C5MD00481K

Götting, C., Hendig, D., Adam, A., Schön, S., Schulz, V., Szliska, C., Kuhn, J. und Kleesiek, K. (2005). Elevated xylosyltransferase I activities in pseudoxanthoma elasticum (PXE) patients as a marker of stimulated proteoglycan biosynthesis. *Journal of Molecular Medicine*, *83*(12), 984–992. doi: 10.1007/s00109-005-0693-x

Götting, C., Kuhn, J., Brinkmann, T. und Kleesiek, K. (1998). Xylosylation of alternatively spliced isoforms of alzheimer app by xylosyltransferase. *Journal of Protein Chemistry*, *17*(3), 295–

302. doi: 10.1023/A:1022549121672

Götting, C., Kuhn, J., Brinkmann, T. und Kleesiek, K. (2002). Xylosyltransferase activity in seminal plasma of infertile men. *Clinica Chimica Acta*, *317*(1–2), 199–202. doi: 10.1016/S0009-8981(01)00793-8

Götting, C., Kuhn, J., Weilke, C., Brinkmann, T., Kleesiek, K., Sollberg, S., Huerkamp, C. und Krieg, T. (1999). Serum xylosyltransferase: a new biochemical marker of the sclerotic process in systemic sclerosis. *Journal of Investigative Dermatology*, *112*(6), 919–924. doi: 10.1046/j.1523-1747.1999.00590.x

Götting, C., Kuhn, J., Zahn, R., Brinkmann, T. und Kleesiek, K. (2000). Molecular cloning and expression of human UDP-D-xylose:proteoglycan core protein β-D-xylosyltransferase and its first isoform XT-II. *Journal of Molecular Biology*, *304*(4), 517–528. doi: 10.1006/jmbi.2000.4261

Gras, C., Ratuszny, D., Hadamitzky, C., Zhang, H., Blasczyk, R. und Figueiredo, C. (2015). miR-145 contributes to hypertrophic scarring of the skin by inducing myofibroblast activity. *Molecular Medicine*, *21*(1), 296–304. doi: 10.2119/molmed.2014.00172

Grossman, C., Dovrish, Z., Shoenfeld, Y. und Amital, H. (2011). Do infections facilitate the emergence of systemic sclerosis? *Autoimmunity Reviews*, *10*(5), 244–247. doi: 10.1016/j.autrev.2010.09.010

Gurtner, G. C., Werner, S., Barrandon, Y. und Longaker, M. T. (2008). Wound repair and regeneration. *Nature*, *453*(7193), 314–321. doi: 10.1038/nature07039

Hardingham, T. E. und Fosang, A. J. (1992). Proteoglycans: many forms and many functions. *The FASEB Journal*, *6*(3), 861–870. doi: 10.1096/fasebj.6.3.1740236

Harvey, A. L., Edrada-Ebel, R. und Quinn, R. J. (2015). The re-emergence of natural products for drug discovery in the genomics era. *Nature Reviews Drug Discovery*, *14*(2), 111–129. doi: 10.1038/nrd4510

Henderson, J., Bhattacharyya, S., Varga, J. und O'Reilly, S. (2018). Targeting TLRs and the inflammasome in systemic sclerosis. *Pharmacology & Therapeutics*, *192*, 163–169. doi: 10.1016/j.pharmthera.2018.08.003

Hinz, B. (2007). Formation and function of the myofibroblast during tissue repair. *Journal of Investigative Dermatology*, *127*(3), 526–537. doi: 10.1038/sj.jid.5700613

Ho, Y. Y., Lagares, D., Tager, A. M. und Kapoor, M. (2014). Fibrosis—a lethal component of systemic sclerosis. *Nature Reviews Rheumatology*, *10*(7), 390–402. doi: 10.1038/nrrheum.2014.53

Hocevar, B. A. (1999). TGF-beta induces fibronectin synthesis through a c-Jun N-terminal kinase-dependent, Smad4-independent pathway. *The EMBO Journal*, *18*(5), 1345–1356. doi: 10.1093/emboj/18.5.1345

van den Hoogen, F., Khanna, D., Fransen, J., Johnson, S. R., Baron, M., Tyndall, A., Matucci-Cerinic, M., Naden, R. P., Medsger, T. A., Carreira, P. E., Riemekasten, G., Clements, P. J., Denton, C. P., Distler, O., Allanore, Y., Furst, D. E., Gabrielli, A., Mayes, M. D., van Laar, J. M., Seibold, J. R., Czirjak, L., Steen, V. D., Inanc, M., Kowal-Bielecka, O., Müller-Ladner, U., Valentini, G., Veale, D. J., Vonk, M. C., Walker, U. A., Chung, L., Collier, D. H., Csuka, M. E., Fessler, B. J., Guiducci, S., Herrick, A., Hsu, V. M., Jimenez, S., Kahaleh, B., Merkel, P. A., Sierakowski, S., Silver, R. M., Simms, R. W., Varga, J. und Pope, J. E. (2013). 2013 classification criteria for systemic sclerosis: an American college of rheumatology/European league against

rheumatism collaborative initiative: ACR/EULAR classification criteria for SSc. *Arthritis & Rheumatism*, *65*(11), 2737–2747. doi: 10.1002/art.38098

Hu, D. und Wan, Y. (2011). Regulation of Krüppel-like factor 4 by the anaphase promoting complex pathway is involved in TGF-β signaling. *Journal of Biological Chemistry*, *286*(9), 6890–6901. doi: 10.1074/jbc.M110.179952

Hu, J., Wang, X., Wei, S. M., Tang, Y. H., Zhou, Q. und Huang, C. X. (2016). Activin A stimulates the proliferation and differentiation of cardiac fibroblasts via the ERK1/2 and p38-MAPK pathways. *European Journal of Pharmacology*, *789*, 319–327. Elsevier. doi: 10.1016/j.ejphar.2016.07.053

Hussein, M. R. (2005). Alterations of mononuclear inflammatory cells, CD4/CD8+ T cells, interleukin 1, and tumor necrosis factor in the bronchoalveolar lavage fluid, peripheral blood, and skin of patients with systemic sclerosis. *Journal of Clinical Pathology*, *58*(2), 178–184. doi: 10.1136/jcp.2004.019224

Ihn, H. (2008). Autocrine TGF-β signaling in the pathogenesis of systemic sclerosis. *Journal of Dermatological Science*, *49*(2), 103–113. doi: 10.1016/j.jdermsci.2007.05.014

Ihn, H., Yamane, K., Asano, Y., Jinnin, M. und Tamaki, K. (2006). Constitutively phosphorylated Smad3 interacts with Sp1 and p300 in scleroderma fibroblasts. *Rheumatology*, *45*(2), 157–165. doi: 10.1093/rheumatology/kei124

Ihn, H., Yamane, K., Kubo, M. und Tamaki, K. (2001). Blockade of endogenous transforming growth factor beta signaling prevents up-regulated collagen synthesis in scleroderma fibroblasts: association with increased expression of transforming growth factor beta receptors. *Arthritis and Rheumatism*, *44*(2), 474–480. doi: 10.1002/1529-0131(200102)44:2<474::AID-ANR67>3.0.CO;2-#

Jinnin, M., Ihn, H., Asano, Y., Yamane, K., Trojanowska, M. und Tamaki, K. (2004). Tenascin-C upregulation by transforming growth factor-β in human dermal fibroblasts involves Smad3, Sp1, and Ets1. *Oncogene*, *23*(9), 1656–1667. doi: 10.1038/sj.onc.1207064

Kaczynski, J., Cook, T. und Urrutia, R. (2003). Sp1- and Krüppel-like transcription factors. *Genome Biology*, *4*(2), 206. doi: 10.1186/gb-2003-4-2-206

Kamato, D., Burch, M., Zhou, Y., Mohamed, R., Stow, J. L., Osman, N., Zheng, W. und Little, P. J. (2019). Individual Smad2 linker region phosphorylation sites determine the expression of proteoglycan and glycosaminoglycan synthesizing genes. *Cellular Signalling*, *53*(November 2018), 365–373. Elsevier. doi: 10.1016/j.cellsig.2018.11.005

Kawakami, T., Ihn, H., Xu, W., Smith, E., LeRoy, C. und Trojanowska, M. (1998). Increased expression of TGF-β receptors by scleroderma fibroblasts: evidence for contribution of autocrine TGF-β signaling to scleroderma phenotype. *Journal of Investigative Dermatology*, *110*(1), 47–51. doi: 10.1046/j.1523-1747.1998.00073.x

Kearns, A. E., Campbell, S. C., Westley, J. und Schwartz, N. B. (1991). Initiation of chondroitin sulfate biosynthesis: a kinetic analysis of UDP-D-xylose:core protein beta-D-xylosyltransferase. *Biochemistry*, *30*(30), 7477–7483. doi: 10.1021/bi00244a016

Khair, M., Bourhim, M., Barré, L., Li, D., Netter, P., Magdalou, J., Fournel-Gigleux, S. und Ouzzine, M. (2013). Regulation of xylosyltransferase I gene expression by interleukin 1β in human primary chondrocyte cells: mechanism and impact on proteoglycan synthesis. *Journal of Biological Chemistry*, *288*(3), 1774–1784. doi: 10.1074/jbc.M112.419887

Kim, K.-J., Liu, X., Komabayashi, T., Jeong, S.-I. und Selli, S. (2016). Natural products for infectious diseases. *Evidence-Based Complementary and Alternative Medicine*, *2016*, 1–1. doi: 10.1155/2016/9459047

Kitabatake, M., Ishikawa, H. und Maeda, H. (1983). Immunohistochemical demonstration of proteoglycans in the skin of patients with systemic sclerosis. *British Journal of Dermatology*, *108*(3), 257–262. doi: 10.1111/j.1365-2133.1983.tb03962.x

Kitagawa, H., Tone, Y., Tamura, J., Neumann, K. W., Ogawa, T., Oka, S., Kawasaki, T. und Sugahara, K. (1998). Molecular cloning and expression of glucuronyltransferase I involved in the biosynthesis of the glycosaminoglycan-protein linkage region of proteoglycans. *Journal of Biological Chemistry*, *273*(12), 6615–6618. doi: 10.1074/jbc.273.12.6615

Klagsbrun, M. (1990). The affinity of fibroblast growth factors (FGFs) for heparin; FGF-heparan sulfate interactions in cells and extracellular matrix. *Current Opinion in Cell Biology*, *2*(5), 857–863. doi: 10.1016/0955-0674(90)90084-R

Kleesiek, K., Reinards, R., Okusi, J., Wolf, B. und Greiling, H. (1987). UDP-D-xylose:proteoglycan core protein β-D-xylosyltransferase: a new marker of cartilage destruction in chronic joint diseases. *Clinical Chemistry and Laboratory Medicine*, *25*(8). doi: 10.1515/cclm.1987.25.8.473

Kubo, M., Ihn, H., Yamane, K. und Tamaki, K. (2002). Upregulated expression of transforming growth factor-beta receptors in dermal fibroblasts of skin sections from patients with systemic sclerosis. *The Journal of Rheumatology*, *29*(12), 2558–2564.

Kuhn, J., Gressner, O. A., Götting, C., Gressner, A. M. und Kleesiek, K. (2009). Increased serum xylosyltransferase activity in patients with liver fibrosis. *Clinica Chimica Acta*, *409*(1–2), 123–126. doi: 10.1016/j.cca.2009.09.013

Kuhn, J., Prante, C., Schön, S., Götting, C. und Kleesiek, K. (2006). Measurement of fibrosis marker xylosyltransferase I activity by HPLC electrospray ionization tandem mass spectrometry. *Clinical Chemistry*, *52*(12), 2243–2249. doi: 10.1373/clinchem.2006.071167

Kuroda, K. und Shinkai, H. (1997). Decorin and glycosaminoglycan synthesis in skin fibroblasts from patients with systemic sclerosis. *Archives of Dermatological Research*, *289*(8), 481–485. doi: 10.1007/s004030050225

Kurzinski, K. und Torok, K. S. (2011). Cytokine profiles in localized scleroderma and relationship to clinical features. *Cytokine*, *55*(2), 157–164. doi: 10.1016/j.cyto.2011.04.001

Lairson, L. L., Henrissat, B., Davies, G. J. und Withers, S. G. (2008). Glycosyltransferases: structures, functions, and mechanisms. *Annual Review of Biochemistry*, *77*(1), 521–555. doi: 10.1146/annurev.biochem.76.061005.092322

Lee, M. H., Lazo, J. S., Li, C.-D., Hadfield, A. F., Maniglia, C. A. und Sartorelli, A. C. (1982). Solubilization of murine melanoma xylosyltransferase and galactosyltransferase activities and their inactivation by dialdehyde nucleosides. *Chemico-Biological Interactions*, *41*(2), 141–153. doi: 10.1016/0009-2797(82)90085-0

LeRoy, E. C., Black, C., Fleischmajer, R., Jablonska, S., Krieg, T., Medsger, T. A., Rowell, N. und Wollheim, F. (1988). Scleroderma (systemic sclerosis): classification, subsets and pathogenesis. *The Journal of Rheumatology*, *15*(2), 202–205. PMID: 3361530

LeRoy, E. C. und Medsger, T. A. (2001). Criteria for the classification of early systemic sclerosis.

The Journal of Rheumatology, *28*(7), 1573–1576. PMID: 11469464

Li, R., Li, Y., Zhang, J., Liu, Q., Wu, T., Zhou, J., Huang, H., Tang, Q., Huang, C., Huang, Y., Zhang, Z., Zhang, G., Zhao, Y., Ma, L., Feng, Y., Mo, L., Han, M. und He, J. (2020). Targeted delivery of celastrol to renal interstitial myofibroblasts using fibronectin-binding liposomes attenuates renal fibrosis and reduces systemic toxicity. *Journal of Controlled Release*, *320*, 32–44. doi: 10.1016/j.jconrel.2020.01.017

Li, Y., Huang, J., Guo, M. und Zuo, X. (2015). MicroRNAs regulating signaling pathways: potential biomarkers in systemic sclerosis. *Genomics, Proteomics & Bioinformatics*, *13*(4), 234–241. doi: 10.1016/j.gpb.2015.07.001

Li, Y., Jiang, D., Liang, J., Meltzer, E. B., Gray, A., Miura, R., Wogensen, L., Yamaguchi, Y. und Noble, P. W. (2011). Severe lung fibrosis requires an invasive fibroblast phenotype regulated by hyaluronan and CD44. *Journal of Experimental Medicine*, *208*(7), 1459–1471. doi: 10.1084/jem.20102510

Lillien, L. (1995). Changes in retinal cell fate induced by overexpression of EGF receptor. *Nature*, *377*(6545), 158–161. doi: 10.1038/377158a0

Liu, J., Dai, W. und Hahn, J. (2014). Mathematical modeling and analysis of crosstalk between MAPK pathway and Smad-dependent TGF-β signal transduction. *Processes*, *2*(3), 570–595. doi: 10.3390/pr2030570

Liu, R.-H., Ning, B., Ma, X.-E., Gong, W.-M. und Jia, T.-H. (2016). Regulatory roles of microRNA-21 in fibrosis through interaction with diverse pathways (Review). *Molecular Medicine Reports*, *13*(3), 2359–2366. doi: 10.3892/mmr.2016.4834

Lu, N., Carracedo, S., Ranta, J., Heuchel, R., Soininen, R. und Gullberg, D. (2010). The human α11 integrin promoter drives fibroblast-restricted expression in vivo and is regulated by TGF-β1 in a Smad- and Sp1-dependent manner. *Matrix Biology*, *29*(3), 166–176. doi: 10.1016/j.matbio.2009.11.003

Lucarelli, P., Schilling, M., Kreutz, C., Vlasov, A., Boehm, M. E., Iwamoto, N., Steiert, B., Lattermann, S., Wäsch, M., Stepath, M., Matter, M. S., Heikenwälder, M., Hoffmann, K., Deharde, D., Damm, G., Seehofer, D., Muciek, M., Gretz, N., Lehmann, W. D., Timmer, J. und Klingmüller, U. (2018). Resolving the combinatorial complexity of Smad protein complex formation and its link to gene expression. *Cell Systems*, *6*(1), 75-89.e11. doi: 10.1016/j.cels.2017.11.010

Ly, T.-D., Kleine, A., Fischer, B., Schmidt, V., Hendig, D., Kuhn, J., Knabbe, C. und Faust, I. (2020a). Identification of putative non-substrate-based XT-I inhibitors by natural product library screening. *Biomolecules*, *10*(10), 1467. doi: 10.3390/biom10101467

Ly, T.-D., Kleine, A., Plümers, R., Fischer, B., Schmidt, V., Hendig, D., Distler, J. H. W., Kuhn, J., Knabbe, C. und Faust, I. (eingereicht). Cytokine-mediated induction of human xylosyltransferase-I in systemic sclerosis skin fibroblasts. *Biochemical and Biophysical Research Communications*.

Ly, T.-D., Plümers, R., Fischer, B., Schmidt, V., Hendig, D., Kuhn, J., Knabbe, C. und Faust, I. (2020b). Activin A-mediated regulation of XT-I in human skin fibroblasts. *Biomolecules*, *10*(4), 609. doi: 10.3390/biom10040609

Ly, T.-D., Riedel, L., Fischer, B., Schmidt, V., Hendig, D., Distler, J., Kuhn, J., Knabbe, C. und Faust, I. (2020c). MicroRNA-145 mediates xylosyltransferase-I induction in myofibroblasts via

suppression of transcription factor KLF4. *Biochemical and Biophysical Research Communications*, 1001–1006. doi: 10.1016/j.bbrc.2019.12.120

Mack, M. (2018). Inflammation and fibrosis. *Matrix Biology*, *68–69*, 106–121. doi: 10.1016/j.matbio.2017.11.010

Magnant, J., de Monte, M., Guilmot, J.-L., Lasfargues, G., Diot, P., Asquier, E., Degenne, D., Boissinot, E. und Diot, E. (2005). Relationship between occupational risk factors and severity markers of systemic sclerosis. *The Journal of Rheumatology*, *32*(9), 1713–1718. PMID: 16142866

Martínez-Godínez, M. A., Cruz-Domínguez, M. P., Jara, L. J., Domínguez-López, A., Jarillo-Luna, R. A., Vera-Lastra, O., Montes-Cortes, D. H., Campos-Rodríguez, R., López-Sánchez, D. M., Mejía-Barradas, C. M., Castelán-Chávez, E. E. und Miliar-García, A. (2015). Expression of NLRP3 inflammasome, cytokines and vascular mediators in the skin of systemic sclerosis patients. *The Israel Medical Association journal: IMAJ*, *17*(1), 5–10. PMID: 25739168

Massagué, J. und Chen, Y. G. (2000). Controlling TGF-beta signaling. *Genes & Development*, *14*(6), 627–644. doi: 10.1101/gad.14.6.627

Maurer, B., Stanczyk, J., Jüngel, A., Akhmetshina, A., Trenkmann, M., Brock, M., Kowal-Bielecka, O., Gay, R. E., Michel, B. A., Distler, J. H. W., Gay, S. und Distler, O. (2010). MicroRNA-29, a key regulator of collagen expression in systemic sclerosis. *Arthritis & Rheumatism*, *62*(6), 1733–1743. doi: 10.1002/art.27443

Meng, E. C., Pettersen, E. F., Couch, G. S., Huang, C. C. und Ferrin, T. E. (2006). Tools for integrated sequence-structure analysis with UCSF Chimera. *BMC Bioinformatics*, *7*(1), 339. doi: 10.1186/1471-2105-7-339

Meurer, S. K. und Weiskirchen, R. (2018). Usage of mitogen-activated protein kinase small molecule inhibitors: more than just inhibition! *Frontiers in Pharmacology*, *9*, 98. doi: 10.3389/fphar.2018.00098

Mia, M. M., Boersema, M. und Bank, R. A. (2014). Interleukin-1β attenuates myofibroblast formation and extracellular matrix production in dermal and lung fibroblasts exposed to transforming growth factor-β1. *PLoS ONE*, *9*(3), e91559. doi: 10.1371/journal.pone.0091559

Mikami, T. und Kitagawa, H. (2013). Biosynthesis and function of chondroitin sulfate. *Biochimica et Biophysica Acta (BBA) - General Subjects*, *1830*(10), 4719–4733. doi: 10.1016/j.bbagen.2013.06.006

Mishra, S., Deng, J. J., Gowda, P. S., Rao, M. K., Lin, C.-L., Chen, C. L., Huang, T. und Sun, L.-Z. (2014). Androgen receptor and microRNA-21 axis downregulates transforming growth factor beta receptor II (TGFBR2) expression in prostate cancer. *Oncogene*, *33*(31), 4097–4106. doi: 10.1038/onc.2013.374

Mori, Y., Chen, S.-J. und Varga, J. (2003). Expression and regulation of intracellular SMAD signaling in scleroderma skin fibroblasts. *Arthritis & Rheumatism*, *48*(7), 1964–1978. doi: 10.1002/art.11157

Mosser, D. M. und Edwards, J. P. (2008). Exploring the full spectrum of macrophage activation. *Nature Reviews Immunology*, *8*(12), 958–969. doi: 10.1038/nri2448

Müller, B., Prante, C., Kleesiek, K., Götting, C. (2009). Identification and characterization of the human xylosyltransferase I gene promoter region. *Journal of Biological Chemistry*, *284*(45), 30775–30782. doi: 10.1074/jbc.M109.016592

Müller, B., Prante, C., Knabbe, C., Kleesiek, K. und Götting, C. (2013). First identification and functional analysis of the human xylosyltransferase II promoter. *Glycoconjugate Journal*, *30*(3), 237–245. doi: 10.1007/s10719-012-9439-5

Müller, S., Disse, J., Schöttler, M., Schön, S., Prante, C., Brinkmann, T., Kuhn, J., Kleesiek, K. und Götting, C. (2006). Human xylosyltransferase I and N-terminal truncated forms: functional characterization of the core enzyme. *Biochemical Journal*, *394*(1), 163–171. doi: 10.1042/BJ20051606

Müller, S., Schöttler, M., Schön, S., Prante, C., Brinkmann, T., Kuhn, J., Götting, C. und Kleesiek, K. (2005). Human xylosyltransferase I: functional and biochemical characterization of cysteine residues required for enzymic activity. *Biochemical Journal*, *386*(2), 227–236. doi: 10.1042/BJ20041206

Murdaca, G., Contatore, M., Gulli, R., Mandich, P. und Puppo, F. (2016). Genetic factors and systemic sclerosis. *Autoimmunity Reviews*, *15*(5), 427–432. doi: 10.1016/j.autrev.2016.01.016

Ng, S. W., Chan, Y., Chellappan, D. K., Madheswaran, T., Zeeshan, F., Chan, Y. L., Collet, T., Gupta, G., Oliver, B. G., Wark, P., Hansbro, N., Hsu, A., Hansbro, P. M., Dua, K. und Panneerselvam, J. (2019). Molecular modulators of celastrol as the keystones for its diverse pharmacological activities. *Biomedicine & Pharmacotherapy*, *109*, 1785–1792. doi: 10.1016/j.biopha.2018.11.051

Ogawa, K., Funaba, M., Chen, Y. und Tsujimoto, M. (2006). Activin A functions as a TH2 cytokine in the promotion of the alternative activation of macrophages. *The Journal of Immunology*, *177*(10), 6787–6794. doi: 10.4049/jimmunol.177.10.6787

Oida, T. und Weiner, H. L. (2010). Depletion of TGF-β from fetal bovine serum. *Journal of Immunological Methods*, *362*(1–2), 195–198. doi: 10.1016/j.jim.2010.09.008

O'Reilly, S. (2016). MicroRNAs in fibrosis: opportunities and challenges. *Arthritis Research & Therapy*, *18*(1), 11. doi: 10.1186/s13075-016-0929-x

Papachristou, D. J., Batistatou, A., Sykiotis, G. P., Varakis, I. und Papavassiliou, A. G. (2003). Activation of the JNK–AP-1 signal transduction pathway is associated with pathogenesis and progression of human osteosarcomas. *Bone*, *32*(4), 364–371. doi: 10.1016/S8756-3282(03)00026-7

Pattanaik, D., Brown, M., Postlethwaite, B. C. und Postlethwaite, A. E. (2015). Pathogenesis of systemic sclerosis. *Frontiers in Immunology*, *6*. doi: 10.3389/fimmu.2015.00272

Pence, H. E. und Williams, A. (2010). ChemSpider: an online chemical information resource. *Journal of Chemical Education*, *87*(11), 1123–1124. doi: 10.1021/ed100697w

Pettersen, E. F., Goddard, T. D., Huang, C. C., Couch, G. S., Greenblatt, D. M., Meng, E. C. und Ferrin, T. E. (2004). UCSF Chimera - a visualization system for exploratory research and analysis. *Journal of Computational Chemistry*, *25*(13), 1605–1612. doi: 10.1002/jcc.20084

Pönighaus, C., Ambrosius, M., Casanova, J. C., Prante, C., Kuhn, J., Esko, J. D., Kleesiek, K. und Götting, C. (2007). Human xylosyltransferase II is involved in the biosynthesis of the uniform tetrasaccharide linkage region in chondroitin sulfate and heparan sulfate proteoglycans. *Journal of Biological Chemistry*, *282*(8), 5201–5206. doi: 10.1074/jbc.M611665200

Pönighaus, C., Kuhn, J., Kleesiek, K. und Götting, C. (2010). Involvement of a cysteine protease in the secretion process of human xylosyltransferase I. *Glycoconjugate Journal*, *27*(3), 359–366.

doi: 10.1007/s10719-010-9283-4

Prante, C., Bieback, K., Funke, C., Schön, S., Kern, S., Kuhn, J., Gastens, M., Kleesiek, K. und Götting, C. (2006). The formation of extracellular matrix during chondrogenic differentiation of mesenchymal stem cells correlates with increased levels of xylosyltransferase I. *Stem Cells*, *24*(10), 2252–2261. doi: 10.1634/stemcells.2005-0508

Prante, C., Milting, H., Kassner, A., Farr, M., Ambrosius, M., Schön, S., Seidler, D. G., Banayosy, A. E., Körfer, R., Kuhn, J., Kleesiek, K. und Götting, C. (2007). Transforming growth factor β1-regulated xylosyltransferase I activity in human cardiac fibroblasts and its impact for myocardial remodeling. *Journal of Biological Chemistry*, *282*(36), 26441–26449. doi: 10.1074/jbc.M702299200

Prydz, K. und Dalen, K. T. (2000). Synthesis and sorting of proteoglycans. *Journal of Cell Science*, *113 Pt 2*, 193–205.

Punta, M., Coggill, P. C., Eberhardt, R. Y., Mistry, J., Tate, J., Boursnell, C., Pang, N., Forslund, K., Ceric, G., Clements, J., Heger, A., Holm, L., Sonnhammer, E. L. L., Eddy, S. R., Bateman, A. und Finn, R. D. (2012). The Pfam protein families database. *Nucleic Acids Research*, *40*(D1), D290–D301. doi: 10.1093/nar/gkr1065

Ratuszny, D., Gras, C., Bajor, A., Börger, A.-K., Pielen, A., Börgel, M., Framme, C., Blasczyk, R. und Figueiredo, C. (2015). miR-145 is a promising therapeutic target to prevent cornea scarring. *Human Gene Therapy*, *26*(10), 698–707. doi: 10.1089/hum.2014.151

Riedel, L., Fischer, B., Ly, T.-D., Hendig, D., Kuhn, J., Knabbe, C. und Faust, I. (2018). MicroRNA-29b mediates fibrotic induction of human xylosyltransferase-I in human dermal fibroblasts via the Sp1 pathway. *Scientific Reports*, *8*(1), 17779. doi: 10.1038/s41598-018-36217-2

Robinson, H. C., Telser, A. und Dorfman, A. (1966). Studies on biosynthesis of the linkage region of chondroitin sulfate-protein complex. *Proceedings of the National Academy of Sciences*, *56*(6), 1859–1866. doi: 10.1073/pnas.56.6.1859

Roch, C., Kuhn, J., Kleesiek, K. und Götting, C. (2010). Differences in gene expression of human xylosyltransferases and determination of acceptor specificities for various proteoglycans. *Biochemical and Biophysical Research Communications*, *391*(1), 685–691. doi: 10.1016/j.bbrc.2009.11.121

Rodnan, G. P. (1962). Progressive systemic sclerosis sine scleroderma. *JAMA*, *180*(8), 665. doi: 10.1001/jama.1962.03050210027006

van Rooij, E., Sutherland, L. B., Thatcher, J. E., DiMaio, J. M., Naseem, R. H., Marshall, W. S., Hill, J. A. und Olson, E. N. (2008). Dysregulation of microRNAs after myocardial infarction reveals a role of miR-29 in cardiac fibrosis. *Proceedings of the National Academy of Sciences*, *105*(35), 13027–13032. doi: 10.1073/pnas.0805038105

Ross, K. R., Corey, D. A., Dunn, J. M. und Kelley, T. J. (2007). SMAD3 expression is regulated by mitogen-activated protein kinase kinase-1 in epithelial and smooth muscle cells. *Cellular Signalling*, *19*(5), 923–931. doi: 10.1016/j.cellsig.2006.11.008

Rostam, M. A., Kamato, D., Piva, T. J., Zheng, W., Little, P. J. und Osman, N. (2016). The role of specific Smad linker region phosphorylation in TGF-β mediated expression of glycosaminoglycan synthesizing enzymes in vascular smooth muscle. *Cellular Signalling*, *28*(8), 956–966. doi: 10.1016/j.cellsig.2016.05.002

Schön, S., Prante, C., Bahr, C., Kuhn, J., Kleesiek, K. und Götting, C. (2006). Cloning and recombinant expression of active full-length xylosyltransferase I (XT-I) and characterization of subcellular localization of XT-I and XT-II. *Journal of Biological Chemistry*, *281*(20), 14224–14231. doi: 10.1074/jbc.M510690200

Sticherling, M. (2012). Systemic sclerosis - dermatological aspects. Part 1: Pathogenesis, epidemiology, clinical findings. *JDDG: Journal der Deutschen Dermatologischen Gesellschaft*, *10*(10), 705–716. doi: 10.1111/j.1610-0387.2012.07999.x

Stochmal, A., Czuwara, J., Trojanowska, M. und Rudnicka, L. (2020). Antinuclear antibodies in systemic sclerosis: an update. *Clinical Reviews in Allergy & Immunology*, *58*(1), 40–51. doi: 10.1007/s12016-018-8718-8

Stoolmiller, A. C., Horwitz, A. L., Dorfman, A. und Kennedy, J. P. (1972). Biosynthesis of the chondroitin sulfate proteoglycan. *Journal of Biological Chemistry*, *247*(11), 3525–3532. doi: 10.1016/S0021-9258(19)45172-7

Sun, Z., Yu, S., Chen, S., Liu, H. und Chen, Z. (2019). SP1 regulates KLF4 via SP1 binding motif governed by DNA methylation during odontoblastic differentiation of human dental pulp cells. *Journal of Cellular Biochemistry*, *120*(9), 14688–14699. doi: 10.1002/jcb.28730

Takagi, K., Kawaguchi, Y., Kawamoto, M., Ota, Y., Tochimoto, A., Gono, T., Katsumata, Y., Takagi, M., Hara, M. und Yamanaka, H. (2011). Activation of the activin A-ALK-Smad pathway in systemic sclerosis. *Journal of Autoimmunity*, *36*(3–4), 181–188. doi: 10.1016/j.jaut.2010.09.004

Tang, M., Cao, X., Zhang, K., Li, Y., Zheng, Q., Li, G., He, Q., Li, S., Xu, G. und Zhang, K. (2018). Celastrol alleviates renal fibrosis by upregulating cannabinoid receptor 2 expression. *Cell Death & Disease*, *9*(6), 601. doi: 10.1038/s41419-018-0666-y

Theis, T., Yoo, M., Park, C. S., Chen, J., Kügler, S., Gibbs, K. M. und Schachner, M. (2017). Lentiviral delivery of miR-133b improves functional recovery after spinal cord injury in mice. *Molecular Neurobiology*, *54*(6), 4659–4671. doi: 10.1007/s12035-016-0007-z

Trott, O. und Olson, A. J. (2009). AutoDock Vina: improving the speed and accuracy of docking with a new scoring function, efficient optimization, and multithreading. *Journal of Computational Chemistry*, 31(2): 455–461. doi:10.1002/jcc.21334

Tsai, C.-Y., Hsieh, S.-C., Wu, T.-H., Li, K.-J., Shen, C.-Y., Liao, H.-T., Wu, C.-H., Kuo, Y.-M., Lu, C.-S. und Yu, C.-L. (2020). Pathogenic roles of autoantibodies and aberrant epigenetic regulation of immune and connective tissue cells in the tissue fibrosis of patients with systemic sclerosis. *International Journal of Molecular Sciences*, *21*(9), 3069. doi: 10.3390/ijms21093069

Varga, J. (2002). Scleroderma and Smads: Dysfunctional Smad family dynamics culminating in fibrosis. *Arthritis & Rheumatism*, *46*(7), 1703–1713. doi: 10.1002/art.10413

Voglmeir, J., Voglauer, R. und Wilson, I. B. H. (2007). XT-II, the second isoform of human peptide *O*-xylosyltransferase, displays enzymatic activity. *Journal of Biological Chemistry*, *282*(9), 5984–5990. doi: 10.1074/jbc.M608087200

Wang, A., de la Motte, C., Lauer, M. und Hascall, V. (2011). Hyaluronan matrices in pathobiological processes: hyaluronan matrices in pathobiological processes. *FEBS Journal*, *278*(9), 1412–1418. doi: 10.1111/j.1742-4658.2011.08069.x

Wang, W., Liu, R., Su, Y., Li, H., Xie, W. und Ning, B. (2018). MicroRNA-21-5p mediates TGF-

β-regulated fibrogenic activation of spinal fibroblasts and the formation of fibrotic scars after spinal cord injury. *International Journal of Biological Sciences*, *14*(2), 178–188. doi: 10.7150/ijbs.24074

Wang, Y., Li, C., Gu, J., Chen, C., Duanmu, J., Miao, J., Yao, W., Tao, J., Tu, M., Xiong, B., Zhao, L. und Liu, Z. (2020). Celastrol exerts anti-inflammatory effect in liver fibrosis via activation of AMPK-SIRT3 signalling. *Journal of Cellular and Molecular Medicine*, *24*(1), 941–953. doi: 10.1111/jcmm.14805

Warnock, D. W. (1991). Amphotericin B: an introduction. *Journal of Antimicrobial Chemotherapy*, *28*(suppl B), 27–38. doi: 10.1093/jac/28.suppl_B.27

Wilson, B. A. P., Thornburg, C. C., Henrich, C. J., Grkovic, T. und O'Keefe, B. R. (2020). Creating and screening natural product libraries. *Natural Product Reports*, *37*(7), 893–918. doi: 10.1039/C9NP00068B

Wilson, I. B. H. (2004). The never-ending story of peptide *O*-xylosyltransferase. *Cellular and Molecular Life Sciences (CMLS)*, *61*(7–8), 794–809. doi: 10.1007/s00018-003-3278-2

Wynn, T. (2008). Cellular and molecular mechanisms of fibrosis. *The Journal of Pathology*, *214*(2), 199–210. doi: 10.1002/path.2277

Wynn, T. A. (2004). Fibrotic disease and the T(H)1/T(H)2 paradigm. *Nature Reviews. Immunology*, *4*(8), 583–594. doi: 10.1038/nri1412

Wynn, T. A. und Ramalingam, T. R. (2012). Mechanisms of fibrosis: therapeutic translation for fibrotic disease. *Nature Medicine*, *18*(7), 1028–1040. doi: 10.1038/nm.2807

Xie, X.-Q. S. (2010). Exploiting PubChem for virtual screening. *Expert Opinion on Drug Discovery*, *5*(12), 1205–1220. doi: 10.1517/17460441.2010.524924

Xu, D., Mu, R. und Wei, X. (2019). The roles of IL-1 family cytokines in the pathogenesis of systemic sclerosis. *Frontiers in Immunology*, *10*, 2025. doi: 10.3389/fimmu.2019.02025

Yamashita, S. (2004). Activin A is a potent activator of renal interstitial fibroblasts. *Journal of the American Society of Nephrology*, *15*(1), 91–101. doi: 10.1097/01.ASN.0000103225.68136.E6

Yan, X. und Chen, Y.-G. (2011). Smad7: not only a regulator, but also a cross-talk mediator of TGF-β signalling. *Biochemical Journal*, *434*(1), 1–10. doi: 10.1042/BJ20101827

Yanagishita, M. (1993). Function of proteoglycans in the extracellular matrix. *Pathology International*, *43*(6), 283–293. doi: 10.1111/j.1440-1827.1993.tb02569.x

Yang, S., Cui, H., Xie, N., Icyuz, M., Banerjee, S., Antony, V. B., Abraham, E., Thannickal, V. J. und Liu, G. (2013). miR-145 regulates myofibroblast differentiation and lung fibrosis. *The FASEB Journal*, *27*(6), 2382–2391. doi: 10.1096/fj.12-219493

Ye, W., Zhou, J., Markova, D. Z., Tian, Y., Li, J., Anderson, D. G., Shapiro, I. M. und Risbud, M. V. (2014). Xylosyltransferase-1 expression is refractory to inhibition by the inflammatory cytokines tumor necrosis factor α and IL-1β in nucleus pulposus cells: novel regulation by AP-1, Sp1, and Sp3. *American Journal of Pathology*, *185*(2), 485–495. doi: 10.1016/j.ajpath.2014.09.021

Yu, Y., Kanwar, S. S., Patel, B. B., Oh, P.-S., Nautiyal, J., Sarkar, F. H. und Majumdar, A. P. N. (2012). MicroRNA-21 induces stemness by downregulating transforming growth factor beta receptor 2 (TGFR2) in colon cancer cells. *Carcinogenesis*, *33*(1), 68–76. doi: 10.1093/carcin/bgr246

Yuan, J., Chen, H., Ge, D., Xu, Y., Xu, H., Yang, Y., Gu, M., Zhou, Y., Zhu, J., Ge, T., Chen, Q., Gao, Y., Wang, Y., Li, X. und Zhao, Y. (2017). miR-21 promotes cardiac fibrosis after myocardial infarction via targeting Smad7. *Cellular Physiology and Biochemistry*, *42*(6), 2207–2219. doi: 10.1159/000479995

Zhang, L. (2005). Integrated approaches for discovering novel drugs from microbial natural products. In L. Zhang und A.L. Demain (Hrsg.), *Natural Products* (S. 33–55). Totowa, NJ: Humana Press. doi: 10.1007/978-1-59259-976-9_2

Zhang, W., Shields, J. M., Sogawa, K., Fujii-Kuriyama, Y. und Yang, V. W. (1998). The gut-enriched Krüppel-like factor suppresses the activity of the *CYP1A1* promoter in an SP1-dependent fashion. *Journal of Biological Chemistry*, *273*(28), 17917–17925. doi: 10.1074/jbc.273.28.17917

Zhao, X., Psarianos, P., Ghoraie, L. S., Yip, K., Goldstein, D., Gilbert, R., Witterick, I., Pang, H., Hussain, A., Lee, J. H., Williams, J., Bratman, S. V., Ailles, L., Haibe-Kains, B. und Liu, F.-F. (2019). Metabolic regulation of dermal fibroblasts contributes to skin extracellular matrix homeostasis and fibrosis. *Nature Metabolism*, *1*(1), 147–157. doi: 10.1038/s42255-018-0008-5

Zhou, R., Wang, C., Wen, C. und Wang, D. (2017). miR-21 promotes collagen production in keloid via Smad7. *Burns*, *43*(3), 555–561. doi: 10.1016/j.burns.2016.09.013

Zhu, H., Li, Y., Qu, S., Luo, H., Zhou, Y., Wang, Y., Zhao, H., You, Y., Xiao, X. und Zuo, X. (2012). MicroRNA expression abnormalities in limited cutaneous scleroderma and diffuse cutaneous scleroderma. *Journal of Clinical Immunology*, *32*(3), 514–522. doi: 10.1007/s10875-011-9647-y

Zhu, H., Luo, H., Li, Y., Zhou, Y., Jiang, Y., Chai, J., Xiao, X., You, Y. und Zuo, X. (2013a). MicroRNA-21 in scleroderma fibrosis and its function in TGF-β-regulated fibrosis-related genes expression. *Journal of Clinical Immunology*, *33*(6), 1100–1109. doi: 10.1007/s10875-013-9896-z

Zhu, H., Luo, H. und Zuo, X. (2013b). MicroRNAs: their involvement in fibrosis pathogenesis and use as diagnostic biomarkers in scleroderma. *Experimental & Molecular Medicine*, *45*(9), e41–e41. doi: 10.1038/emm.2013.71

Zhu, H., Yan, X., Zhang, M., Ji, F. und Wang, S. (2019). miR-21-5p protects IL-1β-induced human chondrocytes from degradation. *Journal of Orthopaedic Surgery and Research*, *14*(1), 118. doi: 10.1186/s13018-019-1160-7

Abkürzungsverzeichnis

3‘-UTR	3‘-untranslatierte Region
ACTA2	α-SMA-Gen
ACVR1B	*Activin receptor-type-IB*
ALK	*Activin receptor-like kinase*
AP-1	Aktivatorprotein-1
AS	Aminosäure
ATP	Adenosintriphosphat
CHO	*Chinese hamster ovary*
COL1A1	Alpha-1-Typ-I-Kollagen-Gen
CS	Chondroitinsulfat
DS	Dermatansulfat
ECM	Extrazelluläre Matrix
EGR	*Early growth response factor*
ERK	*Extracellular signal-regulated kinase*
GAG	Glykosaminoglykan
Gal	Galaktose
GalNAc	*N*-Acetylgalaktosamin
GalT-I	Galaktosyltransferase-I
GalT-II	Galaktosyltransferase-II
GlcA	Glukuronsäure
GlcAT-I	Glukuronyltransferase-I
GlcNAc	*N*-Actetylglukosamin
HA	Hyaluronan
HS	Heparansulfat
IdoA	Iduronsäure
IL	Interleukin
INF-γ	*Interferon-γ*
I-SMAD	Inhibitorische SMAD
JNK	c-*Jun N-terminal kinase*
KLF	*Krueppel like transcription factor*

MAPK	*Mitogen-activated protein kinase*
MH	*Mad-homology*
miRNA	MicroRNA
NHDF	Normale humane Dermalfibroblasten
PG	Proteoglykan
R-SMAD	Rezeptor-aktivierte SMAD
SMAD	*Small mothers against decapentaplegic*
SMAD2	SMAD2-Gen
SMAD3	SMAD3-Gen
SMAD7	SMAD7-Gen
SNV	*Single nucleotide variaton*
SP1	*Specifity protein 1*
SSc	Systemische Sklerodermie
SScF	SSc-Fibroblasten
TF	Transkriptionsfaktor
TGFBR	*Transforming growth factor beta receptor*
TGFBR2	TGFBR2-Gen
TGF-β1	*Transforming growth factor-β1*
TGFB1	TGF-β1-Gen
T_H-Zellen	T-Helferzellen
TNF-α	*Tumor necrosis factor-α*
UPLC-ESI-MS/MS	*Ultra-performance liquid chromatography-electrospray ionization-tandem mass spectrometry*
XT	Xylosyltransferase
Xyl	Xylose
XYLT1	XT-I-Gen
XYLT2	XT-II-Gen
α-SMA	α-Glattmuskelaktin

Publikationen und Kongressbeiträge

Publikationen in *peer-review* Zeitschriften

1. Riedel, L., Fischer, B., **Ly, T.-D.**, Hendig, D., Kuhn, J., Knabbe, C. und Faust, I. (2018). MicroRNA-29b mediates fibrotic induction of human xylosyltransferase-I in human dermal fibroblasts via the Sp1 pathway. *Scientific Reports*, 8(1), 17779. doi: 10.1038/s41598-018-36217-2

2. Fischer, B., **Ly, T.-D.**, Hendig, D., Kuhn, J., Pécheur, E.-I., Reungoat, E., Knabbe, C. und Faust, I. (2019). First description of a compensatory xylosyltransferase I induction observed after an antifibrotic UDP-treatment of normal human dermal fibroblasts. *Biochemical and Biophysical Research Communications*, 512(1), 7–13. doi: 10.1016/j.bbrc.2019.02.150

3. Fischer, B., **Ly, T.-D.**, Schmidt, V., Hendig, D., Kuhn, J., Knabbe, C. und Faust, I. (2020). Xylosyltransferase-deficient human HEK293 cells show a strongly reduced proliferation capacity and viability. *Biochemical and Biophysical Research Communications*, 521(2), 507–513. doi: 10.1016/j.bbrc.2019.10.148

4. **Ly, T.-D.**, Riedel, L., Fischer, B., Schmidt, V., Hendig, D., Distler, J., Kuhn, J., Knabbe, C. und Faust, I. (2020). MicroRNA-145 mediates xylosyltransferase-I induction in myofibroblasts via suppression of transcription factor KLF4. *Biochemical and Biophysical Research Communications*, 1001–1006. doi: 10.1016/j.bbrc.2019.12.120

5. **Ly, T.-D.**, Plümers, R., Fischer, B., Schmidt, V., Hendig, D., Kuhn, J., Knabbe, C. und Faust, I. (2020). Activin A-mediated regulation of XT-I in human skin fibroblasts. *Biomolecules*, 10(4), 609. doi: 10.3390/biom10040609

6. **Ly, T.-D.**, Kleine, A., Fischer, B., Schmidt, V., Hendig, D., Kuhn, J., Knabbe, C. und Faust, I. (2020). Identification of putative non-substrate-based XT-I inhibitors by natural product library screening. *Biomolecules*, 10(10), 1467. doi: 10.3390/biom10101467

7. **Ly, T.-D.**, Kleine, A., Plümers, R., Fischer, B., Schmidt, V., Hendig, D., Distler, H. W. J., Kuhn, J., Knabbe, C. und Faust, I. (eingereicht). Cytokine-mediated induction of human xylosyltransferase-I in systemic sclerosis skin fibroblasts. *Biochemical and Biophysical Research Communications*.

8. Fischer, B., Kuhn, J., **Ly, T.-D.**, Schmidt, V., Kleine, A., Hendig, D., Knabbe, C. und Faust, I. (in Revision). Development of a xylosyltransferase-I-selective UPLC MS/MS activity assay using a specific acceptor peptide. *Biochimie*.

Die hier verwendete Nummerierung der Manuskripte entspricht der zeitlichen Abfolge der Manuskriptveröffentlichungen.

Posterpräsentationen und Kongressbeiträge

15. Jahrestagung der Deutschen Gesellschaft für Klinische Chemie und Laboratoriumsmedizin (2018), Mannheim

- **Posterpräsentation (P018)**

First insights into the senescence associated secretory phenotype and its possible role in pseudoxanthoma elasticum
*J. Tiemann[1]; T. Wagner[1]; **T.-D. Ly**[1]; B. Ibold[1]; O. Vanakker[2]; I. Faust[1]; C. Knabbe[1]; D. Hendig[1]*

- **Posterpräsentation (P019)**

A compound heterozygous XYLT1 deletion in dermal fibroblasts of a patient with short limb skeletal dysplasia leads to abnormal myofibroblast characteristics
*B. Fischer[1]; **T.-D. Ly**[1]; J. Kuhn[1]; D. Hendig[1]; C. Knabbe[1]; I. Faust[1]*

- **Posterpräsentation (P022)**

Regulation of xylosyltransferase I expression by activin A in human skin fibroblasts: signaling pathway and Inhibition of xylosyltransferase-I activity as new approach for the treatment of dermal fibrosis?
***T.-D. Ly**[1]; R. Plümers[1]; B. Fischer[1]; D. Hendig[1]; J. Kuhn[1]; C. Knabbe[1]; I. Faust[1]*

- **Posterpräsentation (P024)**

MicroRNA-29b mediates fibrotic induction of human xylosyltransferase-I
*L. Riedel[1]; B. Fischer[1]; **T.-D. Ly**[1]; D. Hendig[1]; J. Kuhn[1]; C. Knabbe[1]; I. Faust[1]*

Gordon Research Seminar und *Gordon Research Conference* „Tissue Repair and Regeneration" (2019), New London, USA

- **Posterpräsentation**

Activin A mediated regulation of xylosyltransferase-I in human skin fibroblasts and its underlying signaling pathway
***T.-D. Ly**[1]; R. Plümers[1]; B. Fischer[1]; D. Hendig[1]; J. Kuhn[1]; C. Knabbe[1]; I. Faust[1]*

- **Posterpräsentation**

MicroRNA-29b mediates fibrotic induction of human xylosyltransferase-I in human dermal fibroblasts via the Sp1 pathway
*I. Faust[1]; L. Riedel[1]; B. Fischer[1]; **T.-D. Ly**[1]; D. Hendig[1]; J. Kuhn[1]; C. Knabbe[1]*

---

[1] *Institut für Laboratoriums- und Transfusionsmedizin, Herz- und Diabeteszentrum Nordrhein-Westfalen, Universitätsklinik der Ruhr-Universität Bochum, Bad Oeynhausen, Germany*

[2] *Center for Medical Genetics, Ghent University Hospital, 9000 Ghent, Belgium, Center for Medical Genetics, Ghent, Belgium*

16. Jahrestagung der Deutschen Gesellschaft für Klinische Chemie und Laboratoriumsmedizin (2019), Magdeburg

- **Posterpräsentation (P033)**

Xylosyltransferase (XT) deficient human embryonic kidney 293 (HEK293) cells are not viable

*B. Fischer[1]; **T.-D. Ly**[1]; D. Hendig[1]; J. Kuhn[1]; C. Knabbe[1]; I. Faust[1]*

- **Posterpräsentation (P036)**

Evaluation of the effect of heparin, a xylosyltransferase inhibitor, on dermal myofibroblast differentiation

*V. Schmidt[1]; B. Fischer[1]; **T.-D. Ly**[1]; D. Hendig[1]; C. Knabbe[1]; I. Faust[1]*

- **Posterpräsentation (P064)**

Identification of a novel xylosyltransferase-I regulatory mechanism by miRNA-145 in dermal fibroblasts derived from systemic sclerosis patients

***T.-D. Ly**[1]; R. Plümers[1]; B. Fischer[1]; V. Schmidt[1]; D. Hendig[1]; J. Kuhn[1]; C. Knabbe[1]; I. Faust[1]*

[1] *Institut für Laboratoriums- und Transfusionsmedizin, Herz- und Diabeteszentrum Nordrhein-Westfalen, Universitätsklinik der Ruhr-Universität Bochum, Bad Oeynhausen, Germany*

Lebenslauf

Persönliche Daten

Name:	Thanh-Diep Ly
Geburtsdatum, Ort:	07.01.1993, Bad Soden-Salmünster
Staatsangehörigkeit:	Deutsch

Aktuelle Tätigkeit

Wissenschaftliche Mitarbeiterin im Herz- und Diabeteszentrum NRW (seit 11/2017):

Doktorarbeit bei Prof. Dr. med. Cornelius Knabbe am Institut für Laboratoriums- und Transfusionsmedizin, Bad Oeynhausen

Dissertation: „Untersuchungen zur Regulation der humanen Xylosyltransferase-I bei Fibrosen“

Hochschulbildung

Master in Biochemie an der Universität Bielefeld (2015 – 2017):

Masterarbeit: „Untersuchungen zur Inhibition der Fibrogenese durch Hemmung der Xylosyltransferase-Aktivität und Etablierung eines dreidimensionalen in vitro Hautmodells“

Abschluss November 2017: **M.Sc. Biochemie**

Biochemie 1-Fach Bachelor Universität Bielefeld (2012 – 2015):

Bachelorarbeit: „Isolierung und Kristallisation von His-YscY:MBP-YscXΔ31-Proteinkomplexvarianten“

Abschluss September 2015: **B.Sc. Biochemie**

Schulbildung

Integrierte Gesamtschule Enkenbach-Alsenborn, Rheinland-Pfalz (2003 – 2012):

Abschluss März 2012: **Allgemeine Hochschulreife**

Anhang

Anhang 1: Zusatzmaterial von Publikation I

Tabelle 1: Literaturangaben, Bearbeitungsstand und Angaben zum Eigenanteil (**P1**).

Titel	**Activin A-mediated regulation of XT-I in human skin fibroblasts**
Typ	Zeitschriftenartikel
Zeitschrift	*Biomolecules*
Bearbeitungsstand	Eingereicht am 09.03.2020; zur Publikation angenommen am 13.04.2020, online verfügbar am 14.04.2020
DOI	10.3390/biom10040609
Autoren	**Ly, T.-D**.; Plümers, R.; Fischer, B.; Schmidt, V.; Hendig, D.; Kuhn, J.; Knabbe, C.; Faust, I.
Eigenanteil in [%]	Konzeptionelle Gestaltung (80%); Datenaufbereitung (90%); Formalanalyse (100%); Experimentelle Durchführung (90%); Datenpräsentation (100%); Verfassen des ursprünglichen Manuskriptentwurfs und Editierung (100%)

Supplementary Materials

Figure S1 (A-D)

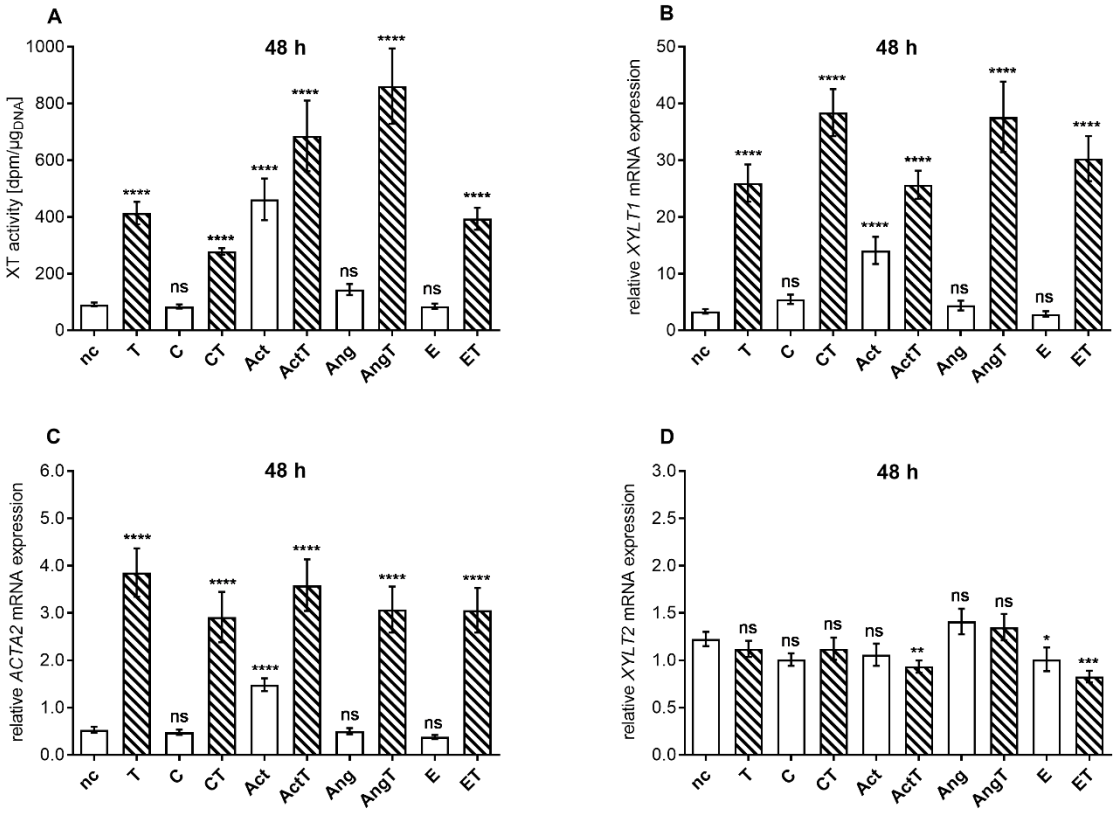

Figure S1. Various Cytokine and growth factor treatments of NHDF. Human primary fibroblasts (n = 4) were cultured the day before the experiment. Cells were serum-starved for 24 h and treated with vehicle (nc), activin A (Act; 50 µg/L), CTGF (C; 50 µg/L), angiotensin-II (Ang; 100 nmol/L), endothelin-1 (E; 100 nmol/L) alone or in combination with TGFβ1 (5 µg/L; T, CT, ActT, AngT, ET) for 48 h. (**A**) Extracellular XT activity was measured in cell supernatants by radiochemical enzyme assay and expressed as dpm per µg of total sample DNA. Relative (**B**) *XYLT1*, (**C**) *ACTA2* and (**D**) *XYLT2* mRNA expression levels were analysed by quantitative real-time PCR. Shown values are means ± SEM for three biological and three technical replicates per experiment. Mann-Whitney *U* test: not significant (ns), $P < 0.05$ (*), $P < 0.001$ (***), $P < 0.0001$ (****).

Figure S2 (A-C)

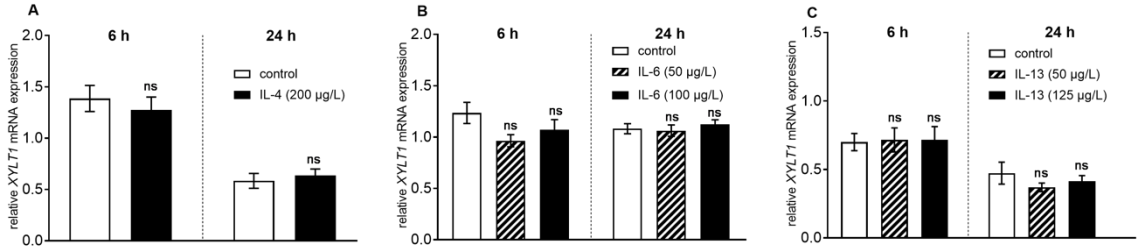

Figure S2. Interleukin treatments of NHDF. Human primary fibroblast cells were treated with (**A**) IL-4 (n = 3), (**B**) IL-6 (n = 2) or (**C**) IL-13 (n = 2) for 6 h and 24 h. Relative *XYLT1* mRNA expression levels

were analysed by quantitative real-time PCR. Shown values are means ± SEM for three biological and three technical replicates per experiment. Mann-Whitney *U* test: not significant (ns).

Figure S3 (A-D)

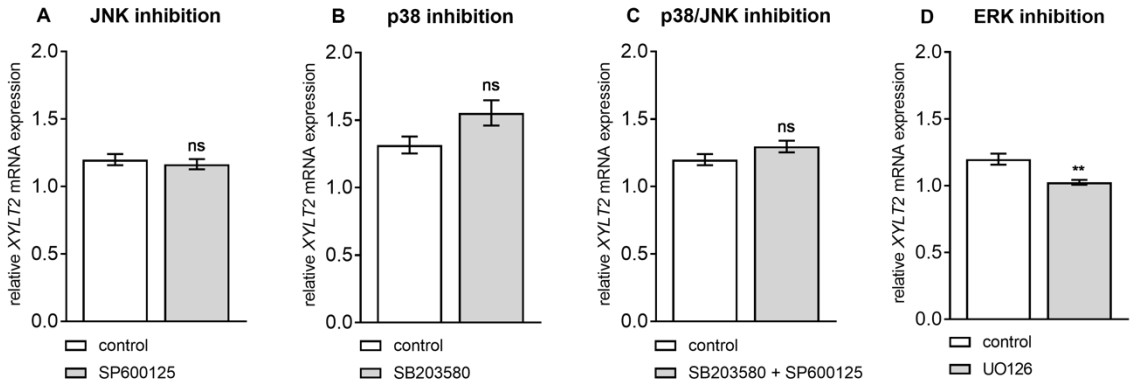

Figure S3. Inhibition of basal *XYLT2* mRNA expression by pharmacological inhibitors to MAPK JNK, p38 and ERK. Human primary fibroblast cells (n = 3) were cultured the day before the experiment. Cells were serum-starved for 24 h and treated with vehicle or (**A**) JNK inhibitor SP600125 (25 μmol/L), (**B**) p38 inhibitor SB203580 (10 μmol/L), (**C**) SP600125 (25 μmol/L) and SB203580 (10 μmol/L) or (**D**) ERK inhibitor UO126 (10 μmol/L) for 6 h. Relative mRNA expression level of *XYLT2* was analysed by qRT-PCR. Shown values are means ± SEM for three biological and three technical replicates per experiment. Mann-Whitney *U* test: not significant (ns), $P < 0.01$ (**).

Figure S4 (A-C)

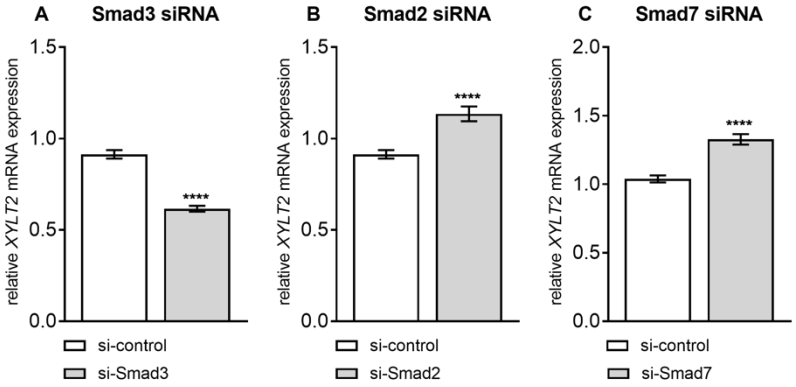

Figure S4. siRNA mediated Smads 2, 3 and 7 knockdowns. Human primary fibroblasts (n=3) were cultured for 24 h before transfection with a negative control siRNA (si-control, 50 or 100 nmol/L) or siRNA targeting against (**A**) Smad3 (si-Smad3, 50 nmol/L), (**B**) Smad2 (si-Smad2, 50 nmol/L) or (**C**) Smad7 (si-Smad7, 100 nmol/L). 24 h post-transfection cells were serum-starved for 16 h and maintained in serum-free media for additional 6 h. Relative *XYLT2* mRNA expression levels were analysed by qRT-PCR. Shown values are means ± SEM for three biological and three technical replicates per experiment. Mann-Whitney *U* test: $P < 0.0001$ (****).

Anhang 2: Zusatzmaterial von Publikation II

Tabelle 2: Literaturangaben, Bearbeitungsstand und Angaben zum Eigenanteil (**P2**).

Titel	**Cytokine-mediated induction of human Xylosyltransferase-I in systemic sclerosis skin fibroblasts**
Typ	Zeitschriftenartikel
Zeitschrift	*Biochemical and Biophysical Research Communications*
Bearbeitungsstand	Eingereicht am 14.01.2021
DOI	
Autoren	**Ly, T.-D.**; Kleine, A.; Plümers, R.; Fischer, B.; Schmidt, V.; Hendig, D.; Distler, H. W. J.; Kuhn, J.; Knabbe, C.; Faust, I.
Eigenanteil in [%]	Konzeptionelle Gestaltung (90%); Datenaufbereitung (80%); Formalanalyse (100%); Experimentelle Durchführung (60%); Datenpräsentation (100%); Verfassen des ursprünglichen Manuskriptentwurfs und Editierung (100%)

Supplementary Material

Figure S1

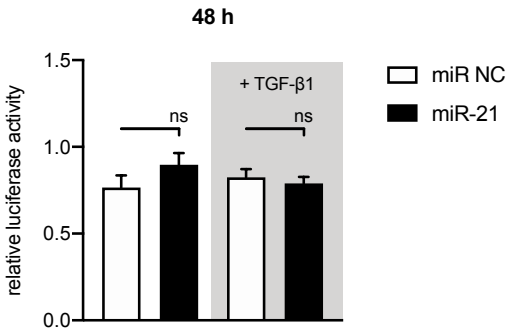

Fig. S1: Regulation of *XYLT1* expression is not mediated by direct miRNA-21 binding to the 3'-UTR. SW1353 cells (180,000 cells/well; 6-well-plate) were cultured for 24 h and simultaneously transfected with a miRNA-21 (miR-21) or miRNA negative control (miR NC) and the luciferase expressing reporter vectors containing the *XYLT1* 3′-UTR. Luciferase activities from the cell lysates were assayed 48 h post-transfection. Firefly luciferase activities were normalized to *Renilla* luciferase activities. Changes in relative luciferase activity resemble the putative interaction of miRNA-21 with the 3'-UTR of *XYLT1*. Values shown are means ±SEM for six biological replicates per experiment. The experiment was performed in presence and absence of TGF-β1 (10 µg/L, gray). Mann-Whitney *U* test: not significant (ns).

Table S1

Tab. S1: Primer sequences and annealing temperatures (T_A) used for qRT-PCR analysis.

Gene	Protein	Sequence	T_A (°C)
B2M	β2-microglobulin	5'-TGTGCTCGCGCTACTCTCTCTT-3' 5'-CGGATGGATGAAACCCAGACA-3'	63.0
RPL13A	ribosomal protein L13a	5'-CGGAAGGTGGTGGTCGTA-3' 5'-CTCGGGAAGGGTTGGTGT-3'	63.0
SDHA	succinate dehydrogenase complex subunit A	5'-AACTCGCTCTTGGACCTG-3' 5'-GAGTCGCAGTTCCGATGT-3'	63.0
TGFBR2	TGF-β receptor II	5'-GTTCAGAAGTCGGATGTGGAA-3' 5'-ACTTGACTGCACCGTTGTTG-3'	63.0
XYLT1	xylosyltransferase-I	5'-GAAGCCGTGGTGAATCAG-3' 5'-CGGTCAGCAAGGAAGTAG-3'	63.0

Table S2

Tab. S2: Target prediction analyses of the miRNA-21 (hsa-miR-21-5p) binding sites that are predicted to target *TGFBR2* using the computational algorithm TargetScan 7.2. Value ranges: Site types (8_{mer}>7_{mer}>$7_{mer\text{-}A1}$>6_{mer}; matching sites in the seed region), context ++ score (1 to −1; the more negative the score, the greater the repression).

Conserved sites	Predicted consequential pairing of target region (top) and miRNA (bottom)	Site type	Context ++ score
Position 206-212 of *TGFBR2* 3'-UTR	5' ...UGACAUUGUCAUAGG-AUAAGCUG...	7mer-m8	−0.1
hsa-miR-21-5p	3' AGUUGUAGUCAGACUAUUCGAU		
Position 5620-5626 of *TGFBR2* 3'-UTR	5' ...UCUUCCUAUUCUAAUUAAGCUAA...	7mer-A1	−0.04
hsa-miR-21-5p	3' AGUUGUAGUCAGACUAUUCGAU		

Anhang 3: Zusatzmaterial von Publikation III

Tabelle 3: Literaturangaben, Bearbeitungsstand und Angaben zum Eigenanteil (**P3**).

Titel	**MicroRNA-145 mediates xylosyltransferase-I induction in myofibroblasts via suppression of transcription factor KLF4**
Typ	Zeitschriftenartikel
Zeitschrift	*Biochemical and Biophysical Research Communications*
Bearbeitungsstand	Eingereicht am 03.12.2019; zur Publikation angenommen am 28.12.2019; online verfügbar am 20.01.2020
DOI	10.1016/j.bbrc.2019.12.120
Autoren	**Ly, T.-D**.; Riedel, L.; Fischer, B.; Schmidt, V.; Hendig, D.; Distler, J.; Kuhn, J.; Knabbe, C.; Faust, I.
Eigenanteil in [%]	Konzeptionelle Gestaltung (60%); Datenaufbereitung (70%); Formalanalyse (100%); Experimentelle Durchführung (70%); Datenpräsentation (100%); Verfassen des ursprünglichen Manuskriptentwurfs und Editierung (100%)

Supplementary Material

Figure S1

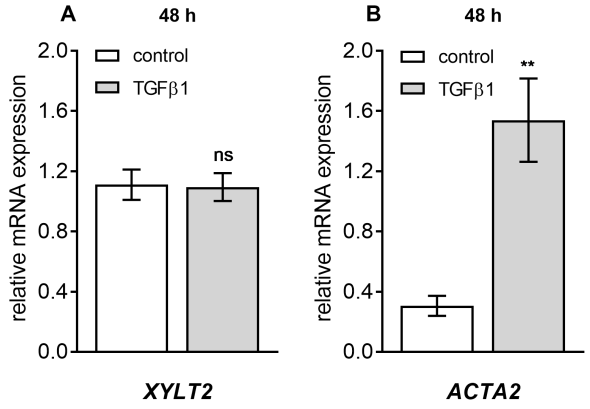

Fig. S1: Effect of TGFβ1 supplementation on *XYLT2 and ACTA2* mRNA expression. The NHDF (n=2) were cultured for 24 h before the experiment. Cells were serum-starved for 24 h and treated with TGFβ1 or vehicle for 48 h. Relative mRNA expression levels of (**A**) *XYLT2* and (**B**) *ACTA2* were analysed by qRT-PCR. Values shown are means ±SEM for three biological and three technical replicates per experiment. Mann-Whitney U test: not significant (ns), **P<0.01.

Figure S2

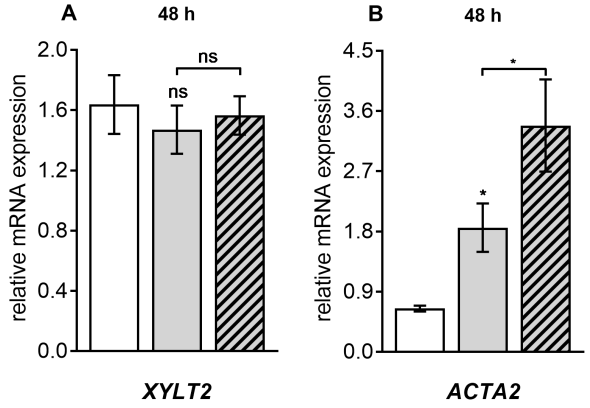

Fig. S2: Effect of miR-145 transfection on *XYLT2 and ACTA2* mRNA expression. The NHDF (n=2) were transfected with a miR-145 mimic (miR-145) or negative control miRNA mimic (miR control). Cells were stimulated 6 h post-transfection with TGFβ1 or vehicle for 24 h. Relative mRNA expression level of (**A**) *XYLT2* and (**B**) *ACTA2* were analysed by qRT-PCR. Values shown are means ±SEM for three biological and three technical replicates per experiment. Mann-Whitney U test: not significant (ns), *P<0.05, **P<0.01.

Figure S3

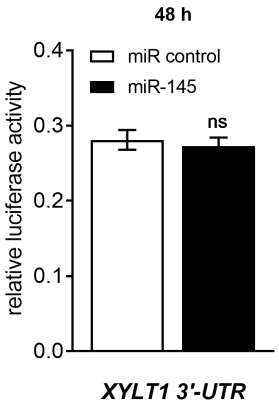

Fig. S3: Regulation of *XYLT1* expression is not mediated by direct miR-145 binding to the 3'UTR. SW1353 cells were cultured for 24 h and co-transfected with a miR-145 mimic (miR-145) or negative control miRNA mimic (miR control) and the firefly luciferase expressing reporter vector containing the *XYLT1* 3′UTR along with the *Renilla* luciferase expressing control vector. Luciferase activities from the cell lysates were assayed 48 h post-transfection. Firefly luciferase data were normalized to *Renilla* luciferase activity. Changes in the relative luciferase activity resemble the putative interaction of miR-145 with the 3'-UTR of *XYLT1*. Values shown are means ±SEM for six biological replicates per experiment. Mann-Whitney U test: not significant (ns).

Tab. S1: Primer sequences and annealing temperatures (T_A) used for qRT-PCR analysis.

Gene	Protein	Sequence	T_A (°C)
ACTA2	alpha-Smooth muscle actin (α-SMA)	5'-CGGAAGGTGGTGGTCGTA-3' 5'-CTCGGGAAGGGTTGGTGT-3'	59.0
KLF4	Krüppel-like factor 4 (KLF4)	5'-ACCCTGGGTCTTGAGGAAGTG-3' 5'-TCTTTGGCTTGGGCTCCTCTG-3'	63.0
RPL13A	ribosomal protein L13a (RPL13A)	5'-CGGAAGGTGGTGGTCGTA-3' 5'-CTCGGGAAGGGTTGGTGT-3'	63.0
SDHA	succinate dehydrogenase complex subunit A (SDHA)	5'-AACTCGCTCTTGGACCTG-3' 5'-GAGTCGCAGTTCCGATGT-3'	63.0

Tab. S2: Overview of selected experimental approved miR-145/KLF4 interactions reported in the literature.

Literature	Details
Minami et al. [27]	Luciferase assay showed the direct binding of miR-145 to the 3′-UTR of KLF4; overexpression of miR-145 decreased KLF4 protein expression in T24 and 253J B-V cells (Warburg effect)
Liu et al. [28]	Overexpression of miR-145 inhibited KLF4 in airway smooth muscle cells (asthma)
Men et al. [5]	Inhibition or overexpression of miR-145 effected KLF4 mRNA and protein levels in rat hepatic stellate cells
Barta et al. [6]	Inhibition of miR-145 in human dermal fibroblasts showed an upregulation of KLF4 (reprogramming of somatic cells to induced pluripotent stem cells)
Yeh et al. [29]	Overexpression and inhibitor experiments showed the differentiation of mesenchymal stem cells to smooth muscle cells via upregulation of miR-145 and the repression of KLF4
Davis-Dusenbery et al. [30]	Luciferase assay showed the direct binding of miR-145 to the 3′-UTR of KLF4; inhibition of miR-145 prevented down-regulation of KLF4 protein expression, TGFβ1 down-regulates KLF4 through the induction of miR-145 in vascular smooth muscle cells

Yang et al. [7]	Overexpression of miR-145 increased α-SMA expression and decreased KLF4 protein expression; miR-145 expression is upregulated in TGF-β1-treated lung fibroblasts (murine lung fibrosis model, human tissue samples)
Xu et al. [31]	Luciferase assay showed the direct binding of miR-145 to the 3′-UTR of KLF4; inhibition of miR-145 expression elevated KLF4 expression in embryonic stem cells

Anhang 4: Zusatzmaterial von Publikation IV

Tabelle 4: Literaturangaben, Bearbeitungsstand und Angaben zum Eigenanteil (**P4**).

Titel	**Identification of putative non-substrate-based XT-I inhibitors by natural product library screening**
Typ	Zeitschriftenartikel
Zeitschrift	*Biomolecules*
Bearbeitungsstand	Eingereicht am 28.09.2020; zur Publikation angenommen am 18.10.2020; online verfügbar am 21.10.2020
DOI	10.3390/biom10101467
Autoren	**Ly, T.-D**.; Kleine, A.; Fischer, B.; Schmidt, V.; Hendig, D.; Kuhn, J.; Knabbe, C.; Faust, I.
Eigenanteil in [%]	Konzeptionelle Gestaltung (90%); Datenaufbereitung (85%); Formalanalyse (100%); Experimentelle Durchführung (85%); Datenpräsentation (100%); Verfassen des ursprünglichen Manuskriptentwurfs und Editierung (100%)

biomolecules

MDPI

Supplementary Materials

Table S1. Results of the NPs library screening assay. The inhibitor (50 μM) was incubated with reaction buffer and equally concentrated XT-I protein solutions derived from CHO-K1 pgsA745 cell line complemented with full-length *XYLT1* expressing plasmid. The XT-I activities shown are means from one experiment performed in technical duplicates and calculated relative to the XT-I activity of the negative control sample containing DMSO.

Compound	CAS Number	Molecular Weight	Name	XT-I Activity [%]
1	53123-88-9	914.18	Rapamycin (Sirolimus)	70
2	56390-09-1	579.98	Epirubicin HCl	95
3	18883-66-4	265.22	Streptozotocin (STZ)	101
4	364622-82-2	438.52	Doripenem Hydrate	86
5	78110-38-0	435.43	Aztreonam	94
6	114-07-8	733.93	Erythromycin	105
7	2022-85-7	129.09	Flucytosine	93
8	72559-06-9	847	Rifabutin	112
9	5536-17-4	267.24	Vidarabine	103
10	486-66-8	254.24	Daidzein	115
11	145-13-1	316.48	Pregnenolone	95
12	467214-21-7	653.21	Alvespimycin (17-DMAG) HCl	120
13	33419-42-0	588.56	Etoposide	114
14	553-21-9	232.32	Costunolide	121
15	4759-48-2	300.44	Isotretinoin	86
16	4618-18-2	342.3	Lactulose	122
17	1397-89-3	924.08	Amphotericin B	25
18	317-34-0	420.43	Aminophylline	122
19	59-67-6	123.11	Nicotinic Acid	126
20	80621-81-4	785.88	Rifaximin	83
21	70458-95-6	429.46	Pefloxacin Mesylate	108
22	723-46-6	253.28	Sulfamethoxazole	121
23	114977-28-5	807.88	Docetaxel	104
24	362-07-2	302.41	2-Methoxyestradiol (2-MeOE2)	114
25	50-02-2	392.46	Dexamethasone (DHAP)	106
26	96036-03-2	383.46	Meropenem	107
27	7681-93-8	665.73	Natamycin	95
28	54965-21-8	265.33	Albendazole	77
29	78613-38-4	353.97	Amorolfine HCl	70
30	61379-65-5	877.03	Rifapentine	50
31	79902-63-9	418.57	Simvastatin	82
32	124832-27-5	360.8	Valaciclovir HCl	74
33	127-69-5	267.3	Sulfisoxazole	95
34	33069-62-4	853.91	Paclitaxel	79
35	2068-78-2	923.04	Vincristine sulfate	87
36	86386-73-4	306.27	Fluconazole	75
37	501-36-0	228.24	Resveratrol	51
38	50-55-5	608.68	Reserpine	89
39	128-13-2	392.57	Ursodiol	98
40	56-75-7	323.13	Chloramphenicol	87
41	13292-46-1	822.94	Rifampin	77
42	59277-89-3	225.2	Aciclovir	71

43	110871-86-8	392.4	Sparfloxacin	89
44	62997-67-5	1056.24	Nystatin (Fungicidin)	52
45	187235-37-6	359.26	PA-824	75
46	56180-94-0	645.6	Acarbose	92
47	112811-59-3	375.39	Gatifloxacin	98
48	220620-09-7	585.65	Tigecycline	59
49	91832-40-5	395.41	Cefdinir	72
50	59-87-0	198.14	Nitrofural	104
51	63-74-1	172.2	Sulfanilamide	118
52	117467-28-4	620.72	Cefditoren Pivoxil	104
53	83905-01-5	748.98	Azithromycin	109
54	98-92-0	122.12	Nicotinamide (Vitamin B3)	116
55	100986-85-4	361.37	Levofloxacin	111
56	73-31-4	232.28	Melatonin	99
57	63968-64-9	282.33	Artemisinin	93
58	446-72-0	270.24	Genistein	94
59	165800-03-3	337.35	Linezolid	103
60	23593-75-1	344.84	Clotrimazole	101
61	58-61-7	267.24	Adenosine	103
62	50-23-7	362.46	Hydrocortisone	122
63	68-35-9	250.28	Sulfadiazine	108
64	773-76-2	214.05	Chloroxine	121
65	68-19-9	1355.37	Vitamin B12	94
66	58-27-5	172.18	Menadione	106
67	25316-40-9	579.98	Doxorubicin (Adriamycin) HCl	113
68	34157-83-0	450.61	Celastrol	38
69	15291-77-7	424.4	Ginkgolide B	100
70	137234-62-9	349.31	Voriconazole	94
71	62893-19-0	645.67	Cefoperazone	83
72	302-79-4	300.4	Tretinoin	84
73	57-83-0	314.46	Progesterone	113
74	79-57-2	460.43	Oxytetracycline (Terramycin)	17
75	474-25-9	392.57	Chenodeoxycholic Acid	113
76	443-48-1	171.15	Metronidazole	109
77	298-81-7	216.19	Methoxsalen	107
78	51-21-8	130.08	Fluorouracil (5-Fluoracil, 5-FU)	137
79	152044-53-6	493.66	Epothilone A	119
80	103060-53-3	1620.67	Daptomycin	86
81	70356-03-5	385.82	Cefaclor	71
82	651-06-9	280.3	Sulfameter	126
83	53-16-7	270.37	Estrone	120
84	50-28-2	272.38	Estradiol	128
85	536-33-4	166.24	Ethionamide	130
86	458-37-7	368.38	Curcumin	43
87	65899-73-2	387.71	Tioconazole	136
88	22832-87-7	479.14	Miconazole Nitrate	149
89	144-82-1	270.33	Sulfamethizole	111
90	68373-14-8	233.24	Sulbactam	138
91	122-11-2	310.33	Sulphadimethoxine	132
92	10212-25-6	261.66	Cyclocytidine HCl	142
93	2922-28-3	171.59	Adenine HCl	146
94	404-86-4	305.41	Capsaicin (Vanilloid)	135

95	15291-75-5	408.4	Ginkgolide A	150
96	9041-93-4	1512.62	Bleomycin sulfate	149
0	67-68-5	78.13	Dimethyl sulfoxide	100

Table S2. Experimental analysis of human XT-I inhibition by celastrol and amphotericin B. K_m and V_{max} values shown were calculated from nonlinear regression (Michaelis-Menten plot) and the corresponding Y-intercept and slope values from the simple linear regression (Lineweaver-Burk plot). Data are means ± SEM of triplicate data points per experiment.

Compound.	**Michaelis-Menten plot**		**Lineweaver-Burk plot**	
DMSO	V_{max} [AU]	12124 ± 626	Y-intercept	$7.8 \pm 1.3 \cdot 10^{-5}$
	K_m [µM]	31.2 ± 3	slope	$2.6 \cdot 10^{-3} \pm 5.09 \cdot 10^{-5}$
Celastrol	V_{max} [AU]	11826 ± 551	Y-intercept	$7.1 \pm 1.1 \cdot 10^{-5}$
	K_m [µM]	53.3 ± 3	slope	$4.5 \cdot 10^{-3} \pm 7.4 \cdot 10^{-5}$
Amphotericin B	V_{max} [AU]	10031 ± 388	Y-intercept	$9.1 \pm 1.5 \cdot 10^{-5}$
	K_m [µM]	27.5 ± 3	slope	$2.8 \cdot 10^{-3} \pm 9.6 \cdot 10^{-5}$

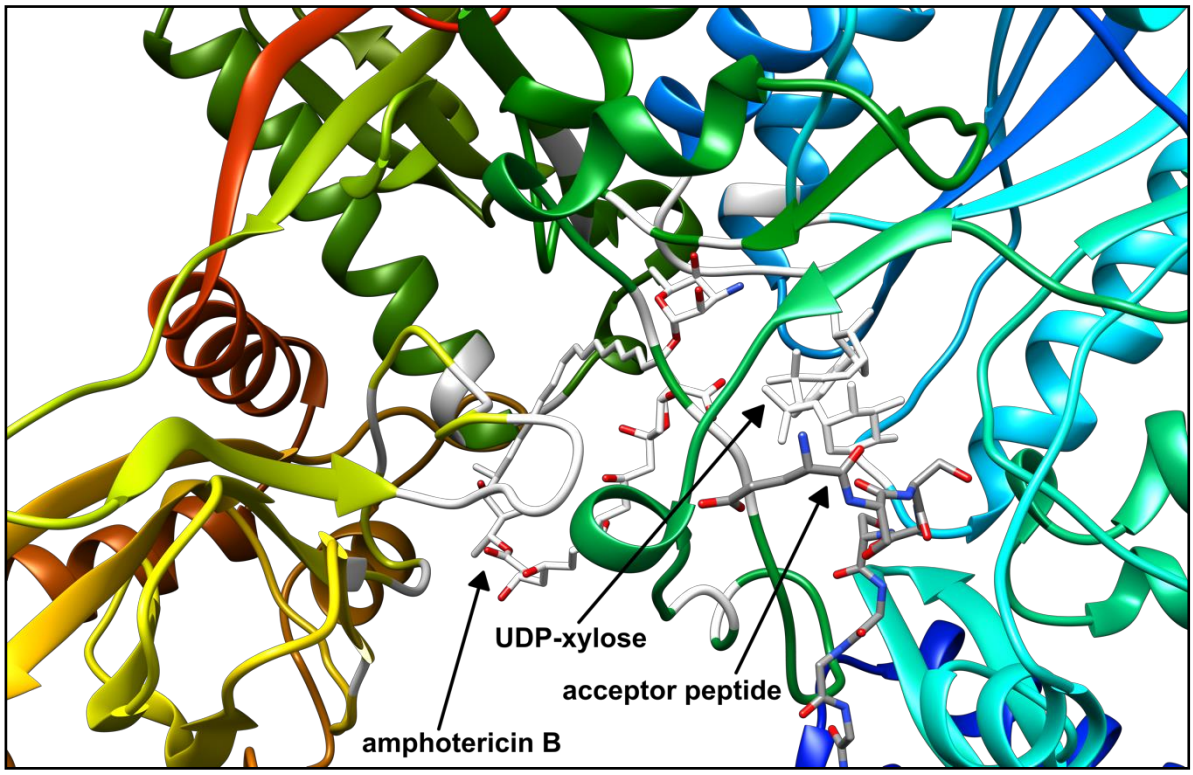

Figure S1. Structure of human XT-I complexed with amphotericin B, UDP-D-xylose and the acceptor peptide. Crystal structure of human XT-I [5] (rainbow colored from the N terminus (blue) to C terminus (red)) complexed with the chimera models #**2** of amphotericin B (white colored), UDP-D-xylose and modified acceptor peptide (atoms: C (grey), N (blue), O (red), P (orange)) are shown in stick representation. All atoms and bonds that meet the criteria < 5.0 Å from amphotericin B were colored in white.

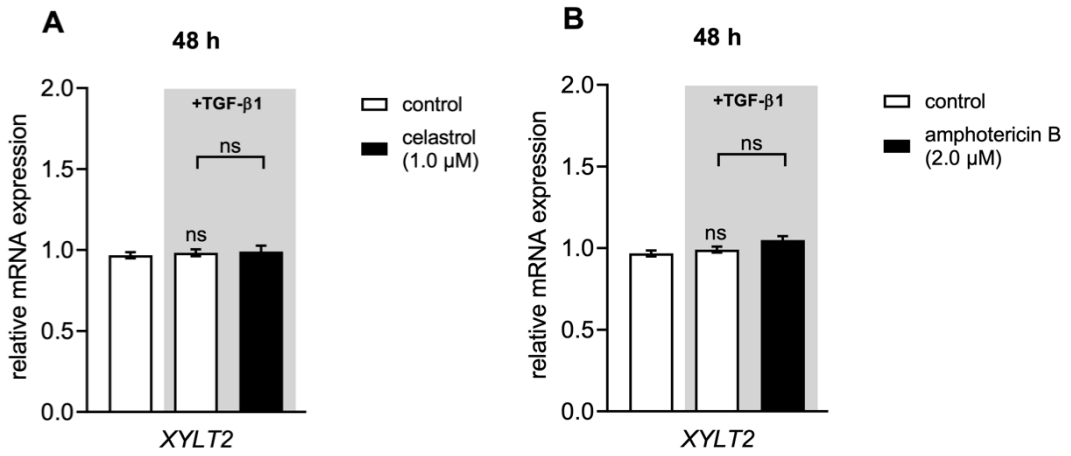

Figure S2. *XYLT2* mRNA expression is not affected by inhibitor or cytokine treatment of NHDF. Human primary dermal fibroblasts (n = 3) were cultured the day before the experiment. Cells were treated for 48 h with vehicle only (control), vehicle or (**A**) 1.0 μM celastrol or (**B**) 2.0 μM amphotericin B with additional TGF-β1 (5 μg/L) supplementation (highlighted in grey). Relative *XYLT2* mRNA expression levels were analyzed by quantitative real-time PCR. Data are means ± SEM of three biological and three technical replicates per experiment. Mann-Whitney U test: not significant (ns).

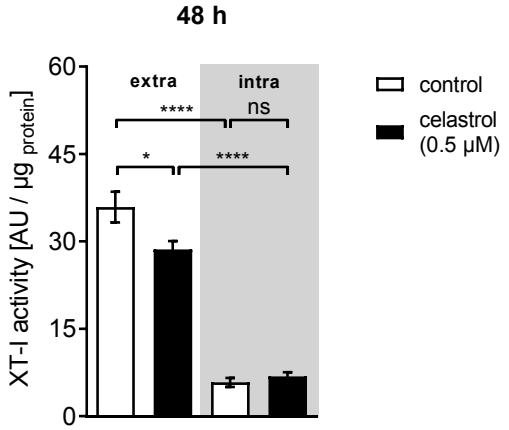

Figure S3. Extracellular XT-I activity reduction by celastrol was not caused by the downregulation of *XYLT1* mRNA expression. Human primary dermal fibroblasts (n = 3) were cultured the day before the experiment. Cells were treated with vehicle (control) or 0.5 μM celastrol for 48 h. Intracellular XT activity (intra, grey) was determined from the cell lysates and the corresponding supernatants were utilized for extracellular XT activity (extra) determination by UPLC-ESI-MS/MS XT-I assay. The XT activity is expressed as arbitrary units (AU) per μg of protein in 1 mL sample. Data are means ± SEM of three biological and three technical replicates per experiment. Mann-Whitney U test: not significant (ns), $p < 0.05$ (*), $p < 0.0001$ (****).

Eigenständigkeitserklärung

Hiermit versichere ich, Thanh-Diep Ly, dass die vorliegende kumulative Dissertation mit dem Titel „Untersuchungen zur Regulation der humanen Xylosyltransferase-I bei Fibrosen“ selbstständig von mir verfasst wurde. Andere als die angegebenen Quellen und Hilfsmittel wurden nicht verwendet. Die Arbeit wurde bisher nicht in anderer Form als Prüfungsleistung vorgelegt.

Ort/Datum Unterschrift